GEOLOGY AND METAMORPHIC HISTORY OF THE

KANMANTOO COPPER DEPOSIT, SOUTH AUSTRALIA

A thesis submitted for the degree of
Doctor of Philosophy to the University
of London

by

William Francis Lindqvist

Imperial College   August, 1969
London

ABSTRACT

The recently discovered Kanmantoo copper deposit is
located in a belt of pelitic rocks that forms part of the
Cambro-Ordovician Kanmantoo Group. These rocks display
typical flysch-type sedimentary characteristics. They were
deposited in a narrow sedimentary trough along the south-
eastern flank of the West Australian Shield and during a
late Ordovician orogeny were severely folded and regionally
metamorphosed to almandine-amphibolite facies grade. No
fragmental volcanic material or lava flows have been recognised
anywhere in the sequence. Intrusive rocks are absent from the
vicinity of the Kanmantoo orebody.

Fine-grained disseminated, non-economic mineralization
consisting of major pyrrhotite and minor chalcopyrite and
sphalerite, occurs through large volumes of the aluminous
and ferruginous country schists and in a few pelitic beds
in the more siliceous rocks further from the orebody.
Textural studies show that these fine-grained sulphides
were present from the earliest recognisable stages of meta-
morphism. Structural and geochemical relationships further
suggest that the sulphur and metals were part of the original
sediments.

The mode of occurrence of the important economic minerali-
zation is altogether different from that of the disseminated
material. It consists of veinlets and bands of coarse-grained
sulphides, oxides and
iron-rich silicates along zones parallel to the axial plane
schistosity. Both Structural and textural relationships
indicate that this mineralization was in its present position
from about the middle stages of metamorphism. Known phase
equilibria data suggest that many of the present day ore
mineral assemblages developed during late and post-metamorphic
times from different assemblages that were more stable at
the elevated temperatures of metamorphism. There is no evidence
that any of the coarse-grained ore mineral components were in
their present location prior to metamorphism. Geochemical

profiles of some major, minor and trace elements through the
ore body show that the sulphur, iron, cobalt, and nickel in
the ore zones may have been derived during metamorphism from
the fine-grained mineralization in the adjacent country
rocks. The copper however appears to have had a more distant
source and is thought to have been possibly introduced into
the ore zones as a chloride dissolved in migrating metamorpho-
genic hydrous fluids.

CONTENTS

Chapter 1

INTRODUCTION

A. OPENING STATEMENT

The Kanmantoo copper deposit is made up of a number of lenses of pyrrhotite-chalcopyrite-magnetite mineralization oriented along the schistosity of the enclosing pelitic rocks. These rocks form part of some 50,000 feet of Cambro-Ordovician geosynclinal flysch-type sediments that were deposited in the narrow, north-south trending Kanmantoo Trough along the south-eastern flank of the Precambrian West Australian Shield. During an Ordovician orogeny the sediments were severely folded and regionally metamorphosed up to almandine-amphibolite facies grade. Small bodies of granite and a few dolerite dykes intruded the sediments during the orogeny but no igneous rocks are exposed in the vicinity of the Kanmantoo deposit.

B. SOME GENETIC ASPECTS OF SULPHIDE ORES IN METAMORPHOSED GEOSYNCLINAL ROCKS

The mineralogical and structural features of the Kanmantoo deposit are similar in many respects to many copper deposits found in metamorphosed geosynclinal regions all over the world. For instance those in the Applachians (Stanton, 1959; Howard, 1959; Kinkel, 1967), in the Palaeozoic schist belts of Japan (Kanehira, 1959), the Norwegian Caledonides (Vokes, 1957) and the Khetri and Singbham copper belts of India (Chowdhury and Das Gupta, 1965; Sen Gupta, 1965). In most of these deposits pyrrhotite is the main iron sulphide phase and chalcopyrite the dominant 'non-ferrous' sulphide; magnetite is usually present in significant amounts. Although such deposits are often described as strata-bound in that in any one region the ore concentrations are confined to parti-cular lithologic horizons or certain lithologic types, individual orebodies or parts of orebodies are generally related more to tectonic structure than to stratigraphy. Most of the ore consists of vein and streaks along rock cleavages, schistosity

planes, shears and fractures. In some places thick zones of
sulphide/wall-rock breccia are developed.

The control of the geometrical features of such ores by
tectonic structures has been recognised for many years but it
was only some 20 years ago that geologists began to question
seriously the previously oft-quoted "post-metamorphic emplace-
ment of ore along favourable structures" concept of ore genesis.
A more critical look was taken at ore textures as well as the
complete geological environment. From well known investigations
such as those of Ramdohr (1951) on the Pb-Zn ores of Broken
Hill, Davis(1954) on the Roan Antelope deposit, and Stanton
(1955) on some pyritic ores of Eastern Australia, considerable
doubt was thrown on many of the conventional criteria for
textural interpretation. Gradually it was realised that many
so-called replacement intergrowths could equally have been
formed by simultaneous crystallization and recrystallization
during metamorphism. This has culminated in the last decade
in a great many papers dealing with metamorphism of sulphide
ores. To keep the subject in perspective it should be pointed
out that neither the concept of metamorphism of ores nor the
recently published observations are by any means novel; modern
sounding observations and criteria for recognising metamorphism
in ores were given by Emmons (1909) and by a number of later
writers including Lindgren and Irving (1911), Kato (1925) and
Newhouse and Flaherty (1930). The possible importance of these
ideas was generally lost in the popularization of the magmatic-
hydrothermal schemes of ore classification that dominated ore
genesis thinking for half a century.

The impetus for much of the recent work on the influence
of metamorphism on the mineralogy, textures and distribution of
sulphide ores has come from the resurgence of syngenetic ideas
for the origin of strata-bound ores; the involvement of the
ore in the metamorphism that affected the enclosing rocks is
a necessary adjunct of the syngenetic theory.

Although Buerger (1928) and Newhouse and Flaherty (1930)
both investigated the deformation characteristics of common

sulphide minerals it was not until the work of Verhoogen (1948), Voll (1960) and Stanton (1964) that the stage was set for more profound experimental work on the effects of metamorphism on sulphide ores. Brett (1964) demonstrated that many replacement-type intergrowths of phases in the Cu-Fe-S system can be formed purely by unmixing of solid solutions during cooling. Roberts (1965) found that galena, chalcopyrite, pyrrhotite and sphalerite readily recrystallized under a confining pressure of 2000 bars at temperatures as low as $100^{\circ}C$. Static annealing experiments by Stanton and Gorman (1968) have shown that equilibrium fabrics in chalcopyrite and sphalerite aggregates can be attained in a matter of days at $200^{\circ}C$. On the other hand Read (1967a) found on heating non-equilibrium pyrite aggregates for about 40 days that grain boundary movements were perceptible at temperatures only above $600^{\circ}C$. Some preliminary heating experiments on inequilibrium magnetite aggregates for periods of up to 7 days showed no visible textural changes under about $750^{\circ}C$ (see p. 118 of this thesis).

This experimental work makes the validity of any interpreted paragenetic sequence of ore minerals even in low-temperature truly epigenetic ores rather dubious but it also presents a difficulty for investigators of suspected syngenetic ores. The recognition of a recrystallized or annealed microstructure in sulphide ore enclosed in metamorphic rocks is not incontrovertible evidence that the ore itself has been metamorphosed. This is an important point since there is already a tendency for recrystallized and annealed ore fabrics to be attributed rather uncritically to the metamorphic event that affected the enclosing rocks. Another interesting point is that in view of the stresses induced in rocks during underground mining operations, it is to be wondered whether many of the softer sulphides have not recrystallized and annealed between the time of driving the underground opening and the collection of the sample. The possibilities of shock metamorphism through blasting also ought to be borne in mind.

C. SCOPE OF THE PRESENT RESEARCH

The ultimate aims of most studies of ores are to determine
the origin of the ore constituents and ascertain the cause for
the ore being where it is and by so doing, advance ore genesis
theory and increase the effectiveness of exploration. Genetic
conclusions for ores in highly deformed and metamorphosed
terrains are usually rather speculative and for this reason
the practical usefulness of research is likely to be one of
ore associations e.g. with certain lithologies, mineralogies
or structures. The general philosophy expounded by Schröcke
(1953) has been followed throughout the field and petrographic
studies; by working inwards from the country rocks to the ore
and using all scales of structural and textural analyses, the
time relationships can be established between metamorphism
and deformation and the involvement of ore minerals in these
events.

This study began early in 1966 with detailed mapping of
the rocks overlying the deposit on a scale of 100 feet to the
inch and the concurrent examination of some 45,000 feet of
diamond drill core that had accumulated by that time. Further
mapping on a scale of 350 feet to the inch was extended outwards
from the deposit to cover about six square miles of the country
rocks to provide additional stratigraphic and structural data
for unravelling the complex structures around the orebody.
As no previous petrological work had been done on the newly
discovered Kanmantoo orebody or on the surrounding rocks, a
major part of the laboratory work has been a petrographic
analysis of the silicate, sulphide and oxide intergrowths.

Once it was established that at least part of the ore
had been metamorphised, mineralogical studies were made on
some of the silicate, sulphide and oxide phases. X-ray
diffraction and electron probe microanalysis techniques were
widely used. Present ore mineral assemblages were then able
to be interpreted in the light of pressure and temperature
estimates based on metamorphic silicate stability relationships.
Whole rock chemical analyses were made of a number of unaltered

country schists to help ascertain their sedimentary nature,
and of a number of altered rocks from the ore zones to determine
what metasomatic changes had occurred. Minor and trace element
data made available for a number of drill holes intersecting
mineralized zones have been an invaluable aid in determining
the possible genetic relationships between metamorphism,
deformation and ore distribution.

D. HISTORY AND DISCOVERY OF THE KANMANTOO DEPOSIT

Copper ores were first discovered in the Kanmantoo
district in 1846 and were worked intermittently by various
syndicates until about 1875 when a total of 5000 tons of
copper metal had been produced. By this time the deepest
workings had reached about 200 feet below the surface where
the ore grade had dropped from an average of about 15% Cu to
2-3%. Various attempts were made to re-open the mines in
subsequent years at times of high copper prices but with little
success. In 1938 a small exploration group called the Austral
Development Company sank a shaft 170 feet deep and put down
four shallow diamond drill holes to test the mineralization
under the old workings but...."the results of the exploratory
work show a large body of highly mineralized material.... it
does not appear however as if the veins showing the higher
values can be linked to make a continuous formation."
(Mining Review, 1939). A subsequent geological appraisal of
the district during the war was made by Dickinson (1942)
who concluded that there were no known copper reserves in the
old mines and that the exploration possibilities had been
fully exploited.

Encouraged by the earlier drilling reports, Mines
Exploration Pty Ltd, the exploration subsidiary of Broken
Hill South Ltd, secured an exploration lease around the old
workings and in 1962 began geophysical prospecting using the
newly developed Induced Polarization (I.P.) electrical
resistivity equipment. A total of 50 line miles of reconnais-
sance work was followed by more detailed investigations over

the workings themselves. Many weakly anomalous I.P. effects were found to be associated with pyritic schist# bands but an important anomaly was found in an elongated zone adjacent to the old workings of one of the larger mines. This I.P. zone was drilled late in 1962 and the first hole intersected 400 feet of sulphide mineralization assaying just on 1% Cu. Since then 42 diamond drill holes totaling over 50,000 feet, and about 35,000 feet of shallow percussive drilling have delineated a substantial but low grade copper deposit extending to 1300 feet below the surface.

E. ACKNOWLEDGEMENTS

Chapter 2

REGIONAL GEOLOGICAL SETTING

A. LOCATION, CLIMATE, PHYSIOGRAPHY

The Kanmantoo copper deposit is situated about 50 miles
east of Adelaide, the capital of South Australia, and is
located about a mile and a half southwest of the township of
Kanmantoo at longitude 140° 01' east and latitude 35° 06' south
(fig. 2-2). This is about a mile west of the main road
connection between Adelaide and Melbourne and less than a mile
east of the main east-west railway link. Access to the orebody
is provided by good, all weather unsealed roads.

With an annual rainfall of 14 inches and an average
monthly temperature between 83°F and 42°F, the area surrounding
the Kanmantoo deposit lies on both the geographic and climatic
boundaries between the semi-arid Murray Basin to the east and
the temperate highlands of the Mount Lofty Ranges overlooking
Adelaide to the west (fig. 2-3). Apart from a few scraggy
species of Eucalyptus and scattered tussocks natural vegetation
is sparse; no vegetation of any type exists in the immediate
vicinity of the old mine workings probably as a result of the
weathering of sulphides in the tailings dumps. Local fauna
include wasps and bees, abundant grasshoppers and flies and
the ubiquitous shingle-back or "sleepy" lizard (Tiliqua rugosa).
Snakes are uncommon.

The moderately undulating topographic forms of the
district have resulted from two distinct cycles of erosion;
a general concordance of summit levels represents a lateri-
tized late Tertiary peneplain, part of which is still preserved
on the Mine Hill overlying the Kanmantoo orebody (fig. 2-1a).
Later minor uplifting movements caused the gentle dissection
of this erosion surface and produced rather mature land forms.
More pronounced uplift in Pleistocene times gave rise to some
local rejuvenation and development of steeply graded streams
and relatively deep gorges in the south western part of the
area. Alluvium filling many of the valleys is dissected by
narrow, steep-walled drainage channels that are dry for most

FIG. 2-I

(a) Looking westwards towards the Mine Hill. Note the lines of old workings along the eastern slopes; the newly discovered orebody is concealed under the eastern edge of the lateritic capping and lies between the points indicated by the arrows. A drainage channel is visible in the valley, and in the foreground there are typical outcrops of the easily weathered quartz-mica schist.

(b) A steep-walled drainage channel cutting through oxidized red-coloured alluvium and exposing fresh quartz-mica schists. Streams run in the channels for short periods after heavy rain.

FIG. 2-1

of the year; these channels are useful locally in exposing
bedrock (fig. 2-1b).

B. THE ADELAIDE GEOSYNCLINE

The Kanmantoo orebody lies within a thick sequence of
lower Palaeozoic meta-sediments known as the Kanmantoo Group
the history of which should be viewed in the context of that
great geological and geographical feature of South Australia,
the Adelaide Geosyncline.

Archaean rocks exposed over much of the western half
of the State form the eastern extension of the well known
West Australian shield region (fig. 2-2). These ancient rocks
were intensely folded, metamorphosed and intruded by igneous
rocks during a number of pre-Cambrian orogenies. In the Upper
Proterozoic, their uplift and erosion provided material to fill
a large depression stretching from Kangaroo Island in the south
to the northern boundary of South Australia. Sedimentation
in this depression, now known as the Adelaide Geosyncline,
is thought by Sprigg (1952) to have occurred principally as
continental outgrowths from the shield areas parts of which
existed to the east at the time. Great thicknesses of sand-
stones and conglomerates were deposited around the shorelines
synchronous with thinner dolomites and shales further from the
coast. Many local unconformities and interbedded chert beds,
evaporites, volcanic sediments, glacial deposits and some
banded iron formations attest to continuous tectonic activity
and ever changing climatic conditions. Towards the end of
the Proterozoic there was widespread development of continental
deposits. The Cambrian began with the deposition of a thick
sandstone formation in the central section of the geosyncline
whilst near the eastern and western coastlines massive
Archaeocyathinae biohermal limestones were formed. By about
the middle Cambrian, general uplift began and sedimentation
over most of the geosyncline ceased except in the extreme
south where local rapid subsidence in the Kanmantoo Trough
stimulated sedimentation into the lower Ordovician.

An orogenic period which followed involved both the

Map legend:

- MESOZOIC BASINS
- PALAEOZOIC GRANITE
- KANMANTOO GROUP
- PROTEROZOIC
- ARCHAEAN

Map labels: WEST AUSTRALIAN SHIELD, Eucla Basin, Gt. Artesian Basin, Lk. Eyre, ADELAIDE GEOSYNCLINE (Flinders Ranges), Murray Basin, Adelaide, Kangaroo Island, Kanmantoo, Southern Ocean

Inset map labels: N.T., QLD., W.A., S.A., N.S.W., VIC.
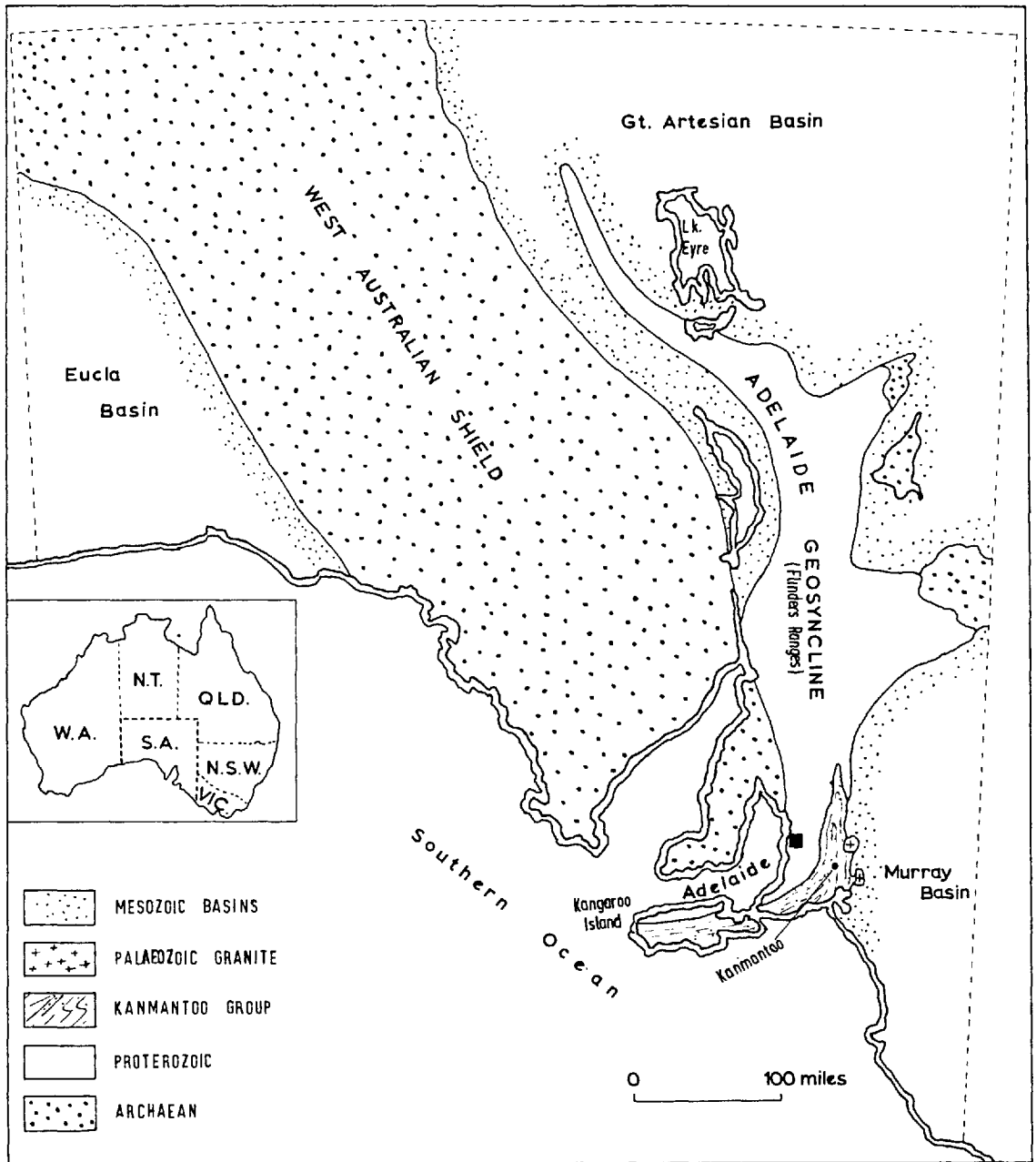
FIG. 2-2   Main Geological sub-divisions of South Australia.

geosynclinal and trough sediments but the folding and meta-
morphism was more severe in the southeast than elsewhere in
the geosyncline. The general absence of later Palaeozoic
sediments prevents the accurate stratigraphic dating of this
orogenic event although sub-horizontal Permian tillites
overlying folded lower Palaeozoic rocks in the far south
(fig. 2-3) at least proves a Palaeozoic age for the folding
(Campana,1954). More recently, potassium-rubidium dating of
minerals in syn-kinematic granites at Victor Harbour by
Evernden and Richards (1962) and at Palmer by White et al.
(1967) places the orogeny in the Ordovician.

A prolonged period of stability following the lower
Palaeozoic orogeny is deduced from the general absence of
Mesozoic sediments over most of the geosynclinal areas.
During the middle and late Tertiary, extensive block faulting
movements were accompanied by local marine sedimentation in
low-lying areas. A general uplift in the late Pliocene and
early Pleistocene produced local fissure eruptions of basalt
on Kangaroo Island and in the southeastern corner of the State.

C. THE KANMANTOO GROUP

The Kanmantoo Group of meta-sediments occupies the
eastern and southern flanks of the Mount Lofty Ranges, a
great anticlinorium stretching northwards from Cape Jervis
to meet with the Flinders Ranges. Figs. 2-3 and 2-4 complement
the following description of the Kanmantoo Group.

1. Sedimentation and Stratigraphy

Except for some isolated brachiopods in the basal
members (Daily, 1963) the Kanmantoo rocks are unfossiliferous
but their dominantly marine origin is almost certainly demon-
strated by their great thickness (50,000 ft), the regional
uniformity of sedimentary characters, the regularity of
bedding and the presence of slump structures. The exact
nature of the contact between the base of the Kanmantoo Group
and the underlying rocks has been a matter of some dispute.
An earlier concept of a faulted contact has been discarded

Legend:
- ALLUVIUM and TERTIARY
- PERMIAN TILLITES
- KANMANTOO GROUP
- CAMBRIAN
- PROTEROZOIC
- ARCHAEAN
- GRANITE GNEISS
- INTRUSIVE GRANITE
- FAULTS

0   10 miles

FLINDERS RANGES

RANGES

LOFTY

MT.

Palmer

ADELAIDE

Nairne

KANMANTOO

MURRAY BRIDGE

Strathalbyn

MURRAY BASIN

GULF ST. VINCENT

PENINSULA

Lake Alexandrina

FLEURIEU

Cape Jervis

Victor Harbour

Rosetta Head
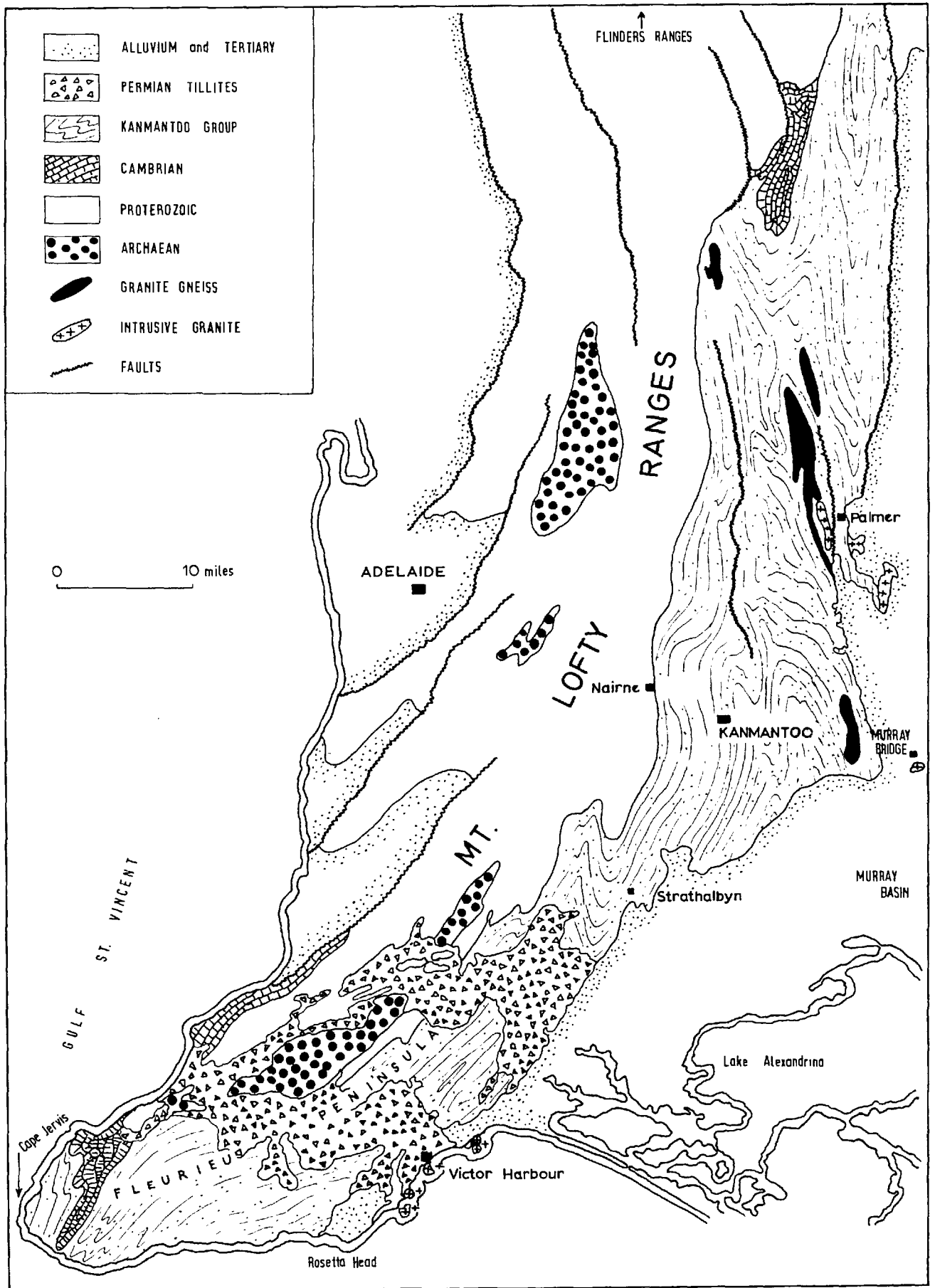
FIG. 2-3   Geology of the Mt. Lofty Ranges, South Australia.

since later mapping has shown some parts conformable upon lower
Cambrian geosynclinal sediments (Kleeman and Skinner, 1959; Daily,
1963) while other parts, are transgressive with local deposition
directly upon eroded Archaean schists (Horwitz et al. 1959).

Monotonous alternations of greywackes, phyllites and
feldspathic sandstones or their metamorphosed equivalents make
correlation within the Kanmantoo Group difficult, nevertheless
a few prominent marker horizons have enabled three formations
to be recognised.

Carrikalinga Head Formation

The lowest formation found locally only on the Fleurieu
Peninsula consists of alternating, thin bands of phyllite
containing a few brachiopods and massive, dark coloured
greywackes.

Inman Hill Formation

The Inman Hill Formation occupies the basal position
over most of the Kanmantoo Group. The predominant rocks are
massive or cross-bedded micaceous quartzites and arkoses with
minor intercalations of quartz-feldspar-mica schist, quartz-
mica schist, andalusite-staurolite schist, and a few lenses of
marble and calc-silicate rocks.

Brukunga Formation

Pelitic schists and meta-greywackes are the dominant
rock-types in this formation. Marking the base of the
Brukunga Formation is one of the most prominent rock-types of
the Kanmantoo Group, the Nairne Pyrite Horizon which has been
traced for at least 65 miles along the regional structure
(Kleeman and Skinner, 195). About 8000 feet stratigraphically
above the Nairne Pyrite Horizon lies a zone of coarse-grained
porphyroblastic andalusite schists called the Paringa Andalusite
Horizon (Mirams, 1962). These rocks are host for the Kanmantoo
orebody and can be traced for more than ten miles south and
five miles north of the Kanmantoo orebody. They weather
commonly to a red-brown colour through the oxidation of the
small amounts of disseminated iron sulphides that they contain.

Scale:
0 ___ 2 miles

Mt. Lofty Ranges

Bremer Fault

Brukunga

● Nairne

Kanmantoo
Orebody

area mapped

Alluvium

● Strathalbyn

Legend:

Alluvium

Paringa Andalusite
Horizon   } BRUKUNGA FORMATION

Nairne Pyrite
Horizon   } INMAN HILL FORMATION

Proterozoic

Pyrite Horizons

Faults
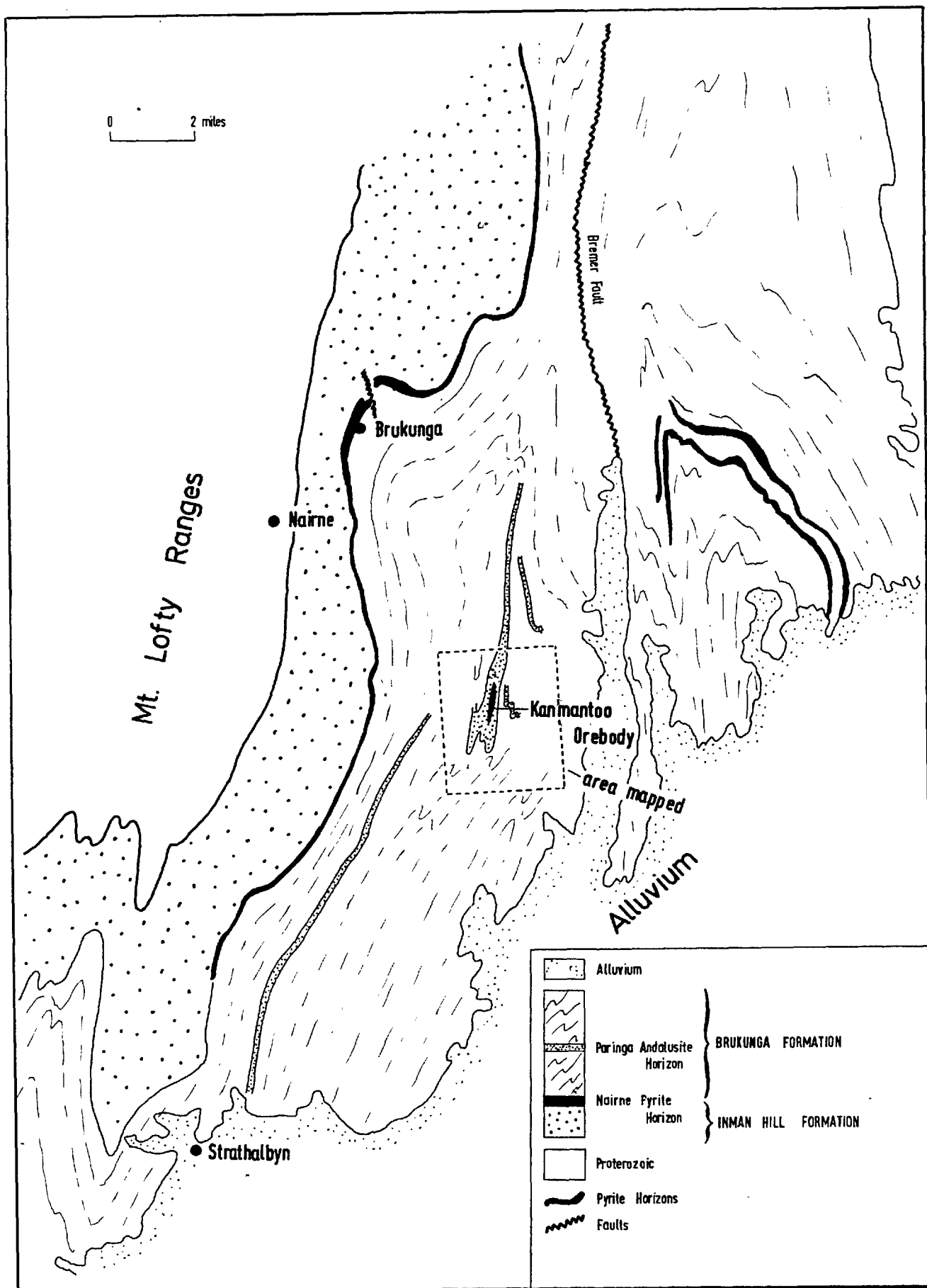
FIG. 2-4   Geological Environment of the Kanmantoo Orebody.

Small showings of chalcopyrite and gahnite (zinc spinel)
occur in a few places along the Paringa Andalusite Horizon
but no mineralization of economic interest has yet been found out-
side the Kanmantoo orebody.

2. The Lower Palaeozoic Orogeny

During the lower Palaeozoic orogeny the rocks of the
Kanmantoo Group were folded into a series of anticlines and
synclines generally plunging between 20° and 50° to the south
and overturned to the west. Metamorphic studies carried out
in the region by White (1956), Kleeman and Skinner (1959),
Mills (1964), Offler and Fleming (1968) and others have
delineated a sequence of metamorphic zones or aureoles out-
wards from the Palmer Granite (fig. 2-3) that are characterised
by the key minerals:

(1) sillimanite + orthoclase
(2) sillimanite + muscovite
(3) andalusite + staurolite
(4) biotite
(5) chlorite

Because of the overall simple structures and the presence of
andalusite-staurolite assemblages the regional metamorphism
has been compared to the Buchan-type of Read (1952) and the
Abukuma-type of Miyashiro (1961); both types are considered
characteristic of relatively shallow depths and fairly high
temperatures.

A number of igneous rocks appear in the Kanmantoo Group
though none are found in the vicinity of the Kanmantoo orebody
or elsewhere cutting the Paringa Andalusite Horizon. White
(1956,66) believes that the granite gneiss near Palmer formed
from pre-existing sediments during metasomatic activity following
the main metamorphic phase but that the Palmer granite was
intruded near the end of this metasomatic period. Dolerite
and meta-dolerite dykes in the northern regions of the Kanmantoo
Group were intruded at a very late metamorphic stage.
Extensive late-metamorphic "shearing" is widespread and is
thought to have controlled much of the late metasomatic

activity such as regional chloritization and widespread
scapolitization (Mills, 1964).

3. Mineralization

In the last half of the 19th century many mines were
active in the rocks of the Kanmantoo Group but the majority
produced only small quantities of silver-lead-zinc and copper
ore some of which contained minor gold and bismuth. Few mines
proved to be economic. Most of the base-metal concentrations
were found along "shear zones" or in quartz fissure-veins
lying parallel or at small angles to the foliation of the
surrounding rocks. Hydrothermal fluids from a nearby or
unknown granite source were widely postulated for the minerali-
zation (LaGanza, 1959) although the common association of
sulphides with high-temperature metamorphic minerals like
sillimanite and garnet has also been recognised (Thomson,
1965). The Palmer granite itself contains sinuous copper
mineralization (Johnson, 1965) but apart from the general
shape of the lodes and a few records of grade, little is known
of the mode of occurrence of the ore.

The Kanmantoo and nearby Callington group of mines were
the largest copper producers (5000 tons). According to
Dickinson (1942) who made his conclusions from old mine records
and an examination of the old, largely collapsed workings, the
ore in this area occurs in veins of tabular or pipe-like
form lying oblique to the crumpled stratification (bedding)
but generally parallel to the foliation of the schists. The
ore is said to have a mesothermal character and formed from
hydrothermal fluids in fracture systems. Similarly Kleeman
and Skinner (1959) considered the Kanmantoo ores to be.....
"localized by shearing and contortion within incompetent
andalusite-staurolite schists".

Near Brukunga there occurs the largest sulphide deposit
in the Kanmantoo Group and the only one currently being worked.
Here the Nairne Pyrite Horizon contains beds of the fahlband
type up to 200 feet thick and assaying up to 15% sulphur in
the form of pyrite, pyrrhotite and minor marcasite. Minor

graphite is widespread. Small amounts of sphalerite, galena,
chalcopyrite and various silver sulpho-salts occur in tension
veins, but these are of no economic interest. Based on
chemical, mineralogical and textural evidence both Skinner
(1958) and later George (1966) conclude that the iron sulphides
were metamorphosed with the enclosing schists. However,
Skinner thinks that the sulphides were deposited as detrital
grains whereas George considers them to be chemical precipitates.
Smaller pyritic and pyrrhotitic mica schist bands are very
common throughout the Kanmantoo Group where they serve as
good local marker beds but assume no direct economic importance.

Chapter 3

GENERAL GEOLOGY AROUND THE KANMANTOO OREBODY

Introduction

The metamorphic rocks around the Kanmantoo orebody are
derived from a suite of sedimentary rocks of mixed arenaceous
to argillaceous compositions. The rocks have been divided on
the basis of mineral assemblages into four main lithological
units (map. 1) although some of these can be further sub-
divided in the structural interpretation (maps 2,3). A
number of minor rock-types are also encountered, some resulting
from original sedimentary variations, some from localised
tectonic-metasomatic processes during metamorphism and others
through weathering.

The individual mappable rock units vary in their degree
of surface exposure because of their differing responses to
both physical and chemical weathering. Widespread interbanding
of the different rock-types at the contacts makes some major
boundaries difficult to fix and monotonous interbanding within
units makes it hard to correlate isolated outcrops. All the
rocks show the effects of deformation and regional metamorphism
but response to these events appears to have varied markedly in
the different lithologies. Sedimentary structures are still
preserved in the arenaceous rocks where folding has been
relatively gentle, and the original sedimentary textures of
detrital quartz and feldspar are largely unchanged except for
the growth of a few micas. But in the more pelitic rocks
deformation has been much more severe and they have been
completely reconstituted into metamorphic mineral assemblages
of the almandine-amphibolite facies.

Chalcopyrite-pyrrhotite-magnetite mineralization which
is found largely within an iron-rich sub-facies of the pelitic
rocks (the lode schists), could be studied only in the diamond
drill core (map. 4) since no ore crops out at the surface.
Even so, valuable evidence of the structural and lithological
setting of the ore was obtained from the upper levels of the
old collapsed mine workings.

This chapter deals with the lithological characteristics of the rocks in the field and discusses in some detail the general features of the sulphide-oxide mineralization.

A. DESCRIPTION OF THE MAJOR ROCKS

1. Quartz-Feldspar Schists

Well exposed around the margins of the area are the tough, fine-grained, siliceous looking quartz-feldspar schists that are light to dark grey in colour and composed mainly of quartz and feldspar with a variable but minor amount of biotite. A lithological banding defined chiefly by rapid alternations in the amount of biotite is widespread and, although the alignment of biotite flakes imparts a schistosity to these rocks, a poorly developed fissility enables the outcrop pattern to be controlled largely by the banding. As a result, the larger folds could be mapped accurately and so provide invaluable control for the interpretation of structure beyond the confines of the orebody. A few biotite-rich, disseminated iron-sulphide horizons were useful in local correlation.

The lithological banding made up of layers from about 1 millimetre to several centimetres thick is undoubtedly bedding because of its association with sedimentary structures exposed in some of the stream beds. Very delicate banding containing many cross-bedding discontinuities and cut-and-fill structures is illustrated in figs. 3-1a,b, the second photograph displaying a curious asymmetrical ripple train that suggests a (local) current direction from west to east. Similar structures have been found in recent sediments of the Mississippi Delta by Davies (1966). In some places there are sequences of arenaceous bands containing multiple ripples with internal laminations, each band being separated from the others by a thin layer of argillitic composition (fig. 3-1c). This photograph illustrates well the slight tectonic disturbance suffered by some of these arenaceous rocks; the poorly reconstituted argillaceous layers demonstrate the partial dependence of metamorphic crystallization on the intensity of deformation. Nearby, where the same horizon of ripple marks

FIG. 3-I

(a)   Gentle cross-bedding in delicately banded quartz-feldspar schists;

the disconformity traces have been marked on the photographs. The

rocks have been slightly deformed and contain some thin quartz veins.

(b)   An asymmetrical ripple train in banded quartz-feldspar schist. The

asymmetry appears to be a primary feature and suggests a local current

direction from west to east.   Note the small cut and fill structure

in the upper part of the photograph. Diameter of coin approximately

3 cm.

(c)   A cross-section through interbanded argillites and arenites; the latter

display internally laminated ripples. Disturbance of some bands may or

may not be penecontemporaneous slumping. The argillaceous bands are

very fine-grained and poorly recrystallized.

(d)   Tectonically deformed ripples on the eastern limb of a small north-south

anticline. The argillaceous bands between the ripples have been completely

recrystallized and exhibit a crude axial plane schistosity sloping downwards

from right to left.

FIG. 3-1

has been exposed on the limbs of a fold, the ripples have
all been moderately deformed and the grain-size of micaceous
layers is visibly increased (fig. 3-1d).

No lithological differences are obvious between the
upper and lower sub-divisions of the quartz-feldspar schists.

2. Quartz-Mica Schists

Between the andalusite-staurolite schists and the
upper and lower arenaceous rocks lie the quartz-mica schist
horizons, each having a thickness of the order of 600 feet.
Again no lithological distinction can be made between the
upper and lower sub-divisions for they both consist predominantly
of quartz, biotite, and muscovite with minor almandine-garnet
and occasional bands of small staurolite and andalusite crystals.
A high mica content produces a good schistosity and a pronounced
fissility which causes rapid erosion through mechanical disinte-
gration. Consequently, the quartz-mica schists occupy most
of the low-lying areas where exposure is poor. Their colour
depends primarily upon the ratio of quartz plus muscovite to
biotite but also to some extent on grain size. For a given
mineralogical composition, the finer the grain size the darker
the appearance of the schist. An erratic but nevertheless
distinct coarsening in grainsize is discernible in both quartz-
mica schist sub-units from near the contacts with the arena-
ceous rocks inwards towards the andalusite-staurolite schist.
The very fine-grained varieties in places could almost be
described as phyllites whereas the exposures in the vicinity of
the aluminous rocks are typical medium grained, quartz-mica
schists (figs. 3-2a,b).

A lithological banding containing rare, gentle cross-
bedding features but no other sedimentary structures is well
developed through most of the quartz-mica schists, and small
folds in this banding in the "phyllitic" schists have a similar
attitude to those in the bedding of nearby quartz-feldspar
schists. Fine banding is generally parallel to the contacts
between thicker lithological units and even if severely
deformed it still retains the appearance of bedding (fig. 3-2c).
Similar folded banding exists in the coarser grained quartz-mica

FIG. 3-2

(a,b) Photomicrograph comparison of fine-grained quartz-mica
schist from near the contact with the quartz-feldspar
schists, with coarser grained quartz-mica schists
close to the Mine Hill. Light mineral is quartz,
elongated minerals are biotite and muscovite and
the opaque phase is ilmenite. Taken in transmitted,
plane polarized light.

(c) Complex small-scale folding in the bedding of quartz-
mica schists. The axial plane schistosity is
parallel to the fractures across the core.

(d) Lithological banding oriented parallel to the
schistosity in quartz-mica schist. This banding is
probably bedding that has been transposed into the
schistosity direction during deformation.
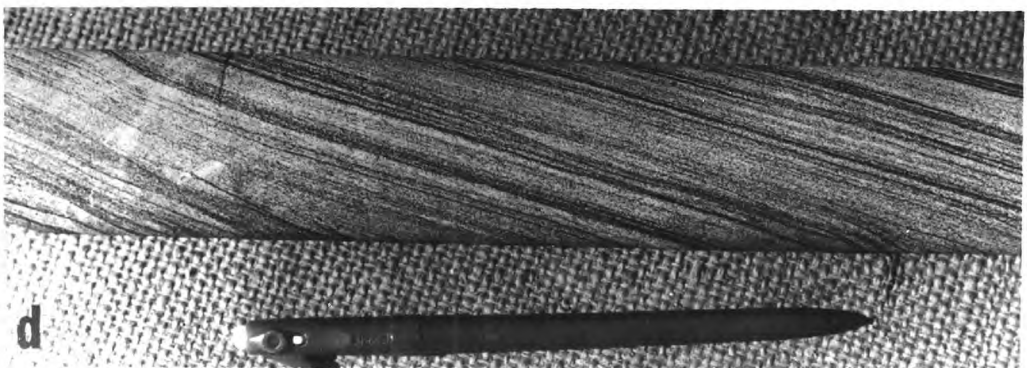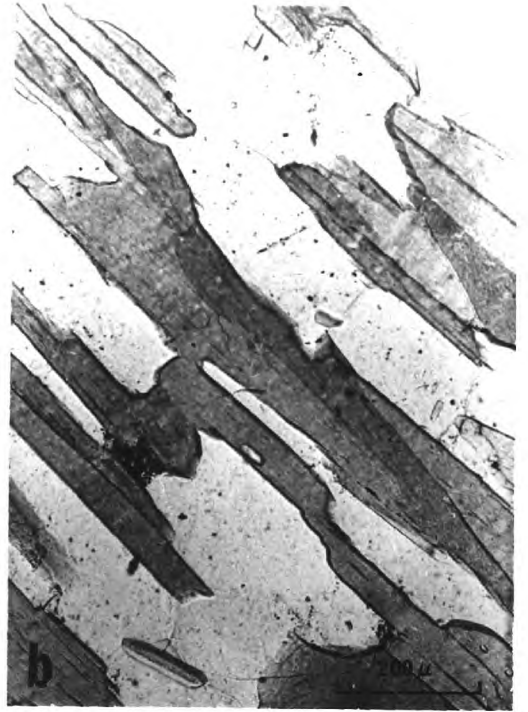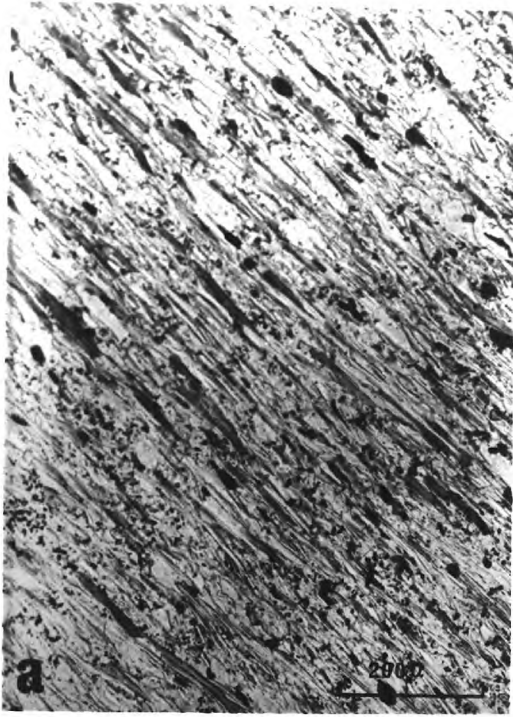
FIG. 3-2

schists but in a number of places a planar banding is developed
parallel or sub-parallel to the schistosity surface (fig. 3-2d).
Banding nearly parallel to the schistosity occurs on the limbs
of many of the tighter folds (see fig. 4-1c) so it seems likely
that this banding is bedding that has been rotated during deform-
ation into an attitude close to that of the axial plane
schistosity. Turner and Weiss (1963, p.92) term such a structure
"transposition foliation" but in the present area it is called
lithological banding and mapped with recognisable bedding as
the same structure.

3. Andalusite-Staurolite Schists

Thin bands containing small to medium size andalusite
and staurolite grains are quite common in parts of the quartz-
mica schists but these bands contrast greatly with the knotty
looking, porphyroblastic andalusite-staurolite schists occupying
the higher ground in the central parts of the area. These
rocks are extremely rich in stumpy andalusite crystals commonly
more than an inch in length (fig. 3-3a), that are set in a
medium grained schistose matrix of quartz, biotite, muscovite,
and garnet with smaller amounts of pale yellow staurolite.
A little fine-grained, disseminated iron sulphide (predominantly
pyrrhotite) is invariably present, the weathering of which
imparts to these schists a hard, red-brown, limonitic skin
that effectively resists erosion.

Dickinson (1942) considered on the basis of the large
size of the andalusite, that the andalusite-staurolite rocks
are simply the more intensely metamorphosed counterparts of
the quartz-mica schists, yet the schistose matrix of the
andalusite rocks is identical in grain-size and texture to
that of the adjacent quartz-mica schists; this would suggest
a more or less parallel metamorphic crystallization history.
On the other hand, a micro-textural study of the different
rocks (ch. 5) shows conclusively that the porphyroblastic
andalusite schists have undergone a more prolonged deformation-
recrystallization history than, for instance, the finer grained
"phyllitic" quartz-mica schists closer to the arenaceous
rocks. But this prolongation would seem better explained as

FIG. 3-3

(a)   Weathered outcrop of typical andalusite-staurolite
      schist. The more resistant andalusite porphroblasts
      stand out in weathering relief from the rather friable
      quartz-garnet-mica schistose matrix. The schistosity
      trace is parallel to the pencil.

(b)   A coarse lithological banding in andalusite-
      staurolite schist composed of alternating
      andalusite-rich and andalusite-poor layers.
      Individual layers can be followed unbroken for
      many tens of feet and they are folded in the
      same style and attitude as undoubted bedding in
      nearby quartz-mica schists. Scale is about 7 inches
      high.

(c)   Andalusite schists of the Kanmantoo Group exposed
      on the coast near Rosetta Head 40 miles southwest
      of the Kanmantoo orebody. The andalusites form zones
      parallel to the bedding but within the zones an
      andalusite banding of tectonic origin is developed
      oblique to the bedding. Length of scale 6 inches
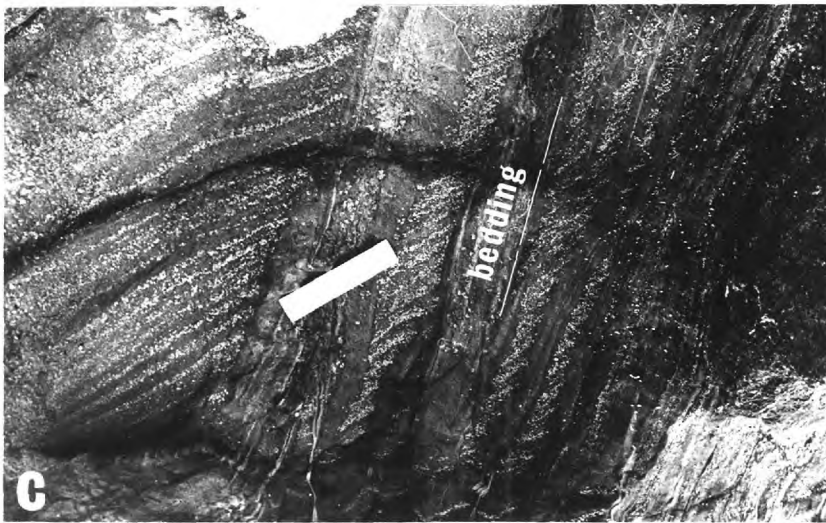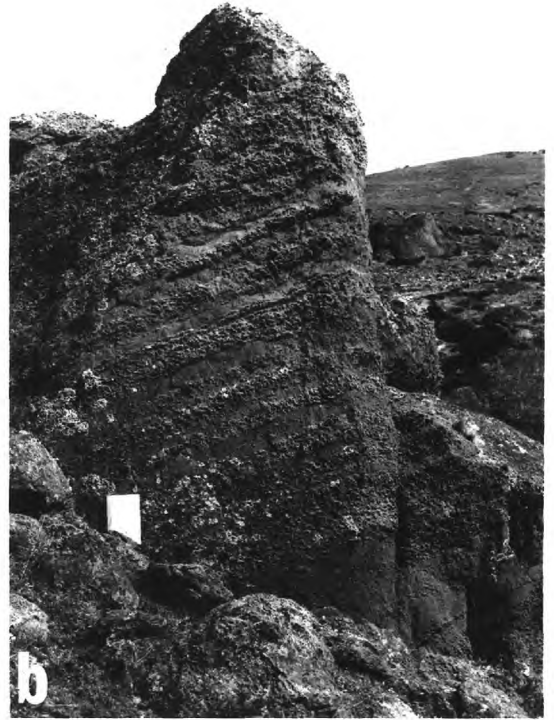
FIG. 3-3

a lithologically controlled response to tectonics rather than
the chance localization of a "metamorphic high" (Dickinson's
suggestion) in otherwise chemically homogeneous rocks.
Chemical analyses of typical samples of quartz-mica and
andalusite-staurolite schists (see table 8-1, chapter 8) show
that there are significant compositional differences between
the two rock-types. This reasoning - that the andalusite-
staurolite schists are a distinct lithological type and there-
fore have stratigraphic significance - is reinforced by the
outcropping of similar rocks for more than 10 miles south and
5 miles north of the Kanmantoo orebody (fig. 2-4). Their
thickness increase in the vicinity of the orebody may be
partly original but largely, it appears to be the result of
tectonic thickening in the hinge regions of folds. In the
limits of the mapped, andalusite zones are never observed to
transgress either small or large lithological contacts, there-
fore this metamorphic unit is concluded to represent a distinct
sedimentary horizon. Kleeman and Skinner (1959) come to
the same conclusion and use the andalusite schist as a strati-
graphic marker horizon in regional mapping.

The andalusite schists contain lithological banding of
two types; (a) the concentration of andalusite porphyroblasts
into rather coarse layers (fig. 3-3b) which are superimposed
on (b) a more delicate matrix layering defined by rapid
alternations in the proportions of quartz and micas (fig. 4-1d).
In similar andalusite schists of the Kanmantoo Group exposed
on the coast near Rosetta Head 40 miles to the southwest
(fig. 2-3), andalusites are developed in zones more or less
parallel to the bedding but within these zones, in thin bands
oblique to both the bedding and the schistosity (fig. 3-3c).
Further examples of this type of andalusite banding from the
same locality are described by Talbot and Hobbs (1966. plate 3)
who conclude that the andalusite bands oblique to the bedding
were produced by some type of metamorphic differentiation
process in situ. They give a similar explanation for a parallel...
"layering made up of an alternations of dark and light bands,
the light bands being narrower than the dark.... in some out-
crops this layering closely resembles bedding..." But at

Rosetta Head neither the andalusite bands nor the parallel
lithological layering (which, as described, is altogether
different from that shown in fig. 4-1d) can be followed continu-
ously for more than a few feet and usually only for a few
inches, whereas in the Kanmantoo area both can be traced
unbroken for tens and sometimes well over a 100 feet. Both
types of banding are always parallel even when folded and no
cross-cutting "bedding" is ever observed. In fact, the banding
is always concordant with major lithological contacts. It
therefore seems extremely likely that both types of banding in
the Kanmantoo orebody area represent original bedding but in
the absence of any confirmatory sedimentary structures they
will continue to be called lithological banding.

4. Lode Schists

The andalusite-staurolite schists enclose and inter-
penetrate a distinctive but at the same time a texturally and
mineralogically very heterogeneous group of rocks that have
been collectively called the lode schists. These rocks occupy
erratic, lens-like positions in the andalusite schists (map. 4)
and for the most part can be described as fine to medium
grained quartz-garnet-biotite ($\pm$chlorite) schists sometimes
containing considerable staurolite but only minor andalusite.
The lode schists are largely concealed beneath the Tertiary
lateritic capping and under the old tailings dumps, and
although a number of lithological sub-divisions could be made
there is little continuity of either exposure or specific
rock-types for more than a few feet along strike. As a result
the schists have been shown (map. 1) as a single metamorphic
unit that most probably represents, within the pelitic rocks,
a relatively iron-enriched, sub-facies of shale. Since the
boundaries between the lode schists and the adjacent andalusite
schists are often very indistinct through intimate interbanding
or severe chloritization, few stratigraphic or structural
inferences can be made from the sketched shape of the litholo-
gical interface (map 4.)

The lode schists contain a complexly folded, lithological
banding defined by rapid alternations of garnet-rich and garnet-

poor layers. The garnet-rich bands are 1-10mm thick and often contain 80 or 90% garnet while the garnet-poor bands are substantially thicker and consist mainly of quartz and biotite (or chlorite). There is no direct evidence that this banding represents original bedding since no sedimentary structures could be found. But neither is there visible any remnant of an earlier, cross-cutting surface. Accordingly this banding has been mapped together with that of the other schists as a lithological banding but where referred to specifically, it will be termed garnet banding.

5. Alteration Zones in the Lode Schists

Within the lode schists and to a small extent in the andalusite-staurolite schists there are narrow, tabular zones from less than an inch up to a few feet in width in which certain metamorphic minerals have grown to a relatively large size. These tabular zones form closely spaced groups and all lie parallel to the schistosity surface (fig. 3-4a). In the drill core individual zones or even groups of zones are difficult to correlate since their mineralogy and thickness persist unchanged for no more than a few inches. Primary silicate assemblages include various proportions of coarse plates of biotite and muscovite, large red dodecahedra of almandine garnet, long prismatic crystals of staurolite and, in some places, fibrous intergrowths of the relatively uncommon iron-rich amphibole, grunerite. Interstitial quartz is minor or lacking but small segregation-like pockets of granular quartz occur at frequent intervals both in these coarse-grained silicate zones and in the adjacent unaltered schists.

That these zones of exaggerated mineral growth have not formed simply by isochemical recrystallization is shown by a comparison of their mineral proportions with those of the adjacent lode schists. For instance a medium-grained quartz-biotite-garnet schist may be suddenly transgressed by a zone containing only coarse grained biotite (or chlorite after biotite) and garnet, and evidence that the contact is not a faulted one is shown in fig. 3-4a where gently folded garnet banding can be traced across the zones with little deviation. A small-scale example of the obliteration of lithological banding by these

FIG. 3-4

(a)   An alteration zone (B) formed along the schistosity
      directions of quartz-biotite-garnet lode schists
      (A and C). The coarse-grained garnet-biotite and
      chlorite after biotite assemblage in the alteration
      zone contrasts with the medium-grained, light coloured
      siliceous lode schists. Small islands of unaltered
      lode schist containing bedding are visible within
      the alteration zone (arrow). There is no evidence
      of any significant shearing or faulting along the
      alteration zones since bedding can be traced across
      them with little deviation or disturbance.
      Diameter of coin approximately 1 inch.

(b)   Bands of pale green calc-silicate schist within
      quartz-mica schist. The lithological contacts
      are parallel to the bedding in the quartz-mica
      schists. Diagonal and circular lines around the
      core were formed during drilling. Diameter of
      core 2.5 inches.
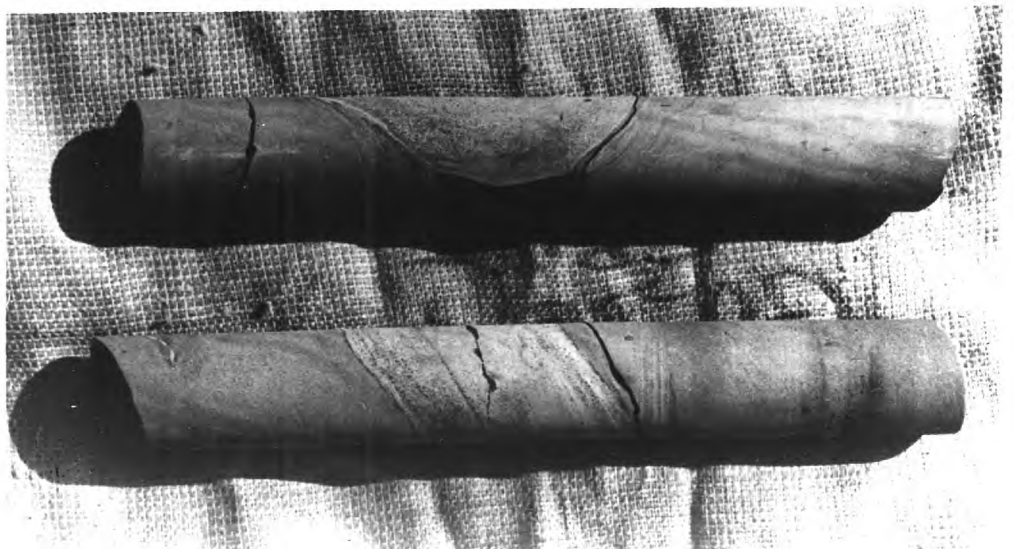
FIG. 3-4

alteration zones is illustrated in fig. 5-7b where folded garnet
bands are clearly truncated by coarse intergrowths of garnet and
biotite. The former schistosity surface is sometimes enhanced
by the mimetic growth of these new coarse-grained micas but
in many places the more or less random growth of new biotite
and muscovite completely destroys the tectonic foliation. The
alteration zone shown in fig. 3-4a is typical of most, inas-
much as it shows positive evidence against any large-scale
faulting or shearing. A close examination of the micaceous
minerals in many zones does however reveal considerable micro-
folding and kinking.

6. The Occurrence of Chlorite

Scattered flakes of chlorite are observed growing across
the schistosity in rocks throughout the area but nowhere is it
as well developed as in some of the alteration zones. Petro-
graphic work (chapter 5) shows chlorite to be a late mineral
that has formed mainly as a breakdown product of earlier
silicates. Biotite has been the most susceptible to altera-
tion whilst staurolite, garnet, andalusite and muscovite have
been variously affected. Since the alteration zones are
composed largely of biotite and garnet and since garnet is the
more resistant to chloritization, considerable volumes of the
alteration zones are essentially chlorite-garnet schists.
In places chloritization has extended out from the alteration
zones into the adjacent schists where it occurs as a new
phase along quartz-quartz interfaces and as a breakdown
product of biotite. Thus some of the lode schists have been
transformed into quartz-chlorite-garnet schists.

In some alteration zones even the garnet has disappeared
and there now exists practically mono-mineralic intergrowths
of coarse-grained, dark green chlorite.

B. MINOR ROCK TYPES

1. Rocks Resulting from Sedimentary Variations

(a) Calc-Silicate Schist

Not exposed at the surface but found as a group of thin
layers in quartz-mica schists in hole no. 39 drilled southeast

of the area in map 4 on section 900 N, is a fine-to medium-
grained quartz-plagioclase-actinolite schist containing minor
disseminated sphene, ilmenite and pyrrhotite. The contacts of
these layers are all parallel to the adjacent lithological
banding (fig. 3-4b). Because of their distinctive pale green
colour such schist layers would make excellent marker bands if
they are exposed in any future mining operations. Judging
from their chemical composition (table 8-1, ch.8) the calc-silicate
schist was probably originally either a muddy dolomitic lime-
stone or, as a remote possibility, andesitic tuff.

(b) Pyritic (pyrrhotitic) Schists

Fine-grained disseminated pyrrhotite and locally pyrite
after pyrrhotite are found through much of the andalusite-
staurolite and unaltered lode schists; these rocks contain
on average about 0.5% sulphur. Disseminated sulphides are
very sparse through the quartz-feldspar and quartz-mica schists
although there are a few bands from one or two inches up to
three or four feet thick and conformable with the bedding that
are visibly enriched in disseminated iron sulphides. Weathering
of the sulphides may produce a pale coloured schist rich in
sericite after biotite which is useful as a local marker for
mapping.

2. Rocks Formed During Metamorphism or Later Events

(a) Mineral Veins

Pegmatitic mineral veins consisting mainly of quartz
but with erratic amounts of muscovite, biotite, aluminium
silicates, apatite and chlorite occur in many shapes, sizes
and structural settings in all rock-types. Only those thicker
than about six inches (a small minority) have been plotted on
map 1. Feldspar veins consisting either of albite or adularia
are located along joint planes and other late fractures. All
these veins constitute an important part of the geological
history and are described in some detail in chapter 7.

(b) Breccia Zones

The sub-vertical breccia zones cutting across the strike
of the rocks (map 1) are up to three feet wide and at least

half a mile long. They appear as linear outcrops of bleached schist breccia in which the fragments are cemented with quartz, or as zones of intense fracturing in which the bleached schist breaks into neat trapezoidal shaped blocks about the size of a hand.

The extent of brecciation gives no indication of the amount or sense of movement along a fault, and the monotonous interbanding of the schist on either side prevents any offset from being observed. The lateral movement must have been rather small since even at major lithological boundaries no measurable offset can be seen. No mineralization apart from quartz has been found associated with breccia exposed on the surface.

C. DESCRIPTION OF THE MINERALIZATION

1. General Statement

The quartz-biotite-garnet lode schists and the included alteration zones are hosts for most of the significant sulphide-oxide mineralization but sparse sulphide mineralization is widespread through much of the adjacent andalusite-staurolite schist. This section deals with the mineralogical composition of the orebody and describes the textural ore-types and their distribution. But first a problem of terminology must be discussed.

2. The Terms - Primary and Secondary

Most orebodies contain ore minerals that have formed at different times (a) when the enclosing rocks were buried well below the surface and (b) when the enclosing rocks were brought near the surface by erosion and subjected to the processes of weathering. Lindgren (1933) terms the earlier minerals hypogene because in most cases they were thought to have been deposited from ascending solutions, and the later minerals supergene because they were formed from descending solutions. Bateman (1950) dislikes the restriction implied by the use of hypogene and prefers the word primary which he defines as ...."those (minerals) forming during the original period or periods of metallization". He uses secondary in place of supergene. Such

terminologies are usually suited to vein-type hydrothermal
mineralization where a clear separation can be made between
the original period of mineralization and later weathering
effects. In a deposit involved in a long history of metamorphism,
metasomatism and deformation this distinction is far from clear.
Accordingly, definitions for a number of terms as used through
this thesis are given below.

Primary refers to all those ore minerals (ore) that are
considered to have been subject to or to have formed at the
elevated temperatures and pressures of metamorphism. The
metamorphic event is considered to have ended with the
cessation of the formation of chlorite. Secondary changes
(see ch.5) are regarded as beginning with the chemical altera-
tion of pyrrhotite to FeS_2 minerals. Ore will be used in its
loose sense as meaning a rock containing ore minerals but when
referring to economic mineralization, ore (senso stricto) will
be used if the in-context meaning is not clear.

3. Mineralogical Composition of the Orebody

The Kanmantoo orebody consists of around 20 million
tons of low-grade material assaying just under 1% copper;
no other metals appear to be present in sufficient quantity
to be economically extractable. The major primary ore mineralogy
is relatively simple - about equal amounts of pyrrhotite,
chalcopyrite and magnetite. These phases are accompanied by
minor sphalerite, ilmenite and primary pyrite and small amounts
of other sulphides and oxides (table 3-1). A list has not
been made of the gangue silicate minerals since none are
peculiar to the mineralized zones.

In the much weaker disseminated mineralization through
the aluminous schists and in odd bands in the quartz-mica schists
pyrrhotite is the dominant ore mineral, chalcopyrite, sphalerite
and ilmenite are present in small amounts while magnetite is
absent. Minor pyrite after pyrrhotite occurs near the surface.

Apart from considerable pyrite and marcasite after
pyrrhotite in the orebody, secondary ore minerals are rather
sparse. Small amounts of copper carbonates occur at or near

TABLE 3-1   Mineralogical Composition of the Kanmantoo Orebody

PRIMARY MINERALS

Major

pyrrhotite	$Fe_{1-x}S$
chalcopyrite	$CuFeS_2$
magnetite	Fe_3O_4

Minor

ilmenite	$FeTiO_3$
sphalerite	$Zn(Fe)S$
galena	PbS
mackinawite	$Fe(Co,Ni)S$
hercynite	$FeAl_2O_4$
bismuth	Bi

Trace

pyrite	FeS_2
cubanite	$CuFe_2S_3$
pentlandite	$(Fe,Ni)_9S_8$
Co-pentlandite	$[Co(Fe,Ni)]_9S_8$
molybdenite	MoS_2
wolframite	$(Fe,Mn)WO_4$
corundum	Al_2O_3
gold	Au

SECONDARY MINERALS

Major

pyrite	FeS_2
marcasite	FeS_2
siderite	$FeCO_3$
goethite	$Fe_2O_3 \cdot H_2O$
hematite	Fe_2O_3

Minor

malachite	$Cu_2(CO_3)(OH)_2$
azurite	$Cu_3(CO_3)_2(OH)_2$
chalcocite	Cu_2S
covellite	CuS
bornite	Cu_5FeS_4
magnetite	Fe_3O_4
rutile	TiO_2
parkerite	$Ni_3Bi_2S_2$
wittichenite	Cu_3BiS_3
sphene	$CaTiSiO_5$

the surface and traces of bornite, covellite and bornite are
found in the upper levels.
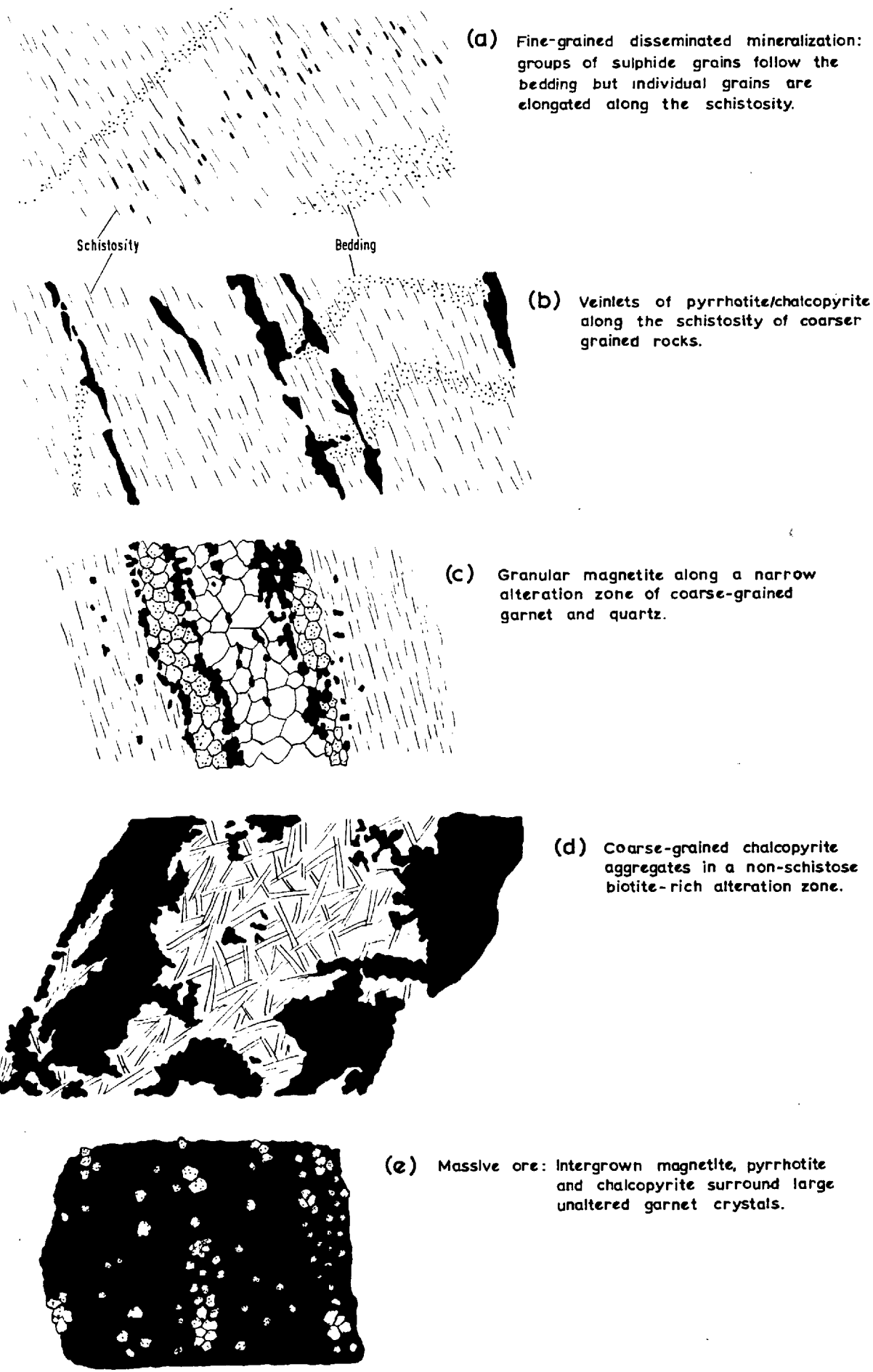
4. Primary Ore-Types and their Distribution

Within the orebody there is a continuous gradation in
ore-types from fine-grained disseminated sulphides to coarse-
grained, practically solid pyrrhotite-chalcopyrite-magnetite
ore. Transition from one ore-type to another at any one place
may be smooth or abrupt. In general there is a fairly close
correlation between the ore-type and the texture of the enclos-
ing rocks; for instance fine-grained sulphide disseminations
are restricted to fine to medium grained schists that have
undergone no visible alteration, coarser streaks and veinlets
of chalcopyrite and pyrrhotite occur in the coarser-grained
schists adjacent to alteration zones or in the schistose parts
of alteration zones themselves while irregular pockets of
sulphides are found either in non-schistose parts of the
alteration zones or in coarse-grained granular quartz veins or
quartz segregations. Descriptions of the different ore-types
are given below and some representative sketches are shown in
fig. 3-5.

(a) Fine-grained Disseminated Mineralization

The most extensive but economically the least important
of the ore-types are the small multi-phase grains of major
pyrrhotite and minor chalcopyrite and sphalerite disseminated
through much of the andalusite-staurolite schists and unaltered
lode schists. Individual sulphide grains are generally well
under a millimetre in length and are always flattened parallel
to the schistosity; groups of grains often form small zones
that follow the lithological banding for a short distance
(fig. 3-5a).

(b) Streaks and Veinlets of Sulphides

The most important type of mineralization in the orebody
consists of streaks and veinlets of pyrrhotite/chalcopyrite
oriented along the schistosity surfaces. These, where suffici-
ently concentrated, constitute ore. In the dimensional
limitations of the drill core no coincidence has been observed
between the distribution of this type of mineralization and

(a) Fine-grained disseminated mineralization: groups of sulphide grains follow the bedding but individual grains are elongated along the schistosity.

Schistosity   Bedding

(b) Veinlets of pyrrhotite/chalcopyrite along the schistosity of coarser grained rocks.

(c) Granular magnetite along a narrow alteration zone of coarse-grained garnet and quartz.

(d) Coarse-grained chalcopyrite aggregates in a non-schistose biotite-rich alteration zone.

(e) Massive ore: Intergrown magnetite, pyrrhotite and chalcopyrite surround large unaltered garnet crystals.

FIG. 3-5   Types of primary ore.

All natural scale.

lithological banding (fig. 3-5b) except where the latter
parallels the schistosity. Individual streaks vary from
1-5 mm in length and veinlets only exceptionally exceed 10 mm
in thickness.

(c) The Mode of Occurrence of Magnetite

Very fine-grained ilmenite is usually the only member of
the Fe-Ti oxide family in the unaltered schists but in and
adjacent to the alteration zones, ilmenite is subordinate to
magnetite. The crystal and aggregate habits of magnetite are
many and varied. Isolated octahedra occur in biotite-rich
schists alongside sulphide concentrations or in the sulphide
concentrations the selves but most of the magnetite exists as
granular to bladed aggregates intergrown with coarse-grained
biotite (or chlorite after biotite), garnet, sulphides and
more rarely quartz, along alteration zones of all sizes (fig.
3-5c).

(d) Coarser Grained Ore

Coarse-grained sulphides, oxides, or sulphides and
oxides may occur as small pockets or bands a few inches across
or as thick concentrations in groups of merging alteration
zones up to 10 or 12 feet across measured normal to the
schistosity planes. In some places ragged aggregates of
chalcopyrite or pyrrhotite are intergrown with non-schistose
alteration zone micas (fig. 3-5d) but the more common ore-type
consists of massive to crudely banded chalcopyrite, pyrrhotite
and magnetite enclosing large numbers of garnet euhedra and
laths of biotite and / or chlorite. There is commonly a
rough segregation of the sulphides into bands parallel to a
foliation defined by both the garnet concentrations and the
alignment of the micaceous minerals (fig. 3-5e). In some
places the sulphide banding visibly swings around magnetite
masses that may have the appearance of being part of a once
continuous oxide band that has been pulled apart (fig. 5-11f).
The location of this coarse-grained sulphide-oxide ore corres-
ponds in practically all cases with the location of late-
metamorphic alteration zones of the type described above.
Alteration zones exist however without accompanying ore mineral
concentrations.

A little coarse-grained pyrrhotite, chalcopyrite and rare magnetite occur through the many small segregation-like granular quartz bands and pockets that have formed in the mineralized rocks (fig. 3-5c). Larger quartz veins are not common in the ore zones but where present they always contain a little pyrrhotite or chalcopyrite but no magnetite interstitial to the silicate grains (fig. 7-3b).

5. Zoning of the Primary Ore

Smooth gradations in the character of the primary mineralization across, along or down through the orebody are practically non-existent. There are however two recognisable types of zoning that are on vastly different scales; one, a district zoning, includes the orebody as a unit and the other which could be termed a domainal zoning, involves small domains within the orebody.

If the area is viewed as a whole, there is more or less a symmetrical disposition of lithologies around the orebody in an east-west vertical section (see maps 3,4). Progressing towards the orebody from the margins of the area, we pass in turn from largely sulphide-free quartz-feldspar and quartz-mica schists into andalusite-staurolite schists that contain weakly disseminated sulphide mineralization. Within these aluminous rocks occur the lenses of quartz-biotite-garnet lode schist that in turn enclose the multitudes of alteration zones with which are associated the important sulphide and sulphide-oxide mineralization.

The small-scale domainal zoning is seen across some of the alteration zones containing coarse-grained sulphide-oxide ore concentrations. For a few inches to a few feet in the unaltered schists on either side of such a zone there may be streaks and veinlets of pyrrhotite/chalcopyrite that rapidly or gradually give way to fine disseminated sulphides further outwards. It is to be emphasised that this type of zoning is rare and it is far more common to find mixtures or erratic developments of streaks, fine-grained disseminations and veinlets of sulphides in between the mineralized alteration zones.

D. WEATHERING CHARACTERISTICS OF THE ROCKS AND ORE

1. General Rock Weathering

Erosion of the quartz-feldspar and particularly the quartz-mica schists is predominantly by mechanical disintegration and removal of the mineral grains by wind and water run-off. Detritus collects in valleys where prolonged weathering and oxidation cause the iron-bearing silicates to break down and form a strongly cohesive red, lateritic clay. This binds and cements the other particles together to produce a material resistant to further erosion except directly by streams (see fig. 2-1b).

The andalusite-staurolite schists erode in a similar manner only in wind-swept locations; for the most part the minor but persistent amounts of fine-grained pyrrhotite they contain breaks down to form a highly resistent skin of limonitic cement. It is most likely that a prolonged process of this type produced the thick lateritic Tertiary peneplain parts of which are still preserved on the Mine Hill (map 1).

The familiar mechanical and chemical stability of quartz in the surface environment is shown by the protrusion of the thicker quartz veins for five to six feet above the general surface level (see fig. 7-1a) and a similar durability is shown by andalusite in areas where the laterite has been stripped off or prevented from forming by rapid erosion. Because of their large size and the sorting action of wind and flowing water, the andalusite crystals have remained behind as eluvial gravel over some areas of the andalusite-staurolite schists. Some thought was given to the economic potential of this material by Mines Exploration Pty Ltd., but the amount was found to be too small.

2. Weathering in Mineralized Areas

(a) Secondary Ore-Mineral Profile Through the Orebody

Information on the occurrence of oxidized and secondary sulphide minerals in the upper parts of the orebody is rather meagre since most of the diamond drill holes are inclined at low angles to the horizontal (see maps 3,4) and secondary ore

in the old workings was completely extracted by the earlier
miners. A proper study of this aspect of the mineralization
will have to await the eventual opening up of the new deposit.
Considerable vertical percussive drilling has been carried out
over the orebody but the rock cuttings were not available for
study.

There is no surface expression of the mineralization
over the newly discovered orebody but in the old workings along
the eastern and western flanks of the Mine Hill (map 1) odd
small exposures of in situ goethite/hematite boxworks can be
seen to contain small specks of chalcopyrite and films of
copper carbonates. Goethite is an oxidation product of the
sulphides whereas most of the hematite has apparently formed
from the magnetite since such material is still reasonably
magnetic.

The depth of oxidation of the wall rocks on the Mine
Hill extends down to about 100 feet where the water table is
met but in the valleys on either side of the Mine Hill, the
water table is intersected at about 20 feet consequently the
zone of oxidation in these areas is rather thin. Small amounts
of chalcocite and covellite occur with copper carbonates through
the oxidized zone but below the water table carbonates disappear
and traces of bornite are seen. The development of these
secondary copper sulphides is very patchy and judging from the
assay results of the percussive drilling, the degree of super-
gene copper enrichment is small. Chalcocite, covellite and
bornite have been found near small fractures down to a depth
of 600 feet.

A large proportion of the pyrrhotite in the orebody has
broken down to concentric intergrowths of secondary pyrite and
marcasite. The distribution of these minerals bears no relation-
ship to topography or depth; they are found evenly developed
through all levels of the orebody but locally are concentrated
in the vicinity of late fractures and joint planes.

(b) Changes in the Wall Rocks
     In the oxidation zone the iron-bearing silicates show

slight alteration to goethite along grain boundaries and in partings and cleavage planes but andalusite, muscovite and quartz appear to be unchanged. In areas of former sulphide mineralization the oxidation of the silicates is in most cases only slightly more advanced. Feldspar veins outcropping in mineralized areas have undergone intensive alteration to a creamy material that varies from a friable powder containing feldspar ghosts to a hard, brittle substance possessing a conchoidal fracture. X-ray diffraction traces show both types of material to be a mixture of quartz, albite and probably kaolinitic clay minerals.

A small area of intense rock alteration is found in some pyrrhotitic schists in the southeastern corner of the region outlined in map 4. Typical of the surface rocks is an extremely white highly fissile quartz-sericite schist containing limonite-stained elongated cavities indicating the position of former sulphide grains. With depth the colour of the schist becomes darker as the sericite content (and the degree of biotite alteration) decreases until at about 300 feet below the surface the original micaceous schist containing about 5% disseminated pyrrhotite appears.

Chapter 4.

STRUCTURE OF THE SCHISTS AND ORE

Introduction

In the course of regional mapping Dickinson (1942),
Grasso and McManus (1954) and Kleeman and Skinner (1959)
have shown the area surrounding the Kanmantoo orebody to
occupy part of the western limb of a regional, southward
plunging syncline (fig. 2-4). No detailed structural investi-
gations of the rocks around the old Kanmantoo mines have been
published.

A study of the schists in the field has disclosed the
presence of a series of major folds, all slightly overturned
to the west, that have an approximately meridional trend and
a general southward plunge of between 10° and 60° (see map. 2).
Typically, the folds in the pelitic rocks are tightly appressed
and consequently difficult to map since the limbs usually
diverge rather gently from the axial plane schistosity.
Folding in the arenaceous rocks is more variable and commonly
quite open, particularly in areas where they become the
dominant lithology. Although the orebody and associated lode-
schists are located within a complex synclinal fold system in
the andalusite-staurolite schists (map. 3), both the position
and extent of the economic mineralization and the lode schists
vary along the strike (map. 4).

The aims of this chapter are to describe, from observa-
tions and measurements made in the field and laboratory, the
geometry of the folding and the geometrical relationships
among the different structures, and to ascertain the sequence
of deformational events. The location and development of the
several types of mineralization will be integrated, as far as
possible, into the resulting tectonic history. In this
manner it is hoped to be able to erect a broad structural
framework on which to hang the many textural details viewed
under the microscope. Some attention will be given to the
mechanism of rock deformation but a detailed investigation of

this subject is beyond the scope of this thesis.

Structure will be discussed on two scales after Weiss (1959):

(1) In terms of hand specimens, single exposures, or a series of closely related exposures (mesoscopic scale).

(2) In terms of the orientation of these mesoscopic structures in fields or domains of any size that contain discontinuously observable features (macroscopic scale).

A. MESOSCOPIC STRUCTURE

A summary of the definitions and relationships of the mesoscopic structures in the schists around the Kanmantoo orebody is given in table 4-1.

1. Initial Structures

A lithological banding (S_O) defined by alternations of metamorphic mineral proportions is found in all rock-types and has been fully discussed in the previous chapter. Because of its association with sedimentary structures in the arenaceous rocks, this banding is undoubtedly bedding but there is no direct evidence that this origin holds for banding in the pelitic schists. However from such evidence as similarities in attitude and fold directions, the absence of recognisable earlier surfaces, and the marked continuity of individual bands it seems likely that this banding also represents original bedding. Tectonic transposition of the banding completely into the plane of the schistosity is not common. All these banding types are folded around similarly oriented fold axial surfaces therefore it seems reasonable to map the former as the same structure.

Other sedimentary structures such as ripple marks and cross-bedding are locally useful for studying the effects of deformation but their rarity makes them of little use for structural analysis.

TABLE 4-1. Definitions and Relationships of the Mesoscopic Structures.

	SURFACE	LINEATION	FOLD
Initial Structures	Lithological banding S_0 (bedding) produced by different proportions of metamorphic minerals.		
Group-1 Structures	Axial plane schistosity S_1 formed by the preferred orientation of platy minerals.	Lineations in S_1 formed by dimensional orientation of platy minerals, micro-crenulations and stretched inclusions.	Small folds in S_0 about S_1 as the axial plane.
Group-2 Structures	Mineral banding in the alteration zones, themselves formed parallel to S_1. Redefinition of S_1 by mimetic growth of new platy minerals.	Possible local slickensiding on S_1 or redefined S_1	Possible modification of group-1 fold profiles. Local bending of S_1.
Group-3 Structures	Axial surfaces of local crenulation and kinking of S_1 Shear bands along S_1.	Crenulation axes parallel to group-1 lineations	Microfolding and kinking of S_1.
Group-4 Structures	Small fractures and joints. Cross-cutting breccia zones.		

2. Group-1 Structures

(a) Schistosity (S_1)

A single schistosity surface defined by the parallelism
of mica (001) crystal faces is present in all rock-types.
The mica-rich schists are extremely fissile along the same
surface but the mica-poor quartz-feldspar schists tend to
fracture along directions parallel to S_0. The schistosity
surface is always sub-parallel to the axial plane of the
group-1 mesoscopic folds in S_0 (hence the prefix in map 1).

(b) Lineations in S_1

The schistosity surface contains a number of lineations
but by far the most widespread is a very fine mineral lineation
produced by the preferred orientation of the long dimensions
of the mica crystals. This is seen on the S_1 surface as a
striation or a microcrenulation (fig. 4-1a). A parallel
though somewhat coarser lineation is the alignment of the
long dimensions on the undulations in S_1 produced by its
swinging around andalusite porphyroblasts (fig. 4-1b). A
rare lineation found in a single exposure of andalusite-
staurolite schist south of the Mine Hill is the parallelism
of the long axes of rather large inclusions (fig. 4-1c). The
origin of these inclusions is uncertain but they are probably
deformed pebbles or siliceous concretions of some kind. Their
tectonic significance is discussed in section E of this chapter.

(c) Folds in S_0

Mesoscopic folds in the lithological banding are not
uncommon although not a great many measureable exposures could
be found. The folds are extremely variable in amplitude,
wavelength and profile even in the same rock-type but all have
in common a relatively uncomplicated style, the same axial
plane orientation (S_1) and a tendency to plunge to the south.
Even so, in a single outcrop the plunge of adjacent folds can
vary by as much as 40°.

The larger mesoscopic folds in the quartz-feldspar
schists usually exhibit a concentric type of profile and so

<u>FIG. 4-1</u>

<u>Group-1 Mesoscopic Structures</u>

(a) Coarse mineral lineations on an axial plane
     schistosity surface.

(b) A lineation formed by the alignment of long
     dimensions of schistosity undulations around
     andalusite porphyroblasts (arrow).

(c) Similar folding in banded andalusite-staurolite
     schist. Note the well developed axial plane
     schistosity and a small fault sub-parallel to it.
     Five elongated inclusions are just visible in the
     upper part of the picture, one of which is arrowed.

(d) More open folding in coarser grained andalusite-
     staurolite schist. The andalusite porphyroblasts
     are concentrated in zones parallel to the more
     obvious matrix banding (S_0) which is produced by
     rapidly changing proportions of quartz, biotite,
     muscovite and garnet. This banding is deduced to
     represent compositional variations in the original
     argillaceous sediments.
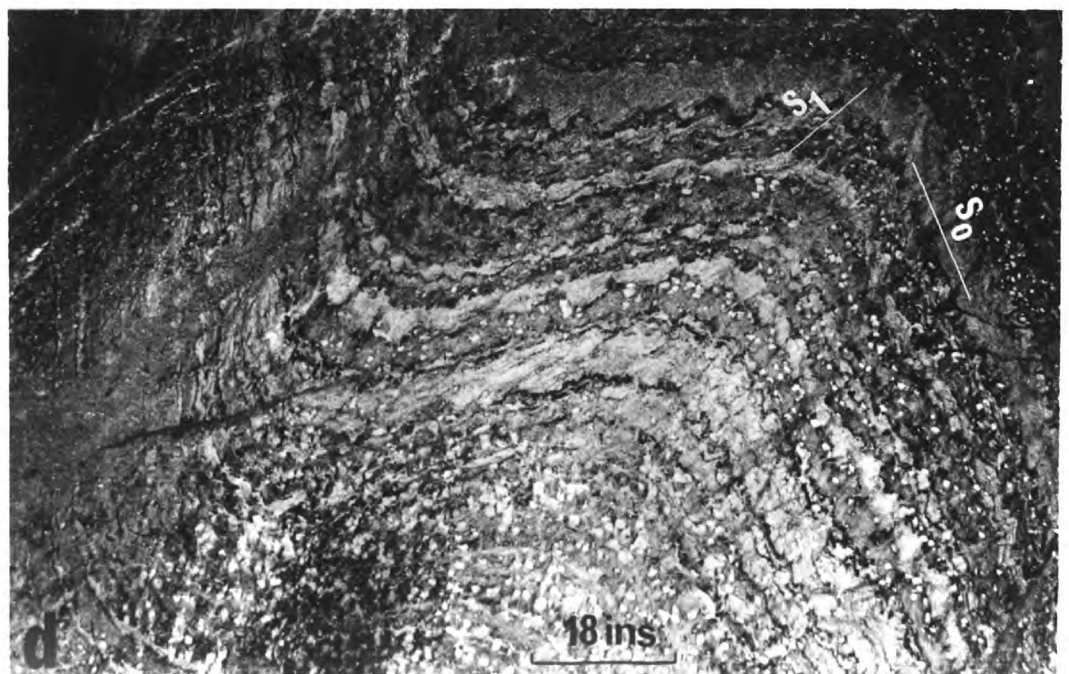
FIG. 4-1

too do any smaller folds occurring on the limbs of the larger
structures(fig. 4-2a). Folds in the more micaceous rocks
generally have a _similar_ shape although individual fold
profiles can vary from more or less symmetrical (figs. 4-2b,c)
to highly asymmetrical (fig. 4-2d). The complexity of this
small-scale folding prevents any stratigraphic sense being
made from large sections of the drill co#re (see fig. 3-2c).

Good exposures of mesoscopic folds are found in andalusite-
staurolite schists in road cuttings south of the Mine area.
Fig. 4-1c is a photograph taken looking down the fold axis.
Although such folds clearly have a similar type of profile,
a detailed examination of their morphology shows that few are
truly similar. This is shown by the isogonic relationships
on a tracing of the photograph in fig. 4-2e. Dip isogons are
lines joining top and bottom surfaces of a folded bed at points
where the respective tangents are equally inclined to the axial
plane (Ramsay, 1967). In ideal concentric or parallel folds
the dip isogons are oriented normal to the tangents whereas
in ideal similar folds having a constant limb thickness
measured parallel to the axial plane, the dip isogons are
parallel to one another and to the axial plane. A shortened
form of the classification scheme of Ramsay (1967) is shown in
table 4-2.

TABLE 4-2.	Geometrical classification of folds.
class	characteristics
1	Folds with dip isogons converging towards the inner arc.
1a	Strongly convergent isogons
1b	Concentric folds
1c	Weakly convergent isogons
2	Folds with parallel isogons
3	Folds with isogons diverging towards the inner arc.

<u>FIG. 4-2</u>

<u>Group-1 Mesoscopic Folds</u>

(a)   Concentric style folds on the limb of a larger
      fold in quartz-feldspar schist.

(b,c) Sub-symmetrical similar-type folds in quartz-mica
      and andalusite-staurolite schist.

(d)   Asymmetrical similar folding in quartz-mica schist.

(e)   Isogons drawn on a tracing of the folding illustrated
      in fig. 4-1c. For explanation see text.

(f)   Different geometrical orders of folding visible in
      andalusite staurolite schist. The identity of the
      axial plane attitudes and axial directions of the
      different folds suggests that they are all of the
      same age.

(a)   1.0 ft

(c)   3.5 ft

(b)   1.5 ins

(d)   1.5 ins

B   Isogons

C

E

D

F

A   (e)

1.0 ft

1st order
2nd order
3rd order   S₁

S₀

1.5 ft   (f)
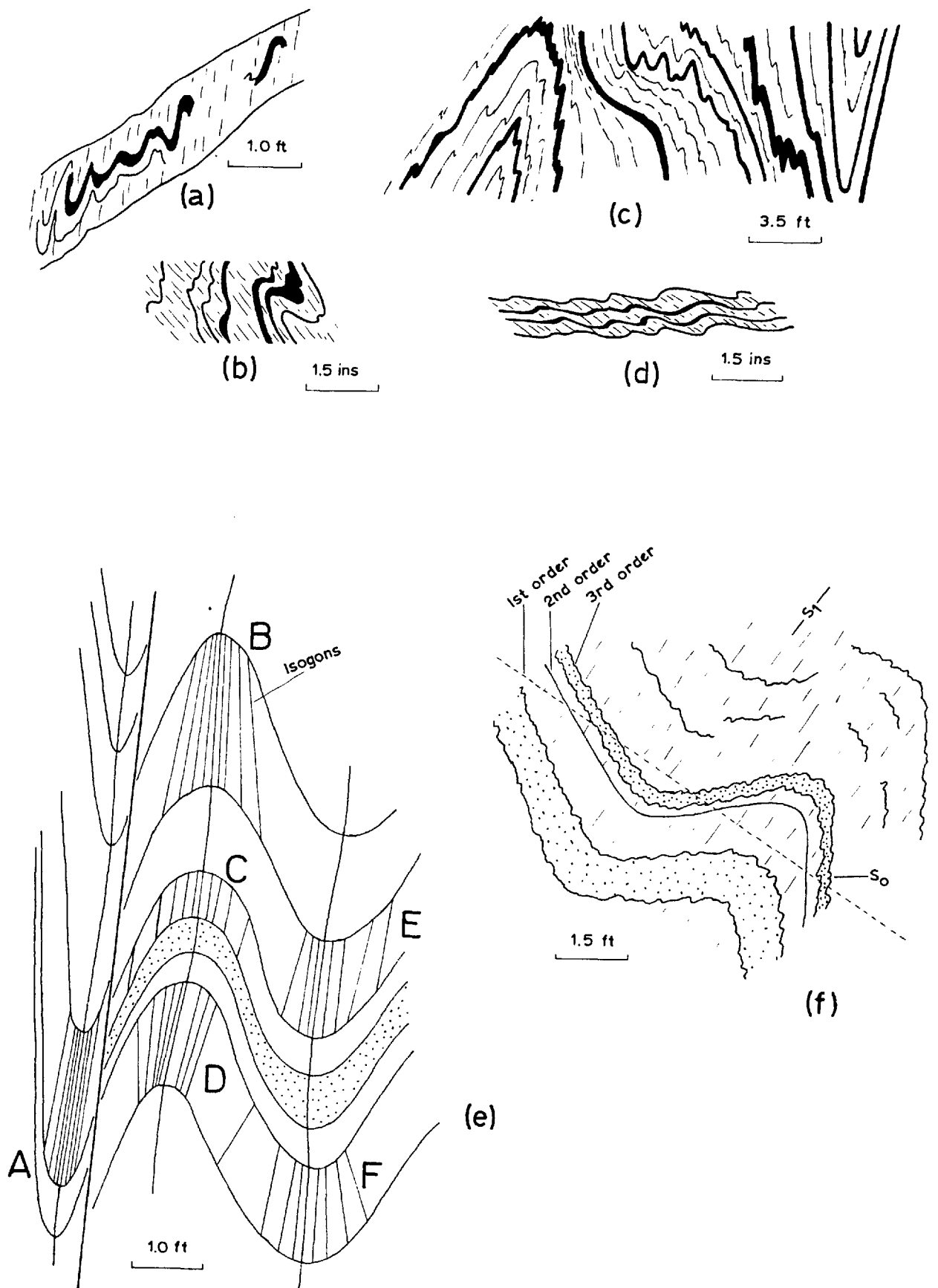
FIG. 4-2

In fig. 4-2e folds D and F are class 1c, folds A, C and E are
close to class 2 and fold B is class 3. Of particular interest
is the change in fold class in the sequence B-C-D along the
same axial surface since this change complies with the predic-
tion of Ramsay (op cit, p.371) that;

> "An important property of certain types of folds is
> that they are unable to affect an unlimited number
> of layers of material without alteration in shape....
> where dip isogons either diverge or converge towards
> the inner fold arc they cannot continue to do this
> indefinitely.... folds in these categories must
> either change their type from layer to layer or
> develop some structural discontinuity in the material."

A further example of "similar" folding in andalusite-
staurolite schists is shown in fig. 4-1d but here the real
change in fold shape is difficult to assess since the photo-
graph is taken looking upwards obliquely onto the irregular
wall of a mine opening. This figure and a tracing of the
folding in it (fig. 4-2f) illustrate well the different orders
of fold size to be found in the Kanmantoo area. Hobbs (1965)
has pointed out the danger of trying to make a macroscopic
structural interpretation from a number of random bedding
facings measured on small outcrops since the bedding in the
small structures need not reflect the gross attitude of bedding
on the larger scale. In view of the monotonous nature of some
of the banded schists and the lack of marker beds in the
Kanmantoo area, the author was fortunate in having mappable
first order folds in the arenaceous rocks, long continuous
exposures of micaceous schists in road and railway cuttings
and in some of the old workings, and a large number of major
lithological intersections in the diamond drill core.

3. Group-2 Structures

The most prominent of the group-2 structures are the
alteration zones described in chapter 3. The exaggerated growth
and segregation of minerals into zones parallel to the group-1
schistosity surface have produced a mineralogical banding of
metamorphic-tectonic origin. In some areas the original
schistosity surface is preserved and even enhanced by the
mimetic growth of the new coarse-grained micas and chlorite

along it whereas in other areas S_1 has been obliterated by the growth of new minerals across it. The group-1 mineral lineations are often preserved as slickenside-like striations particularly in areas where the schistosity itself has been buckled (fig. 4-3c).

Near the group-2 alteration zones the group-1 mesoscopic folds in S_0 are marked by erratic changes and even reversals of plunge and by an increase in morphological complexity. Fig. 4-3 shows some typical fold profiles in garnet banding in lode schists near alteration zones. The disharmonic folding is very similar to the two-dimensional interference patterns of superposed folding produced experimentally by Ramsay (1962, fig. 14E) and Cary (1962, fig. 10). No new axial surface structure corresponding to this possible super- posed folding has been observed but it seems probable that this fold modification is a result of movements that are somehow associated with the formation of the alteration zones.

4. Group-3 Structures

No direct evidence is available on the relative ages of the three structures in this group. However they all appear to have been formed well after the metamorphic climax since the minerals at the discontinuities are all strained and show no signs of recrystallization.

(a) Crenulations in S_1

Crenulations of the schistosity or slaty cleavage are common elsewhere in the Kanmantoo Group (Mills, 1964) but in the Kanmantoo mines area they occur in only two isolated quartz- mica schist outcrops. The crenulations may be in the form of minute concentric folds (fig. 4-4a) or else chevron-type folds (fig. 4-4b). In both types the axial surface strikes east-west and dips steeply southwards and the lineation produced by the crenulation axes has the same attitude as the group-1 mineral lineations. No cleavage structure parallel to the axial planes of the crenulations is developed.

FIG. 4-3

Group-2 Folds in Lode Schists Near Alteration Zones

(a,b) Disharmonic folding in garnet banding (stippled)
around an axial plane schistosity parallel to S_1.
These complex profiles appear to have been formed
by modification of simple group-1 mesoscopic folds.

(c) A further example of disharmonic folding in lode
schists. Note the slightly bent axial plane
schistosity.

FIG. 4-4

Group-3 Mesoscopic Structures

(a) Crenulations in schistosity S_1.

(b) Chevron folding in S_1. An undulating axial surface
is produced by some folds dying out and new folds
developing.

(c) Shallow dipping kink banding of the axial plane
schistosity S_1.

(d) Internal shear banding along the S_1 surfaces.
Bedding (S_0) is visibly offset across the shear bands.

all natural scale
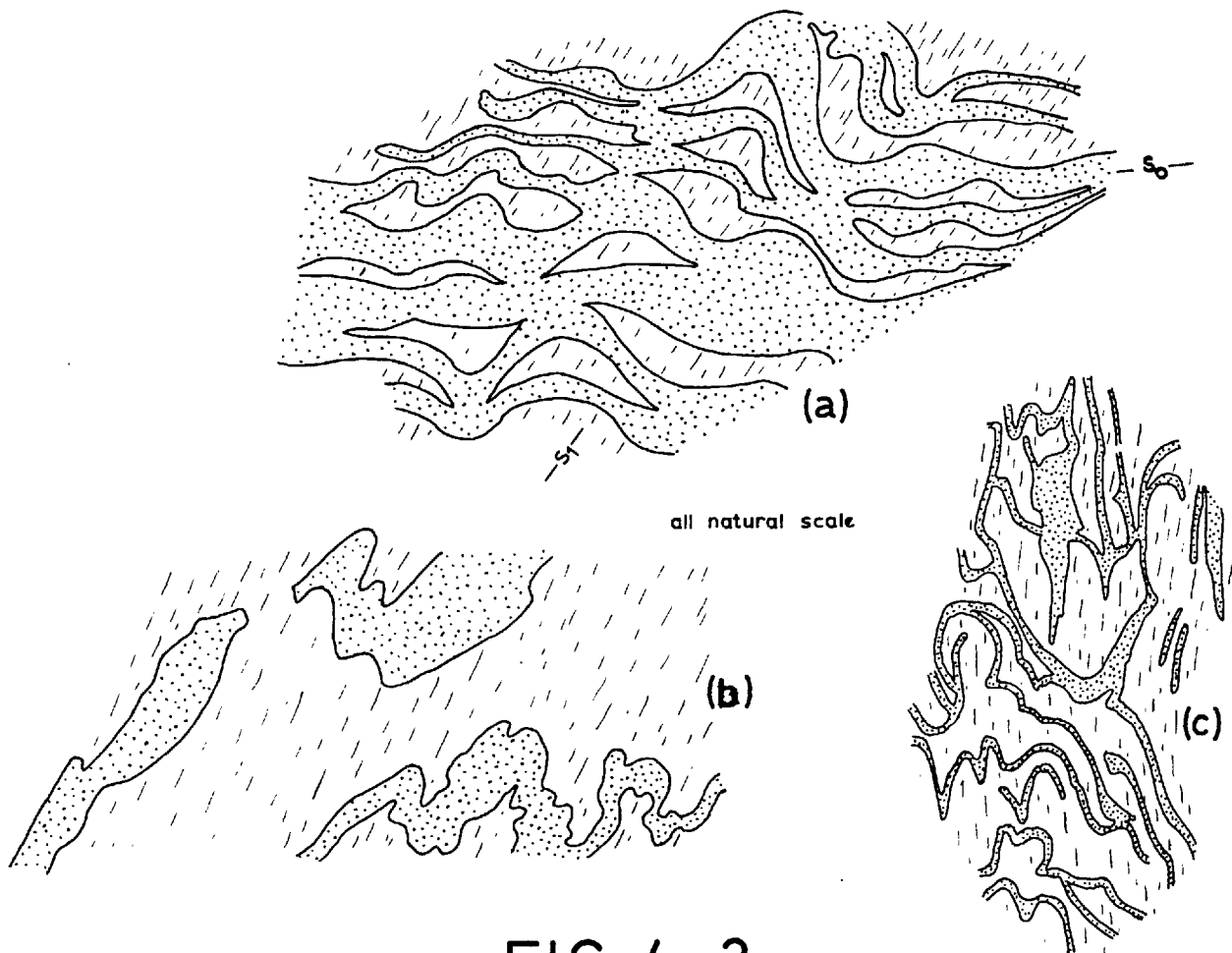
FIG. 4-3
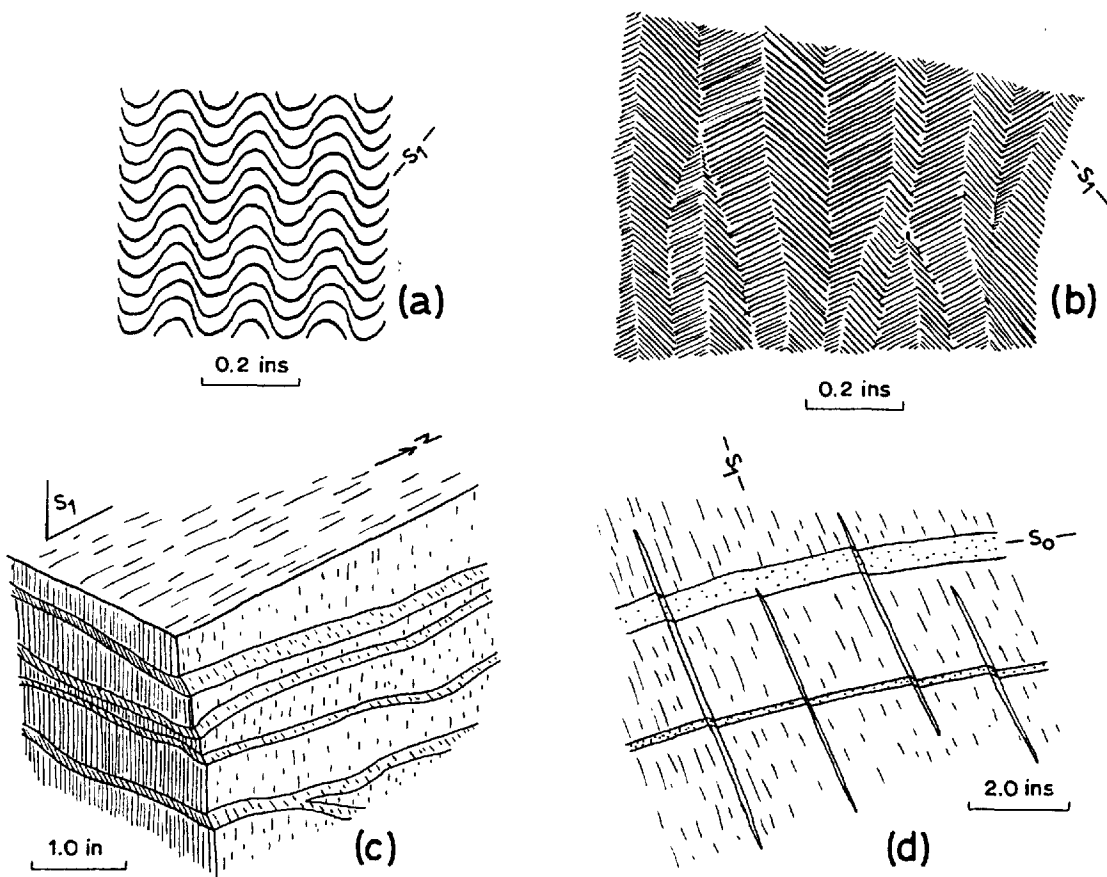
FIG. 4-4

(b) Kink Bands in S_1

In a few outcrops of quartz-mica schists, S_1 is deformed into a series of small monoclinal kink structures similar in appearance to the single limbs of chevron folds. Individual kinks vary from 0.1 to 3 inches in width and in a single outcrop or even a hand specimen they may form an interlacing system with some kinks dying out and others criss-crossing or merging (fig. 4-4c). The kink planes are gently dipping in all directions but whatever their attitude, the sense of movement across a kink is always with the upper part moving towards the west. Recent deformation experiments on phyllite by Paterson and Weiss (1966) have shown that kinking can develop at many combinations of temperature and confining pressure. Kinking is therefore no indicator of any specific physical conditions of the rocks at the time of deformation. But the kinks in the Kanmantoo rocks are thought to have formed long after metamorphism because both micas and quartz are bent and visibly strained around the kink plane.

(c) Shear Bands along S_1

These unusual structures are found in quartz-mica schists in only one small section of the drill core but are worth mentioning since similar features, as far as is known, have not been described in the literature. In hand specimen the shear bands appear as sets of narrow lenticular stripes up to 2mm thick and 12 inches long oriented along a slightly curving schistosity surface (fig. 4-4d). In thin section the bands consist of fractured and undulose quartz and rather bleached looking biotite having a stringy fibrous appearance. They are termed shear bands because their intersections with S_0 produce an offset of the latter that always has the same sense. The displacement corresponds to the western side of the core moving down relative to the eastern side.

5. Group-4 Structures

This group comprises structures produced late in the geological history when the rocks deformed by rupture rather than by folding. Small fractures and faults are not very

obvious on the surface (see fig. 4-1c) but are quite common in the drill core both within and beyond the orebody. These small structures occur parallel to the schistosity as well as transgressing it at all angles. Included in this group is a set of prominent east-west joints partly infilled with adularia or albite, that control the outcrop pattern for short distances. The most important of the brittle structures from the point of view of size are the large breccia zones cutting across the fold trends; these have been described in chapter 3.

B. MACROSCOPIC STRUCTURE

1. Interpretation of Structural Data

Where folds are essentially homoaxial and provided field measurements of bedding are not biased (for instance if one limb is preferentially exposed), the style of large scale folding may be able to be deduced from the way poles to the bedding, group themselves around a great circle of a stereogram (Ramsay, 1964). The attitude of the fold axis is defined by the normal to the great circle on which the poles to bedding fall (β in fig. 4-5). The poles of the fold shown in fig. 4-5a spread fairly evenly over part of a great circle whereas in the tight fold in fig. 4-5b, the poles are arranged in two closely spaced groups about the axial plane trace. In the case of isoclinal folding (fig. 4-5c) the style of folding is obvious (or else folding is not recognised at all) but the orientation of the fold axis can be found only by direct measurements of the fold hinge in the field.

In areas having undulating fold axes it is usually necessary to divide the area into essentially homoaxial sub-areas before fold styles and directions can be determined with confidence. Accordingly, the Kanmantoo area has been divided into six sub-areas (numbered 1 to 6 in map 2) plus the Mine area. The six sub-areas as a group are called the outer area. All the structural data in map 1 are plotted on lower hemisphere equal area projections that appear in the enclosure termed map 5. The positions of the great circles on these projections are all based on contoured identical
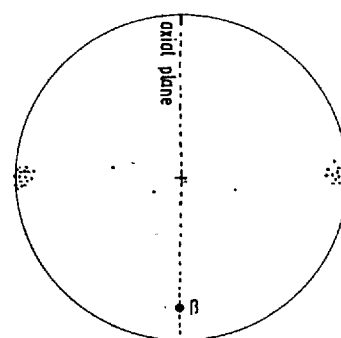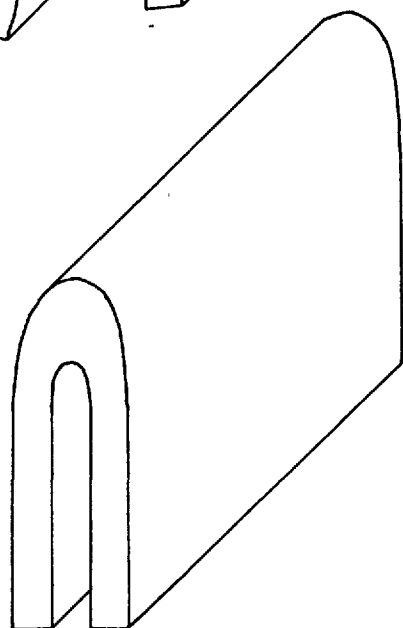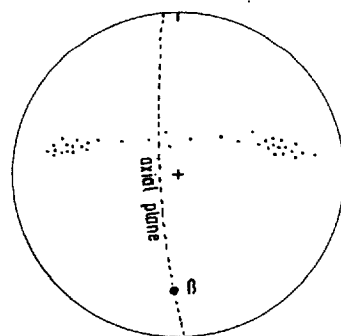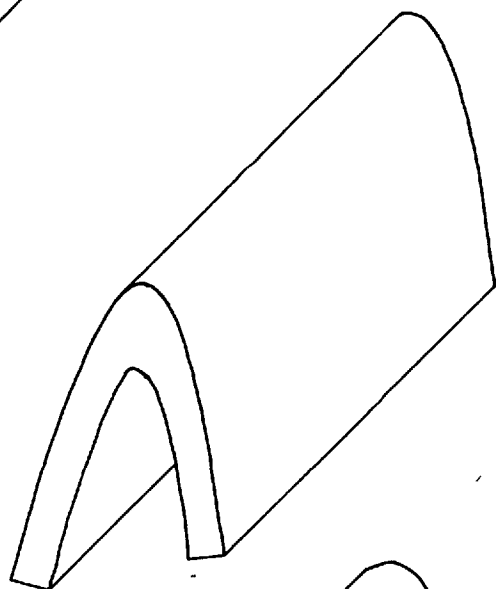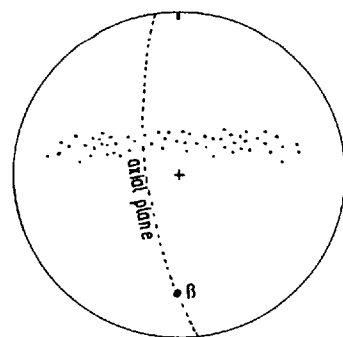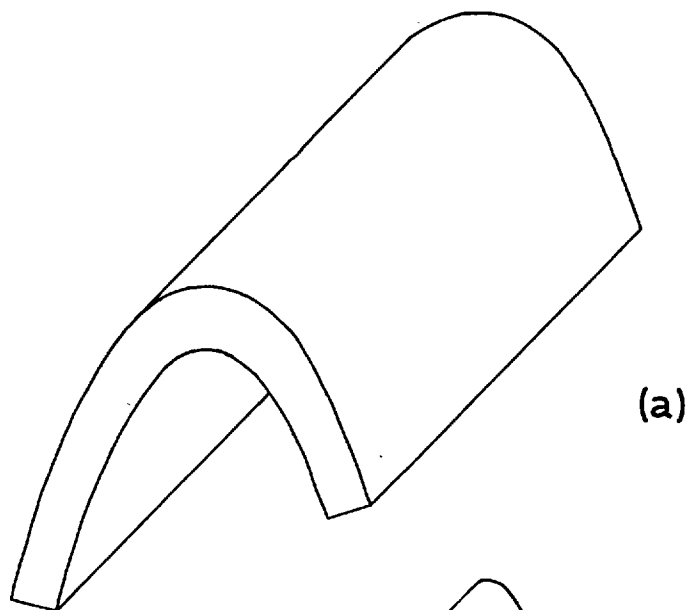
(a)

(b)

(c)

FIG. 4-5

Stereographic projections of bedding poles
for different types of folds.

projections (not shown).

2. Geometry of the Folding

In the field there is a tendency for the broad concentric-
type macroscopic folding to be confined to the arenaceous rocks
and the tighter, similar-type folding to the micaceous rocks
but a glance at map 2 shows that this is not always so. The
tight folding in sub-areas (1) and (2) is reflected in
projections a and b (map 5) where most of the bedding poles
plot at high angles to the axial plane trace. More open
folding in the other sub-areas is deduced by the rather more
even distribution of poles along the great circles. Fold
directions are indicated by the positions of the axes $\beta_{1,2,3}$
etc. Despite moderate variations in the axial directions in
these sub-areas, S_O poles for the outer area fall along a
reasonably defined great circle (projection i) that gives an
overall axial direction (β_i) trending 171° and plunging 45°
south. This relatively uncomplicated geometry does not hold
for the area as a whole (projection h), where the wide departure
of poles from any single great circle indicates a fold geometry
within the mine area rather different from that of the outer
area. In the mine area, southward plunges of the few mappable
macroscopic folds of only a few degrees (map-2) are confirmed
by the distribution of S_O poles in projection g. Here a major
fold axis (β_x) trending 176° and plunging 10° south is
accompanied by a suggestion, albeit not very strong, of a
minor axial direction (β_y) trending about 250° and plunging
about 5° to the west. No axial surface structure correspond-
ing to this possible east-west folding is present but it is
interesting that the area displaying this complex macroscopic
geometry is also the area containing most of the alteration
zones and the disharmonic mesoscopic folds. The interpreted
very tight folding in much of the mine area (maps 2 and 3) is
confirmed by the concentration of S_O poles far from the axial
plane trace in projection g.

3. Relationship of the Mesoscopic Structures to Folding

(a) Axial Plane Schistosity

When S_1 poles are plotted for the whole area (projection j), a single point maximum defines an "average" schistosity surface striking $008°$ and dipping $75°$ east; no difference in the S_1 populations can be detected between the mine and outer areas. The individual, as well as the overall fold axes (excepting βγ) fall on, or close to the S_1 trace (projection i). Thus if allowance is made for the small errors in measuring and plotting these structures, it is clear that S_1 is close to the axial plane of both the mesoscopic and macroscopic folds. On a macroscopic scale S_1 appears essentially unfolded.

(b) Small Folds

Even in a single outcrop mesoscopic folds exhibit a wide variation in plunge so it is not surprising that their axes show a greater scatter than do the axes of the larger structures. When plotted for the whole area (projection k), the mesoscopic folds fall along the axial plane trace but in the outer area alone (projection l), they form a small south-ward plunging group scattered about the macroscopic fold axes. The coincidence of small fold axes with those of the larger structures is well known in many metamorphic and non-metamorphic terrains and requires no comment. While there are insufficient small fold measurements from the mine area for meaningful conclusions to be drawn (projection m), there is a tendency for the axes to plunge shallowly both northwards and southwards thus forming a group around the B_x macroscopic axis.

(c) Lineations in S_1

Mineral lineations, micro-crenulations and "stretched" inclusions from the whole area plot as a point maximum having a trend of $125°$ and a plunge of about $72°$ to the southeast (projection n). This maximum falls on the schistosity trace but is about $35°$ from the overall fold axis B_i. The non-coincidence of the lineation with either the fold axis or a normal to it has been reported in other parts of the Kanmantoo Group by Kleeman (1954) who, however, could offer no explanation

for it. This question is taken up again in section E of this
chapter.

(d) Group-3 Structures

Axes of the crenulations in S_1 are sub-parallel to the
fine group mineral lineations in S_1 but the genetic connection
between them is unknown. The attitudes of the kink planes
(projection o) appear to bear little relation to the macro-
scopic fold geometry. It is interesting that the rotational
sense of movement deduced from both the kink bands and the
shear bands corresponds with the eastward dip of the axial
plane schistosity (assuming that it was formerly sub-vertical).
Again any genetic relationships between these structures are un-
known.

(e) Group-4 Structures

Poles to the prominent set of east-west joints are
grouped around the macroscopic fold axes in projection p.
Such structures are generally termed "a-c" joints because
they are sub-parallel to the a-c geometrical axes of the
folds. Billings (1962) thinks that such joints form from the
slight extension of the rocks along the fold axes due to the
stress relief attending the erosion of the overlying rocks.

All but one of the breccia zones strike within a 70°
quadrant (projection q). This geometry probably has some
relationship to the regional stress pattern during Tertiary
faulting and is not related directly to the earlier fold-
generating deformation.

C. RELATION OF MINERALIZATION TO MESOSCOPIC STRUCTURE

Because primary ore is exposed only in diamond drill
core having a maximum diameter of about $2\frac{1}{2}$ inches (internal
diameter of size NX diamond bit), the effective study of
mineralization-structural relationships is restricted to
structural domains of the same order of magnitude. This is
not serious for planar or linear structures that (in this case)
remain so over large areas, but the dimensional limitation
places such structures as folds with amplitudes and wavelengths
greater than a few inches beyond both observation and sensible
extrapolation.

1. Initial and Group-1 Structures

Concentrations of sulphide grains along the S_0 lithological banding are found only in the fine-grained disseminated mineralization. One example, illustrated in fig. 3-5a, shows relatively large sulphide poly-grains elongated along the schistosity surface of quartz-mica schist and forming a zone coincident in space with S_0. The folded schist specimen sketched in fig. 4-6a contains very fine-grained pyrrhotite-chalcopyrite mineralization that is practically invisible to the eye. However the folding is clearly outlined by the distribution of sulphide grains as shown in the tracing of a sulphide-iron chromographic contact print in fig. 4-6b (for details of chromographic techniques see Williams and Nakhla, 1951).

It is clear that the disseminated sulphide grains are always flattened along S_1 although it should be noted that the shapes of the grains within the schistosity surface are far from being equidimensional. This is visible in the dimensional variation of sulphide grain traces around the surface of drill core and is illustrated by the two sketches in figs 4-6c,d. Accompanying histograms of sulphide grain lengths measured under a microscope using a micrometer ocular, show that the sulphide grains are elongated parallel to the lineation. If pyrrhotite and chalcopyrite, in this case, were to be regarded as ordinary rock-forming minerals then these observations would most likely be sufficient evidence to suppose the geometrical features to be a result of metamorphism. But it can always be argued that structurally guided, post-metamorphic replacement could conceivably produce the same sulphide-structure relationships and such a possibility, on the present evidence, is difficult to refute. These time relationships are discussed further in the next chapter.

2. Group-2 Structures

Although zones of ore minerals have not been observed coincident with the complex group-2 fold profiles, the location of mineralization along the group-2 planar structures i.e.
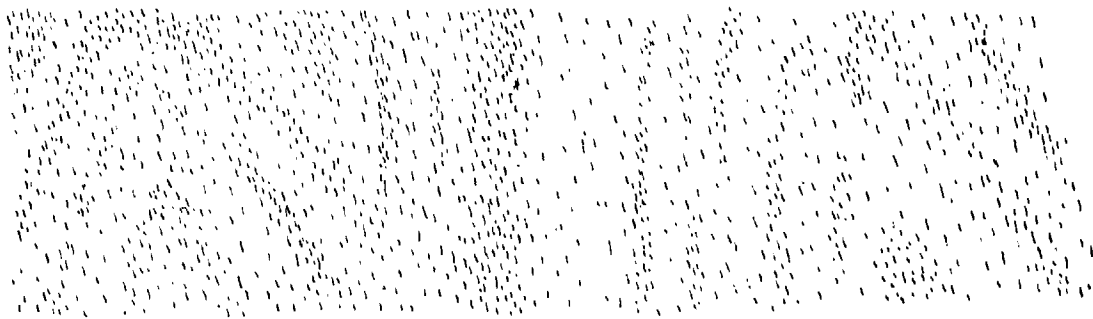
FIG. 4-6

Relationships Between Mineralization and Structure

(a)   Traces of folded bedding on the finely-ground surface
      of a micaceous schist specimen.

(b)   Distribution of fine-grained disseminated pyrrhotite-
      chalcopyrite mineralization as revealed by a sulphide-
      iron chromographic contact print of the surface of
      (a) above. Individual sulphide grains are aligned
      along the axial plane traces but groups of sulphide
      grains clearly follow the bedding.

(c,d) Elongation of individual disseminated sulphide
      grains along the lineation direction as revealed
      by measurement of grain lengths on two perpendicular
      sections through the same specimen.

(e,f,g) Schematic cross-sections based on section 1250N through
      the Kanmantoo orebody, illustrating different
      relationships of orebody shape to structure depending
      on the grade of material regarded as ore. Case (e)
      is perfectly concordant, case (f) is strata-bound
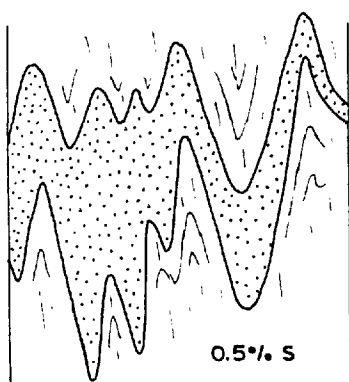   and case (g) is discordant.
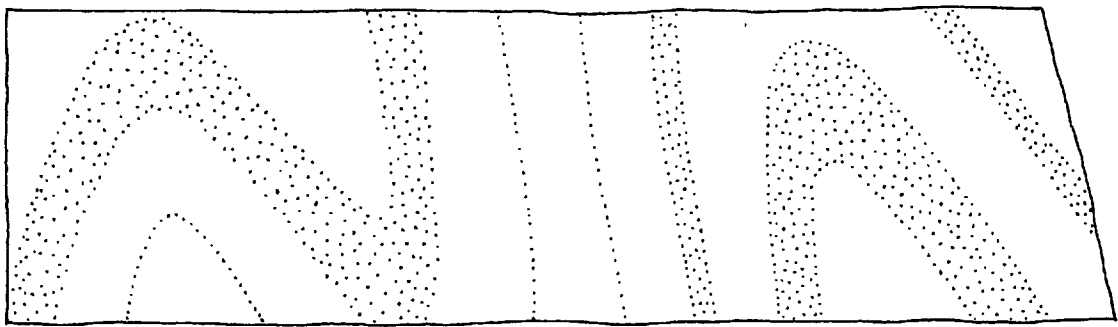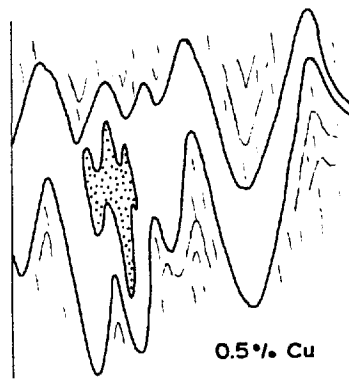
(a)

Natural scale

(b)
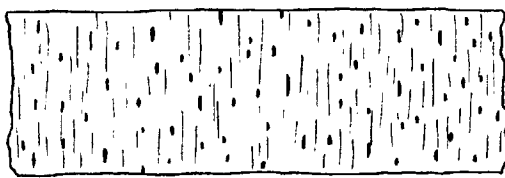
Perpendicular to schistosity
and lineation. (c)

276 grains
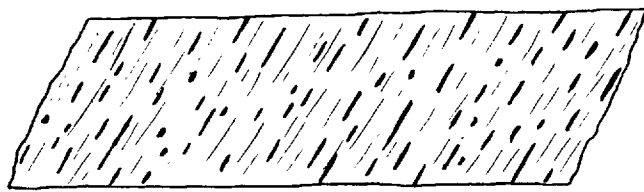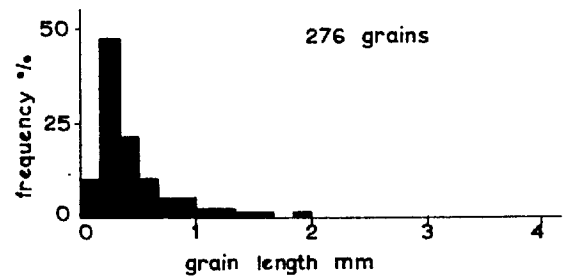
Perpendicular to schistosity.
Parallel to lineation (d)

278 grains

0.5% S (e)

0.5% Cu (f)
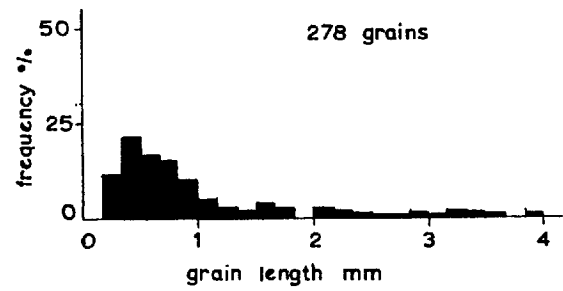
1.5% Cu (g)
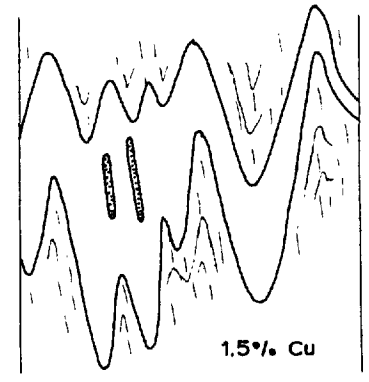
FIG. 4-6

schistosity planes and alteration zones, is a dominant structural feature of the coarser grained ore. Where the rock fabric remains schistose, the sulphide streaks and veinlets remain similarly oriented (fig. 4-7a) and if the schistosity surface is contorted or redefined in a different direction, any associated sulphides follow the new surface (fig. 4-7b). Sulphide grains or intergrowths in rocks whose schistosity surface has been destroyed by random growth of new micas, usually themselves lack a preferred dimensional orientation (fig. 3-5d). Thicker sulphide/magnetite zones are generally oriented along the group-2 mineralogical bands (alteration zones) that lie parallel to the schistosity of the adjacent rocks (fig. 4-7c).

Although the mineral lineation on the group-2 schistosity surfaces is often accentuated both by slickenside-like striations and by the oriented growth of long prisms of non-isometric minerals like staurolite and grunerite, the relationship of the coarser-grained mineralization to this lineation is difficult to assess. The change in dimensions of sulphide grain traces around the core surface is a poor guide because of the wide variation in sulphide grainsize. Even so, there does seem to be a tendency for the smaller sulphide streaks to be elongated along the lineation direction and, in one specimen, the "silicate" lineation is visible as striations in pyrrhotite at the sulphide-silicate interface.

3. Group-3 Structures

No sulphide/magnetite mineralization is found associated with any of the group-3 structures. Micro-folding and kinking of mica grains within some sulphide masses (fig. 4-7c) may have been caused by movements responsible for the group-3 structures.

4. Group-4 Structures

The mineralization displays basically two distinct relationships to the brittle structures. In fractures or small faults along which no sulphide or silicate alteration has taken place - in other words in internal or local dislocations - primary sulphides may infill parts of the structures

FIG. 4-7

(a) Streaks of chalcopyrite/pyrrhotite along the schisto-
sity surfaces of garnet-biotite-chlorite schist from
an alteration zone. Slightly reduced.

(b) Quartz-biotite-garnet lode schist from near an
alteration zone showing truncation of one set of
schistosity surfaces by another set. Chalcopyrite/
pyrrhotite streaks and veinlets follow both sets of
surfaces. Note the sulphides along the truncation
boundary. Garnets show up as the small rounded
pale-grey spots. Slightly reduced.

(c) Coarse-grained chalcopyrite/pyrrhotite mineraliza-
tion along a small garnet-biotite-chlorite alteration
zone in quartz-biotite-garnet lode schist. Many of
the micaceous laths in the sulphides are microfolded.
Note the small sulphide grains disseminated through
the lode schists parallel to S_1 (arrowed) Slightly
reduced.

(d) Thin section of a banded lode schist consisting of
biotite-rich bands (grey zones) and quartz-rich bands
(lighter zones). Pyrrhotite-rich mineralization
(black) consists of streaks and veinlets along the
schistosity planes (S_1). In the lower-left part
of the photograph pyrrhotite has apparently migrated
into small internal fractures one of which offsets
the banding.

(e) Columnar adularia crystals line the walls of a joint
in andalusite-staurolite schist. A large pyrite cube
has formed in the joint cavity and growing perpendicular
to the pyrite faces are columnar aggregates of dark
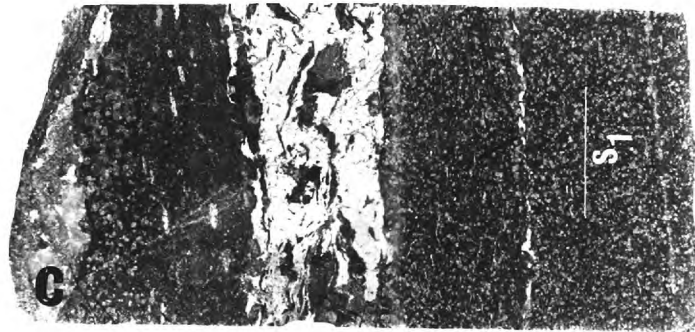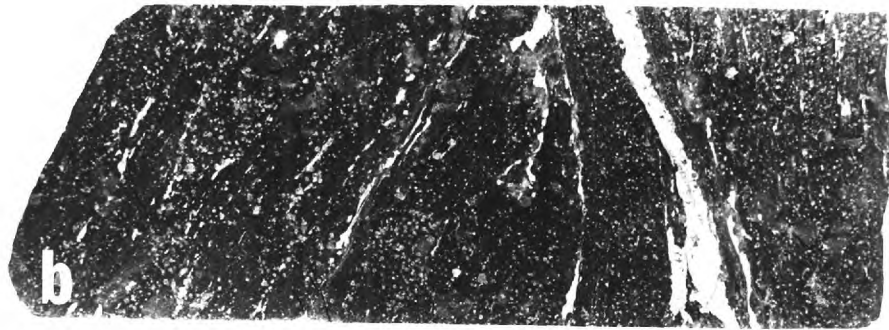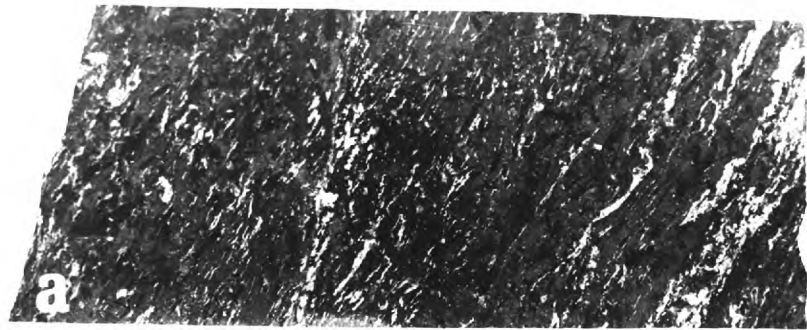blue iron-chlorite (arrowed).

FIG.4–7

in a manner that suggest migration from a nearby location
(fig. 4-7d). The other relationship is found in open fractures
or joints; these must have been favoured as conduits by ground
waters and consequently are the main loci for primary mineral
breakdown and the growth of secondary sulphides like pyrite
(fig. 4-7e).

D. RELATION OF MINERALIZATION TO MACROSCOPIC STRUCTURE

1. The Shape of an Orebody

In the scientific investigation of an ore deposit the
problem of the overall shape or structure of an orebody is
not so much the geometrical projection of the object onto
paper as the geological significance of the shape to be
projected. In simplest terms, an orebody is a volume of
rock bounded by an imaginary surface dividing material that
can be economically exploited,from material that cannot.
In some cases this economic shape clearly coincides with the
shape of a geological feature and in other cases it does not.
For instance, in some of the very rich massive pyritic deposits
of Cyprus or the bedded phosphates of Morocco, the orebody
consists of material that can be regarded as a separate and
valid rock-type that would have the same shape irrespective
of its being ore. However in many low-grade deposits this
relationship may not hold; the valuable mineral may be a
minor phase distributed through one or more rock-types and
the actual surface defining the orebody will follow an assay
boundary which would probably vary according to economic
factors like metal price and mining efficiency. Geologically,
such an orebody is not strictly a separate entity.

Consider as an illustrative example, the three sketches
in figs. 4-6e,f,g that are based on a cross-section through
1200 north in map 4. If economics allow material in the
Kanmantoo area containing greater than 0.5% sulphur to be ore
then the shape of the orebody will appear as a conformable
deposit as in section (e). On the other hand if 50 feet of
material containing less than 0.5% copper is the cut-off

grade then section (f) would be the resulting shape. An orebody containing material with not less than about 1.5% Cu is shown in section (g). Clearly there is a transformation from more or less complete stratigraphic concordancy to complete discordancy depending on the grade of ore considered. Caution must therefore be exercised in assessing the genetic significance of the shape of a low-grade orebody. Perhaps the best scheme would be to contour metal or sulphur contents but to be of use this method would probably require more assay values than are generally available.

The ore shown in maps 3 and 4 is based on a cut-off grade of 50 feet assaying 0.5% Cu.

2. Overall Structural Relationships

The structure of the andalusite-staurolite schists enclosing the lode schists and the orebody can be described as a tightly folded synclinorium slightly overturned to the west (map 3). From near the centre of this synclinorium to the north of the orebody (map 4) the lode schists and associated alteration zones, which together enclose most of the economic mineralization, occupy lens-like positions along the synclinal keel. Towards the south however, the lode schists, alteration zones and mineralization are all less strongly developed and are found mainly near the quartz-mica schist contacts.

The overall form of the orebody is difficult to envisage because of the erratic changes in its profile from section to section (map 4). Perhaps the simplest description would be that it is made up of a series of lenses flattened parallel to the axial plane schistosity and following the trend of the country schists. Whether these lenses join up into a complexly folded continuous unit is not known but there is little evidence to suggest any coincidence between their distribution and the macroscopic folding. Neither is their any evidence for the orebody as a whole or any of its constituent lenses having any long dimension parallel to either the schist lineation or the fold axial trends as has been found in similar deposits in Japan (Kanehira, 1959) and Quebec (Stevenson, 1937).

Thus although the orebody is far from being a typical cross-
cutting feature it could hardly be described as a stratiform
deposit.

E. OBSERVATIONS BEARING ON THE MECHANISM OF DEFORMATION

1. Some Principles of Deformation

The term strain is given to the change in shape or
volume of a body induced by the application of stress. Strain
includes both elastic and permanent deformation but in studying
rocks the latter is the main concern. This is called finite
strain but it is usually shortened to strain; a term synonymous
with deformation. The strain is called homogeneous when lines
or planes within a body remain so after deformation although
their demensions and angular relationships will have altered.
There are two types of homogeneous strain; one called pure
shear or pure strain is produced by three pairs of coaxially
opposed, mutually perpendicular forces (principal stresses)
acting on a body (fig. 4-8a) and the other called simple shear,
is produced by opposed, non-coaxial forces acting as a couple
(fig. 4-8b). The type and degree of homogeneous strain in a
given body can be described in terms of a strain ellipsoid
developed from an initial spherical sample of the unstrained
body; the long, intermediate and short axes of the ellipsoid
are designated X,Y and Z. In homogeneous pure shear the
axes of the strain ellipsoid do not change their orientation
as strain progresses, whereas in homogeneous simple shear
the long axis of the ellipsoid rotates asymptotically towards
the shear plane. The direction of shear on the shear plane
is termed kinematic-a (Ka), the kinematic-b direction being
perpendicular to Ka in the shear plane and the kinematic-c
direction being perpendicular to the shear plane (Turner, 1948).

The generation of a fold from a planar element cannot be
produced by homogeneous deformation; some inhomogeneous or
differential strain is necessary. There does not seem to be
much argument that parallel folds are formed by buckling and
flexural slip but ideas on the formational mechanism of

FIG. 4-8

(a)   Deformation of a cube by homogeneous pure shear.
      Principal axes of the strain ellipsoid do not
      rotate during deformation.

(b)   Deformation of a cube by homogeneous simple shear.
      At least two principal axes of the strain ellipsoid
      rotate during deformation.

(c,d) Formation of a <u>similar</u> fold by inhomogeneous
      simple shear. The long axes of the strain
      ellipses converge strongly towards the fold
      crest.

(e,f) Modification of the fold profile of (d) above by
      progressive homogeneous pure shear; there is no strain
      along the fold axis. The folds become tighter but
      retain their <u>similar</u> profiles, and the long axes of
      the strain ellipses appear to rotate so as to become
      nearly parallel to one another and to the axial
      plane.

(a)

(b)

(c)

(d)

(e)

(f)
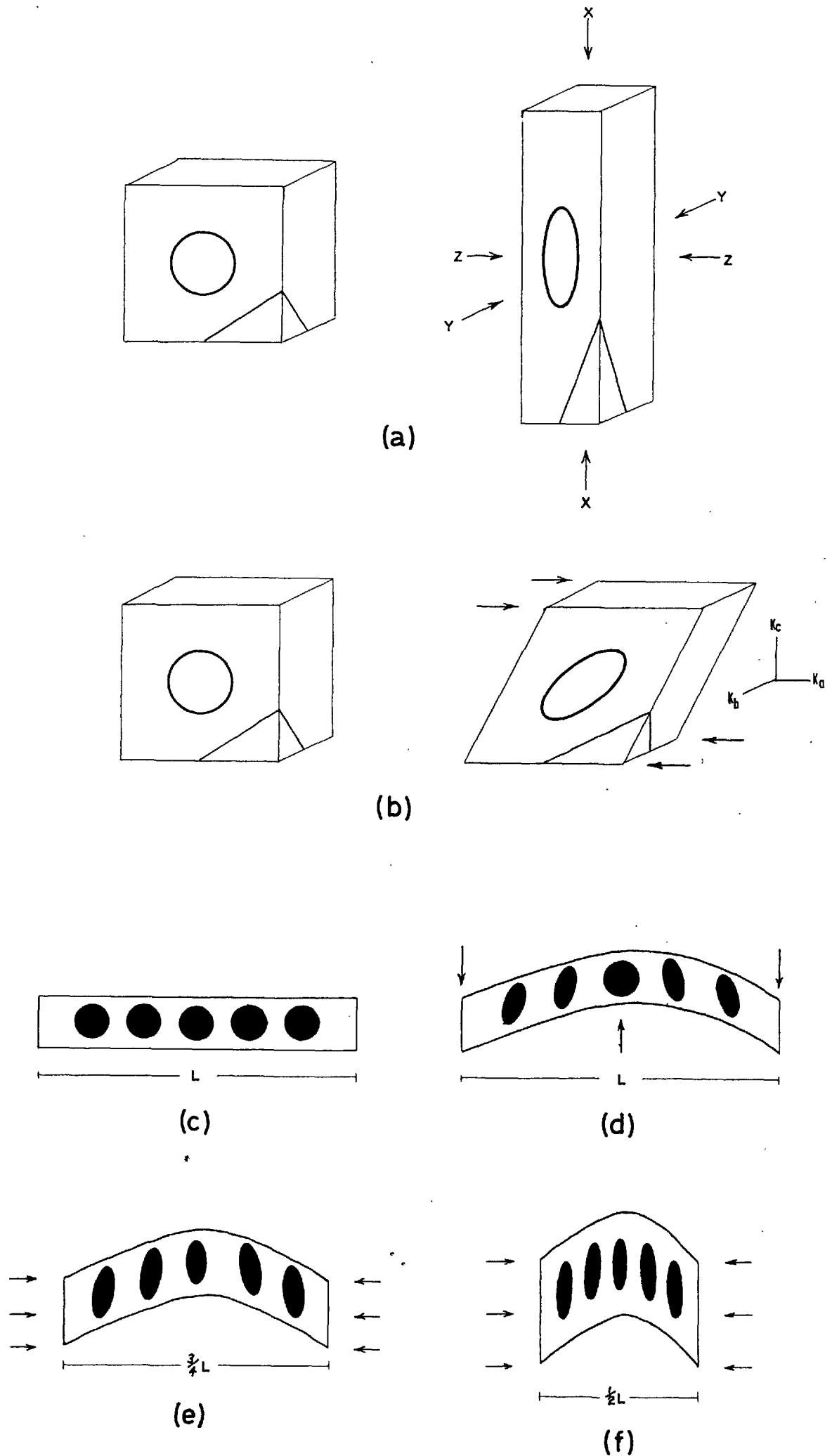
FIG. 4-8

similar-type folds are not so uniform. The common occurrence
of an axial plane cleavage or schistosity in similar folds has
been taken by many authors to indicate fold formation by a
process of differential simple shear or non-affine slip
(Turner, 1948) along the cleavage surfaces. In this process
strain ellipses which indicate only two dimensional strain,
form a fan shaped pattern with the long axes converging towards
the hinge (fig. 4-8c,d). Ramsay (1967) considers that for
ideal similar folds there seems to be no other satisfactory
explanation but he points out that folds produced in this way
will retain their similar profiles if homogeneously deformed
by any amount and in any direction. This phenomenon is
illustrated in figs. 4-8e,f where the fold profile of fig 4-8d
is subject to simple compression (two dimensional pure shear).
Note the progressive elongation and rotation of the strain
ellipses to become nearly perpendicular to the compression
direction.

Schistosity surfaces have been variously thought to
represent the plane of slip (simple shear), the plane of
flattening parallel to the X-Y plane of the strain ellipsoid
(pure shear), and the normal to the axis of principal compressive
stress (Turner and Weiss, 1963). According to Wilson (1961),
mineral lineations or microcrenulations on schistosity planes
are commonly parallel to the associated fold axes and are
therefore parallel to kinematic-b. Lineations perpendicular
to the fold axes are called "a" lineations because they are
thought to be parallel to kinematic-a or the direction of slip.
If the schistosity plane is regarded as the X-Y plane then "a"
lineations are parallel to the long (X) axis of the strain
ellipsoid (Ramsay, 1967). Earlier, Cloos (1946) pointed out
many cases of lineations neither parallel nor perpendicular
to the fold axes and perhaps his advice that...."each case
must be studied and should be stated so that the reader can
form his own opinion".... should be heeded.

2. Evidence from Folds

Fig 4-9a shows a folded andalusite band in a section cut
perpendicular to S_1 and the fold axis. Zoning in the andalusites

FIG. 4-9

(a) Tracing of a folded andalusite band viewed along
     the fold axis, and its approximate length on
     unfolding. In the inner andalusite zone the
     inclusion fabric is parallel to the folding whereas
     in the thinner outer zones the inclusion fabric is
     parallel to the external schistosity.

(b) Two mechanisms whereby the andalusite band could
     have been folded; in the first the band buckles
     while the surrounding schists deform by pure shear
     and in the second the band buckles while the
     schists deform by simple shear along the schisto-
     sity direction.

(c) Tracing of folding in fig. 4-1c. Outlines of the
     "stretched" inclusions are shown in black. The
     hollow shapes represent the forms and orientations
     of strain ellipses that would result if the folding
     was caused by inhomogeneous simple shear along the
     schistosity planes.

(d) Tracing of an adjoining fold. Description as
     for fig. 4-9c.

(e) Sketch of a section through the centre of one of
     the "stretched" inclusions in the plane of the
     minor and intermediate ellipsoidal axes. For
     explanation see text.

natural scale

(a)

(b)

(c)

1.0 ft

(d)

1.0 ft

(e)

natural scale
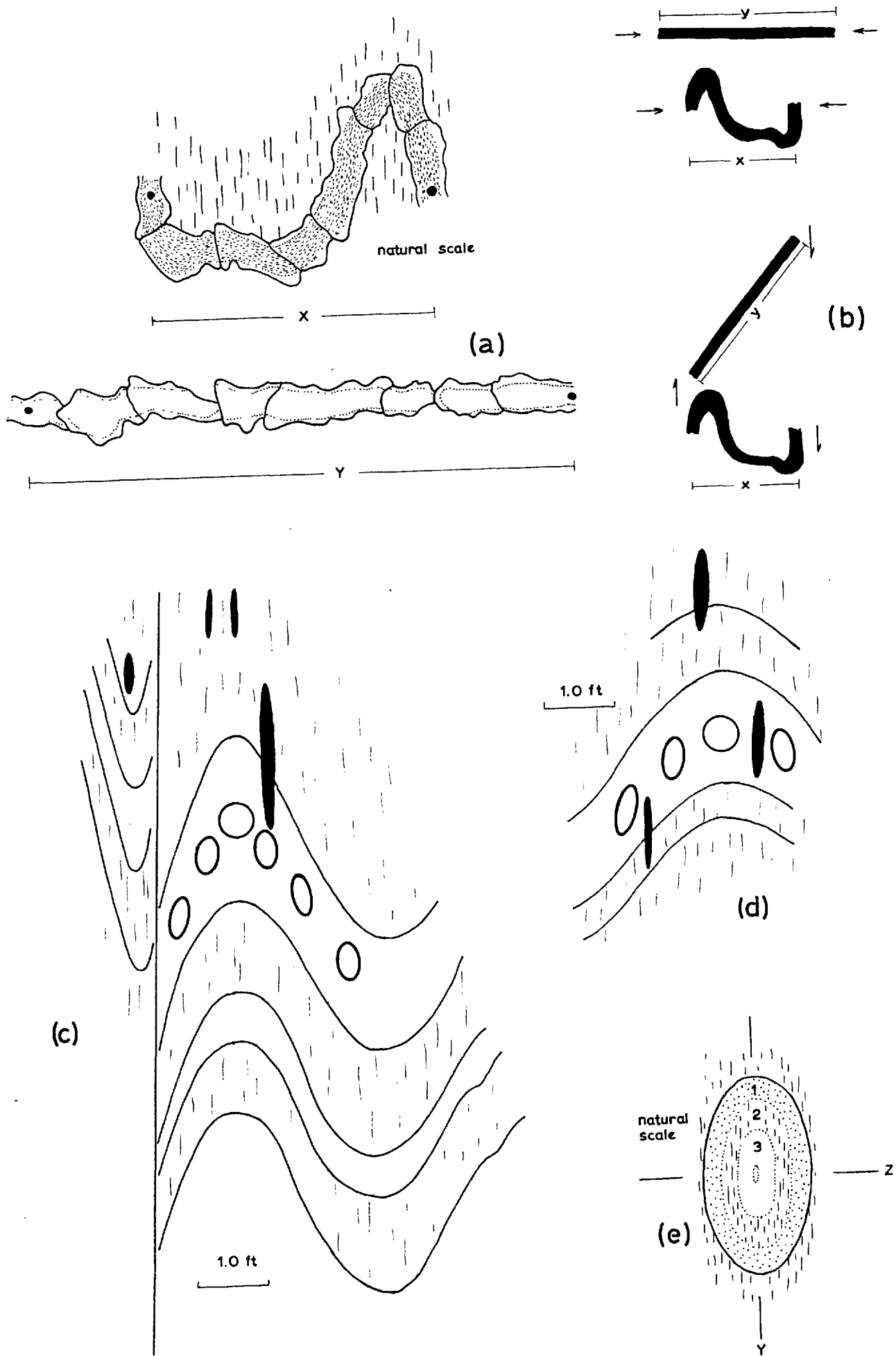
FIG. 4-9

is quite obvious in hand specimen; in the inner zones small mica and ilmenite inclusions are parallel to the folded surface whereas inclusions in the thinner outer zones are oriented parallel to the external schistosity. This indicates that the bulk of the andalusite grew in a more or less planar layer before being buckled into a fold. Some of the andalusites are bent but there is little evidence that they are stretched or compressed therefore it seems reasonable to suppose that the length of the andalusite band measured in the fold is close to its original pre-folded length. This would indicate a component of shortening of the schist in a direction perpendicular to S_1 and by comparing distance x with the unfolded length y in fig. 4-9a a rough estimate of this component is possible:

$$x = 25 \text{ units} \qquad y = 48 \text{ units}$$

component of shortening perpendicular to S_1

$$= \frac{y - x}{y} \times \frac{100}{1} = 48\%$$

Unfortunately there is no way of distinguishing between pure and simple shear since the two mechanisms illustrated in fig. 4-9b could produce identical folds in the andalusite band.

3. **Evidence From "Stretched" Inclusions**

The nearly ideal similar fold profiles in figs. 4-1c and 4-2c are strong evidence for at least partial formation by differential simple shear, but the folds by themselves, give no indication of the amount of homogeneous strain that may have taken place. Some of the associated elongated inclusions that are found in a small group in a single exposure south of the Mine Hill (map 1) vary in shape from almost perfect ellipsoids to slightly irregular forms, and internally may be nearly structureless, concentrically banded or finely cross-banded. All are slightly lighter in colour than the adjacent schist and all are elongated along the S_1 planes (solid shapes in figs. 4-9c,d).

One inclusion collected for laboratory study is almost a perfect ellipsoid flattened in the S_1 plane and elongated parallel to the mineral lineations. A section cut perpendicular to the long (X) axis and sketched in fig. 4-9 c has the following features: the external schist has a well developed lepidoblastic texture and contains about 60% quartz, 35% biotite and 5% garnet. Zone (1) is quartz-rich with a little garnet and biotite, zone (2) contains about 80% quartz and 20% biotite showing a preferred orientation parallel to the external S_1, and zone (3) contains progressively less biotite towards a small core having mineral proportions similar to the external schist. The external micas do not show any tendency to swing around the inclusion but stop abruptly at the margin. The exact origin of the inclusion is not known but neither is it important. What is important, is that (a) this textural evidence indicates that the inclusion during deformation acted as a nearly passive body having similar mechanical properties to the enclosing rock and (b) the nearly perfect ellipsoidal shape suggests the inclusion was formerly a sub-spherical body - two essential features if inclusions of this kind are to be used as valid indicators of strain (Hobbs and Talbot, 1966).

If both sets of folds in figs. 4-9c,d were produced by differential simple shear acting along the S_1 planes, then circles inscribed on the undeformed rock would, after folding, be expected to give a strain ellipse pattern shown by the hollow shapes. Note the characteristic variation in strain and ellipse orientation in different parts of the folds, particularly the zero strain indicated in the hinge region, and compare these with the parallelism of the actual inclusions (solid shapes). Note also the weak relationship between the indicated strain of the inclusions and their positions in the folds. On the other hand, compare the shapes and distributions of the inclusions with the hypothetical situation in fig. 4-8f where weakly slip-folded layers have been subject to 50% of subsequent shortening - clearly there is a striking resemblance. If then, the inclusions are indicators of

homogeneous pure strain involving a shortening perpendicular
to S_1 and extension parallel to the lineation, their dimensions
are of some quantitative significance. External measurements
and calculations made on the ellipsoidal inclusion described
above yielded the following results:

$$X = 11.9 \text{ cm} \qquad Y = 5.6 \text{ cm} \qquad Z = 2.8 \text{ cm}$$

if we assume the inclusion was originally a sphere of diameter
D then.

$$\frac{4 \pi}{3} \frac{D^3}{8} = \frac{4 \pi}{3} \times 11.9 \times 5.6 \times 2.8$$

$$D = 5.8 \text{ cm}$$

D is very close to the length of the Y axis and therefore
indicates virtually no extension or shortening in the schistosity
plane in a direction perpendicular to the mineral lineations.
The extension (E) in a direction parallel to the lineations is
given by;

$$E = \frac{X - D}{D} \times \frac{100}{1} = 105\%$$

and the shortening (S) in a direction perpendicular to S_1
becomes;

$$S = \frac{D - Z}{D} \times \frac{100}{1} = 52\%$$

This latter figure is remarkably similar to the shortening
calculated for the domain containing the folded andalusite
band.

It therefore seems reasonable to suppose that; (1)
the profiles of the similar folds, at least in the area considered,
are the result of a moderate amount of homogeneous pure strain
superimposed on originally only gently folded S_o layers,
(2) the schistosity S_1 in its present form represents a
surface of flattening parallel to the X-Y plane of the strain
ellipsoid and not simply a set of slip or simple shear planes,
and (3) the mineral lineations on S_1 are parallel to the X
axis of the strain ellipsoid and therefore indicate the
direction of extension.

SUMMARY

1. The earliest recognisable surface - the lithological banding (S_O) - has been proved to be bedding in part and deduced to be bedding elsewhere.

2. The group-1 mesoscopic structures and the main fold geometry of the area appear to have been formed during a single deformational event. This event probably lasted through most of the progressive metamorphism. Folding initially may have been by a combination of buckling and inhomogeneous simple shear under an east-west compression system, but the resulting fold profiles have probably all been modified to some extent by locally homogeneous pure shear. Folding is generally tighter in the more micaceous lithologies so these must have absorbed most of the compression by extending in the lineation direction. It should be noted that ideally homogeneous pure shear probably did not exist except in very small domains since the rapid changes in the plunge of mesoscopic fold axes suggests that the degree of extension varied along (as compared to about)a given schistosity plane.

3. The non-correspondence of the extension direction with a normal to the original bedding planes accounts for the acute angle between the lineation and the fold axes.

4. The minor deformational event or events following the major folding and responsible for the alteration zones probably took place in late metamorphic times. Despite some evidence in slicken side-like striations and warped schistosity planes, no major shearing or displacement has been found across any alteration zone so it seems likely that stress field associated with their formation had a dilational or tensile component perpendicular to the schistosity planes. Such a stress field could exist only after the movements responsible for folding when compression perpendicular to the schistosity planes was relaxed. The resulting low pressure zones could then have acted as loci for metasomatic activity that accelerated the growth of the metamorphic silicates.

5. The complex mesoscopic fold profiles existing in schists near the alteration zones are difficult to reconcile with such postulated dilational movements. No explanation can be confidently offered for their formation.

6. The uncommon group-3 mesoscopic structures appear to be younger than the deformation event associated with the alteration zones so they are probably the result of slight tectonic disturbances sometime between the waning stages of metamorphism and the brecciation and fracturing connected with Tertiary faulting movements.

7. The weakly disseminated sulphide minerals in the aluminous and ferruginous chists are geometrically identical to the other schist-forming minerals in that they are flattened in the schistosity plane, elongated in the lineation direction and in a few places form zones parallel to the bedding. This is good evidence that the sulphide constituents are pre-tectonic and therefore probably pre-metamorphic in age and possibly even syngenetic with the original sediments.

8. Coarse-grained sulphide and sulphide-oxide ore is practically all within or adjacent to the alteration zones. There is little doubt that in its present position this is epigenetic mineralization.

9. The orebody as a whole consists of a series of lenses flattened along the schistosity surfaces. There is no clear coincidence either between the distribution of these lenses and the macroscopic fold structure or between the long dimensions of the lenses and the lineation or fold directions.

10. No significant primary sulphide mineralization appears to be connected with the group-3 or group-4 brittle structures. Many of the joints and fractures probably acted as conduits for ground water since they play an important part in the location of some secondary minerals.

11. A brief list of the deduced sequence of events in the tectonic history is given in table 4-3

TABLE 4-3. Interpretation of the Tectonic History of the Rocks Enclosing the Kanmantoo Orebody.

EVENT	STRUCTURES PRODUCED		ORE HISTORY
	Mesoscopic	Macroscopic	
O	Bedding. Ripple marks and other rare sedimentary structures	Probable sub-horizontal bedding surface.	Possibel syn-genetic deposition of the constituents of the disseminated mineralization.
B_1	North-south folds in S_O. Axial plane schistosity S_1. Mineral lineations in S_1.	Major, slightly non-homoaxial north-south fold structure. Planar axial plane schistasity surface. "a" lineations.	Growth of dissemina-ted sulphide grains; these become flatten-ed parallel to S_1 and elongated in the mineral lineation direction.
B_2	Segregation and growth of silicate minerals along zones parallel to the S_1 schistosity surface. Local redefinition of S_1 by new micas. Possible modifica-tion of fold profiles by differ-ential movements in S_1.	Possible slight east-west folding superposed on main north-south geometry.	Development of coarse-grained sulphide streaks and veinlets along schists adja-cent to alteration zones. Growth of oxide and sulphide ore minerals within the alteration zones.
B_3	Local kinking, crenulation and shearing of S_1.	Sub-horizontal kink plane structure.	Unknown; probably minor deformation and recrystallization of ore minerals
B_4	Small fractures and faults. Jointing. Breccia zones.	Joint system sub-perpendicular to B_1 fold axes. East-west trending, sub-vertical breccia zone system.	Extensive but variable deformation, solution and redeposition of ore minerals. Intensive alteration of some phases.

Chapter 5

PETROGRAPHIC ANALYSIS OF THE TEXTURES

Introduction

According to Crook (1933), the divorce of the study of ore deposits from that of rocks began almost from the commencement of scientific work in geology around about the time of Hutton and Werner. The feeling that mineral veins were "things apart" had persisted to the time of writing. Crook appeals as much to students of ore deposits to treat their studies as petrogenetic investigations as to petrographers not to take too narrow a view of their science. Such sentiments are also expressed by some modern writers (e.g. Amstutz, 1960) but the study of rocks now incorporates such a vast field of specialized techniques, that anyone contemplating a general study of an ore deposit is virtually forced to select a limited number of methods of investigation. Although it could be argued that this selection ought to be based purely on scientific grounds, there is often the need to consider aspects of direct practical importance as well. Fortunately the interests of both science and industry coincide in the knowledge of the geometrical features of the ore. A study of the smaller geometrical relationships i.e. the textures or microstructures, is important in mineral beneficiation processes and is essential for determining or confirming any age differences in mineral formation. Such chronological considerations are a necessary step to speculating on ore genesis.

A. SOME PRINCIPLES OF TEXTURAL INTERPRETATION

1. Paragentic Studies of Ores

The development of ore microscopy from about the turn of the century, was contemporaneous with the growth of ideas on the migration of metal-laden fluids through rocks (Van Hise, 1900) that culminated in the widespread, though far from universal, acceptance of the hydrothermal schemes

of classification for metalliferous deposits (e.g. Lindgren, 1933). Criteria for recognising mineral replacement, infilling and superposition were used to determine the simultaneous, sequential and overlapping histories of mineral deposition from hydrothermal fluids (Bastin, 1931; Schwartz, 1951; Edwards, 1954). Although such paragentic criteria were, and still are, applied successfully to many vein-like deposits, many workers recognised the need for caution in their application to ores where the textures may have been modified since the original mineral deposition.

Most base-metal sulphide ores in metamorphosed geosynclinal rocks exhibit textures that are notoriously difficult to interpret. That non-supergene replacement textures exist in all such ores is indisputable since the growth of any mineral in a solid medium must involve replacement processes. Argument can stem only from the interpretation of the replacement textures. Do they signify introduction of mineral constituents from (a) the mantle, (b) nearby igneous rocks, (c) the adjacent metamorphosed rocks, or (c) the immediate domain of the mineral? Are replacement or replacement-like textures the result of simultaneous or sequential crystallization prior to metamorphism, recrystallization and grain-boundary adjustment during metamorphism, or phase unmixing and mineral segregation during cooling? The logical first step in answering these questions is to ascertain whether or not the textures are indicative of, or compatible with, the metamorphism of the ore and associated rocks.

2.   Solid State Concepts in Textural Interpretation

In recent years increasing interest has been shown in the application of plastic deformation, recrystallization and surface tension phenomena to the interpretation of rock and ore textures. Most of the fundamental work has been done on metal and ceramic systems but important contributions in a geological context are papers by Voll (1960), McLean (1965), Stanton (1964), McDonald (1967) and Stanton and Gorman (1968).

The plastic deformation of crystal aggregates is thought to take place partly by grain boundary sliding but principally by atomic slip and twinning both of which require the generation of point and line crystallographic defects and their movement through the crystal lattices. During deformation, lattice strain associated with the rising number of defects causes the internal energy of the crystals to increase until eventually, the crystal structures may undergo a change that tends to reduce this internal strain energy. One process by which they can do this, called recrystallization, involves the nucleation of unstrained grains from the deformed material and the growth of these nucleii until they completely replace the strained host grains. If the material is held at a moderate temperature for a time after recrystallization, the new grain boundaries may undergo annealing adjustments in response to the surface tension forces that tend to reduce the interfacial or grain boundary area and therefore the surface energy of the crystalline aggregate.

Studies of surface tension phenomena go back at least to the work on soap bubbles by Lord Kelvin in 1887 and the importance of surface tension in controlling the interfacial geometry of annealed metal aggregates was first studied by Desch in 1919. According to Verhoogen (1948) the physical interpretation of surface tension is as follows: atoms on the surface of a solid have a resultant force tending to pull them into the grain at right angles to the surface but if these forces are resolved for the grain as a whole, the surface can be shown to be in a state of tension i.e. the surface is tending to pull the grain in on itself. In an annealed crystal-line aggregate the equilibrium geometry at any triple junction will depend on the nature of the three phases in contact. If the phases are the same and are more-or-less isotropic with respect to surface energy, the angle of meeting of two phases (dihedral angle) will be close to 120° but it the phases are different, the differing values of the surface tensions for the three interfaces will produce a grain boundary configuration that obeys the triangle of forces law. Following the

work by Smith (1948) on two-dimensional dihedral angle
relationships in single-phase and multi-phase annealed metal
aggregates, Stanton (1964) measured dihedral angles in single
and two-phase sulphide ores and found equilibrium conditions
to be widespread. Stanton concluded from this work that
conventional paragenetic sequences for such ores are illusory
since all grain shapes are the result of interfacial energy
phenomena; all the textures could be explained by simple
grain coarsening, deformation, recrystallization and annealing
in the solid state during metamorphism.

In the case of idiomorphic crystals growing in an
anhedral granular matrix of another phase, grain-boundary
geometry is no criterion for recognising textural equilibrium
or simultaneous growth of crystal and matrix. The configura-
tion of the crystal-matrix interface is a function of the
symmetry and forms displayed by the crystal. Furthermore,
consideration of grain-boundary geometries alone can not
readily distinguish a pre-metamorphic ore from a post-metamorphic
epigenetic ore introduced under conditions at which annealing
can take place. One solution to the problem of recognising
metamorphism in ores is to return, somewhat paradoxically, to
a paragenetic study of the sequence of mineral growth by
making use of many of the textural dating techniques developed
for silicate intergrowths in metamorphic petrology.

3. Textural Analysis of Metamorphic Rocks

The question of time in plutonism is the subject of
an important contribution by Read (1949) who rejects the dictum
of Becke that metamorphic minerals in a rock are of simultaneous
formation and states that...."One of the fundamental branches
of plutonic geology is concerned with textures as indicating
the time relationship of rock components...." Textural
analysis is based on the presence of relics of older metamorphic
events preserved in the textures of younger metamorphic events.
The techniques have been developed gradually since Clough and
Hill (1897) first noticed that.... "inclusions in albite
porphyroblasts run in different directions from the foliation

of the rocks enclosing them.... there is the suggestion that
the albite may have received a twist...." Structures produced
during deformation can be used as relative time markers to
date metamorphic mineral growth. Where one structure is
produced three possible periods of crystal growth may be
recognised; prior to deformation, during deformation, and
after deformation. Similarly where two sequential structures
are produced, five periods may be recognised. Different
terminologies exist in the literature since some workers have
used structures to date mineral growth whilst others have
used mineral growth to date structures. The terminology of
Spry (1963) shown in Table 5-1 is used throughout this thesis.

TABLE 5-1. Different terminologies for the time
relationships between deformation and
crystal growth.

Read (1949)	Spry (1963)	Zwart (1962)
Post-crystalline deformation	Pre-tectonic crystal growth	Pre-kinematic crystal growth
Para-crystalline deformation	Syn-tectonic crystal growth	Syn-kinematic crystal growth
Pre-crystalline deformation	Post-tectonic crystal growth	Post-kinematic crystal growth

Fig. 5-1 illustrates some of the typical textural
relationships used to date the growth of minerals; the
techniques are particularly applicable to metamorphosed
pelitic rocks because of the wealth of porphyroblasts usually
present. The inclusion fabric of a porphyroblast is convention-
ally termed S_i (internal) while the external fabric is termed
S_e.

By the use of these textural techniques some interesting
accounts have been given on the interplay of metamorphism and
deformation in many metamorphic terrains e.g. in the Scottish
Highlands (Read, 1952; Johnson, 1968), in the European Alps

Pre-tectonic mineral growth

S_i

S_e

S_i

S_e
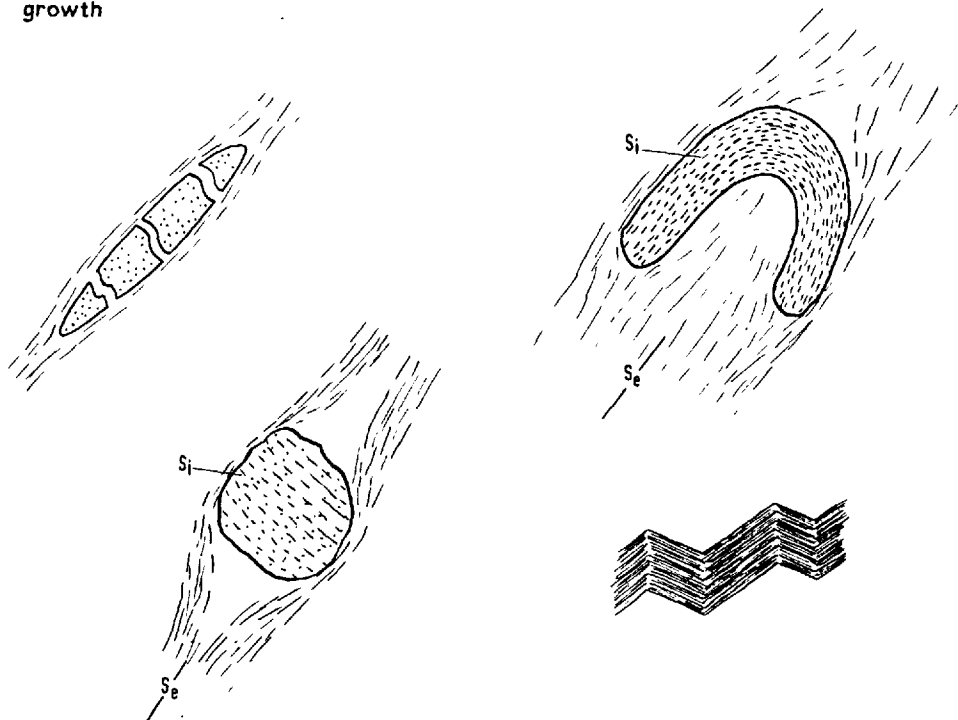
Syn-tectonic mineral growth
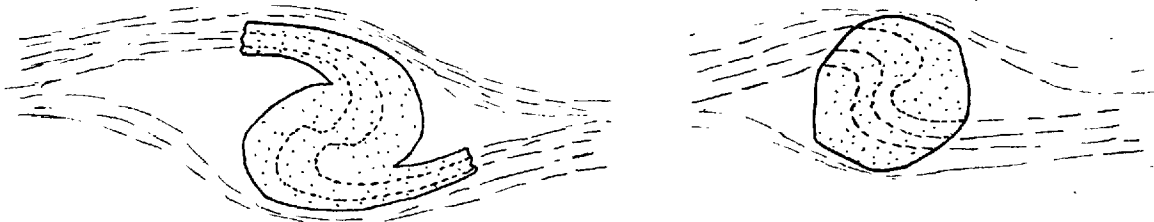
Post-tectonic mineral growth
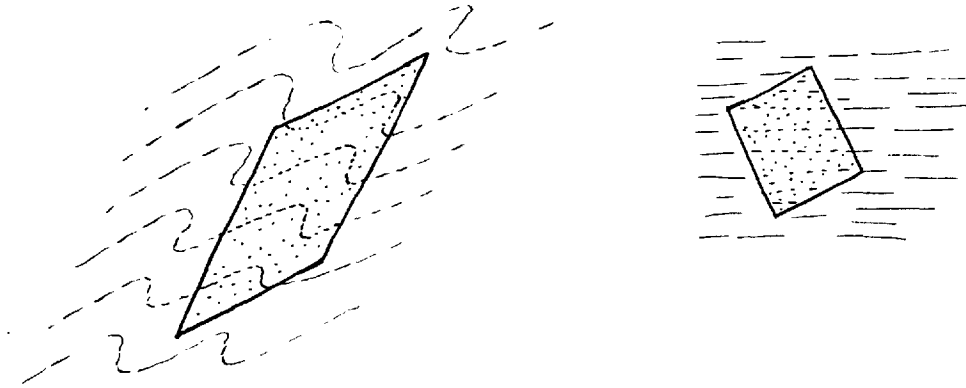
FIG. 5-1

Textures illustrating some time relationships between mineral growth and deformation.

(Zwart, 1958, 62,63; Read,1967b) and in Tasmania (Spry, 1963).
Few serious systematic studies along the same lines appear to
have been made on sulphide orebodies in metamorphosed rocks. A
number of accounts of metamorphic effects recognised in opaque
minerals in sulphide ores has appeared in recent years e.g.
Moh et al. (1963), Kinkel (1962, 67), Kalliokoski (1965),

Han (1968) and Markham (1968), but many of these authors
either give a list of the metamorphic features they have
observed, or else relate in a general way mineral textures
to schistosity surfaces or fractures. Little attempt has
been made at integrating the opaque mineral textures into the
detailed deformational and metamorphic history of the enclosing
rocks

B. ROCKS OUTSIDE THE ALTERATION ZONES

1. Quartz-Feldspar Schists

Very uneven grain size, irregular grain boundaries, and
severe internal strain in the larger grains indicate consider-
able textural disequilibrium in the quartz-feldspar schists.
Typically, these rocks display a mortar-type texture of
large grains or poly-grains of quartz and plagioclase set in
an interstitial matrix of quartz, feldspar, and oriented
brown biotite (figs. 5-2a,b). Muscovite flakes where present,
generally cut across the biotite trends. Accessory minerals
include a few small pale pink subhedra of garnet, thin needles
of rutile within some larger quartz grains, small prisms of
monazite and apatite and ragged to prismatic brown to green
tourmaline.

Unlike the even grained quartzo-feldspathic schists
25 miles to the northeast (White, 1956), metamorphic reconsti-
tution of these arenaceous rocks appears far from complete.
It is difficult to prove that the larger quartz and feldspar
grains are detrital but the evidence pointing in this direction
are (a) the larger unstrained grains are surrounded by slightly
strained to unstrained matrix minerals and (b) metamorphic

FIG. 5-2
(all photographs taken in transmitted light)

(a,b)   Photomicrographs showing the characteristic mortar
        texture of the quartz-feldspar schists. The first
        picture is in plane polarized light and the second
        under crossed nicols. Recrystallization of the quartz
        grains (clear phase) and the cloudy feldspar (arrow)
        is predominantly along the external grain boundaries.
        The rough alignment of biotite laths that have
        formed from the clay matrix defines the schistosity
        S_1. Dark grain at left is a detrital? monazite crystal.

(c)   Post-tectonic chlorite flake growing across the S_1a
        schistosity. Elongated inclusions of quartz and
        ilmenite preserve the schistosity trends within the
        chlorite. Extremely elongated dark material along
        the cleavages of the chlorite is rutile that
        probably formed with the chlorite during the break-
        down of biotite. Transmitted plane polarized light
        (PPL).

(d)   Garnet porphyroblast in coarser grained S_1b quartz-
        biotite matrix. There is a small central zone in
        the garnet containing sub-planar quartz inclusions,
        but the sigmoidal quartz and ilmenite inclusion
        fabric in the outer zone indicates a period of syn-
        tectonic garnet growth. Dark pleochroic haloes in
        the biotite are formed around minute radioactive
        inclusions of monazite. Section cut perpendicular to
        schistosity and parallel to the lineation.
        Transmitted PPL.

(e)   Disseminated pyrrhotite/chalcopyrite grains (black)
        along the S_1b schistosity surfaces. A large post-
        tectonic andalusite porphyroblast has replaced the
        biotite (medium grey) but has grown around and not
        affected the sulphide grains. Other minerals are the
        rounded garnets (G) and fractured staurolite (St).
        Transmitted ordinary light.
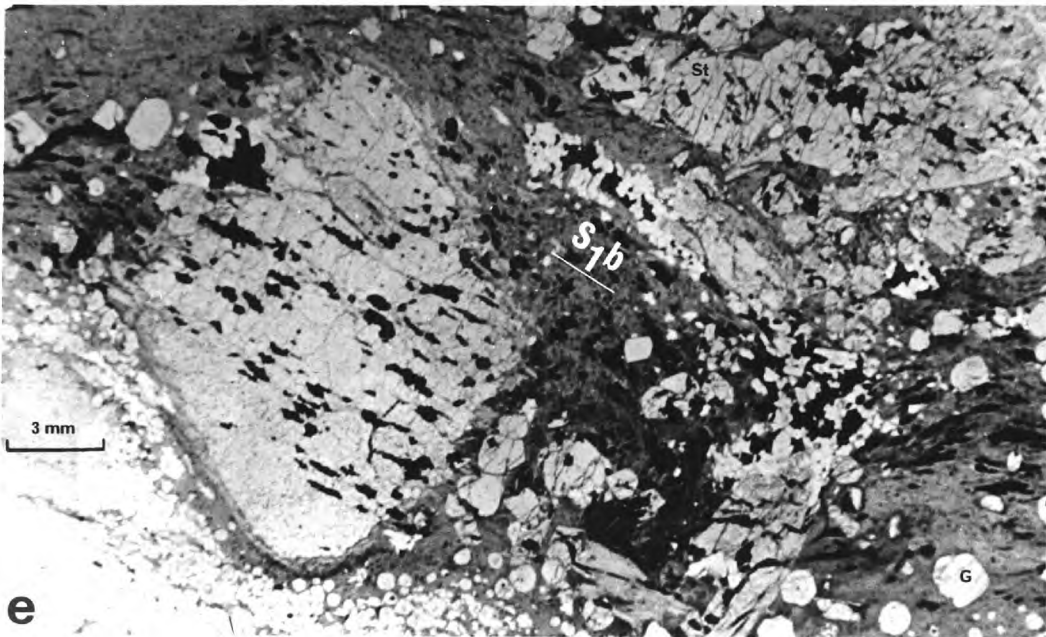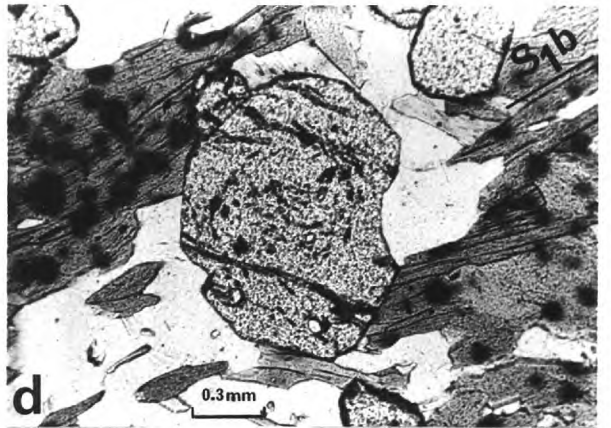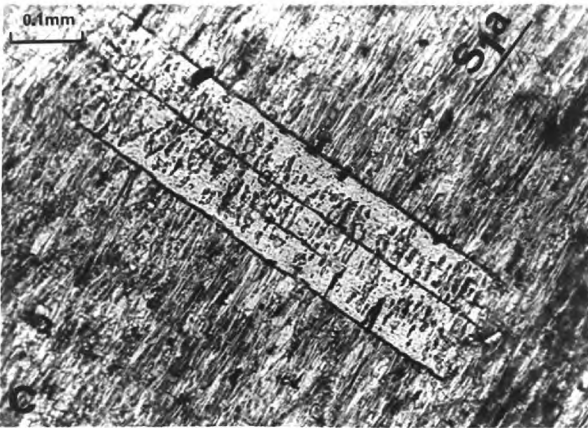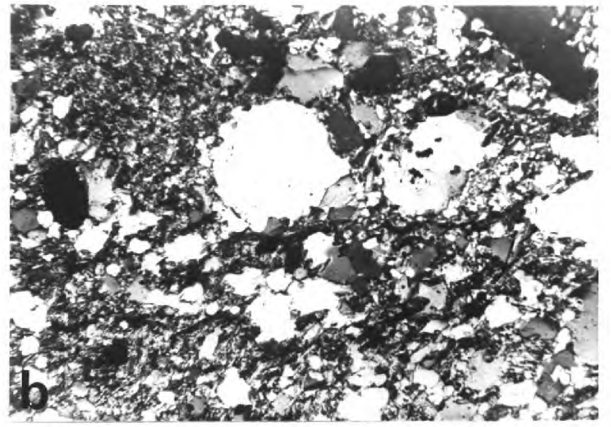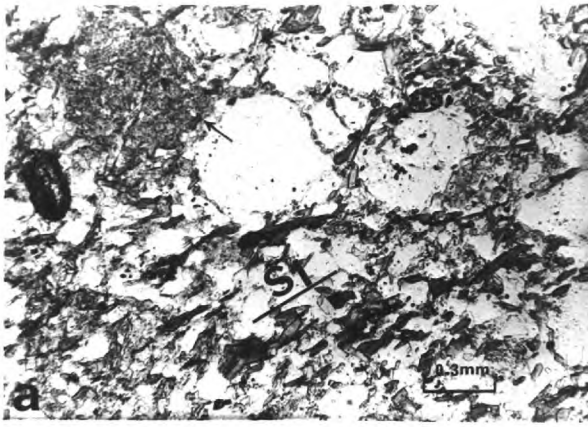
FIG.5-2

minerals such as the micas and garnets grow through the matrix and are never found along the interfaces of the quartz poly-grains.

2. Quartz-Mica and Andalusite-Staurolite Schists

It is convenient to describe these two rock-types together because (a) each is interbanded to a limited extent in the other, (b) they differ in mineralogical proportions but not in mineral assemblages, and (c) there are important contrasts in matrix-porphyroblast relationships depending on the matrix grain-size. The rocks as a whole can therefore be divided into two groups based on the coarseness of the matrix.

(a) Finer Grained Types

The finer grained micaceous rocks are restricted to the outer parts of the area near the contacts with the arenaceous rocks. The matrix is made up of a lepidoblastic intergrowth of highly elongate biotite, muscovite and quartz (see fig. 3-2a). Other minerals include minor garnet, andalusite, chlorite and accessory ilmenite, monazite and tourmaline. Feldspar is rare.

Micas show no tendency to swing around garnets but stop abruptly at their margins; elongate quartz and ilmenite grains continue through the crystal as inclusions (fig. 5-3a). Chlorite displays the same matrix relationships (fig. 5-3b). Clearly both these phases have grown by replacement after the formation of the S_1 fabric and are therefore post-tectonic to B_1. Fig. 5-2c shows two intersecting oxide inclusion trends in a post-S_1 chlorite porphyroblast. The opaque grains parallel to the external fabric are mechanical inclusions of ilmenite whereas the dark, elongate phase along the chlorite basal planes is rutile. This rutile probably formed from the titanium released from the biotite lattice during its replacement by chlorite.

Scattered through the finer grained micaceous schists are a number of augens composed of a fine mosaic of quartz plus possible feldspar accompanied by varying amounts of biotite, muscovite, tourmaline, chlorite and dusty iron oxides. Many augens possess a small core of an unknown, pale-brown

FIG. 5-3

Textural Relations of Porphyroblasts in Fine-grained Schists

(a) Post-tectonic garnet porphyroblasts in an S_1a matrix. Light inclusions are quartz and dark inclusions ilmenite.

(b) Post-tectonic chlorite porphyroblast in S_1a matrix.

(c) Quartz-rich augens in fine-grained schist. In sections cut perpendicular to the schistosity and parallel to the lineation (first sketch) the augen mica fabric is continuous with the external schistosity and suggests syn-tectonic growth. Augens cut perpendicular to the lineation generally display a network mica intergrowth (second sketch).

(d) Post-tectonic andalusite porphyroblasts in fine-grained schists. The andalusites are intimately associated with augens and in many cases completely or partially replace them.

(a)

0.2 mm

$-S_1a-$

(b)

0.2 mm

$-S_1a-$

(c)

1.0 mm

1.5 mm

S_1a

(d)
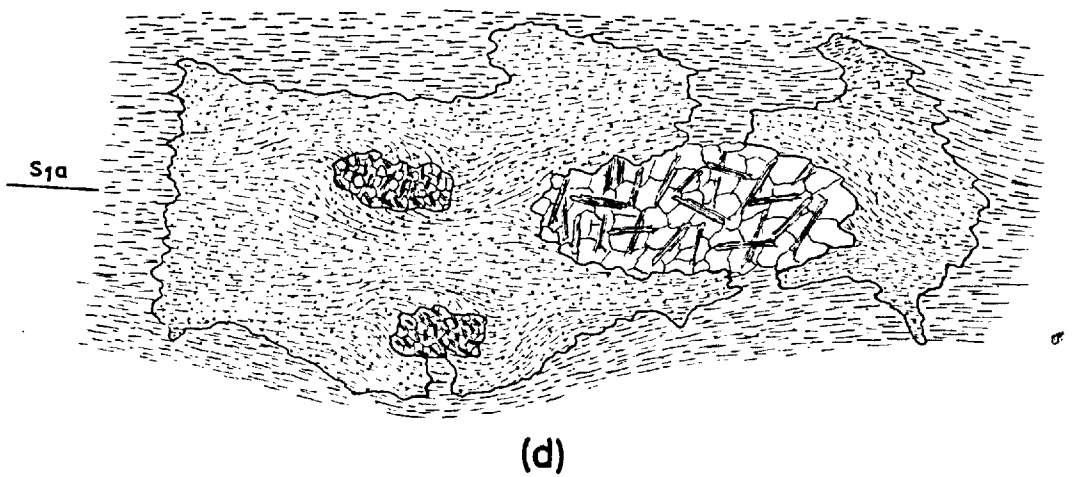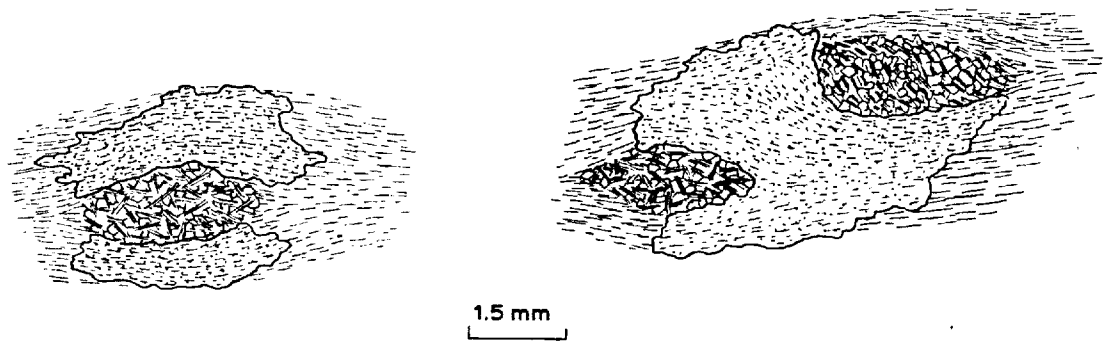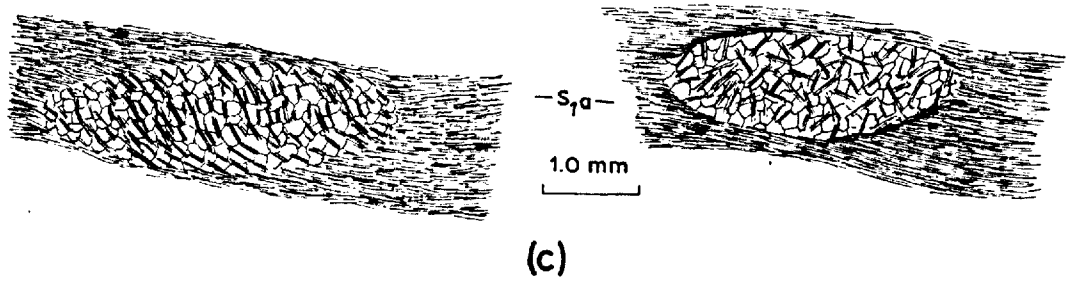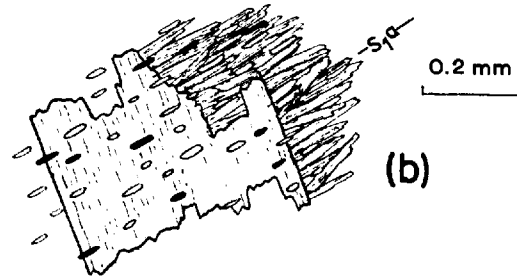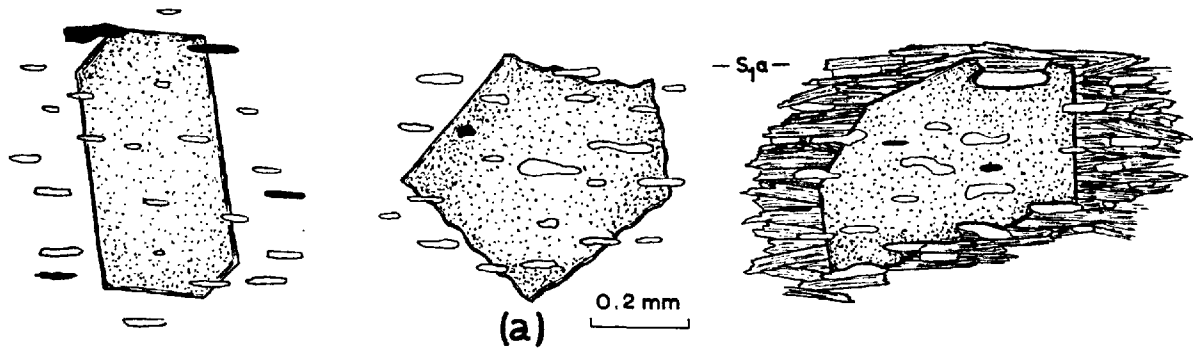
FIG. 5-3

faintly crystalline substance that is either isotropic or ultra fine-grained. The external schistosity swings rather weakly around most augens which internally, display both an erratic network of micaceous laths and sigmoidal mica patterns concordant with S_e (fig. 5-3c). Both types of internal fabric may be found in a single section although the sigmoidal pattern is more common in sections cut perpendicular to the foliation and parallel to the lineation. Such relationships indicate that the augens were formed during the deformation that produced the external schistosity, therefore they are syn-tectonic to B_1. The exact origin of the augens is not known but it would seem likely that they are either alteration products of a former syn-tectonic mineral i.e. cordierite, or represent some kind of concretionary growth feature.

Although the augens occur alone, any andalusites in these fine grained rocks are generally intergrown with them (fig. 5-3d). Important features of these andalusites relevant to their time of growth are as follows: (1) S_e tends to swing around the augens but passes unhindered through the andalusite i.e. S_i is concordant with S_e, (2) there may be slight flattening of the external fabric around some andalusites but the size of external matrix grains and inclusions is very similar, (3) andalusite appears to be replacing and inheriting the fabric of some augens, and (4) in some andalusite porphyroblasts the inclusion fabric if interpreted as a syn-tectonic one pre-supposes opposite senses of rotation during the growth of a single crystal - clearly this is impossible. It seems reasonable to conclude that the andalusites are post-tectonic to B_1 and that they grew in a favourable chemical environment somehow associated with the pre-existing augens. The "folded" andalusite inclusion fabrics are therefore truly helicitic in that they represent a pre-existing folded surface.

(b) Coarser Grained Types

The matrix of these rocks is made up of a lepidoblastic intergrowth of varying proportions of biotite, muscovite and quartz (see fig. 3-2b). Important features of the larger andalusite prophyroblasts (fig. 5-4a) that occur in these rocks

FIG. 5-4

Porphyroblastic Minerals in Coarser-grained Schists

(a) Zoned andalusite porphyroblasts in S_1b quartz-
mica matrices. In the inner zones the quartz, mica
and oxide inclusions are very small and clearly
discordant with S_1b; this indicates that the andalusite
cores are pre-tectonic to S_1b. This inner inclusion
fabric is very similar to the fabric in the andalusites
in fig. 5-3d and suggests that these andalusite cores
are of a similar i.e. early post-S_1a age. The outer
andalusite zones contain much coarser inclusions and
probably vary in age from early syn-S_1b to post-S_1b.
Note the coarse granular quartz and a few large
muscovite flakes associated with andalusites; some
of this material migrated into pressure shadow zones
during tectonism but much of the muscovite appears
to have formed during post-S_1b alteration of andalusite.

(b) Garnet porphyroblasts in coarser-grained schists.
In the upper sketch the rims of the garnets appear to
be post-tectonic to the S_1b biotite fabric. The garnet
cores contain fine quartz and ilmenite inclusions in
planar fabrics having orientations that vary from grain
to grain; this suggests a pre-S_1b age for the inner
zones. The lower sketch shows large garnets included
in a poikiloblastic andalusite but it is difficult to
decide which mineral is the earlier.

(c) Post-S_1b staurolite porphyroblasts displaying euhedral
faces against biotite but irregular boundaries against
quartz aggregates (first sketch) and andalusite (lower
part of second sketch); the quartz inclusions formerly
in the andalusite are inherited by the staurolite.
Note how garnet always displays its crystal faces
towards staurolite (upper part of second sketch).

(d) Folded garnet bands in medium-grained lode schists. In
the first example the garnets are late syn-tectonic to
post-tectonic with respect to S_1b, but in the second
fold garnet growth is clearly pre-tectonic to S_1b.

(a) 2.0 mm

(b) 0.3 mm

(c) 0.7 mm

(d) 0.5 mm

(e)
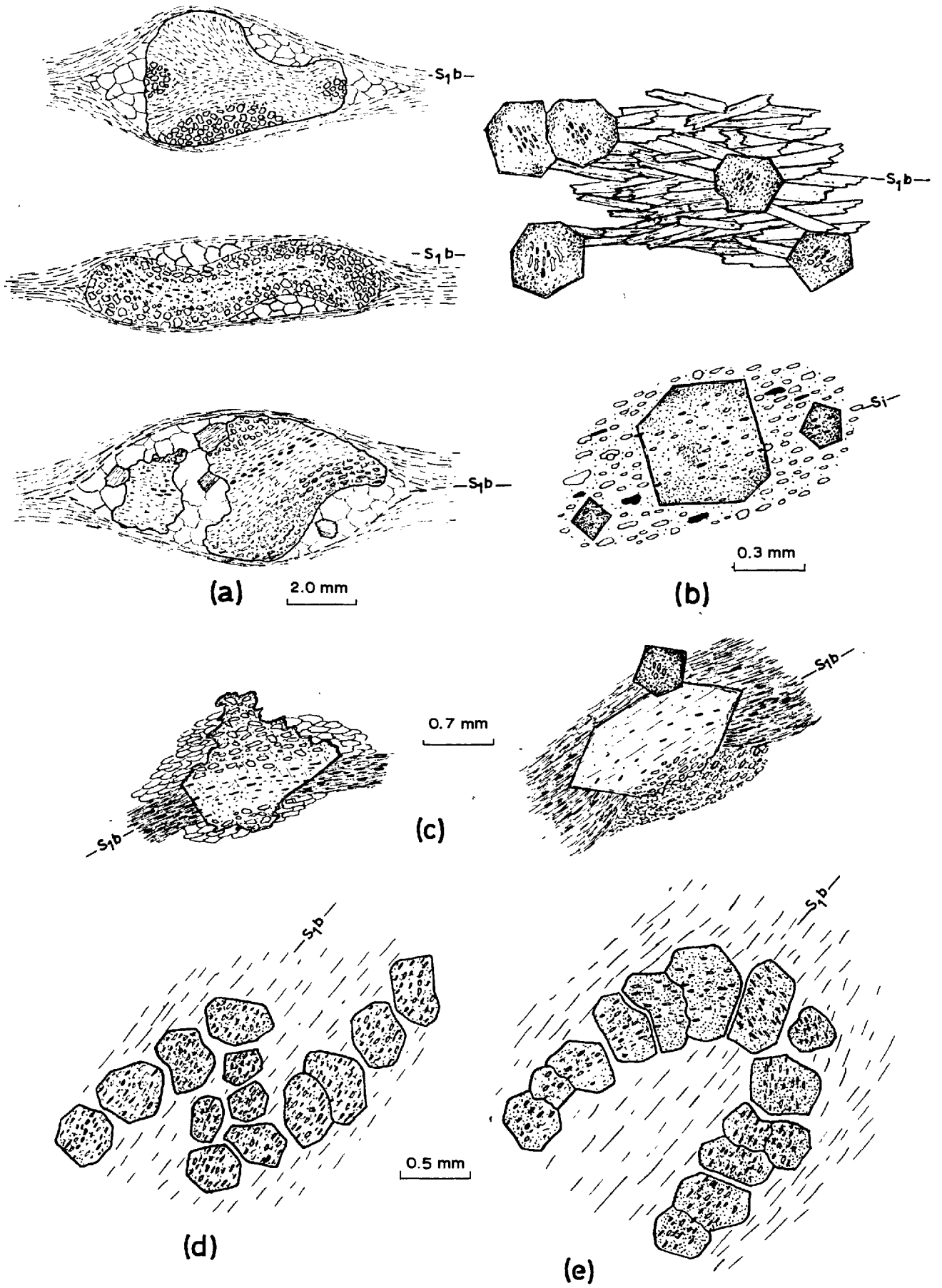
FIG. 5-4

are: (1) S_e always swings around the crystals and the resulting pressure shadow zones are filled with coarse granular quartz $\pm$ muscovite, (2) the crystals are usually zoned with a core of fine grained inclusions and a rim or partial rim of coarser grained inclusions, (3) the core inclusion size is similar to that of the non-zoned andalusites in the finer grained rocks (fig. 5-3d) while the rim inclusions approach the size of the adjacent matrix, (4) the core fabric is always discordant with S_e while the rim fabric is concordant or else indistinct, and (5) the core fabric frequently displays opposing senses of rotation in a single grain. Clearly these andalusites display two intermittent stages of growth; the cores are older than the schistosity while the rims are about the same age as the schistosity. It would seem reasonable to interpret the similarities between these andalusite cores and the andalusites of the finer grained schists as indicating similarity in age. But it has been shown that the axial plane schistosity and mineral lineation over the whole area have constant orientations yet andalusite apparently of the same age, is post-tectonic to S_1 in some areas and pre-tectonic to it in others. The only feasible explanation seems to be that the age of the schistosity surface varies throughout the area. The interpreted sequence of events in table 4-3 must therefore be modified; henceforth the deformation event (events) attending the development of the finer grained "phyllitic" schists is termed B_1a and the resulting schistosity surface S_1a. The second deformation event associated with the coarser matrix is termed B_1b and the coarser schistosity S_1b.

Garnets are rather larger and more numerous than in the fine-grained rocks and they occur as subhedral to euhedral grains through both the matrix and andalusite porphyroblasts. All garnets contain trains of small quartz and ilmenite inclusions in their central regions but the rims are generally inclusion-free. The inclusion fabric of garnets within andalusite porphyroblasts is continuous with the host internal fabric so

there is little indication of relative age (fig. 5-4b). Out-side the andalusite, the garnet core fabric is oriented at all angles to the S_1b micas that stop abruptly at the garnet margins. The cores are therefore probably pre-B_1b and the rims post-B_1b in age. Evidence for a syn-B_1b age for some garnets is shown in the section viewed perpendicular to the schistosity and parallel to the lineation in fig. 5-2d; sub-planar quartz inclusions in the core are followed outwards by a spiral pattern of ilmenite and quartz inclusions that indicates rotation of the crystal during growth.

Porphyroblasts of staurolite up to 1 mm in length display varying degrees of morphological perfection depending on the material with which they are in contact (fig. 5-4c). Staurolite exhibits well developed crystal faces against biotite which is always truncated and not deflected at the porphyroblast margin. In some places staurolite appears to be replacing andalusite and inheriting its inclusion fabric but the staurolite-garnet relationships are usually difficult to interpret. In any case, staurolite is a post-tectonic mineral and is probably late post-B_1b in age (see fig. 5-5e).

3. Quartz-Biotite-Garnet Lode Schists

The matrix of the unaltered lode schists is richer in quartz, poorer in biotite and generally lacking in muscovite compared with the other schists. But the similarity of matrix grain size of these rocks with the other coarser grained schists indicates that the schistosity surface is probably S_1b. The only additional textural information obtained from these rocks is on the age of the garnet that occurs commonly in isoclinally folded bands around the schistosity surface.

Fig. 5-4d shows garnets having a planar to gently curved inclusion pattern that has a constant orientation everywhere in the fold. S_i is continuous with S_e. Such relationships indicate late syn-tectonic to post-tectonic garnet growth.

In the second example shown in fig. 5-4e, many of the garnets are in contact with one another and the continuous inclusion fabric follows faithfully around the fold profile. Growth of this garnet is clearly pre-tectonic to S_1b. Such an almost solid garnet band should have considerable rigidity and is likely to have deformed by buckling rather than by the passive rotation of individual garnet grains.

4. <u>Matrix Age Relationships</u>

The preferred orientation of the matrix forming minerals quartz, biotite, muscovite and (in places) disseminated opaque minerals, defines the structures and therefore the time markers on which depends the interpretation of the age relationships of the porphyroblasts. It would therefore seem necessary to consider briefly the age of the matrix irself.

According to Flinn (1965), the rapid increase in the number and activity of crystallographic defects in minerals produced by the application of differential stress to rocks, considerably speeds up the diffusion rates of atoms that in turn hasten recrystallization and chemical reactions. Deformation proceeds through repeated straining and recrystallization of some existing phases and by the growth of new phases at the expense of chemically less stable older ones. Harris and Rast (1960) point out that the increasing inclusion size from the centre to the outside of syn-tectonic garnet proves that the matrix grain size coarsens during deformation.

The anisotropic matrix fabric developed is a combination of the elongated shape of minerals like quartz and the parallel growth of platy minerals like biotite and muscovite, but the precise age of these minerals relative to the cessation of metamorphism is difficult to determine. It seems likely that the oriented matrix minerals undergo final recrystallization in the presence of at least a weak differential stress field since clearly post-tectonic minerals are able to grow at any angle to the schistosity surface.

C. DISSEMINATED MINERALIZATION

1. Grain Boundary Relationships

Although disseminated sulphide and oxide grains show an increase in size as the silicate matrix coarsens, their shapes and grain boundary relationships are largely independent of grain-size. Pyrrhotite is the dominant sulphide while chalcopyrite and sphalerite occur in minor, more or less equal amounts. Oxides are represented almost exclusively by ilmenite.

No matter whether a sulphide grain is a single crystal, a polycrystal or a multiphase aggregate, it is always flattened in the plane of the schistosity and its long dimension is generally parallel to the lineation. This preferred dimensional orientation is not accompanied by any obvious preferred crystallo- graphic orientation. Representative sulphide-silicate inter- growths are illustrated in fig. 5-5a. Sulphide-mica interfaces are usually planar along the mica (001) cleavage direction but moderately interpenetrating across the mica end terminations. Both muscovite and biotite are optically unchanged in the presence of sulphides and the latter mica, shows red-brown to pale fawn pleochroism right up to the sulphide boundary. Gently curving to planar sulphide-quartz interfaces are very similar to quartz-quartz interfaces and there is little tendency for sulphides to tongue along silicate grain boundaries or vice versa. Ilmenite grains, which are generally smaller than the associated sulphides, occur as single platy crystals oriented with their basal (0001) faces parallel to the mica (001) planes (fig. 5-5b). Ilmenite-mica end terminations are irregular to strongly interpenetrating but ilmenite generally displays both its planar basal faces as well as its prismatic faces against quartz. In some of the S_1b fabrics, a few larger ilmenite subhedra have grown across the schistosity surface.

If the sulphide grains plus quartz were to be grouped as phase A and ilmenite plus micas as phase B, clearly the resulting fabric would be typically lepidoblastic one. Thus it does not seem unreasonable to suppose that all these minerals

FIG. 5-5

Textural Relationships Between Disseminated Ore Minerals
and Silicates

(a) Pyrrhotite-rich sulphide grains (stippled) inter-
     grown with lepidoblastic quartz (clear) and mica.

(b) Disseminated ilmenite (cross-hatched) intergrown
     with lepidoblastic quartz and mica.

(c) Intergrowths of disseminated sulphides (light stipple)
     with post-tectonic garnet in fine-grained schists.

(d) Intergrowths of sulphides with garnet porphyroblasts
     in coarser-grained schists.

(e) Elongated sulphide grains trapped within post-tectonic
     staurolite (clear) and garnet (heavy stipple). The
     helicitic sulphide inclusion fabric suggests that the
     rocks were slightly deformed after the formation of
     S_1b but prior to staurolite and garnet growth.

(a)

0.15 mm

(b)

0.1 mm

(c)

0.2 mm

(d)

0.3 mm

(e)

1.2 mm

S_1b
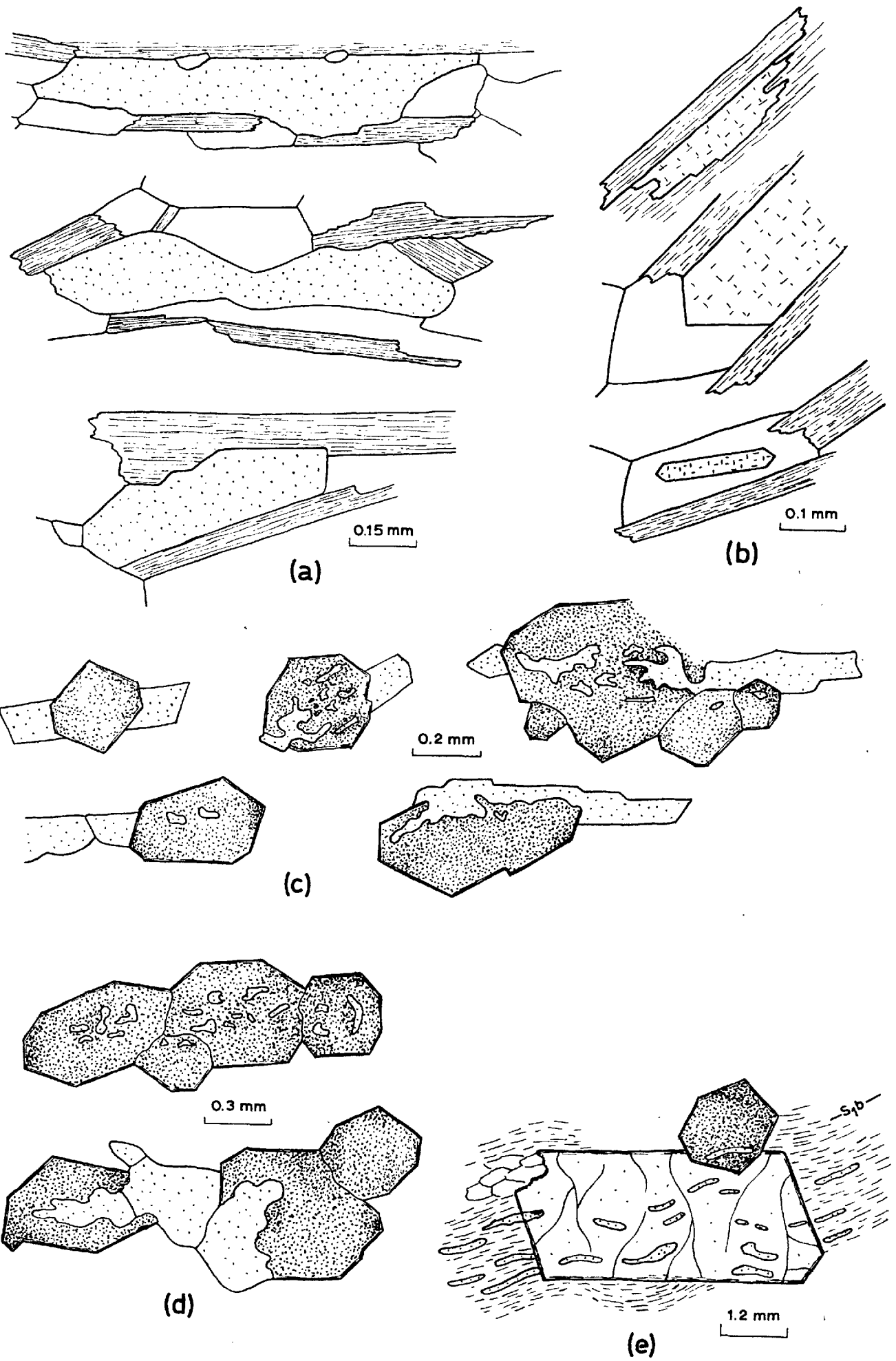
FIG. 5-5

and their intergrowths have developed more-or-less simultaneously.

2. Intergrowths with Porphyroblasts

(a) Garnet

Garnets in both S_1a and S_1b matrices display near perfect euhedral outlines in contact with the micas but generally subhedral boundaries in contact with quartz. Important features of garnet-sulphide intergrowths in the finer grained schists (fig. 5-5c) are as follows; (1) garnet oulines are both euhedral and irregular towards external sulphides but are always irregular towards internal sulphides, (2) sulphide inclusions are often but not always accompanied by external sulphide grains, (3) sulphide inclusions tend to be distributed in zones parallel to the schistosity rather than scattered erratically through the garnet, and (4) the shallow penetration of most external sulphides into the garnets (where this does occur) suggests that most of the inclusions are physically isolated grains, i.e. they are not two dimensional intersections of sulphide tongues. Again the sulphides appear to have acted essentially as a matrix phase in being trapped within the growing garnets. In the coarser grained rocks both the external sulphides and the garnets themselves are rather larger (fig. 5-5d). The sulphide inclusions concentrated in the central regions of the garnets are similar in size to those in the finer grained rocks. Some ilmenite-garnet relationships are illustrated in figs. 5-2d and 5-3a.

(b) Andalusite and Staurolite

Minute ilmenite laths pass through post-B_1a andalusite in fig. 5-3d but the non-coincidence of andalusite and sulphides in these fine-grained schists prevents their textural relations being studied. An example is given in fig. 5-2e of a disseminated sulphide - andalusite intergrowth in a coarser grained schist. The sulphide grains lie along the S_1b schistosity and clearly pre-date the growth of the andalusite porphyroblast that partially encloses them. A similar relationship is shown between disseminated sulphides and the staurolite crystal in

fig. 5-5e; in this example S_1b had been slightly crenulated prior to the growth of the staurolite as is evident from the helicitic sulphide inclusion fabric within the porphyroblast.

3. Internal Structures of Grains
(a) Sulphides

Pyrrhotite, the dominant sulphide, may occur alone as apparently homogeneous anhedral single crystals or polycrystals (fig. 5-6a) or else intergrown with minor chalcopyrite and small amounts of other sulphides. Pyrrhotite grain boundaries vary from strongly curved to essentially planar, and $120°$ dihedral angles at triple junctions appear to be rare.

Pyrrhotite-chalcopyrite intergrowths are extremely varied (fig. 5-6b). The important geometrical relationships are (1) chalcopyrite occurs almost always as a single grain at any position along the margin of the sulphide grain or totally enclosed within it, (2) the continuity of the sulphide grain margin is unaffected in passing from one sulphide phase to another, (3) pyrrhotite-chalcopyrite interfaces are usually gently curved although they vary from planar to finely sutured, (4) judging from cross-sectional shapes, chalcopyrite varies in habit from irregular bodies to near euhedral plates, and (5) the plates are always internal although they may be continuous with anhedra along the grain margin. These intergrowths appear inconsistent with either the attainment of internal textural equilibrium (a matter of days for chalcopyrite at a temperature of $200°C$ according to Stanton and Gorman, 1968) or the replacement of either phase by the other (why is there only a single grain of each phase present?). More likely, the sulphide grains were formerly single or double Fe-Cu-S solid solutions and the present textural relations arose by unmixing and segregation phenomena during cooling.

Intergrowths of other minor sulphide phases that are common in the disseminated mineralization are illustrated in fig. 5-6c. Pentlandite is found as small flame-like bodies as well as oriented lamellae through pyrrhotite whilst ragged

<u>FIG. 5-6</u>

<u>Internal Microstructures of Disseminated Sulphides</u>
<u>and Oxides</u>

(a) Polycrystalline microstructures in some pyrrhotite
     grains.

(b) Two-phase sulphide grains made up of pyrrhotite and
     a single sub-grain of chalcopyrite.

(c) Multiphase sulphide grains. Pentlandite blebs
     are confined to pyrrhotite while both sphalerite
     and mackinawite are always in contact with or
     enclosed in chalcopyrite.

(d) Very rare two-phase sulphide grains consisting of
     pyrrhotite and galena.

(e) Polycrystalline ilmenite grains in calc-silicate
     schist. Much of the ilmenite is partially replaced
     by sphene.

(a)

0.15 mm

(b)

0.15 mm

(c)

0.1 mm

(d)

0.15 mm

(e)

0.15 mm
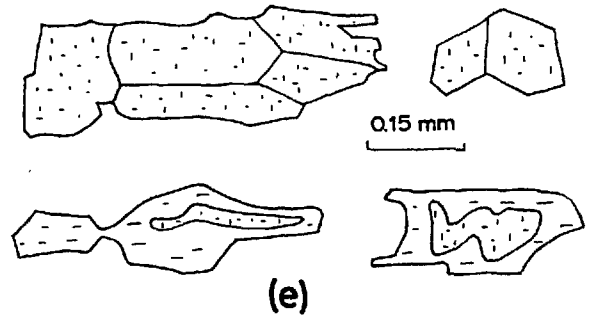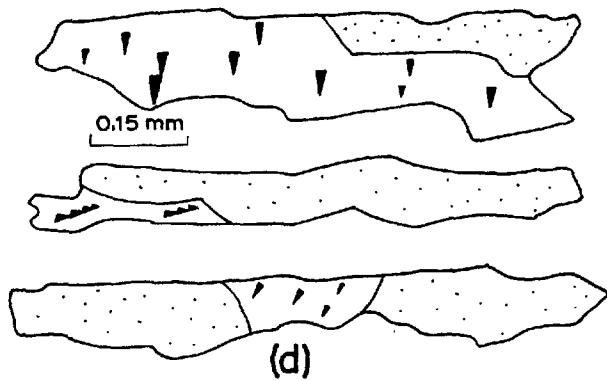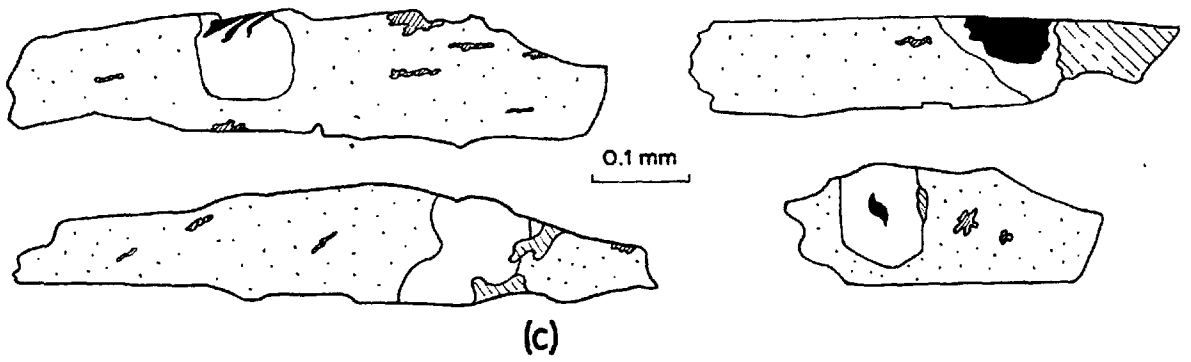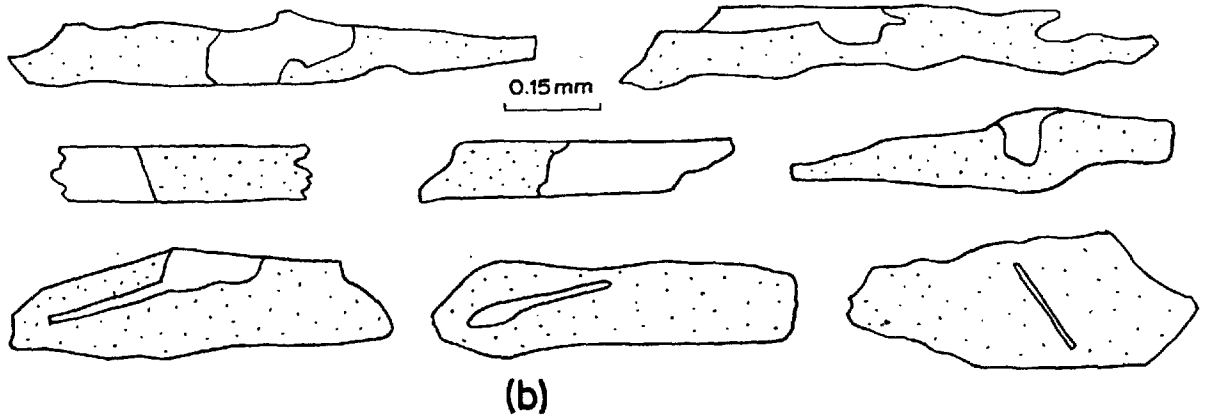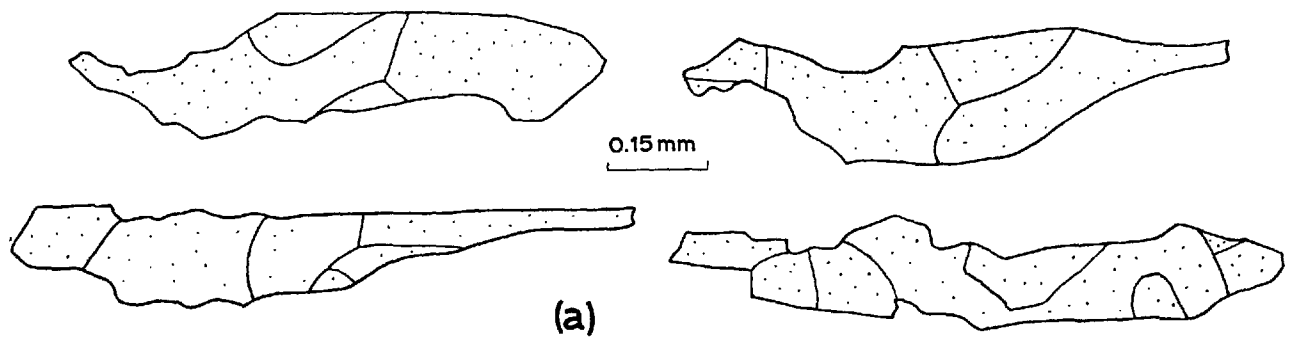
	Pyrrhotite		Sphalerite
	Chalcopyrite		Galena
	Mackinawite		Ilmenite
	Pentlandite		Sphene

FIG. 5-6

grains of sphalerite and wisps of mackinawite (tetragonal FeS)
are located along chalcopyrite-pyrrhotite or chalcopyrite-
silicate interfaces and within chalcopyrite grains. Sphalerite
may in turn contain minute lamellae of chalcopyrite. Any exsolution
history is evidently much more complex than can be explained by
phase relationships in the Cu-Fe-S system alone. Galena is
a very rare phase in the disseminated mineralization but where
present it is intergrown with pyrrhotite in a similar manner to
chalcopyrite (fig. 5-6d).

(b) Oxides

Ilmenite grains are generally homogeneous single crystals
except for a few visibly bent grains that display oblique
lamellar twinning presumably along the (01$\bar{1}$2) planes (Berry
and Mason, 1959). Another exception is the ilmenite in the
thin calc-silicate schist bands where some single crystals
and polyhedral ilmenite aggregates are replaced and pseudo-
morphed in varying degrees by sphene (fig. 5-6e).

D. ROCKS IN AND ADJACENT TO THE ALTERATION ZONES

1. General Statement

As this section covers localized mineralogical and
textural modifications of existing metamorphic rocks, it is
convenient to discuss the post-B_1b stage of the metamorphic
history in terms of mineral development rather than the large
variety of minor rock-types developed. The exact nature and
number of local movements (the B_2 tectonic phase) associated
with the formation of the alteration zones is difficult to
determine but it appears likely that movements began soon after
the B_1b event and continued intermittently until the end of
chloritization. Many of the new mineral intergrowths have
apparently formed under tectonically static conditions since
the micas show no preferred orientation. In parts of the
alteration zones and nearby rocks where a schistosity has
been preserved by the parallel growth of new micaceous minerals
either mimetically or during deformation, the same minerals
probably grew simultaneously in adjacent, non-deforming areas

in non-parallel orientation. As a result mineral-penetrative
structural relationships have limited use for dating mineral
growth; deductions are based largely on inclusion textures and
mineral associations.

2. Andalusite

Growth of andalusite continued after the B_1b tectonic
phase (fig. 5-2e) but appears to have ceased before or during
the first B_2 movements when andalusite began to be extensively
replaced by other phases.

3. Biotite-Garnet-Staurolite

These three phases constitute the bulk of the melanocratic
minerals in the alteration zones and display a variety of inter-
relationships according to the degree of overlapping growth.

(a) Biotite

Coarse-grained biotite is pleochroic from dark red-
brown to pale fawn and shows three main growth habits; first
there is the schistose biotite found in zones cross-cutting and
often obliterating folded S_0 banding (fig. 5-7b), secondly
there is the network intergrowth of platy crystals of the type
shown in fig. 5-7a, and thirdly there are the large, erratically
oriented, amoeboidal biotite porphyroblasts replacing quartz
and andalusite in schists adjacent to the alteration zones
(figs. 5-8a,b). The large numbers of pleochroic halos are
caused by radiation damage from the small prismatic inclusions
of monazite.

(b) Garnet

Red to pink almandine-rich garnet is a persistent
porphyroblastic mineral that appears to have grown or to have
remained stable over a large part of the metamorphic history.
Post-B_1b garnets are common throughout most of the unaltered
coarser grained schists but seldom have the crystals reached
more than 0.75mm in size. The sudden increase in garnet size
to 2-5 mm in the alteration zones is typified in fig. 5-7b
where folded bands of pre-S_1b garnets are truncated by a zone
of coarsely intergrown biotite and post-B_1b garnet. Isolated

FIG. 5-7

Silicate Intergrowths In and Near Alteration Zones

(a) Non-schistose aggregate of biotite, garnet (stippled)
     and staurolite. Both staurolite and garnet appear
     to have grown at the expense of biotite but the
     staurolite-garnet relationships are usually
     difficult to determine.

(b) A folded garnet band in unaltered quartz-garnet-
     biotite lode schist is truncated and obliterated
     by an alteration zone containing coarse-grained
     garnet and poorly schistose biotite; no quartz
     is present.

(c,d) Late post-tectonic growth of garnets and staurolite
       in lode schists adjacent to an alteration zone.

(e) Intensive alteration of an andalusite poikiloblast
     to coarse-grained aggregates of muscovite.
     Granular material is quartz.

(f) A large muscovite porphyroblast growths across and
     largely replaces schistose biotite, and corrodes
     both staurolite and garnet (stippled) porphyroblasts.

(a) — scale: 1.0 mm

(b) — S₁b — Alteration zone. — S₁a? — scale: 0.7 mm

(c) — scale: 1.5 mm

(d) — S₁b — scale: 0.5 mm

(e) — scale: 0.5 mm

(f) — scale: 0.6 mm
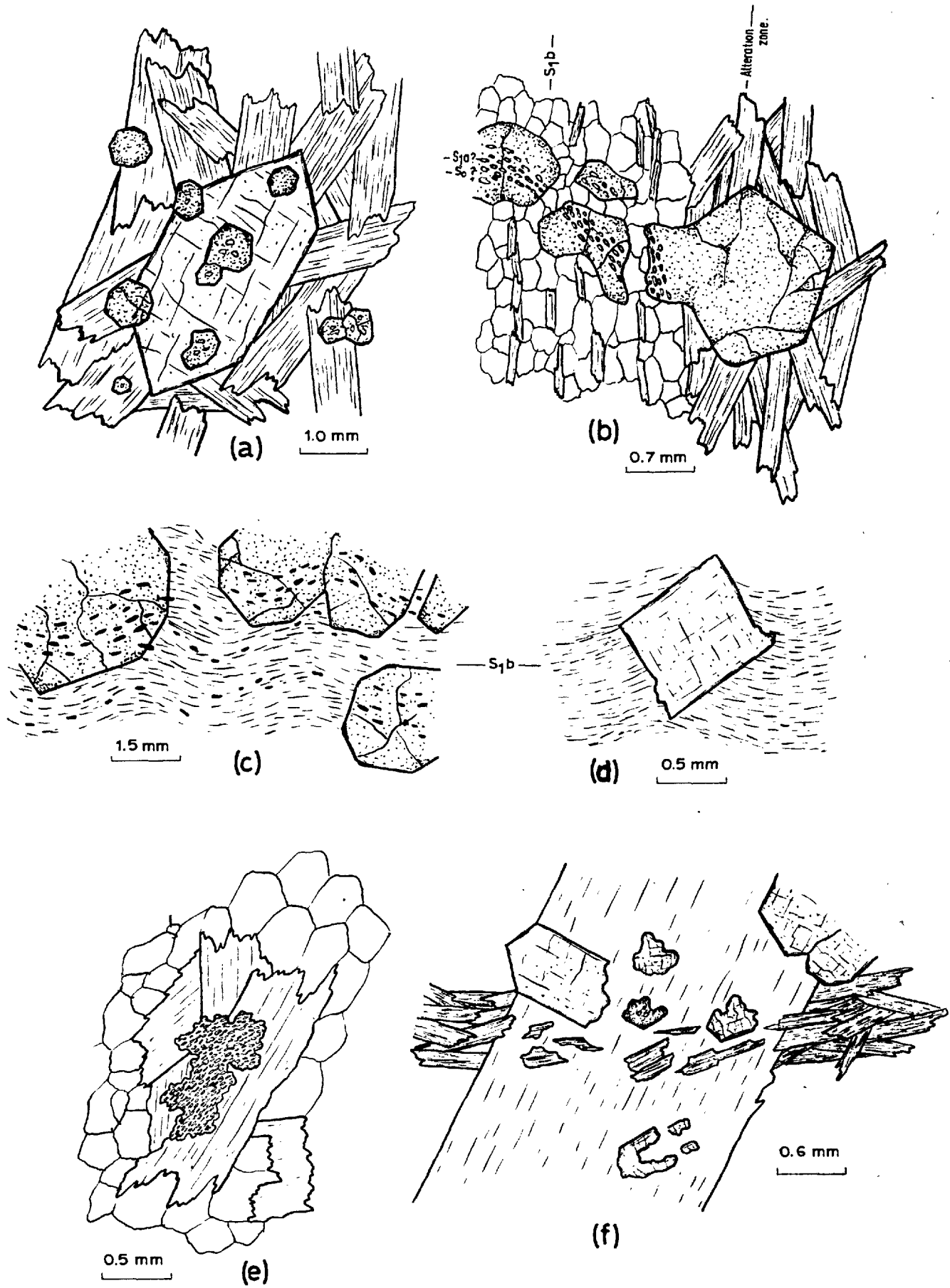
FIG. 5-7

garnets in contact with the mica are nearly perfect dodeca-
hedrons but in areas where the garnets have coalesced, crystal
faces are largely lost due to the development of interference
boundaries. Garnet-garnet interfaces are generally quite
irregular and there is little evidence of any annealing
adjustments (fig. 5-8c). Some textures show evidence that
garnet growth has been mainly at the expense of biotite. For
instance ilmenite inclusions in garnet often display a
preferred orientation parallel to external biotite grains
(fig. 5-7c) but the greater density of ilmenite grains within
the garnet suggest some of the oxide is a reaction product
of garnet growth. A possible reaction scheme could be:

$$K_2(Fe,Mg,Mn,Ti)_2(OH)_2AlSi_3O_{10}) \rightarrow [Fe(Mg,Mn)]_3Al_2(SiO_4)_3 +FeTiO_3 +$$
$$SiO_2 + H_2O + K_2O$$
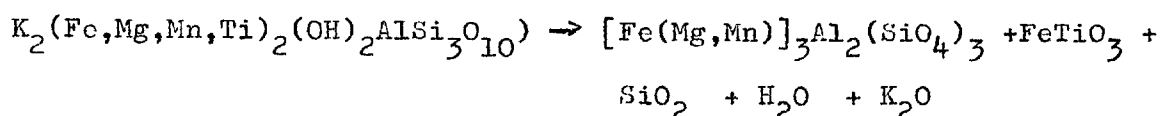
i.e. Biotite $\rightarrow$ Garnet + Ilmenite + other products

In other instances the garnet itself seems to exercise some
crystallographic control over inclusion distribution as in
fig. 5-8d where a zone of ilmenite and sulphide inclusions
parallels the crystal faces of the garnet host.

(c) Staurolite

Staurolite is the most spectacular of the alteration
zone silicate minerals since it commonly occurs as large
golden orange (yellow in thin section) hexagonal prisms up
to 30 mm in length. Indications that the period of greatest
staurolite growth was later than that of many of the other
phases are (1) staurolite grows across S_1b biotite surfaces
that were crenulated during early B_2 movements (figs. 5-5c,
5-7d), (2) most textural relations suggest staurolite growth
at the expense of pre-existing biotite and andalusite (fig.
5-4c), and (3) unfractured staurolite prisms enclose large
garnet euhedra (fig. 5-7a).

Although there is clear evidence of corrosion of many
phases by staurolite, its origin is far from clear. Winkler
(1965) gives the following reaction;

chloritoid + pyrophyllite $\rightarrow$ Staurolite + quartz + water

He points out that small inclusions of quartz support such a
scheme. Quartz inclusions do occur in the Kanmantoo staurolites
(fig. 5-4c) but these are almost certain to be simple mechani-
cal inclusions of quartz trapped during staurolite growth.

FIG. 5-8

Silicate Intergrowths In and Near Alteration Zones

(a) Post-tectonic amoeboidal biotite porphyroblast in quartz-rich lode schist. Small chlorite laths growing along the quartz-quartz interfaces (arrowed) form a crude schistosity. that swings around the biotite. Transmitted PPL.

(b) Late amoeboidal biotite (dark) replaces poikiloblastic andalusite and inherits part of its quartz inclusion fabric. Dark circular patches in the biotite are pleochroic haloes around minute radioactive monazite crystals. Transmitted PPL.

(c) Coarse-grained garnet aggregate in an alteration zone. Small dark inclusions are ilmenite. Curved and irregular grain boundaries and few 120° dihedral angles suggest that this is a primary growth fabric rather than an annealed one. Transmitted PPL.

(d) Ilmenite, pyrrhotite and chalcopyrite inclusions in a zone parallel to the external faces of a large garnet porphyroblast. Reflected PPL.

(e) Very small worm-like inclusions of quartz form a myrmekitic pattern in the interior of a large staurolite crystal. Dark grains are ilmenite. Transmitted PPL.

(f) Intimate intergrowth of chlorite (lighter phase) with biotite in a schistose alteration zone. Note the pleochroic halos in both phases. Transmitted PPL.

(g) Complete alteration of biotite in a garnet-biotite alteration zone assemblage produces a garnet-chlorite rock of the type illustrated here. Transmitted PPL.

(h) Acicular aggregates of rutile (dark) in chlorite that has formed from biotite. Transmitted PPL.
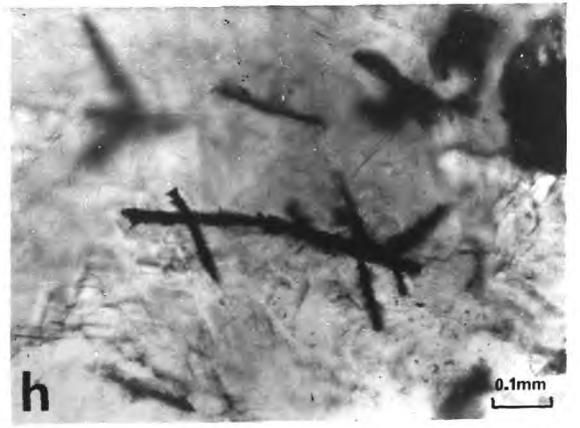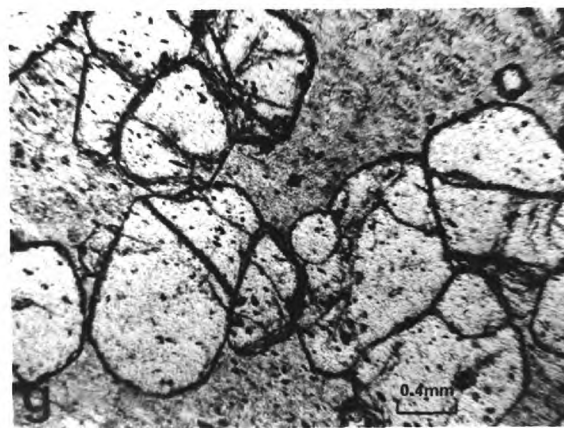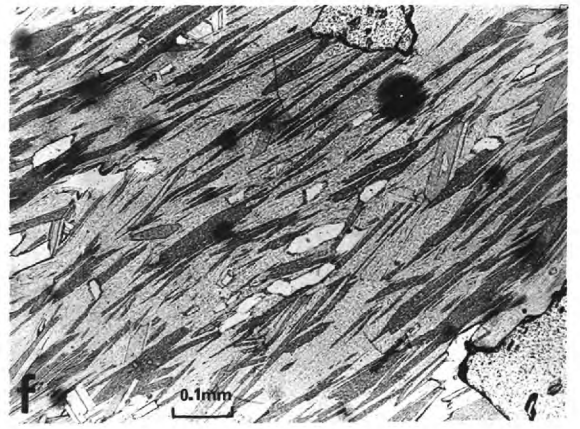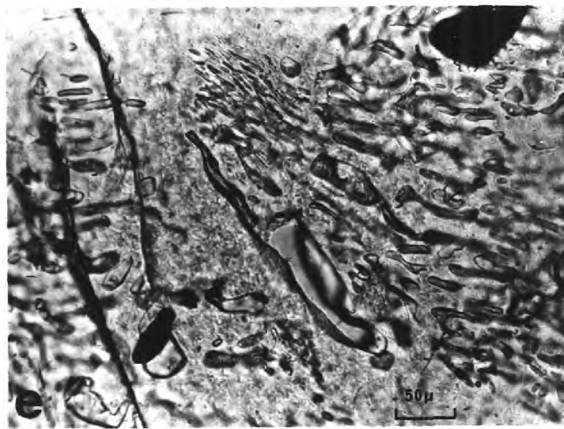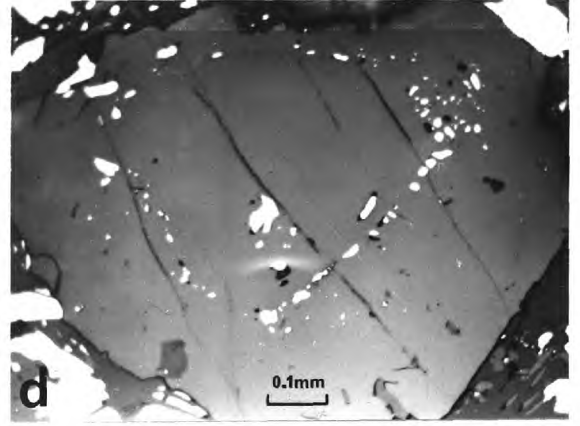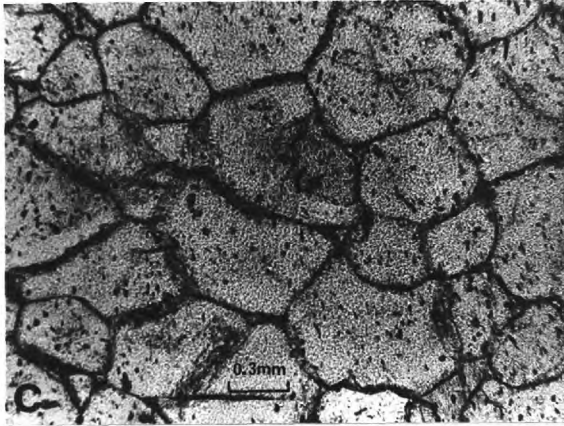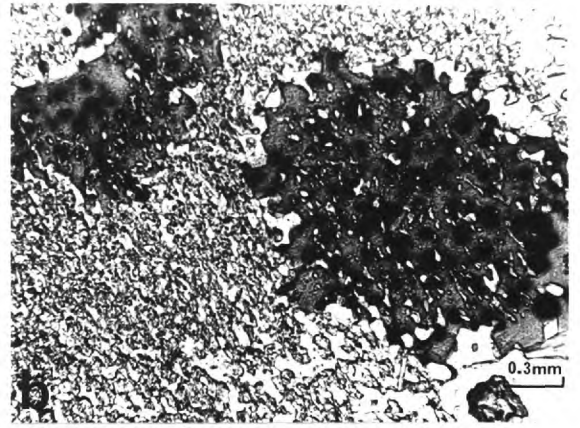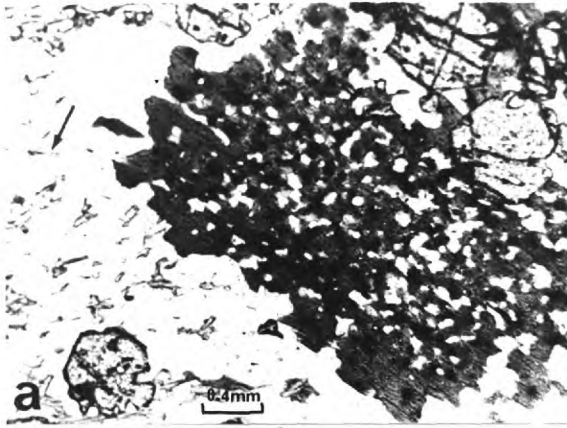
FIG. 5-8

More difficult to explain are the very fine worm-like quartz
inclusions that often occur together with the larger granular
quartz inclusions (fig. 5-8e). These may be some kind of
reaction product or possibly incompletely replaced pre-existing
quartz.

4. Muscovite

Muscovite occurs as a matrix mineral equal in importance
to biotite through much of the unaltered schists. Most thin
sections contain in addition, a few larger post-tectonic
muscovite flakes growing across the schistosity in the manner
of the chlorite in fig. 5-3b. Coarse muscovite flakes may
also be intergrown with granular quartz in the pressure shadow
zones of pre-B_1b andalusites (fig. 5-4a) while in the alteration
zones and adjacent rocks, andalusite is extensively altered
externally and internally to aggregates of muscovite and quartz
(fig. 5-7e). The replacement of alteration zone biotite and
corrosion of other phases by muscovite is common (fig. 5-7f)
and the frequency with which unstrained muscovite grows across
weakly fractured biotite, indicates slight deformation between
the growth of the two coarse grained micas. This alteration-
zone muscovite is clearly a late phase.

5. Sillimanite

Sillimanite is a comparatively rare mineral in the area
as a whole but is not uncommon in small amounts in rocks
adjacent to alteration zones or in areas rich in late muscovite.
It always occurs as minute needles or felted masses (fibrolite)
which are difficult to identify under the microscope due to
optical interference from enclosing minerals. However, the
provisional identification has been confirmed by X-ray diffrac-
tion photographs of small samples extracted from thin sections.
Sillimanite is intergrown with a variety of minerals but the
zones in which it is found nearly always show signs of slight
deformation, particularly micro-shearing of biotite and fractur-
ing or optical straining of staurolite. Although there is a
clear tendency for sillimanite to show its greatest development

in the vicinity of andalusite and staurolite, only a few
needles actually occur within these phases; instead sillimanite
is concentrated along their grain boundaries (figs. 5-9a,b),
within adjacent deformed biotite (fig. 5-9d) and along biotite-
quartz or quartz-quartz interfaces (fig. 5-9c). Sillimanite
appears to pre-date muscovite flakes in some areas (fig. 5-9e)
and post-date them in others (fig. 5-9d). It is noteworthy
that there is no sign of sillimanite in the small group-3
shear bands described in chapter 3.

Chinner (1961) describes sillimanite from the Scottish
Dalradian that clearly pre-dates staurolite, post-dates parts
of the kyanite, and is intergrown (or inferred to have been
intergrown) with biotite. The strict geometrical relationship
between the orientation of sillimanite and the biotite cleavage
Chinner interprets as control of sillimanite nucleation and
growth by the biotite structure. No permanent breakdown of
biotite is visible and he suggests that Al and Si for sillimanite
growth were derived mainly from solution of nearby unstable
kyanite. This association of sillimanite with biotite
is evidently very common but Pitcher (1965) thinks that the
reaction producing sillimanite is quite independent of poly-
morphic inversion. It would seem unwarrented to invoke any
general reaction scheme for the formation of sillimanite
since its time of formation with respect to that of the other
phases will depend both on the P-T path of metamorphism and
on the chemistry of the rocks and environment.

In the Kanmantoo Mines area, sillimanite appears to
have formed largely at the expense of andalusite and staurolite
but has nucleated and grown in rather haphazard orientation
along various phase boundaries, in fractures and within minerals.
Positive evidence against epitaxial growth of sillimanite in
biotite is seen in the groups of sub-parallel sillimanite needles
passing undeviated through deformed biotite laths that have
widely varying orientations (fig. 5-9d). The small deformation
zones were probably important as conduits for the solution,
transport and precipitation of Al and Si and for allowing

FIG. 5-9

Textural Relations of Sillimanite

(a) Sillimanite needles in a coarse-grained intergrowth
of biotite (B), andalusite (A), garnet (G), staurolite
(St), and quartz (Q).

(b) Fibrolitic sillimanite along the interface between a
corroded looking staurolite grain and granular quartz,
and along fractures within the staurolite.

(c) Sillimanite needles along biotite-quartz interfaces.

(d) Sillimanite (Sill) concentrated in deformed biotite
along the margin of a large andalusite porphyroblast.
The small shear zones in the rock are later than
the large post-tectonic muscovite flake.

(e) Post-tectonic muscovite flake cutting across a
schistose biotite fabric is intergrown with
andalusite (A) and granular quartz. Small
sillimanite needles formerly intergrown with
biotite are not replaced by the later muscovite.
Stippled grains are garnet.

Textural Relations of Grunerite

(f) Needles and prismatic crystals of grunerite in quartz-
rich lode schist adjacent to an alteration zone.
Elongated dark grains are ilmenite and stumpy dark
grains are magnetite.

(g) Grunerite needles and granular quartz form an
interstitial phase to large garnets in an alteration zone.

(h) Sulphide inclusions in garnet indicate garnet growth
after the formation of the crudely foliated grunerite-
rich matrix.

(i) The ilmenite and pyrrhotite/chalcopyrite inclusion fabric
in garnet aggregates suggests that the large prismatic
grunerite crystals have grown at the expense of the garnet.

(j) Grunerite crystals and granular quartz form a matrix
around large biotite and garnet porphyroblasts.

(a) 0.5 mm
(b) 0.5 mm
(c) 0.5 mm
(d) 1.0 mm
(e) 0.5 mm
(f) 0.6 mm
(g) 0.4 mm
(h) 0.3 mm
(i) 0.4 mm
(j) 0.3 mm
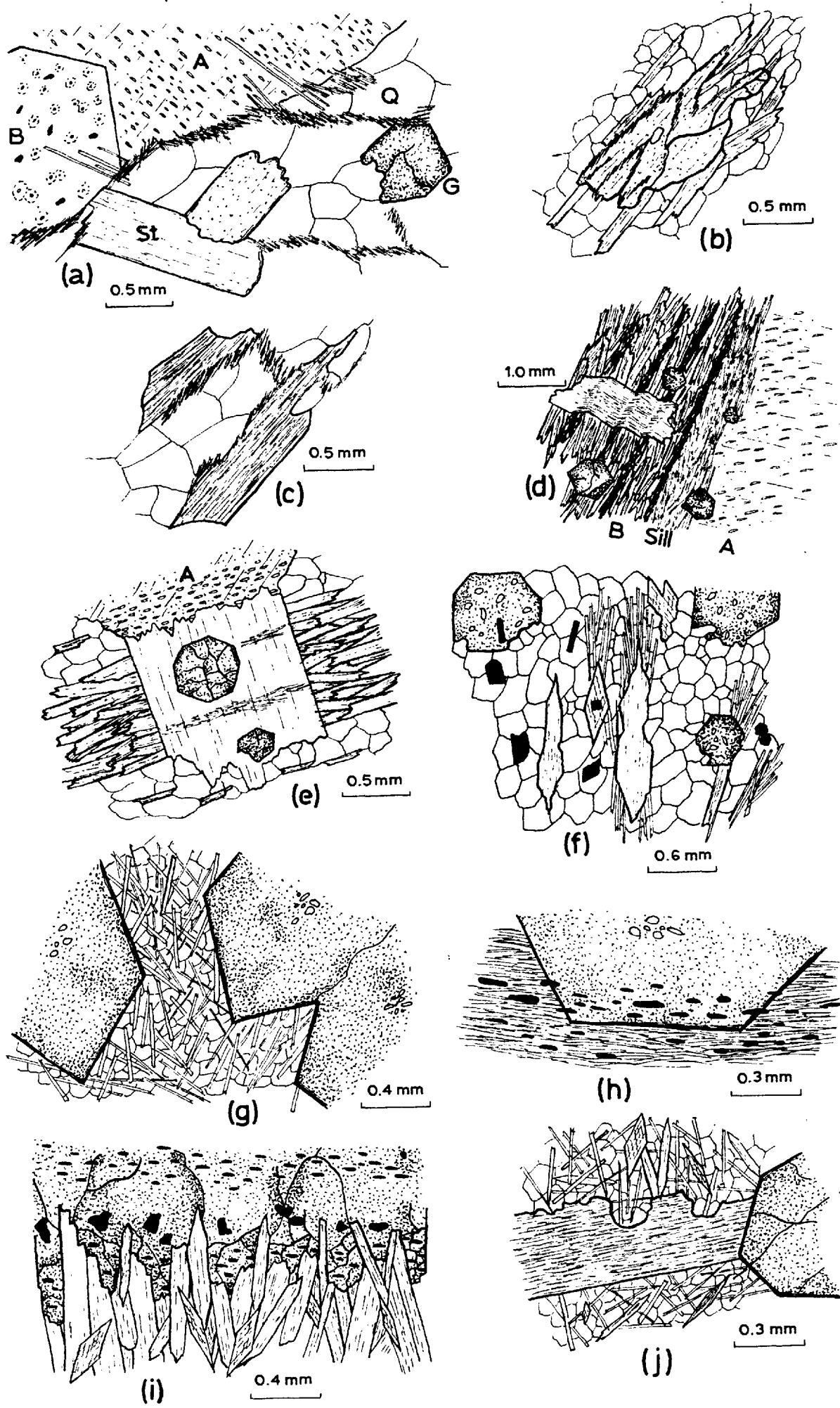
FIG. 5-9

reactions involving the generation of water to proceed at an accelerated rate e.g. the reaction given by Turner and Verhoogen (1960);

$$staurolite + quartz \longrightarrow sillimanite + almandine + H_2O$$
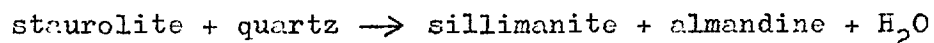
6. Iron Amphibole

A white fibrous to prismatic amphibole found in a few places in and adjacent to alteration zones, is faintly pleochroic from very pale fawn to colourless in thin section and occurs both as slim needles and subhedral prisms intergrown with both quartz and garnet. The needles are very similar in appearance to fibrolitic sillimanite but X-ray diffraction traces showed both the fibrous and coarsely crystalline material to be a monoclinic amphibole with lattice spacings similar to the iron-rich amphibole grunerite. Grunerite is also indicated in a qualitative electron probe analysis which shows the presence of major Fe, minor Mg and trace Mn; neither Ca nor Al could be detected.

In amphibole-bearing quartz-biotite-garnet lode schists, a few amphibole needles and subhedral prisms are scattered through the granular quartz matrix (fig. 5-9f) but in nearby alteration zones containing both more abundant and coarser garnet, the interstitial quartz is loaded with networks of amphibole needles (fig. 5-9g). Growth of garnet after the amphibole needles is suggested by the sulphide inclusion relationships shown in fig. 5-9h while in some of the vein-like concentrations of coarse grained amphibole that cut across the rocks, garnet near the vein walls appears to be replaced by amphibole prisms (fig. 5-9i). In some areas a few subhedral porphyroblasts of biotite or chlorite after biotite are present but it is difficult to conclude whether the mica is being replaced by amphibole or, if it is in the process of growing (fig. 5-9j).

7. Chloritization

Although it is impractical to discuss chlorite intergrowths

without referring to the closely associated oxide-sulphide
mineralization, it would be a useful introduction to the ore
textures to describe the important chlorite-silicate relation-
ships. Regional chloritization is widespread but minor and
consists mainly of a few post-tectonic flakes cross-cutting
the schistosity (fig. 5-2c), growing in augens and replacing
the margins of andalusite. In lode schists and nearby altera-
tion zones chlorite is an important mineral. Where biotite is
lacking or exists only as large poikiloblasts chlorite grows
as small oriented flakes along the quartz-quartz interfaces
and defines a crude schistosity surface that swings around
the earlier biotite grains (fig. 5-8a). In schistose biotite
bands, biotite and chlorite form intimate intergrowths (fig.
5-8f). Many biotite-chlorite intergrowths give no indication
which is the earlier phase (fig. 5-10a) while others leave no
doubt that chlorite is the later mineral (fig. 5-10b).

As chloritization becomes more severe, biotite porphyro-
blasts themselves begin to break down (fig. 5-10c) and in
quartz-poor rocks a very common "intermediate" rock type is a
garnet-chlorite schist in which the garnet euhedra appear
quite fresh with little visible alteration (fig. 5-8g).
Such intergrowths may constitute a locally stable mineral
assemblage but in some sections garnet itself shows partial
breakdown to chlorite in otherwise perfectly fresh biotite-
rich and staurolite-rich rocks (fig. 5-10d,e). The near final
products of chloritization appear to be the zones up to one
foot or more across containing about 95% of coarse-grained
radiating aggregates of dark green chlorite. In such zones
former biotite is nearly all altered to chlorite but remnants
of muscovite and garnet are clearly visible (figs. 5-10f,g).
Staurolite appears to be very stable and apart from severe
fracturing shows little alteration. New minerals formed
within these chlorite aggregates include suhhedra of blue
pleochroic corundum, green, blue and brown zoned tourmaline
and colourless apatite (figs. 5-10h,i,j). Large platy euhedra
of ilmenite partly altered to rutile may also be present
(fig. 5-10k) and quite often the associated chlorite is loaded
with minute radiating acicular aggregates of rutile (fig. 5-8h).

<u>FIG. 5-10</u>

<u>Chlorite Relationships in the Alteration Zones</u>

(a,b) Chlorite (light phase) intergrown with deformed biotite.

(c) Large biotite porphyroblast partially replaced by radial aggregates of chlorite.

(d) Advanced alteration of garnet to radial aggregates of chlorite while adjacent schistose biotite is completely fresh.

(e) Partial alteration of garnet to chlorite within a slightly fractured but completely fresh staurolite crystal.

(f) Partial alteration of the more resistant muscovite grains to chlorite.

(g) Where both biotite and garnet are breaking down to chlorite the outlines of the former garnet crystals are made visible by the slighter lighter coloured and finer-grained chlorite that has formed from the garnet.

(h,i,j) New phases that appear in chlorite-rich alteration zones. These are respectively corundum, apatite and zoned tourmaline.

(k) Large plates of ilmenite intergrown with coarse radial aggregates of chlorite. The ilmenite (dark) has partially altered to granular rutile.

(a)

0.2 mm

(b)

(c)

0.5 mm

(d)

0.2 mm

(e)

0.5 mm

(f)

0.3 mm

(g)

0.5 mm

(h)

0.5 mm

(i)

0.2 mm

(j)

0.1 mm

(k)

0.5 mm
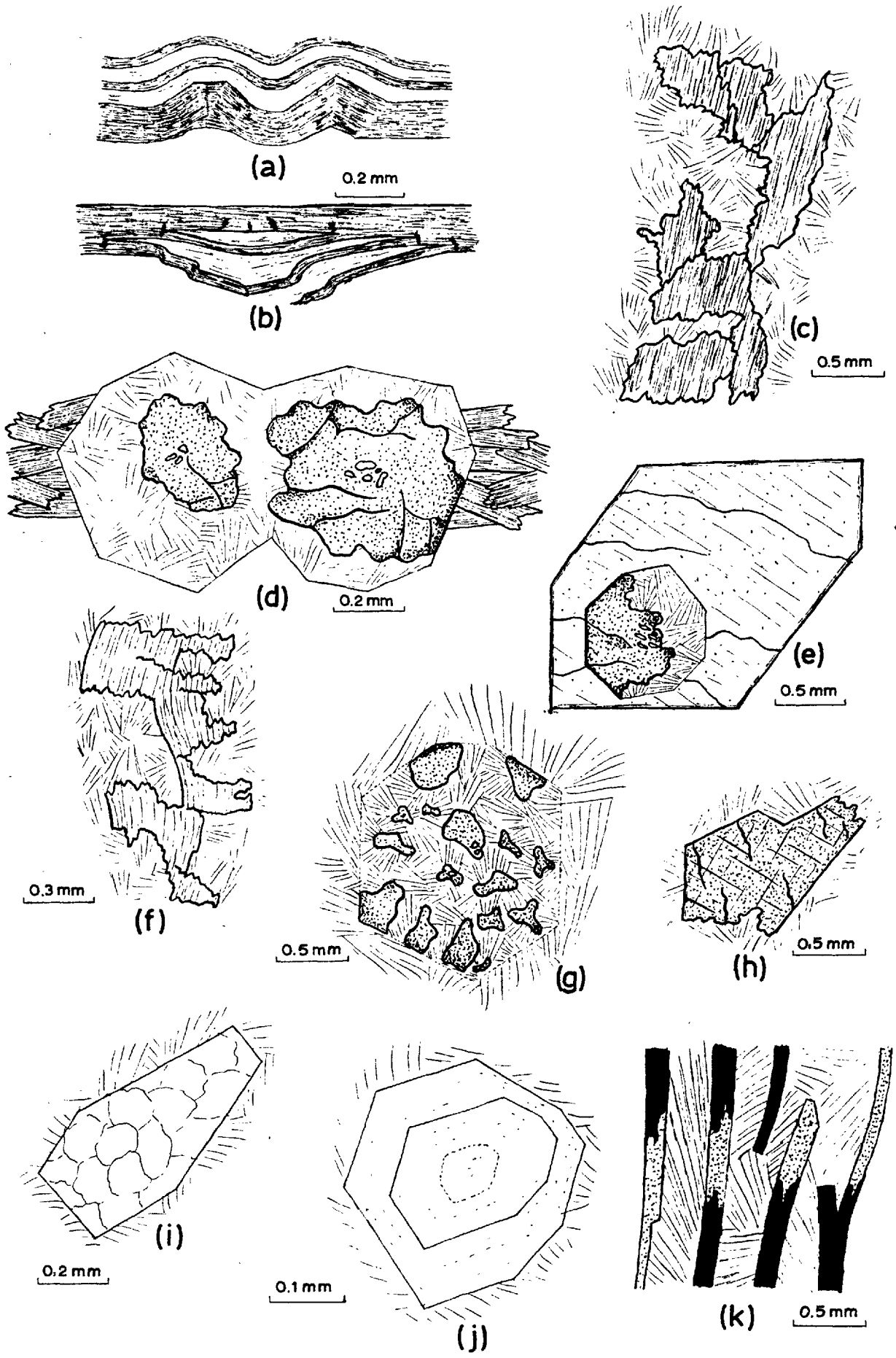
FIG. 5-10

Despite clear petrographic indications that the chlorite
is a late mineral formed principally as a breakdown product
of earlier minerals, there is no direct evidence to postulate
any great time interval between the cessation of pre-chlorite
mineral growth and the onset of chloritization. The common
occurrence of deformed earlier minerals as well as deformed
chlorite in chloritized areas suggests that the small localized
movements making up the B_2 tectonic phase continued during the
chloritization period. Such movement zones probably had an
important influence on the location and intensity of chlorite
growth by mechanically preparing the earlier minerals for
breakdown and for providing passageways for the metasomatic
transport of reactants and products.

E. DEVELOPMENT OF THE COARSE-GRAINED PRIMARY ORE TEXTURES

1. General Statement

Combinations of (a) probably overlapping silicate,
oxide and sulphide crystallization and recrystallization
histories, (b) unmixing features in both the sulphide and
oxide assemblages, (c) a number of minor movements during the
B_2 tectonic phase, and (d) secondary mineralogical and textural
changes in much of the coarse-grained ore, would be expected
to produce such a wealth of textural relationships that the
imprint of time would be difficult to recognise. But by
using precisely the same textural criteria for the opaque
mineral intergrowths as used for the silicates, plus a few
additional techniques, a substantial amount of the minerali-
zation can be fitted into the metamorphic history. Minor
opaque phases will be mentioned in this section only where
they are important in dating; a fuller account of the ore
mineralogy is given in chapter 6.

2. Magnetite and Associated Oxide Relationships

Magnetite euhedra in a chlorite-free alteration zone
assemblage of biotite, muscovite and garnet are shown in fig.
5-11a and a similar euhedral magnetite crystal surrounded by

FIG. 5-11

(a) Magnetite euhedra (black) in a chlorite-free altera-
tion zone assemblage of quartz (clear), garnet
(high relief) and biotite. Transmitted PPL.

(b) An octahedral magnetite crystal (Mt) intergrown
with chalcopyrite (Cp) and concentric pyrite
(Py) after pyrrhotite. Note the pale grey
lamellar phase parallel to the octahedral faces
of magnetite and the smaller very dark slim
lamellae oblique to the octahedral planes.
Reflected PPL.

(c) Electron scanning photograph of the area out-
lined by the black dashed line in (b) above.
The pale grey phase and dark lamellae are
clearly shown.

(d,e) X-ray scanning photographs for Ti and Al confirm
the optical indentifications of the pale grey phase
as ilmenite and the dark phase as hercynite. No
Mg is detectable in either phase.

(f) Finely ground surface of a coarse-grained ore
specimen. Large masses of magnetite (Mt) are
surrounded by roughly banded pyrrhotite (Po)
and chalcopyrite (Cp). Within the sulphides are
plentiful garnet crystals (thick arrow) and micro-
folded biotite or chlorite after biotite (thin arrow).

(g) A similar ore specimen in which part of the pyrrhotite
has been altered to networks of pyrite. Note the
faintly mottled appearance of the magnetite.
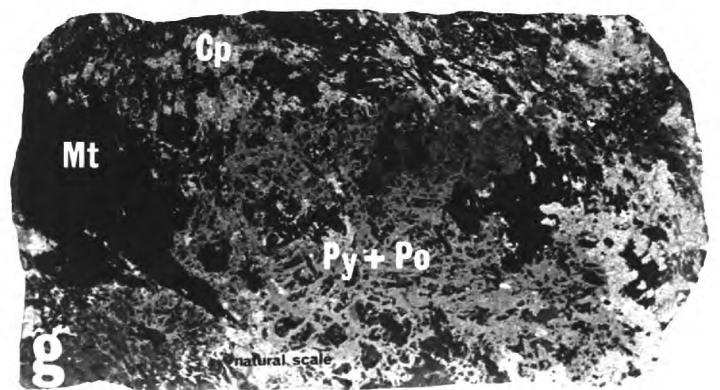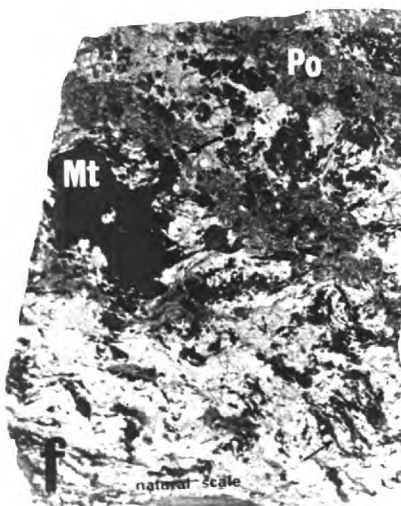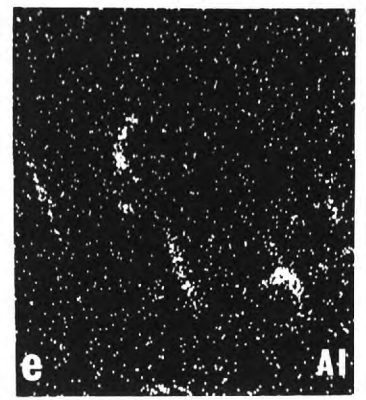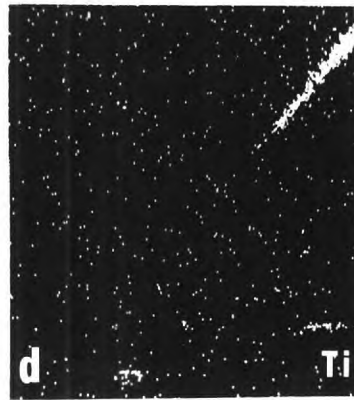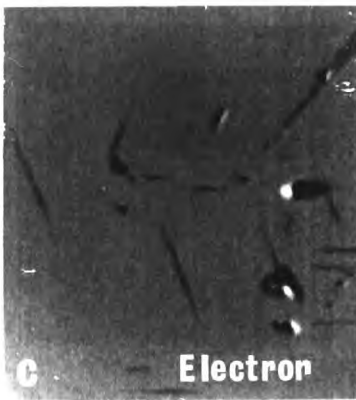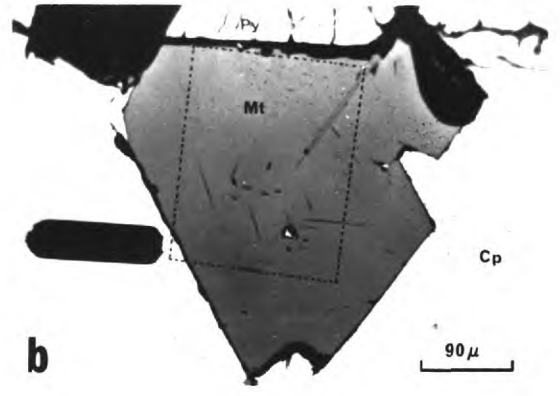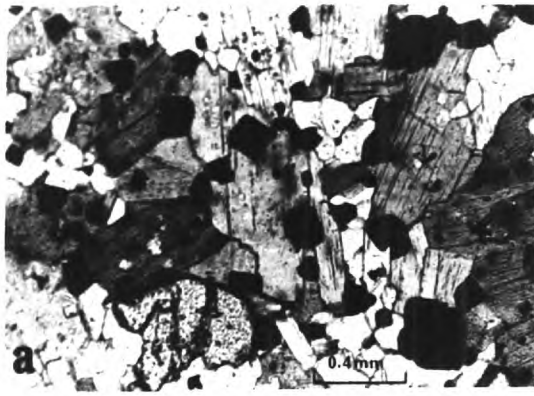
FIG. 5–11

coarse-grained sulphides is illustrated in fig. 5-11b.
Accompanying electron and X-ray scanning photographs for part
of the octahedral magnetite crystal in fig. 5-11b show that
the medium grey lamellar phase parallel to the octahedral
faces is ilmenite. The smaller, very slim black (transparent)
lamellae oblique to the octahedral faces are probably the iron-
aluminium spinel, hercynite ($FeAl_2O_4$) since no Mg could be
detected. These intergrowths give no indications of the
relative age relationships between the magnetite and the
external phases.

(a)   Deformation Microstructures

Such magnetite euhedra as described above appear to be
undeformed but in many places larger magnetite grains and
aggregates are found where there is evidence of post-magnetite
deformation. For instance in fig. 5-11f a crude external
foliation in both the sulphides and silicates swings around
the magnetite aggregate and in fig. 5-11g the magnetite has a
distinctly mottled appearance in hand specimen suggestive of
internal deformation. In polished section, the magnetite in
fig. 5-11f appears to be relatively homogeneous except for an
irregular fabric of minute transparent inclusions and small
ilmenite lamellae, but after etching the surface with a 50%
aqueous HCl solution for about 60 seconds, a complex sub-
structure is revealed (fig. 5-12a). Evidence against this
internal structure being a post-tectonic magnetite intergrowth
around pre-existing folds is shown by (a) a faint but distinct
anisotropy detectable in the unetched magnetite (undeformed
magnetite appears essentially isotropic), (b) strained ilmenite
lamellae bent around the magnetite microfolds, (c) the chaotic
pattern of structures through the magnetite mass, and (d) no
similar microfold structures in the external phases. The
orientation of the included ilmenite lamellae (arrow in fig.
5-12a) indicates that the magnetite sub-grain boundaries
revealed by etching are more-or less parallel to the octahedral
planes.

An enlarged view of the magnetite sub-structure in

FIG. 5-12

Some Microstructures in Etched Magnetite

(a) Complex bladed deformation-like microstructure in the
magnetite of fig. 5-11.f. The orientation of the
ilmenite lamellae (arrows) suggests that the
magnetite sub-grain boundaries are parallel to the
octahedral planes. Light phase is chalcopyrite and
the dark material chlorite.

(b) B-type magnetite areas show virtually no etch reaction
and display no sub-structure whereas A-type areas
show both a marked surface etch effect and a fine
lamellar sub-structure. Arrows point to some ilmenite
lamellae. Black stumpy grains are hercynite.
Oil immersion.

(c) A very irregular interface between an A-type and
a B-type area. Note the slightly curved ilmenite
grain (arrowed). Oil immersion.

(d,e) Further examples of strongly interpenetrating
interfaces between A-type and B-type magnetite.
Oil immersion.

(f) Magnetite showing a transition from a bladed
microstructure to a fine granular aggregate
Medium grey phase (arrows) is hercynite. For
further explanation see text.
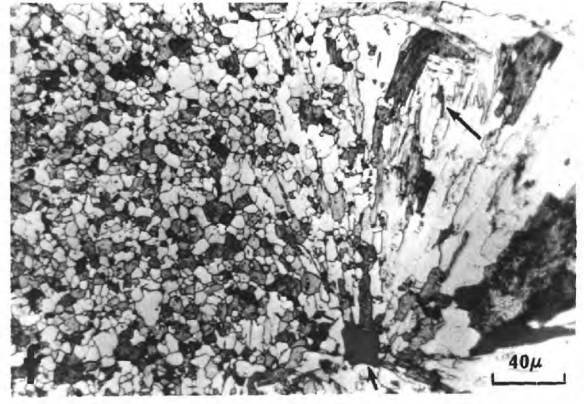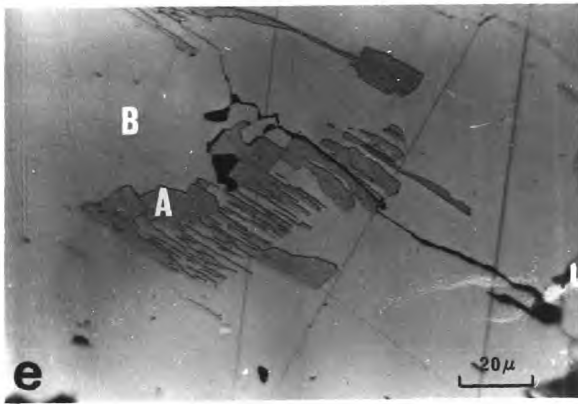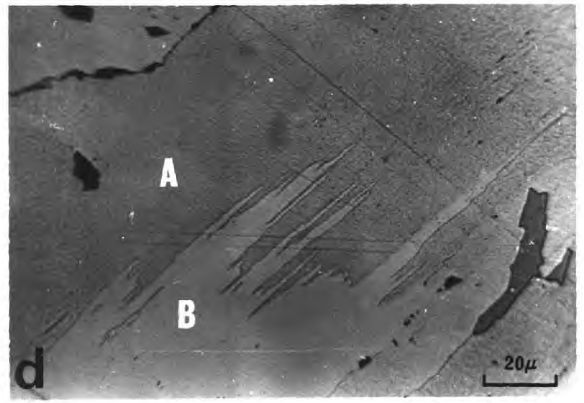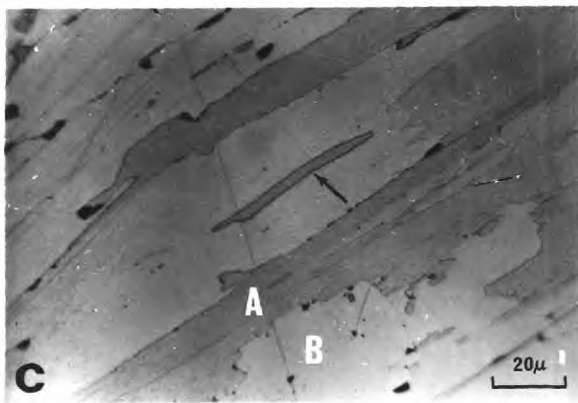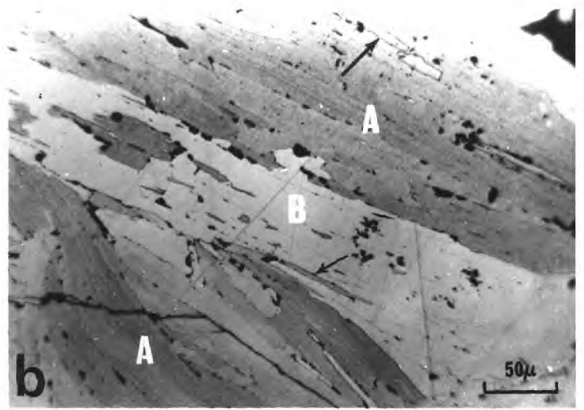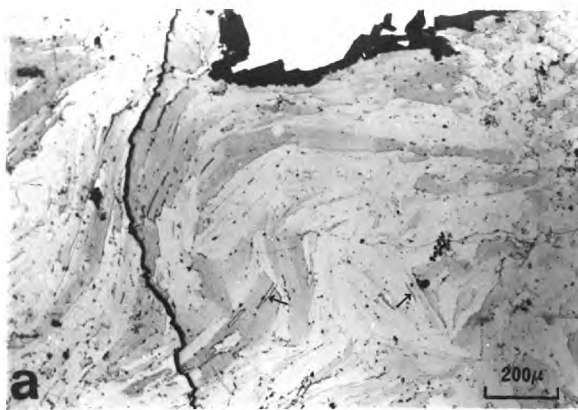
FIG. 5-12

fig. 5-12b contains a number of important features. In the
moderately etched areas marked A, the just visible sub-grain
boundaries are all relatively straight and parallel and the
similar etch reaction on all sub-grains indicates similar
crystallographic orientations. No sub-structure is visible in
the barely etched areas marked B apart from small ilmenite
lamellae (arrowed) and the larger magnetite "inclusions"
having an etch intensity similar to area A. Although
following the general octahedral directions, the A-B interfaces
in detail are quite irregular. An even more irregular A-B
boundary is shown in fig. 5-12c and what probably are two-
dimensional interference traces of A-B type interfaces, are
illustrated in figs. 5-12d,e. The almost negative etch
reaction of the B-type areas could indicate simply a different
crystallographic orientation relative to the adjacent A-type
areas but the constancy of this differential etch reaction
relationship implies some other factor operating, a factor
independent of lattice orientation. A likely possibility
seems to be a difference in the density of crystallographic
defects since the greater the number of defects the more rapid
is the etchant attack.

Grühn (1919) made magnetite deform experimentally at
room temperature but at high confining pressures by poly-
synthetic twinning in the octahedral planes, and Hornstra
(1960) reports that in sintering experiments with spinel
(senso stricto), plastic deformation takes place largely by
atomic slip also in the octahedral planes. On an atomic scale,
these plastic deformation phenomena are the result of the
creation and movement of point and line defects within the
crystal lattice. Accordingly, the following provisional
explanation is given for the magnetite features described
above. The magnetite deformed principally by atomic slip in
the octahedral planes and produced the microstructures preserved
in the A-type areas (mechanical slip along (111) partings is
considered to be insignificant in the physical conditions
under which the deformation is thought to have occurred).
Subsequently, relatively unstrained B-type grains were formed

either by lattice recovery and grain boundary migration from
slightly less strained A-type areas or by nucleation and growth
of completely new unstrained grains, i.e. recrystallization.
In either case, the most rapid direction of A-B interface
migration appears to be along, rather than across the prevail-
ing octahedral slip planes.

(b) Recrystallization Microstructures
        In some areas of the large magnetite mass in fig. 5-11f,
there is a rapid transition from the lamellar type deformation
intergrowth to the fine-grained polyhedral granular aggregate
illustrated in fig. 5-12f. The magnetite mass in fig. 5-11g
consists of a similar but even finer grained polyhedral
aggregate as shown in fig. 5-13a. These microstructures also
are invisible on a freshly polished surface and are best
revealed by etching with a 50% aqueous HCl solution for between
one and three minutes. Such aggregates look suspiciously like
the textures formed in highly strained metals and ceramic
materials after the temperature has been raised sufficiently
to induce recrystallization. Thus the magnetite in the Kanmantoo
orebody appears to show all variations between undeformed
crystals, deformed material and completely recrystallized
aggregates.

        There is considerable evidence that the recrystallized
magnetite has not undergone any annealing adjustments. Fig
5-13a illustrates that the grain-size is quite variable and
a high magnification view given in fig. 5-13b shows that the
grain shape is variable as well. Planar interfaces and 120°
dihedral angles at triple junctions are both comparatively
rare.

(c) Ilmenite and Hercynite Intergrowths
        The minor oxides intergrown with and genetically
related to the magnetite undergo some interesting textural
and morphological changes that also suggest considerable
structural re-arrangement within the host.

        The tapered lamellae and subhedral grains of ilmenite
in the undeformed magnetite (fig. 5-11b) are to be compared

FIG. 5-13

(all photographs taken in reflected plane
polarized light)

(a)   An inequigranular magnetite microstructure revealed
by etching with HCl. Although this may be a
recrystallization feature there is no evidence
of any annealing; there is a considerable varia-
tion in grain size, grain boundaries are not very
straight and 120° dihedral angles appear to be rare.
Black areas are both holes and hercynite grains.
Oil immersion.

(b)   Magnified view of the granular magnetite micro-
structure reveals a considerable variation in
grain shape and a wealth of non-equilibrium grain
boundaries. Oil immersion.

(c)   Euhedral ilmenite plates within a deformed
magnetite host. Hercynite (black phase) occurs
as stumpy grains within the magnetite and both
as stumpy and elongated grains along the magnetite-
ilmenite interface. Surface unetched. Oil immersion.

(d)   Habit of ilmenite in magnetite that possesses a
microstructure intermediate between lamellar and
granular. Small tongues of ilmenite project
along magnetite-magnetite grain boundaries.
Etched surface. Oil immersion.

(e)   Ilmenite in magnetite displaying a crude granular
microstructure. The ilmenite appendages appear
to have penetrated further along the magnetite-
magnetite interfaces and in some cases have isolated
small islands of magnetite. Etched surface.
Oil immersion.

(f)   Where magnetite shows a well developed granular
microstructure, ilmenite displays a poikiloblastic
habit and encloses many magnetite islands. Note
the granular habit of the hercynite (black phase).
Lightly etched surface. Oil immersion.
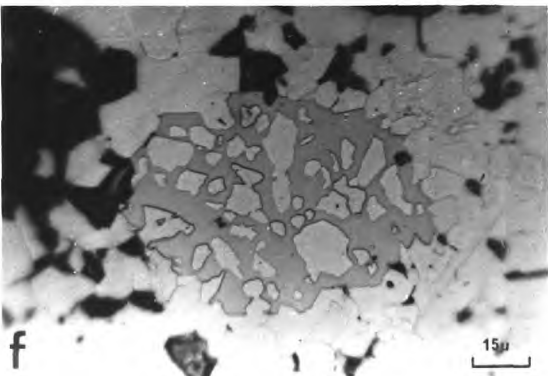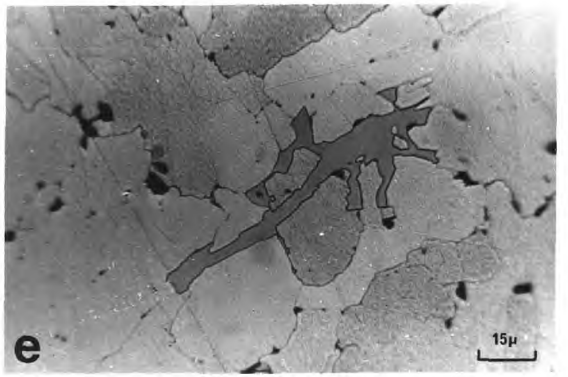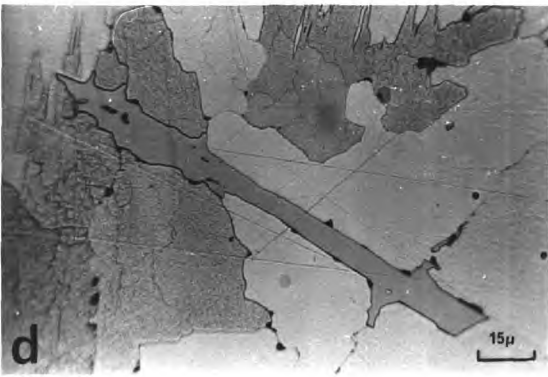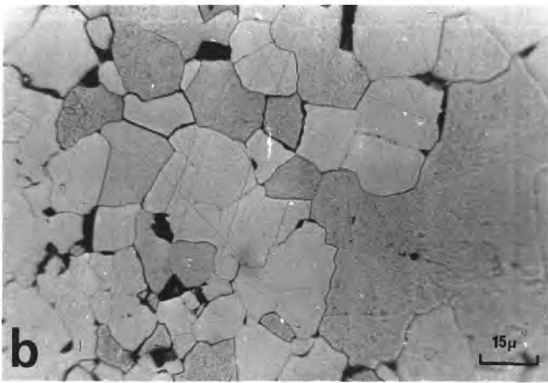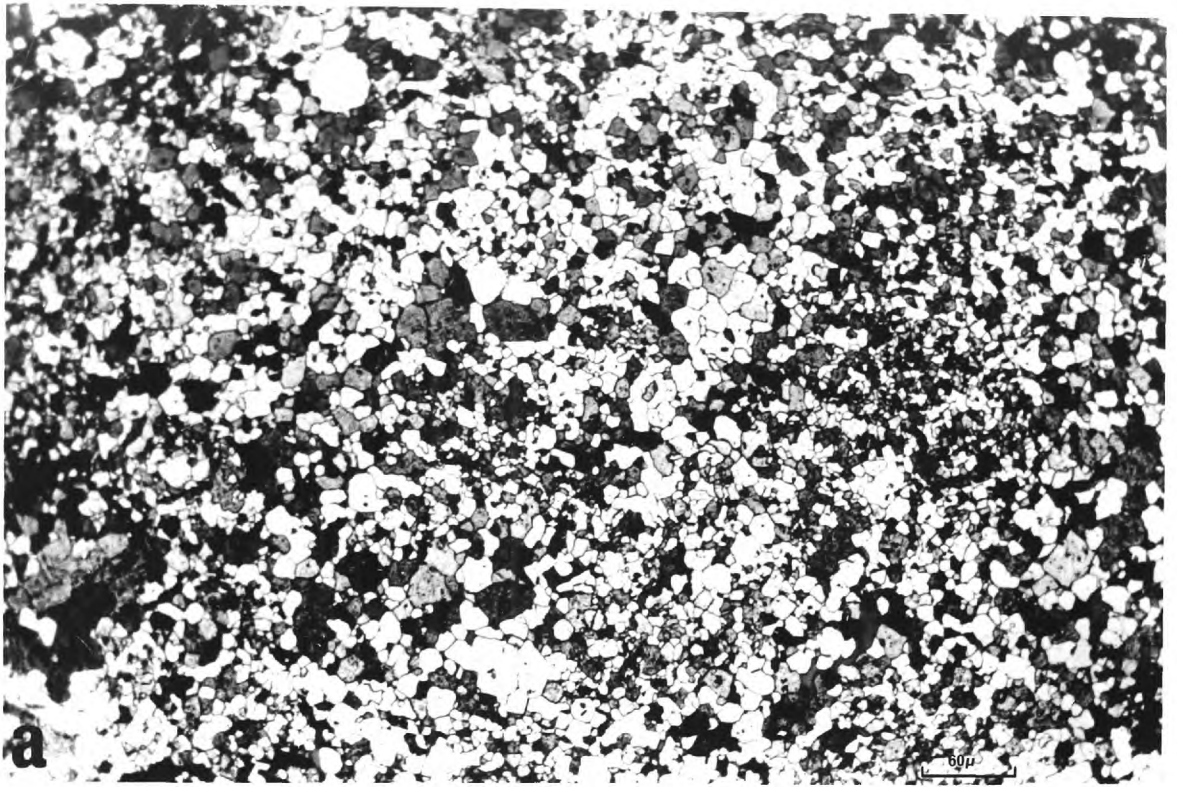
FIG. 5-13

with the perfect hexagonal ilmenite plates found in the deformed
magnetite (fig. 5-13c). Where the apparently unstrained B-type
grains form, these ilmenite plates begin to develop branch-like
outgrowths along the magnetite-magnetite grain boundaries
(fig. 5-13d) and where recrystallization proper has begun,
such branches have grown out around and completely enclosed
magnetite grains (fig. 5-13e). Where magnetite recrystallization
is essentially complete, the end products of this ilmenite
growth are the ragged poikiloblasts enclosing a large number
of anhedral magnetite islands (fig. 5-13f).

In undeformed magnetite, hercynite may occur as stumpy
inclusions along the magnetite-ilmenite lamellae interfaces
but more commonly it forms slim lamellae along the cubic planes
of the host (fig. 5-11b). In deformed magnetite aggregates,
hercynite collects along the sub-grain boundaries and at
magnetite-ilmenite interfaces but within the magnetite sub-
grains, it forms intersecting cube-like intergrowths (fig.
5-14a). During recrystallization of the magnetite, most of
the hercynite was apparently expelled into the grain boundaries
eventually to grow as anhedral grains and become part of the
spinel aggregate (see figs. 5-12f, 5-13b,f). Hercynite in
this position is often difficult to distinguish from holes
and silicate inclusions in an etched polished section but is
easily recognised as a pale green isotropic mineral in thin
section.

Ilmenite lamellae have their (0001) planes lying
parallel to the magnetite (111) surfaces in such an orientation
that the oxygen positions of the two lattices are very nearly
coincident (Edwards, 1954). The lattice strain energy associ-
ated with this interface is probably fairly low for even in
deformed magnetite where ilmenite may have had an opportunity
to reduce its surface area, the platy habit is retained.
Magnetite has a unit cell edge of 8.395Å compared to 8.159Å
for hercynite, so the atomic misfit across the common (100)
interface must be considerable. The resulting comparatively
high interfacial strain energy between these two spinel phases

FIG. 5-14

(all photographs in plane polarised light)

(a) Cube-like aggregates of hercynite in magnetite displaying a bladed microstructure. Lightly etched surface. Oil immersion.

(b) Minute, possibly exsolved hercynite euhedra in granular magnetite. surface unetched. Oil immersion.

(c) Inclusions of hercynite (black) and chalcopyrite (white) in the interior of an undeformed magnetite crystal. Some of the sulphide grains are dimensionally oriented along the magnetite cubic directions in the same way as the hercynite. Oil immersion.

(d) Ragged inclusions of sulphide (chalcopyrite and pyrrhotite) and magnetite (pale grey) in the interior of a large garnet porphyroblast. Note the minute chalcopyrite and pyrrhotite inclusions within the magnetite (arrow).

(e) A large garnet (Gn) porphyroblast surrounded by a fine granular aggregate of magnetite. Note the small areas of magnetite displaying a bladed-type microstructure. The garnet is largely unfractured but part of it is pseudomorphed by chlorite (Chl). The time relationship between the chalcopyrite (Cp) and the chlorite is unknown. Surface etched with HCl.

(f) Magnified view of the area outlined in white in the previous photograph. An ilmenite poikiloblast in granular magnetite (arrowed) appears to have been truncated by the garnet (now chlorite) dodecahedral face. Etched surface.

(g) Evidence that some of the chlorite (Chl) is an alteration product of magnetite (Mt); small ilmenite lamellae in the chlorite (arrowed) have the same form and network pattern as ilmenite in the adjacent magnetite. Some of the sulphide inclusions in the magnetite also appear to retain their original positions in the later chlorite.
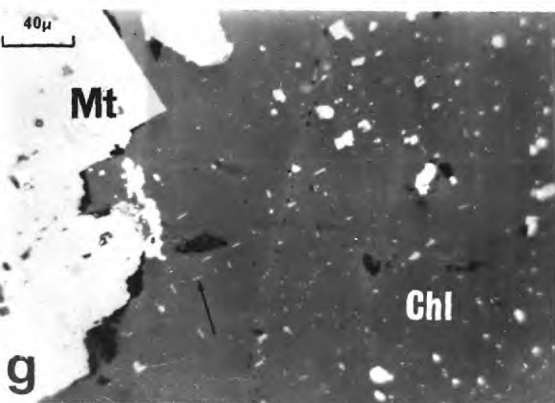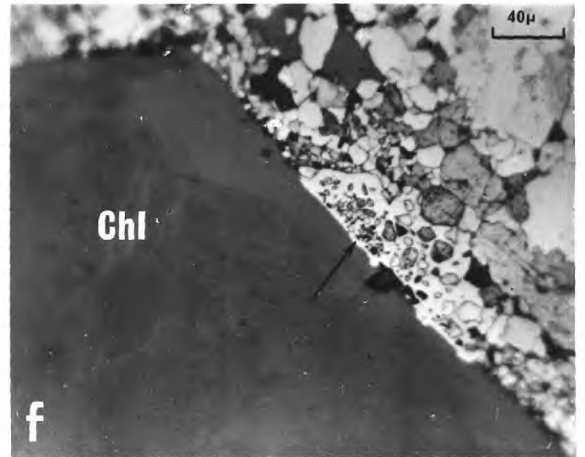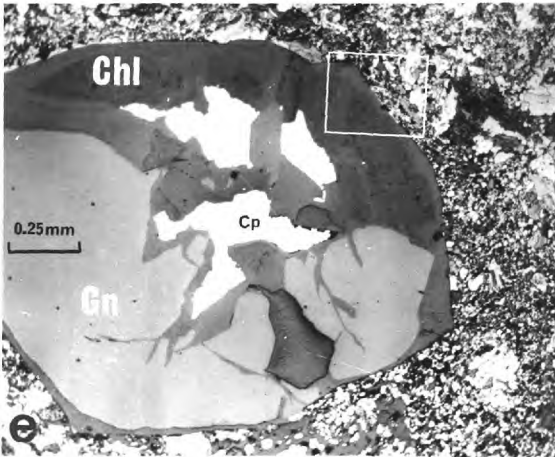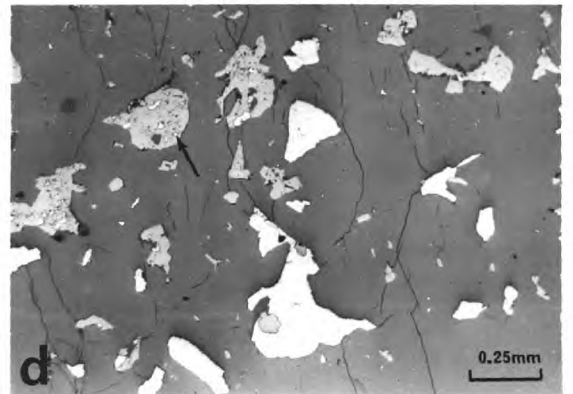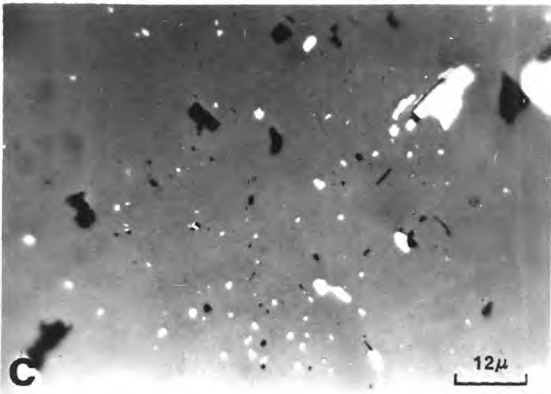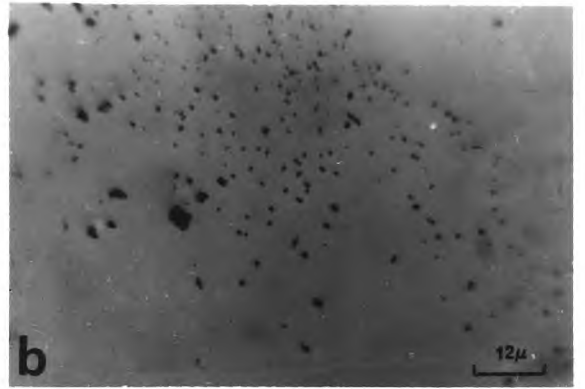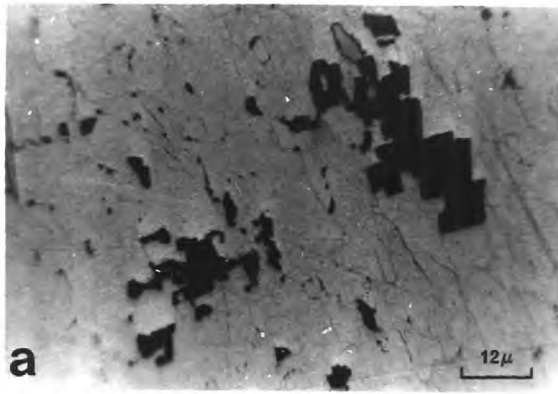
FIG. 5-14

probably explains why hercynite collects along grain boundaries or attempts to minimise its surface area by forming into cubes. The surface energies would be reduced even further if the still finely dispersed ilmenite and hercynite could recrystallize into a smaller number of larger grains (see Ewer, 1968). This is probably part of the driving force for the precipitation of these minor phases into the grain boundaries during recrystallization of the magnetite. Evidently the magnetite lattice was able to retain some aluminium during recrystallization for minute oriented euhedra of hercynite are quite common in individual recrystallized magnetite polyhedra (fig. 5-14b). X-ray powder diffraction photographs of undeformed, deformed and recrystallized magnetite all give a unit cell edge close to that of pure Fe_3O_4 and no cations beside Fe and traces of Ti could be detected under the electron probe microanalyser.

3. Some Oxide-Sulphide-Silicate Relationships

This section describes some key intergrowths that form the basis for the interpretation of most of the complex textures in the coarse-grained mineralization.

(a) Magnetite-Sulphides

Undeformed non-recrystallized magnetite crystals are often loaded with minute single phase, two phase and multi-phase inclusions of chalcopyrite, pyrrhotite, pentlandite and mackinawite; chalcopyrite is the most common. Individual inclusions vary from anhedral forms to elongated "euhedral" grains oriented along the magnetite cubic planes parallel to adjacent hercynite lamellae (fig. 5-14c). The inclusion size varies from about 100 microns down to the limits of optical resolution of the ore microscope (about 0.5 microns). Sulphide inclusions may or may not be accompanied by external sulphides and in many places predominantly chalcopyrite inclusions occur with external pyrrhotite and vice versa. If identical treatment is to be given to silicate, oxide and sulphide intergrowths, these sulphide inclusions have to be

regarded as having been trapped during the growth of the magnetite (assuming of course that they have not exsolved from a former oxide-sulphide solid solution).

(b) Garnet

Two important garnet-ore mineral intergrowths are the following: (a) garnets frequently enclose ragged inclusions of both sulphides and magnetite with the latter, in turn, enclosing minute inclusions of sulphides (fig. 5-14d), and (b) undeformed garnets are found totally enclosed within masses of both deformed and recrystallized magnetite (fig. 5-14e). A detailed examination of the garnet-oxide interface in fig. 5-14f reveals a truncated looking ilmenite poikiloblast that suggests replacement of the oxides by the garnet. The only reasonable conclusion that can be made from these relationships is that garnet growth has continued after both the deformation and recrystallization of magnetite and that therefore garnet growth post-dates the formation of at least some of the sulphides.

(c) Chlorite

Chlorite is clearly pseudomorphing the garnet in fig. 5-14e. Although magnetite occurs as near perfect euhedra in the rare cases where it is intergrown with unaltered biotite (fig. 5-11a), magnetite boundaries are quite irregular in the more common intergrowths with chlorite. Magnetite-chlorite textures are difficult to interpret but a detailed study of chlorite along the oxide grain boundaries reveals micro-structures of the type shown in fig. 5-14g; small oriented ilmenite lamellae (arrowed) plus numerous sulphide inclusions remain unaltered after the host magnetite is replaced by chlorite.

(d) Intergrowths in Grunerite-Bearing Alteration Zones

In some parts of these zones anhedral aggregates of pyrrhotite and chalcopyrite form a continuous phase around large garnet idioblasts and smaller ilmenite subhedra (fig. 5-15a). Such an intergrowth could be interpreted according to certain ideas of Stanton (1964) and Schreyer et al. (1964)

FIG. 5-15

(all photographs except g taken in reflected
plane polarized light)

(a) An intermixture of pyrrhotite and chalcopyrite
(light grey) forms a continuous phase around
large garnet euhedra. The medium grey elongated
grains are ilmenite.

(b) Pyrrhotite (Po) and quartz together form a
continuous phase interstitial to euhedral
garnets. Note the small inclusions in both the
quartz and sulphide.

(c) Magnified view of the quartz polished surface
shows that the inclusions are traces of small
grunerite needles.

(d) Similar inclusions of grunerite in the pyrrhotite.

(e) Large poikiloblast of magnetite (Mt) enclosing
euhedral garnets and anhedral inclusions of
pyrrhotite and chalcopyrite. Groups of pyrrhotite
grains display simultaneous extinction positions.

(f) Traces of grunerite needle inclusions in magnetite.
Note the grunerite needles in the sulphide
inclusion in the upper right.

(g) Large ilmenite porphyroblasts (Il) intergrown
with garnets containing quartz inclusions. The
repeated twinning in the ilmenite is probably of
deformation origin. Taken under partially crossed
nicols.
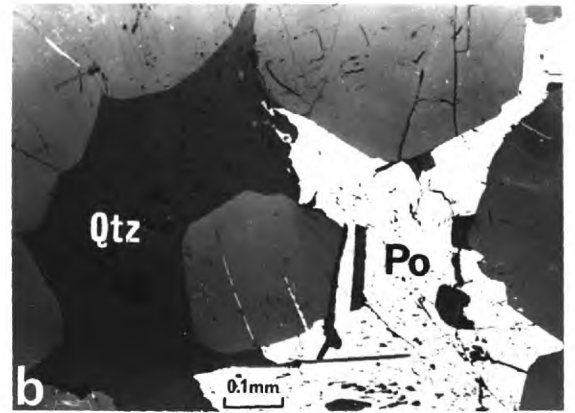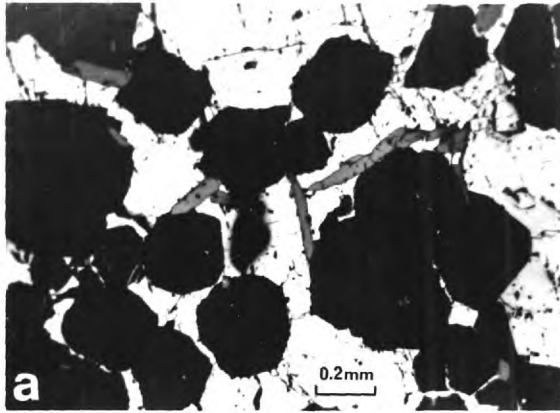
FIG. 5-15

as the result of relative interfacial tensions during essentially simultaneous crystal growth. But it has already been shown fairly conclusively that there are clear sequences of mineral growth in the Kanmantoo mineralization so such an explanation would simply be avoiding the difficulties of interpretation.

In some places quartz and sulphide together act as interstitial material to the garnets (fig. 5-15b) and an interesting feature is that amphibole needles appear in both phases (fig. 5-15c,d). It is difficult to imagine amphibole needles nucleating and growing in the interior of sulphide grains so it seems likely that the sequence of events was (1) development of the quartz-amphibole intergrowths followed by (2) replacement of quartz but not amphibole by the sulphides.

Very large magnetite poikiloblasts grow in the grunerite zones and enclose large euhedral garnets as well as numerous groups of anhedral sulphide inclusions (fig. 5-15e). A close examination of the magnetite near the sulphide inclusions and near magnetite-quartz interfaces reveals many amphibole needles in this mineral as well (fig. 5-15f). Thus it appears that magnetite in this case has grown later than all the other phases by replacement of quartz and partial replacement of the sulphides. Ilmenite porphyroblasts display similar relationships towards garnet as does magnetite but they contain neither sulphide nor amphibole inclusions (fig. 5-15g).

Clearly these growth relationships are very complex in detail but there emerges the important conclusion that there has been considerable replacement among the silicates, the sulphides and the oxides. For such phenomena to take place there must have been a good deal of movement of sulphide constituents through at least some parts of the alteration zones.

4. Some Deformation Relationships

(a) General Statement

Tectonic movements occurring in the alteration zones

during and after chloritization have caused the brittle deformation of hard minerals like garnet, staurolite, magnetite and pyrite, the bending and kinking of layer-lattice minerals such as biotite, muscovite, chlorite and molybdenite, the lamellar twinning of ilmenite and chalcopyrite, and the plastic deformation of quartz and pyrrhotite. Deformation of some phases such as bismuth and chalcopyrite even at this late stage, may still have been by a process of simultaneous plastic strain and recrystallization. The activity of aqueous fluids in the zones of local deformation was probably much greater than in the adjacent schists and may even have constituted the greatest single factor in the movement of mineral components.

A clear separation in time or space of the mineralogical and textural changes accompanying this late tectonic activity under conditions of retrogressive metamorphism, from the secondary changes brought about by percolation of surface waters, is almost impossible to establish. Therefore an arbitrary division has to be made; secondary changes are regarded as beginning with the chemical alteration of pyrrhotite to FeS_2 minerals.

(b) Representative Textures

In many deformed intergrowths of sulphide and micaceous minerals the sulphide penetrates with no sign of any replacement for varying distances along the silicate cleavage (fig. 5-16a). An example of a more complex sulphide-mica intergrowth is given in fig. 6-16b; in many cases the sulphide is the enclosing phase and it is difficult to find conclusive evidence on which mineral is corroding which. The mica is usually clearly deformed but lamellar twinning in chalcopyrite is no evidence of deformation since similar twinning is found in secondary material that has definitely not been deformed. Simultaneous deformation of many mica-pyrrhotite intergrowths is usually more obvious since strain effects in this sulphide are less subtle than in chalcopyrite. An example is given in fig. 5-16c where folded partings and undulose extinction zones

FIG. 5-16

(a) Slim tongues of chalcopyrite (Cp) penetrating along the cleavages of chlorite. Oil immersion.

(b) Complex intergrowth of chalcopyrite with deformed chlorite (black). Oil immersion.

(c) Simultaneous deformation of chlorite (Chl) and pyrrhotite (Po) indicated by the parallelism of the folded silicate cleavages and sulphide partings. Note also the radial undulose extinction zones in the pyrrhotite. Some of the deformed pyrrhotite appears to have recrystallized into granular aggregates (arrowed). Taken under partially crossed nicols.

(d) Chalcopyrite (Cp) penetrating along the basal partings of a bent ilmenite grain.

(e) Chalcopyrite infilling fractures in garnet (Gn) and grunerite (Gr).

(f) "Exploded" rutile (Rt) aggregate after ilmenite; the outline of the former ilmenite crystal is clearly visible. Chalcopyrite and a little chlorite form a continuous phase around the disoriented rutile grains. Pyrrhotite occurs frequently along the boundaries of such rutile-chalcopyrite intergrowths but is not found as part of the intergrowth.

(g) Ragged aggregates of chalcopyrite interstital to coarse-grained vein quartz. Note the small sulphide tongues along the quartz-quartz grain boundaries.

(h) Multitudes of sulphide crystallites extend out from the chalcopyrite tongues for short distances along the quartz-quartz grain boundaries. The photograph was taken with an oil immersion objective focused below the polished surface of the specimen.
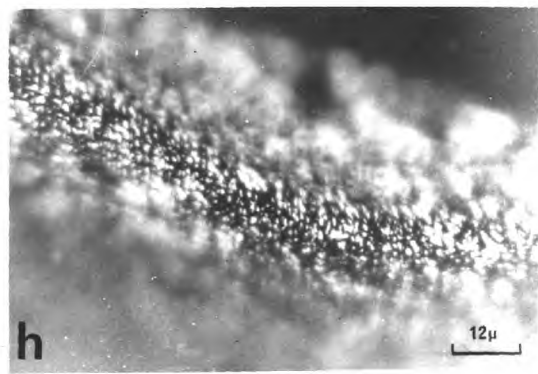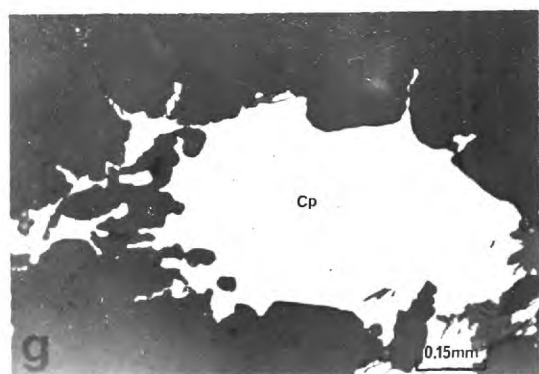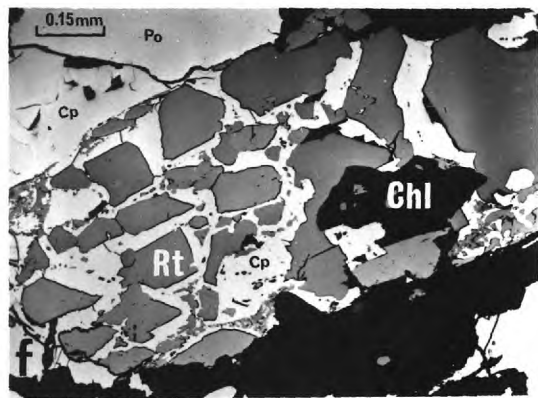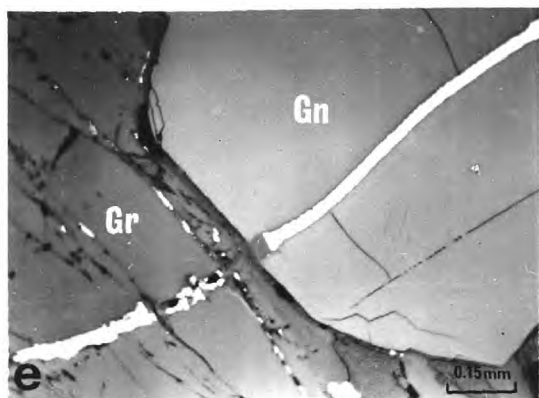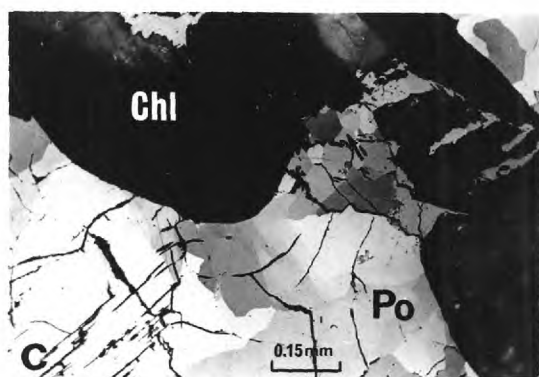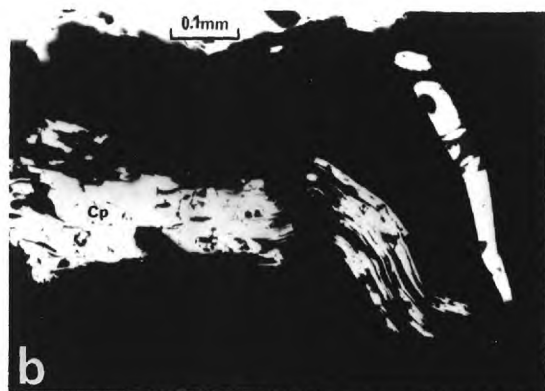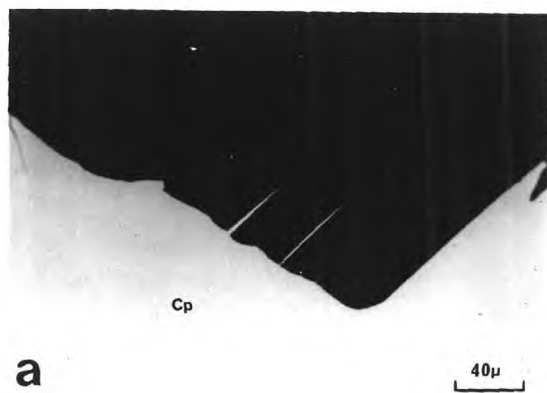
FIG. 5-16

in the sulphide correlate with the folded cleavage in the
adjacent mica. Note the small polyhedral pyrrhotite area
(arrowed) which may be the result of partial recrystalliaztion
following deformation.

Common relationships between the hard and soft minerals
are the infilling of fractures in oxides and brittle silicates
by chalcopyrite and native bismuth (figs. 5-16d,e). Fractured
ilmenite is sometimes partly or wholly altered to rutile (fig.
5-10k); where rutile does not occupy the whole volume of the
former ilmenite grain, the spaces between the rutile network
are filled with quartz, chlorite or sulphides (fig. 5-16f).

A small fraction of the total chalcopyrite and pyrrhotite
occurs in the granular quartz pockets and veins that have
developed in all rock-types. The quartz is nearly always
highly strained and full of fluid inclusions (see ch. 7) but
associated sulphides are usually strain free. In fact the
typical interstial intergrowth shown in fig. 5-16g suggests
the sulphides are replacing the quartz, an interpretaion that
seems to be supported by the many zones of minute sulphide
crystallites that extend outwards for a few millimetres along
quartz-quartz interfaces and along healed fractures (fig. 5-16h).

(c)   The Occurrence of "Primary" Pyrite

All the marcasite and nearly all the pyrite in the
Kanmantoo orebody appear to have formed directly or indirectly
from the breakdown of pyrrhotite. These secondary minerals
occur as very fine-grained concentric intergrowths or as
rather porous looking, crystalline material truncating the
concentric textures and containing minute mineral inclusions
and numerous cavities. Fractures are generally of the shrinkage
type.

However there are a few pyrite grains up to 20mm in
size that have an altogether different appearance to this
secondary pyrite. These are intergrown with unaltered pyrrhotite
and chalcopyrite (fig. 5-17a) and enclose large euhedra of
garnet, staurolite and magnetite (fig. 5-17b); the magnetite

FIG. 5-17

Primary Pyrite Relationships

(a) Euhedral primary pyrite (Py_1) intergrown with chalcopyrite (Cp) and pyrrhotite (o).

(b) Coarse-grained fractured primary pyrite enclosing porphyroblasts of magnetite (Mt) and garnet. Pyrrhotite and chalcopyrite occur both as minute inclusions in the magnetite and as infillings along fractures in the pyrite.

(c) Tectonic fractures in primary pyrite infilled with quartz. The primary pyrite is in contact with a lower reflectivity secondary pyrite (Py_2) which has an extremely irregular boundary with chalcopyrite (Cp).

(d) Fractures in primary pyrite infilled with major pyrrhotite and minor chalcopyrite. corrosion of the pyrite by these other sulphides is only slight.

(e) An unusual intergrowth of secondary pyrite along fractures in primary pyrite. It is possible that this secondary pyrite is an in situ alteration product of former fracture-filling pyrrhotite of the type illustrated in the previous photograph.
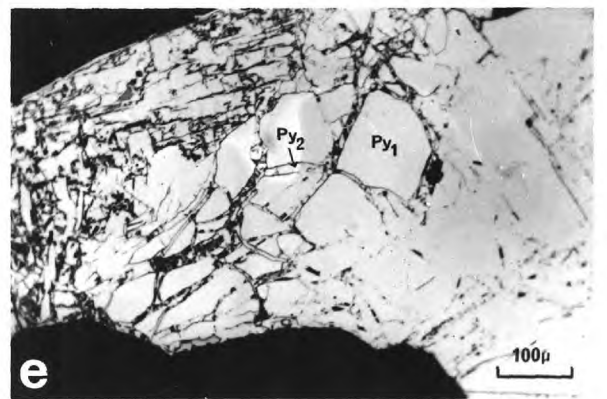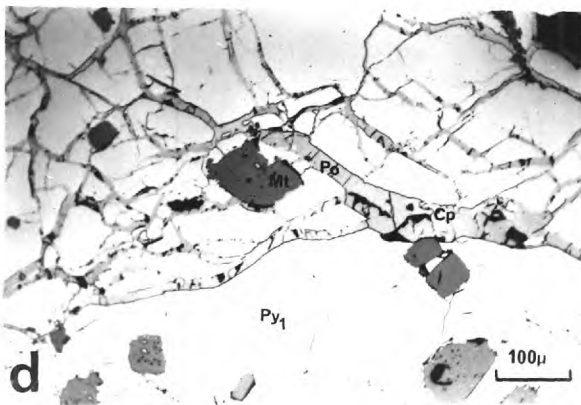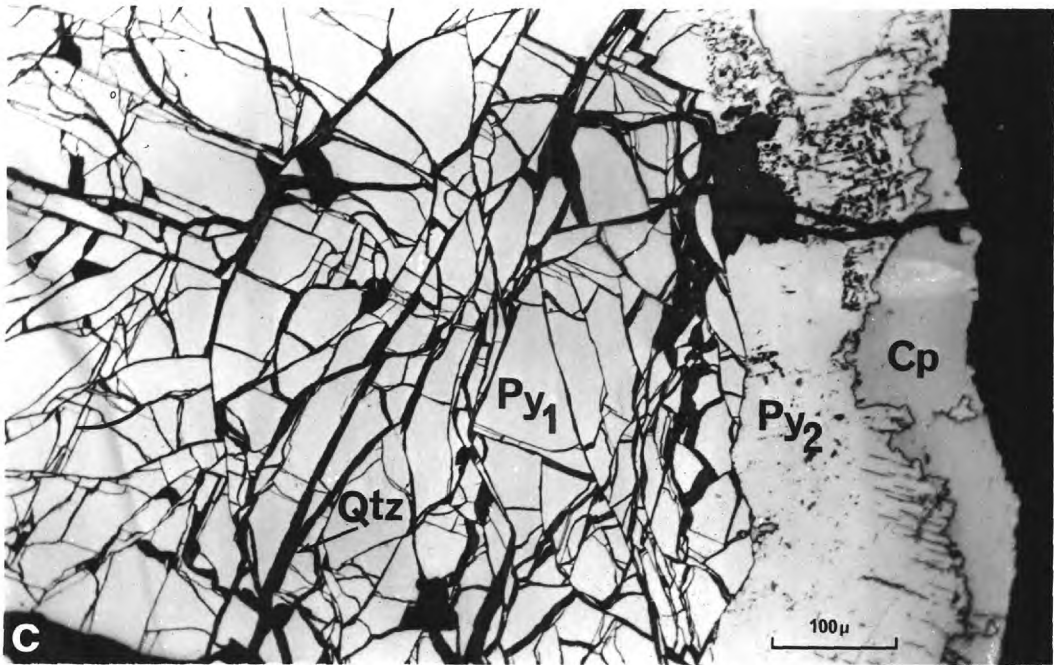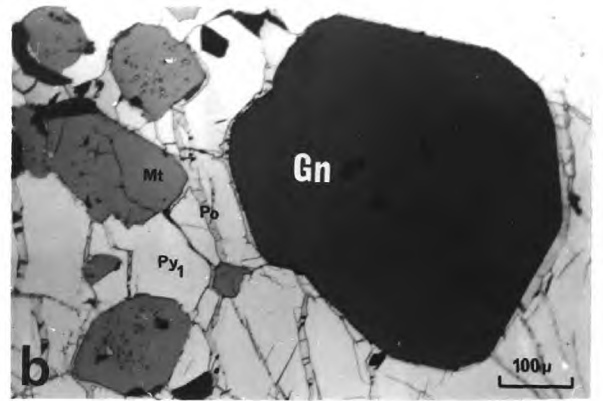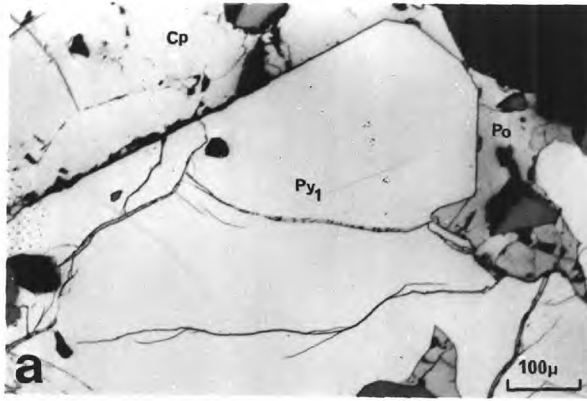
FIG. 5-17

in turn may contain minute inclusions of chalcopyrite and
pyrrhotite. Fractures are of the tectonic type and are generally
infilled with quartz or by pyrrhotite and chalcopyrite (figs.
5-17c,d). In some places this homogeneous looking pyrite (Py_1)
is in contact with a porous looking pyrite (Py_2) of slightly
lower reflectivity (fig. 5-17c); neither by X-ray powder
diffraction nor by electron probe microanalysis could any
distinction be made between these two pyrites. Another inter-
growth of the two pyrites is shown in fig. 5-17e where the
lower reflectivity phase actually infills fractures in the
homogeneous pyrite. This lower reflectivity material is very
similar in appearance to much of the secondary pyrite that is
forming from pyrrhotite and so it seems likely that to have
had the same origin.

The growth of the higher reflectivity pyrite appears
to post-date not only the garnet, staurolite and magnetite
but also the chalcopyrite and pyrrhotite inclusions in the
magnetite. On the other hand it pre-dates the formation of
the pyrrhotite and chalcopyrite in the fractures as well as
the secondary pyrite. It therefore seems reasonable to regard
this pyrite as primary and that it attained its present form
during late metamorphic times.

F. SOME SECONDARY MINERALS AND THEIR INTERGROWTHS

1. The Formation of Secondary Iron Sulphides

Undeformed secondary pyrite and marcasite are found
throughout the orebody and show an erratic distribution
related neither to surface topography nor to the location of
supergene copper sulphides. These FeS_2 phases show two distinct
modes of occurrence; (1) pyrite and marcasite clearly related
to the breakdown of pyrrhotite and (2) pyrite not associated
directly with pyrrhotite.

(a) Alteration of Pyrrhotite to Marcasite and Pyrite

Progressive changes in the breakdown of pyrrhotite are

shown in the hand specimen illustrations of fig. 5-18.
Concentric intergrowths of marcasite and pyrite grow initially
along and out from narrow hairline fractures which form a
three dimensional network through the larger pyrrhotite
aggregates (fig. 1-18a). In a more advanced stage of alteration
shown in fig. 5-18b, the FeS_2 mineral networks have isolated
small volumes (islands) of pyrrhotite. There is generally a
small gap between the pyrrhotite and FeS_2 boundaries which
suggests there has been a loss of some iron during the altera-
tion process, and this is supported by the presence of cavities
formed through the dissolution of some of the pyrrhotite.
islands. The end products of pyrrhotite alteration are the
granular aggregates of pyrite and marcasite containing numerous
cavities in which crystal faces have developed (fig. 5-18c).
Small areas of the earlier concentric FeS_2 intergrowths as
well as the initial hairline fractures are still clearly
visible.

Microscopically, the secondary pyrite-marcasite inter-
growths appear complex and varied although certain geometrical
features are common to all. Concentric intergrowths usually
occur in a number of layers all of which have their convex
surface directed towards the adjacent pyrrhotite (fig. 5-19a,b).
Certain sections displaying complex concentric intergrowths
e.g. fig. 5-19d, are probably the result of a two-dimensional
view through intersecting sets of botryoidal concentric layers
that have different curvatures. In a few places the interface
between one set of concentric layers and another is perfectly
planar (fig. 5-19a) but in general, the only common occurrence
of planar interfaces is at the boundaries between FeS_2 inter-
growths and euhedral silicate crystals (fig. 5-19d).

The lighter coloured, more homogeneous looking layers
in the concentric intergrowths consist of fine to medium grained
radial aggregates of marcasite or marcasite in pyrite, or
granular aggregates of pyrite. The darker porous looking
layers in between consist of very fine-grained material; X-ray
powder photographs show different zones to contain marcasite,

FIG. 5-18

Progressive Changes in the Alteration of
Pyrrhotite to Pyrite and Marcasite
(photographs slightly enlarged)

(a) An aggregate of pyrrhotite (Po) and magnetite (Mt)
     in contact with garnet-biotite schist (Sc) displays
     incipient alteration to fine-grained FeS_2 minerals
     along hairline fractures (arrowed).

(b) Pyrrhotite in a more advanced stage of alteration.
     Note the small pyrrhotite islands completely
     surrounded by finely banded FeS_2 zones; dissolution
     of these pyrrhotite islands results in small cavities
     (arrowed) in which pyrite and marcasite crystal faces
     develop.

(c) The final product of pyrrhotite alteration:
     granular aggregates of pyrite and a little marcasite
     containing numerous cavities lined by FeS_2 crystals.
     Some of the initial hairline fractures (arrowed) and
     the early concentric FeS_2 intergrowths are clearly
     visible. The lighter areas are caused by the evapora-
   tion of moisture from the surface of the specimen
   during photography.
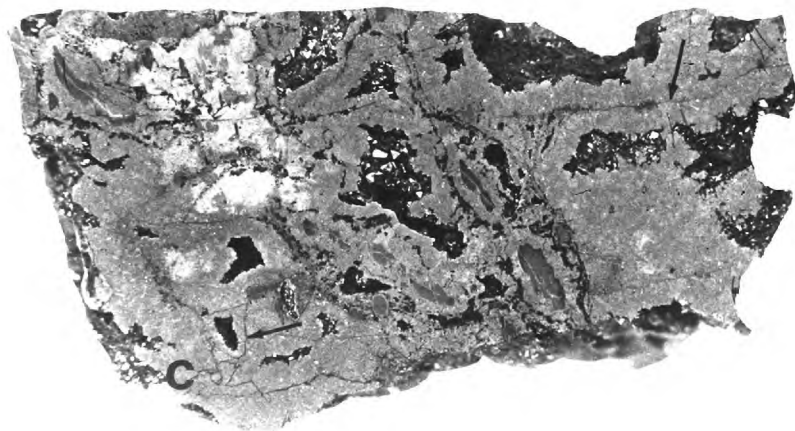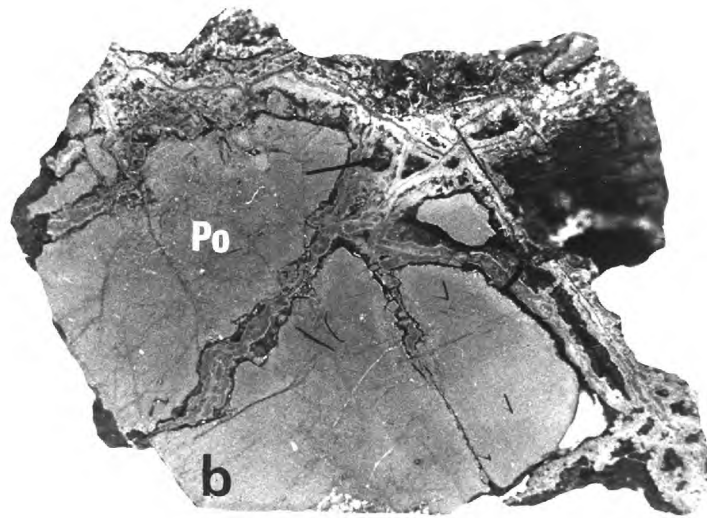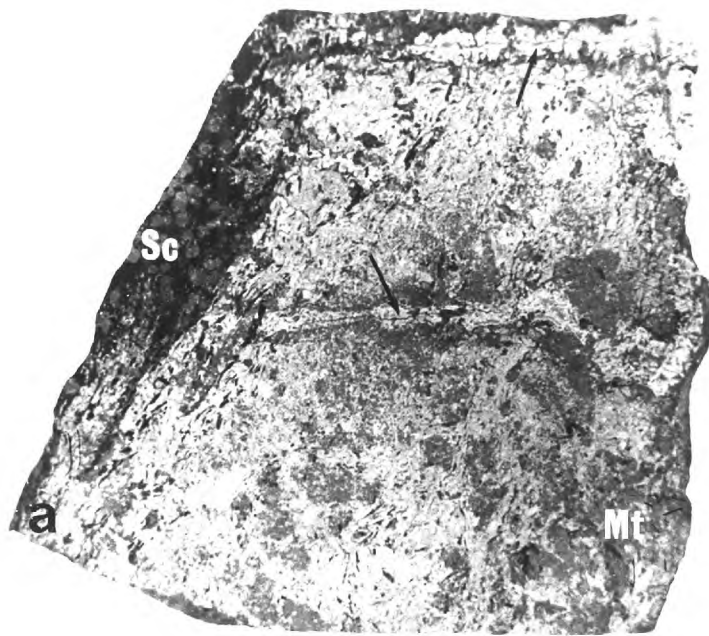
FIG. 5—18

FIG. 5-19

Textures of Some Secondary Minerals

(a,b) Concentric layers of very fine-grained marcasite and pyrite (darker material) and medium-grained crystalline pyrite (arrowed) display their convex surfaces towards the pyrrhotite (Po). Note the siderite (Sd) infilling the hairline fracture in the second photograph.

(c) Coarse-grained pyrite that apparently recrystallizes from the concentric, fine-grained FeS_2 layers. Lines of ragged pyrrhotite and magnetite inclusions follow the growth zones of the pyrite.

(d) Complex concentric FeS_2 aggregates interstitial to large staurolite (St) porphyroblasts. The arrow points to what appear to be concentric shrinkage or syneresis cracks.

(e) Secondary coarse-grained pyrite aggregates lining a cavity . The bladed shape of the individual pyrite grains is also characteristic of nearby marcasite aggregates which do not display this type of micro-fracture pattern. This suggests that the pyrite has inverted from marcasite and the fracture pattern is a result of the slight density increase accompanying the inversion.

(f) Pyrite veinlets along fractures in rutile.

(g) Pyrite infilling fractures along vein quartz and growing as a poikiloblast in the same material.

(h) Chalcopyrite (Cp) pseudomorphing secondary pyrite around a cavity.

(i) Chalcopyrite being replaced by supergene hornite (Bn).

(j) Intergrowth of supergene bornite and supergene chalcocite (Cc).
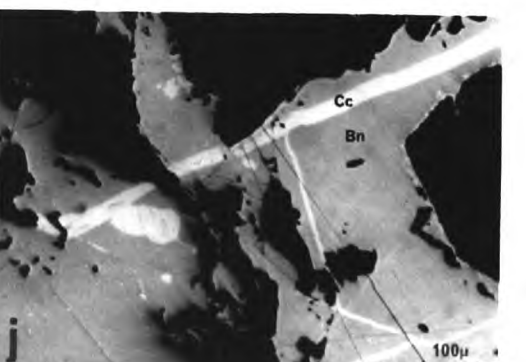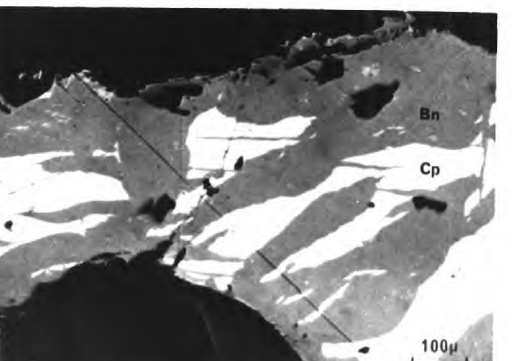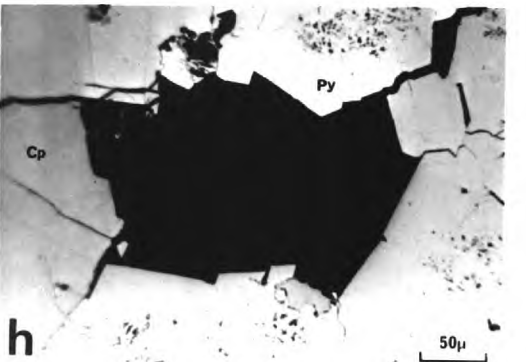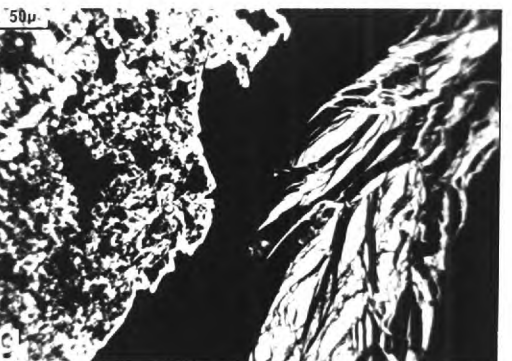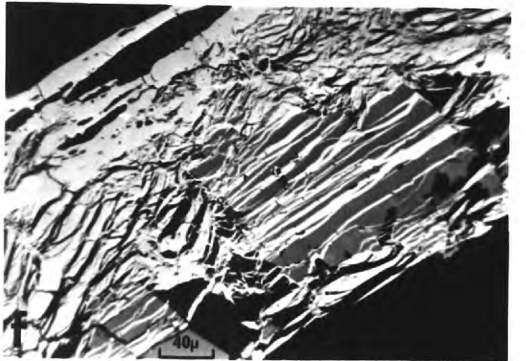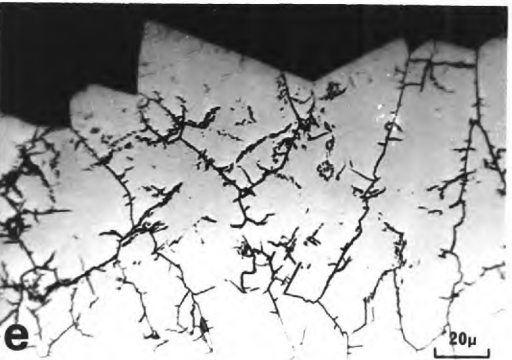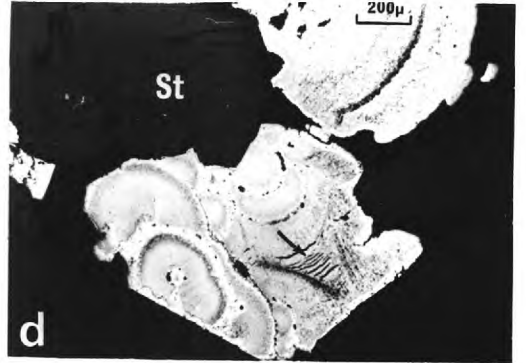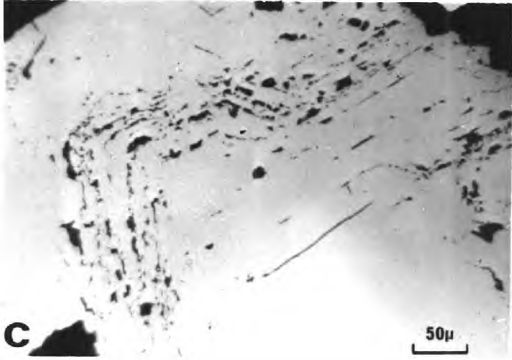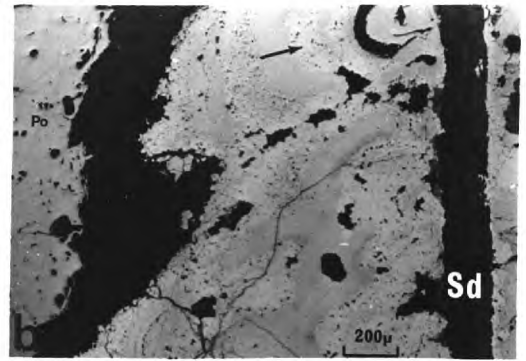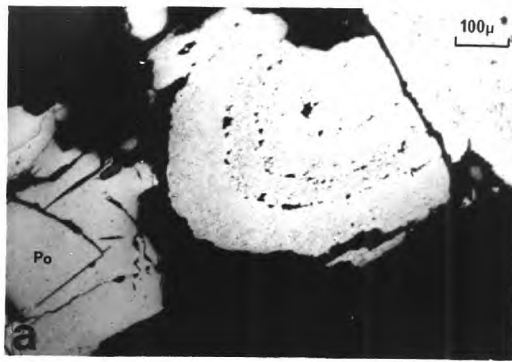
FIG. 5-19

marcasite plus pyrite or rarely pyrite alone. In addition
small amounts of quartz, siderite, possible troilite and other
unidentified compounds may be present. No correlation has
been able to be made between the appearance or position of a
zone in an intergrowth and its mineralogical composition.

To a varying degree through all this secondary FeS_2
material, the concentric fine-grained layers are truncated by
aggregates of coarsely crystalline pyrite or pyrite plus
marcasite. Granular pyrite grains display euhedral growth
zones and in many cases contain lines of minute ragged inclusions
of pyrrhotite and magnetite following the zonal growth structure
(fig. 5-19c). This pyrrhotite may or may not be unreplaced
primary material but the magnetite appears to have formed
during the growth of the pyrite. Neither the granular pyrite
nor the bladed marcasite in pyrite aggregates display any
significant fracturing but a feature of the not uncommon
bladed pyrite aggregates is a distinctive fracture pattern
along and outward from the grain boundaries (fig. 5-19e).

The origin of these secondary FeS_2 minerals is clearly
related to the breakdown of primary pyrrhotite but the precise
course crystallization and recrystallization in the FeS_2 inter-
growths is difficult to determine. Some of the morphological
features of the concentric intergrowths appear consistent
with their being originally finely-divided gel-like material
governed to a large extent by surface tension forces. Such a
material would attempt to reduce its free surface by assuming
a near spherial form and reduce its internal surface by
crystallizing or recrystallizing into larger grains. If a
newly formed layer or set of layers were to begin recrystalliz-
ing inwards from both its free surface and attachment surface,
a rigid "shell" would probably be formed; any further
recrystallization and possible accompanying dehydration would
lead to shrinkage phenomena of the type arrowed in fig. 5-19d.
These partially crystalline concentric intergrowths were
probably still relatively unstable and in many places appear to
have undergone recrystallization to the coarse-grained aggregates
of pyrite and marcasite.

In some cases pyrite and marcasite appear to have formed
as contemporaneous recrystallization phases but in other cases
pyrite is pseudomorphic after marcasite. In the example given
in fig. 5-19e the fractures are most likely the result of the
volume change during the inversion of marcasite to more dense
pyrite.

(b) Pyrite not Associated Directly with Pyrrhotite

A little late pyrite that has clearly been introduced
from outside the site of deposition rather than derived from
adjacent pyrrhotite is found along mineral fractures (fig.
5-19f) and as nearly poikiloblastic intergrowths within vein
quartz (fig. 5-19g).

2. Other Secondary Minerals

The chemical mobility of chalcopyrite even at this late
stage is shown in fig. 5-19h where it pseudomorphs secondary
pyrite euhedra lining a cavity. A small quantity of chalco-
pyrite in the orebody is therefore secondary.

In contrast to the secondary FeS_2 phases, the distribu-
tion of the minor secondary copper sulphides bears a close
relationship to surface topography. Below about 100 feet a
little chalcopyrite may be rimmed and veined by bornite (fig.
5-19i) but just below the surface chalcopyrite is largely
missing. The common assemblage is one of bornite rimmed and
veined to varying degrees by chalcocite containing a few
minute blades of covellite (fig. 5-19j).

On the surface primary magnetite is partially martitised
to network intergrowths of hematite, while all the sulphide
minerals have been altered to box-work masses of hematite
containing films of copper carbonates.

SUMMARY
1. The degree of deformation and metamorphic reconstitution
of rocks in this comparatively small area, varies from slight
in the arenaceous lithologies where detrital quartz and feld-
spar appear to be preserved, to intense in some of the central
alteration zones where the rocks have undergone repeated
movements and prolonged mineral growth.

2. A study of the textural relationships between porphyro-
blastic minerals and matrix structures suggests that the area
(volume) responding to deformation and accompanying metamor-
phism has contracted with time towards the central lode schist
aones. The B_1a and B_1b tectonic events have produced structures
with similar attitudes but of different ages.

3. Intergrowths of the fine-grained disseminated sulphides
and ilmenite with the matrix and porphyroblastic silicates
indicate that the opaque minerals were present in the rocks
from the earliest recognised stage of metamorphism.

4. In the coarse-grained ore associated with the alteration
zones there is substantial textural evidence that magnetite,
ilmenite, pyrrhotite and most of the chalcopyrite, the principal
ore minerals, crystallized and recrystallized with most of
the silicate phases over a long period that began at least as
early as immediately after the B_1b tectonic event. Accompanying
this period of widespread crystal growth has been e tensive
replacement among many minerals.

5. In the ore zones mineral textures having the appearance
of being annealed are rare. This is probably the result of
continual minor movements throughout the late stages of the
thermal history and the considerable movement, growth and
replacement of minerals continuing right up to the present day.

6. There are a few grains of pyrite that texturally appear
to have been present during metamorphism and are therefore
primary, however practically all the pyrite and associated
marcasite are secondary alteration products of pyrrhotite.
Some of the chalcopyrite has apparently been able to move
about rather freely since it partially replaces late phases
like chlorite, rutile after ilmenite and secondary pyrite
after pyrrhotite.

7. Thus there is strong evidence that a small fraction of
the sulphides existed in the schists from early metamorphism
and that a large part of the ore was present from about
the middle stages of metamorphism. Despite this, there is

no positive textural evidence to prove or disprove the
possibility that sulphides in the ore zones were present
prior to the metamorphic events.

8. A schematic representation of the mineral development in
the Kanmantoo orebody with respect to the deformation markers
B_1a, B_1b etc. is given in fig. 5-20. Areas above the base-
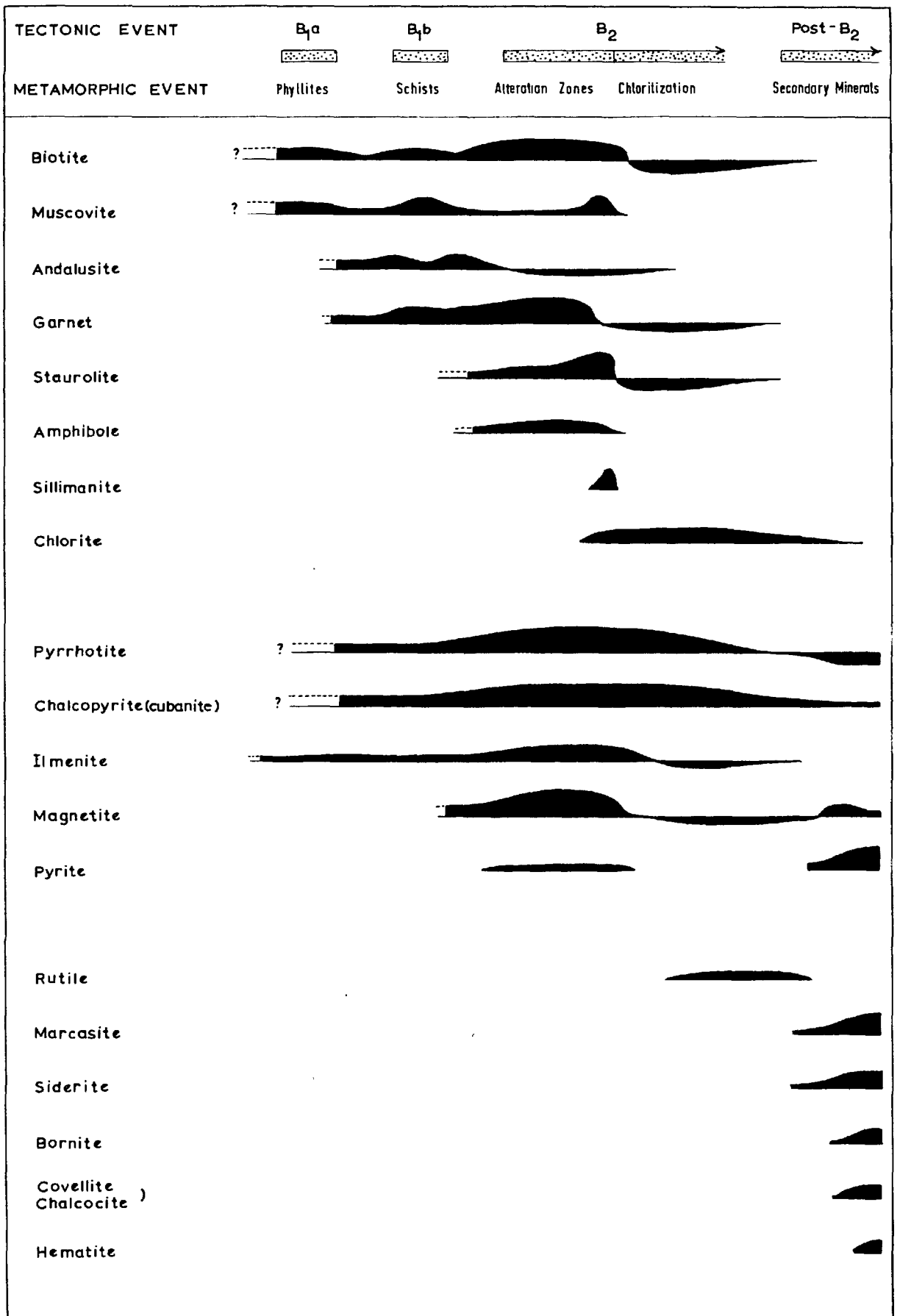line for each mineral indicate times of growth whereas areas
below indicate replacement.

FIG. 5-20 Mineral growth and replacement relationships in and around the Kanmantoo orebody.

chapter 6

MINERALOGY AND PHASE RELATIONSHIPS

Introduction

Textural relationships clearly demonstrate that much of the sulphide-oxide mineralization has been subjected to the elevated temperature and pressure conditions of metamorphism. At almandine-amphibolite temperatures of about $600^{\circ}C$ there is negligible solid solution among the common schist-forming silicates therefore it can safely be assumed that most of the silicate assemblages and intergrowths have been "frozen" from the time of metamorphism. Since the common sulphide systems at this temperature display extensive partial or complete solid solution relationships among many phases, the same assumption cannot be made for the sulphide intergrowths and mineralogy. In this chapter the pressure-temperature path of metamorphism is inferred from the known stability fields of certain silicates. Then the important ore minerals are described and an attempt made to resolve the present sulphide assemblages with known phase equilibria data of the relevant systems.

A. INSTRUMENTAL PROCEDURES

1. X-ray Powder Diffraction

X-ray diffraction analyses were done using both a Philips 11 cm powder camera and a Philips wide-range goniometer. Mineral grains as small as 50 microns could be X-rayed successfully by digging them out of thin and polished sections with a finely pointed steel needle or with a special diamond indentor mounted in a Leitz Duromet microhardness microscope. Microsamples were prepared by picking up the resulting mineral particles in a small drop of cow-gum, grinding the material between two clean glass slides and mounting the resulting powder impregnated gum-ball on the end

of a very thin glass fibre. Larger mineral and rock specimens were ground and prepared either as smears on glass slides or as cavity mounts in standard aluminium holders.

For routine mineral identification no internal standards were used and both films and diffractometer traces were measured without applying any corrections. In calculating unit cell dimensions from powder photographs, allowance was made for film shrinkage and $K\alpha_1$ and $K\alpha_2$ X-ray wavelengths instead of $K\alpha$ average were used where high-angle reflections were resolved into two lines. Cell sizes for a number of garnets were calculated from powder photograph measurements on an IBM 7094 computer using a slightly modified, least squares type programme devised by Burnham (1962).

Where accurate 2θ positions of particular reflections were required in goniometer samples a step-scanning technique was employed. The goniometer was made to advance in stages of 0.01 degrees 2θ and held at each position for either a fixed time when the number of counts were recorded or for a fixed number of counts when the time was recorded. The output appeared simultaneously both in graphical and digital form.

2. Electron Probe Microanalysis

Most of the mineral analytical work was done on a Cambridge Microscan Mk. 2 instrument that incorporates an X-ray take-off angle of 20° measured from the specimen surface and a semi-focusing, vacuum-type X-ray spectrometer. Gypsum, LiF and Pentaerythritol (P.E.T.) analysing crystals enable the complete Bragg angle from 10° to 65° to be covered. An accelerating voltage of 25 KV was employed and for quantitative work, the X-ray intensities recorded on a scaler were corrected for statistical counting error and for atomic number, fluoresence and absorption effects according to the empirical method of Kelly (1969). A small amount of qualitative work was done on a Cambridge Geoscan instrument. Polished surfaces of specimens were always coated with carbon to make them electrically conducting and both pure metals and analysed minerals were used as standards.

3. Reflectivity

Reflectivity values, helpful in aiding identification
of certain opaque minerals, were measured with a Reichert
reflex spectral photometer described by Singh (1965). This
instrument was mounted on a Reichert Zetopan reflecting
microscope and all measurements were made at a wavelength of
589 nm. The reflectivity standard was a polished (111) section
of pyrite calibrated by the National Physical Laboratory.

B. PHASES AND ASSEMBLAGES BEARING ON CONDITIONS OF
METAMORPHISM

1. Composition and Zoning of Garnets

Textural evidence given in chapter 5 indicates a long
history of garnet growth beginning when the rocks were andalusite-
bearing phyllites and continuing well into the B_2 tectonic
phase. The large garnets are restricted to the coarser-
grained, post-B_1b alteration zones in which most of the
important mineralization is located therefore this mineral,
together with associated larger crystals of staurolite, biotite
and chlorite, afford a ready mineralogical guide to ore in the
area. However, there are no obvious visual features in any of
these phases that can be associated with the presence or
absence of ore so it was decided to investigate the garnet
mineralogy further to see if any compositional peculiarities
were present in mineralized or non-mineralized rocks.

Skinner (1956) showed that the end members of the garnet
group had widely varying unit-cell edges therefore cell sizes,
at least in two-component garnets, should be a sensitive
indicator of composition. Microsamples prepared from whole
small garnets and from the cores and rims of large garnets in
various rock-types were X-rayed in an 11cm powder camera using
iron filtered cobalt radiation. From the twenty two lines up
to the (12.2.2) reflection that could be measured on most
photographs, the best-fit cell edges and standard errors of

measurement were computed. In the results shown graphically
in Fig. 6-1a samples (1) and (2) are from fine-grained sulphide-
free quartz-biotite-muscovite schists, samples (3) and (4) are
from unmineralized, coarse-grained garnet-quartz-grunerite
alteration zones while the remaining samples are from sulphide
and sulphide-oxide bearing alteration zones of various types.
A semi-quantitative electron probe traverse across one large
garnet was made to help interpret the X-ray data (fig. 6-1b).

The important relationships revealed in fig. 6-1 are:
(a) in all but one sample the large garnets show a significant
compositional zoning, (b) this zoning as demonstrated by
the elemental variation across a garnet of sample no. 10
is caused by a sharp decrease in the MnO/FeO ratio from the
core to the rim, (c) CaO and MgO contents are very small,
(d) small garnets in fine-grained schists are richer in
spessartine than the small garnets associated with large
garnets in alteration zones, and (e) the indicated composi-
tions of the large garnet rims and the small garnets in the
alteration zones are close to pure almandine.

Thus while there is considerable variation in the degree
of zoning in garnets from different rock-types, clearly there
is no zoning feature that can be correlated with the presence
or absence of sulphide minerals.

While it was earlier supposed that the decreasing MnO
content of Ca-poor garnets in higher grade metamorphic rocks
was a good indicator of the P-T conditions of metamorphism
(Miyashiro, 1953) and recent studies of equilibrium garnet
compositions in the garnet-mica system by Dahl (1968) support
this supposition, it appears that pressure-temperature deductions
from garnet compositions must always be treated with caution.
In particular, allowance must be made for the influence of
host-rock composition on garnet composition (Atherton, 1965)
and account must be taken of possible zoning which is evidently
very common in garnets (Atherton and Edmunds, 1966). Harte
and Henley (1966) think that different zones in spessartine-
almandine garnets may be the result of a grade effect whereby
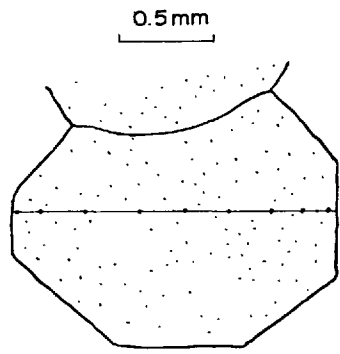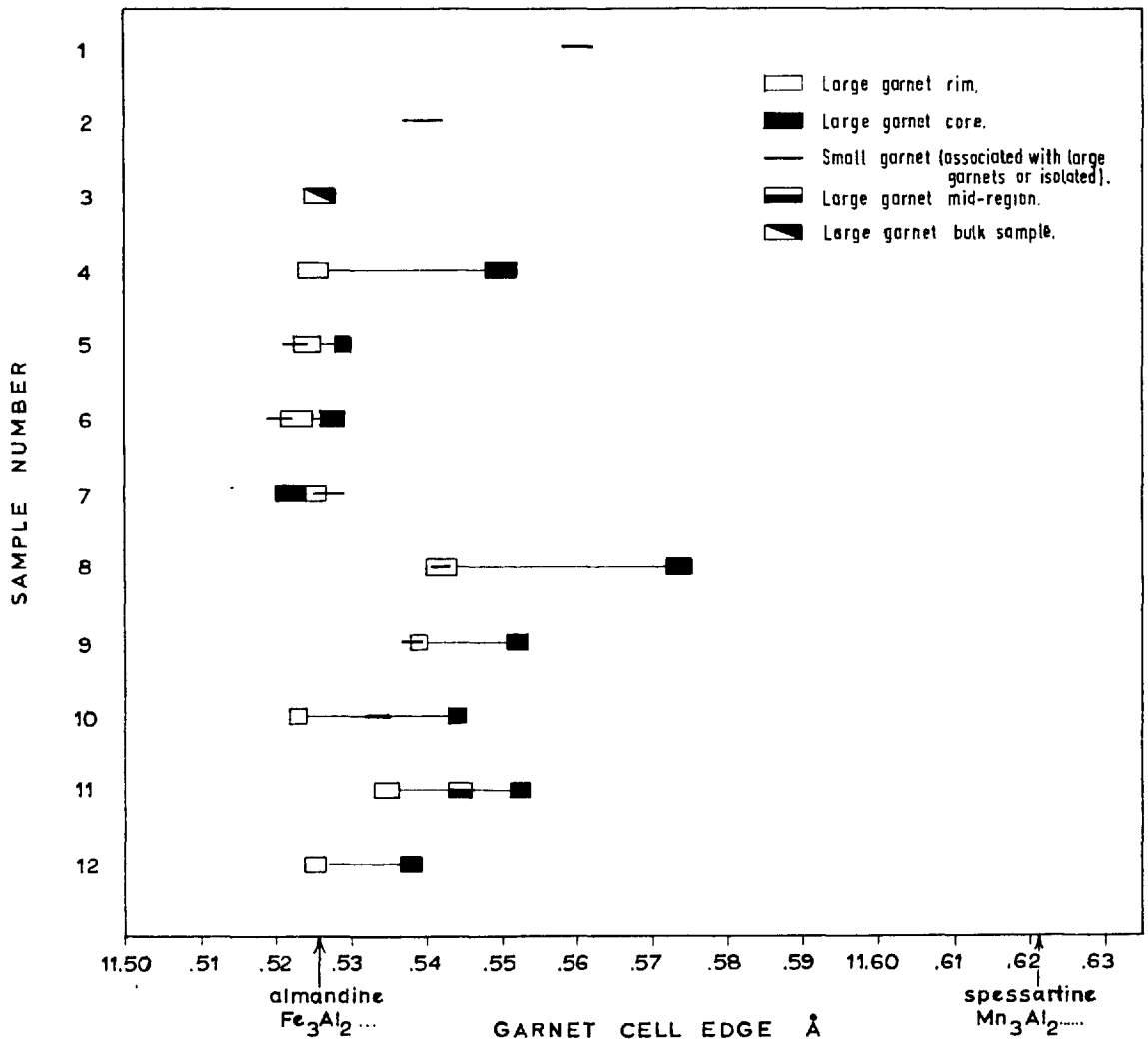
(a) Cell edges of some garnets from the wall and country rocks of the Kanmantoo orebody (see text).
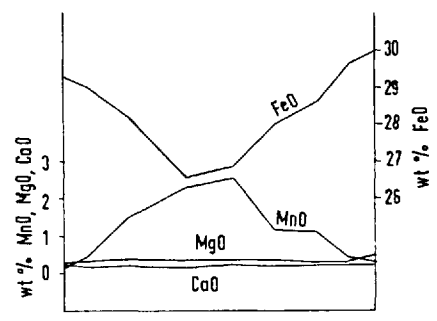
(b) Electron probe traverse across a large garnet from sample number 10.

FIG. 6-1

iron becomes increasingly stabilized in the garnet lattice
with increasing temperature but the interpretation of similar
zoning by Hollister (1966) as the fractionation of Mn from
the rock by garnet growth rather than as a reflection of
increasing temperature, is supported by the work of Leake
(1968) on garnets from the Galway granite. These igneous
garnets which are presumed to have grown in conditions of
falling temperature, are also found to have "normal" Mn-rich
cores and Fe-rich rims. Leake's work would seem to preclude
any inferences being made on the pressure-temperature conditions
of garnet growth in the Kanmantoo rocks from the present data.

2. Aluminium Silicates

For some time the stability fields of the three aluminium
silicate minerals - andalusite, sillimanite and kyanite -
have promised to provide valuable data on the physical condi-
tions of metamorphism. However in a recent review of the
aluminium silicate polymorphs, Pitcher's (1965) opinion that
"... the stability relationships of the naturally occurring
aluminium silicates have not yet been closely enough simulated
in the laboratory for estimates to be made of the P-T condi-
tions of metamorphic processes..." is supported by the great
variance in the results of different workers. For instance,
Clark et al. (1957) gave a triple point at $260^{\circ}C/8$ kb while
Newton (1966) gave the same point at approximately $500^{\circ}C/4$ kb.
Fortunately recent experimental work has produced results
more in accord with petrologic expectations. The stability
field determinations of Althaus (1967) have been adopted for
the P-T diagram in fig. 6-2 because they agree closely with
other reaction curves involving Al_2SiO_5 phases as well as
with the most recent triple point determination by Gilbert,
Bell and Richardson (1968).

In the schists around the Kanmantoo orebody andalusite
growth began immediately after the B_1a tectonic phase and
continued until soon after the B_1b phase when it began to be
replaced largely by coarse-grained aggregates of quartz and
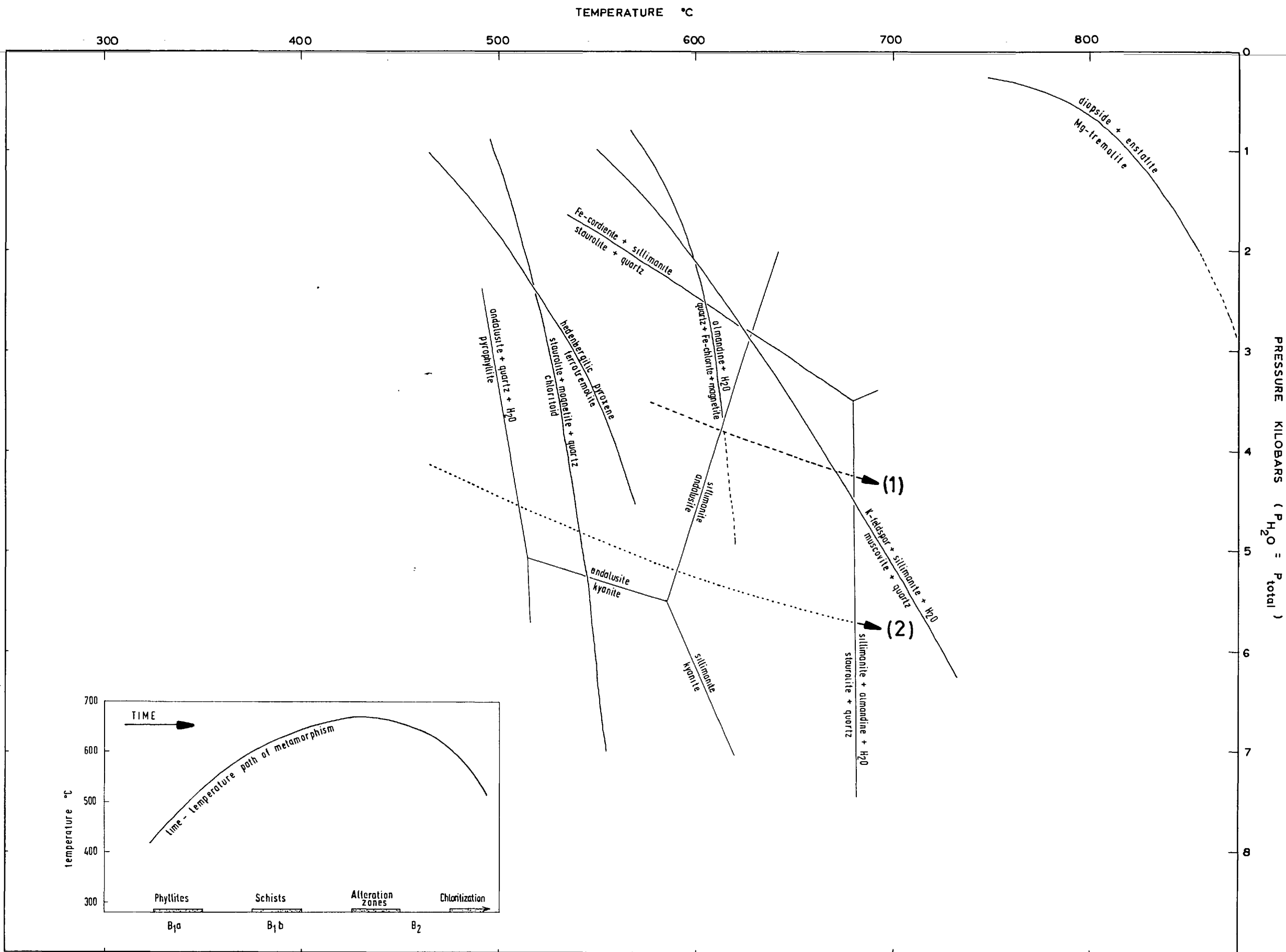muscovite. The small amount of sillimanite present probably

FIG. 6-2 Physical conditions of metamorphism defined by stability fields of some silicate minerals.

began to form around this stage since the coarse-grained
post-tectonic muscovite and sillimanite appear to be broadly
comtemporaneous. Kyanite is absent but is found in rocks of
similar composition in the nearby localities of Brukunga and
Strathalbyn (fig. 2-4). Thus it appears that the P-T conditions
of metamorphism reached the sillimanite stability field but
there is regional evidence that they were close to the kyanite
field as well (see fig. 6-2).

3. Stability Fields of Other Phases

As the compositions and thus the P-T stability fields
of iron-oxides and iron-bearing silicates are dependent on
the oxygen fugacity (f_{O_2}) of the environment, experimental
work on synthetic systems containing iron and oxygen has to
be done under controlled f_{O_2} conditions. The usual technique
for controlling f_{O_2} is to hold the charge in a container into
and out of which oxygen can diffuse freely and to surround
this container with an assemblage of buffer phases sensitive
to changes in f_{O_2}. Such oxygen buffers work on the principle
that at a given temperature and total pressure, the oxygen
fugacity is fixed as long as all the phases in the buffer
are present; any tendency for the f_{O_2} of the charge to change
is prevented by a change in the amount of one of the buffer
phases that either releases or absorbs oxygen. The relevant
reactions in the QFM (quartz + magnetite - fayalite) and the
magnetite - hematite buffer assemblages are given below:

$$3SiO_2 + 2Fe_3O_4 \rightleftharpoons 3Fe_2SiO_4 + O_2$$

$$3Fe_2O_3 \rightleftharpoons 2Fe_3O_4 + \tfrac{1}{2}O_2$$
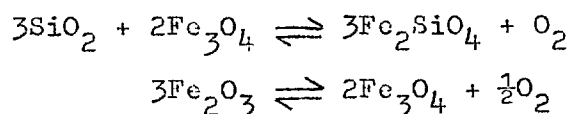
The common occurrence of quartz + magnetite and the absence
of both fayalite and primary hematite in the Kanmantoo rocks
indicate that the oxygen fugacities were always between the
values defined by these two reactions (see fig. 6-4g).

The lower stability curve for staurolite taken from
Ganguly and Newton (1968) and the other staurolite stability

curves from Richardson (1968) were all determined under f_{O_2} conditions defined by the quartz + magnetite - fayalite buffer. The position of the lower temperature stability curve on fig. 6-2 agrees well with the interpreted appearance of staurolite considerably after the beginning of andalusite growth but prior to the development of sillimanite. In a few places sillimanite needles along corroded-looking margins of staurolite in contact with quartz suggest that the high-temperature stability curve of staurolite may just have been reached. The absence of Fe-cordierite in the Kanmantoo rocks indicates a pressure in excess of 3.5 kb but if a P-T path such as (1) in fig. 6-2 were followed, then the muscovite + quartz stability limit as determined by Evans (1965) would be exceeded and potash feldspar would be expected to be present. More likely is a path such as the dotted one (2) since it remains in the stability field of muscovite + quartz and passes close to the kyanite field as suggested by the presence of kyanite in nearby rocks.

Two tremolite stability curves are plotted in fig. 6-2; the ferrotremolite curve was determined by Ernst (1966) using a QFM oxygen buffer and the Mg-tremolite curve by Boyd (1959) using a magnetite -wüstite buffer. Both the optics of the pale-green amphibole in the calc-silicate schist bands and the whole rock chemical analysis (table 8-1. ch.8) suggest the mineral is an actinolite with an FeO/MgO ratio of near 1:1. The stability curve for such a mineral is probably about mid-way between the two end-member tremolite curves, a position that would be fairly close to the inferred P-T conditions around the metamorphic climax. Not much information is available on the stabilities of phases in the grunerite - cummingtonite series of amphiboles although Kopp and Harris (1967) synthesised grunerite at $400^\circ C$ at 1.6 kb fluid pressure. However, petrographic indications are that the iron-amphibole in the Kanmantoo rocks was stable at much higher values than these.

In fig. 6-2 it is assumed that $P_{H_2O} = P_{fluid} = P_{rock}$ but it should be pointed out that the equilibrium temperatures

of dehydration reactions are lower if P_{H_2O} is less than P_{rock} (Althaus, 1968).

4. Some Remarks on the Conditions of Formation of Chlorite

The general views of Turner and Verhoogen (1960) and Winkler (1965) that retrogressive minerals are the result of re-equilibration to lower temperature conditions in local areas where water becomes available for hydration reactions have been challenged recently by Carpenter (1967). He thinks that in some cases, "low-grade" assemblages adjacent to "high-grade" assemblages may have formed at the same time as the latter but under more hydrous conditions in the low-pressure zones of fold crests. In deducing the age and conditions of growth of chlorite in the Kanmantoo rocks the important points to be considered are; (a) chlorite is best degeloped in the alteration zones along which deformation was locally prolonged, (b) in almost all cases chlorite is a breakdown product of other minerals particularly of biotite but to a lesser extent of garnet and magnetite, and (c) chlorite is a rare mineral in those siliceous mineral veins containing a high-temperature silicate assemblage. But the very existence of the mineral veins is considered to be a result of diffusion along tectonically induced pressure gradients into low-pressure zones and primary fluid inclusions in many minerals associated with vein formation indicate a water-rich environment (see chapter 7). Thus there seems to be little doubt the chlorite in the alteration zones is a truly retrogressive mineral although this is not to imply that it is all of low-temperature origin. At 3 kb fluid pressure in a system with the f_{O_2} controlled by a QFM buffer, Hsu (1968) determined the equilibrium temperature between iron-chlorite and almandine to be close to $600^{\circ}C$ (see fig. 6-2). The alteration of biotite to chlorite is complex since the commonly observed volume by volume replacement requires in addition to introduction of water and extraction of alkalis, transfer of other material as well. The temperature of the biotite-chlorite reaction is dependent on many factors including mineral compositions and the ratio

of K^+ to H^+ in the system (McNamara, 1966).

5. General Deductions on the Conditions of Metamorphism

The approximate pressure-temperature path thought to have been followed during the progressive metamorphism is shown dotted in fig. 6-2. An inferred temperature of around $675^{\circ}C$ and pressure of just over $5\frac{1}{2}$ kb reached during the metamorphic climax compare reasonably well with corresponding values of $650^{\circ}C$ and about 4 kb estimated for the metamorphism over the greater part of the Kanmantoo Group by Offler and Fleming (1968). The pressure estimate of these workers is based on the earlier aluminium silicate stability determinations of Newton (1966). A time-temperature graph inset in fig. 6-2 shows the order of temperatures that were probably operative during the various tectonic and inter-tectonic events.

Although the rocks around the Kanmantoo orebody come within the almandine-amphibolite facies of Turner and Verhoogen (1960), the metamorphism can be better described according to the facies classification of Miyashiro(1961) as belonging to the intermediate-pressure series.

C. ORE MINERALOGY

1. Pyrrhotite Relationships

(a) General Optical Character and Composition

Pyrrhotite is volumetrically the most important primary sulphide phase in both the coarser grained mineralization of the orebody and in the fine-grained disseminated mineralization found in parts of the adjacent schists. Optically, the pyrrhotite varies from pale pink to pale brown and is characteristically strongly bireflectant and anisotropic. Completely undeformed material is apparently rare since nearly all grains or aggregates, particularly in the coarser ore, display a strong undulose extinction similar to that seen in strained quartz in thin section. Some of the deformation

boundaries may be true deformation twin planes, but their general converging or irregular geometry points more to some type of polygonization structure produced by the ordering of strain-induced lattice defects after deformation (figs. 6-3a,b). These photographs illustrate also the delicate lamellar microstructure visible through much of the pyrrhotite when viewed under partially crossed nicols. One of the lamellar phases is always optically continuous with material that forms along both the pyrrhotite internal and external grain boundaries. There is no obvious correlation between the intensity of strain effects in the pyrrhotite and the incidence of these lamellar intergrowths.

X-ray powder diffraction traverses across the (102) reflection of pyrrhotite that shows little or no lamellar microstructure produce a single symmetrical peak of the type shown in fig. 6-4a, thereby indicating a hexagonal structure. Furthermore, weak superlattice reflections at 5.70 $\overset{o}{A}$ and 4.80 $\overset{o}{A}$ (fig. 6-4b) show that this hexagonal pyrrhotite is the high temperature-type stable at temperatures above about $320^{o}C$ (see fig. 6-4e). X-ray traverse across the same 2 Θ position for pyrrhotite displaying a dense lamellar intergrowth all show a split (102) peak with the smaller peak on the high 2 Θ side of the larger (figs. 6-4c,d). According to Desborough and Carpenter (1965) this split peak indicates that the lamellar intergrowth is a mixture of hexagonal and monoclinic phases the latter stable at temperatures below about $320^{o}C$.

A convenient method for determining the composition of hexagonal pyrrhotite is given by Arnold and Reichen (1962) who found a close relationship between the (102) spacing i.e. d_{102} and the metal(s) content provided the total concentration of Cu, Ni, Zn etc. was less than about 0.5%. Their graph is reproduced in fig. 6-4f and X-ray data for seven pyrrhotites from the Kanmantoo orebody are given in table 6-1. The pyrrhotite compositions ranging from 46.40 to 47.40 atomic percent Fe are plotted at an arbitrary temperature position in fig. 6-4e (heavy line).

FIG. 6-3

(a,b) Lamellar pyrrhotite composed of intergrown monoclinic
(arrowed) and high temperature hexagonal phases. The
pyrrhotite in both illustrations has been plastically
deformed and displays undulose extinction effects.
Partially crossed nicols. Oil immersion.

(c) Granular intergrowth of pyrrhotite (Po),
chalcopyrite (Cp) and cubanite (Cb). Cobalt-
pentlandite (Pn) occurs both as a stumpy anhedral
grain in the pyrrhotite and as a slim lamella through
the cubanite. Oil immersion.

(d) Complex twinning in coarse-grained chalcopyrite.
Bright lamellae running diagonally through the
chalcopyrite are mackinawite (Mk). Partially
crossed nicols.

(e) Regular lamellae of cubanite (Cb) running in two
directions through chalcopyrite.

(f) Exsolved sphalerite stars(Sl) in chalcopyrite.
Note the slim mackinawite lamellae passing through
the chalcopyrite.

(g) A thin layer of sphalerite along the interface
between magnetite (Mt) and chalcopyrite. This
sphalerite has probably also exsolved from the
chalcopyrite but has been precipitated along the
grain boundary. Oil immersion.

(h) Small inclusions of native bismuth and a minute
inclusion of gold in pyrrhotite.

(i) Coarse-grained granular intergrowth of sphalerite
and galena (Gn). Minute blebs of pyrrhotite and
rare chalcopyrite follow crystallographic directions
in the sphalerite. Some pyrrhotite also occurs in
galena near the phase boundary.
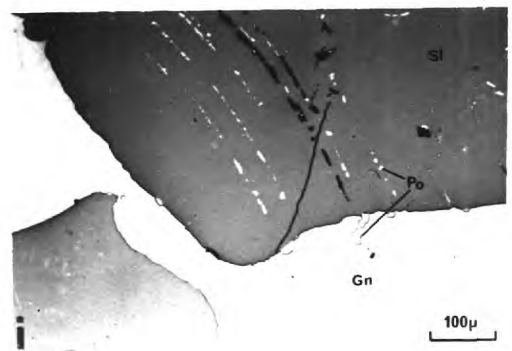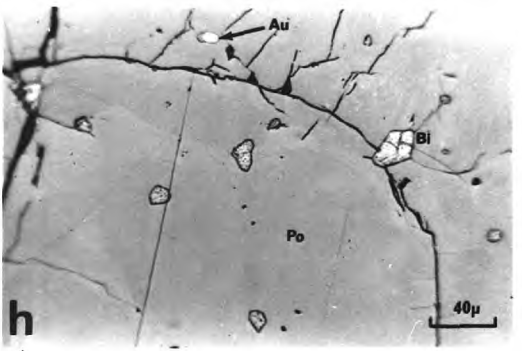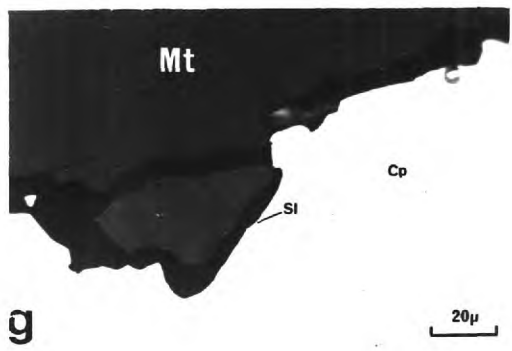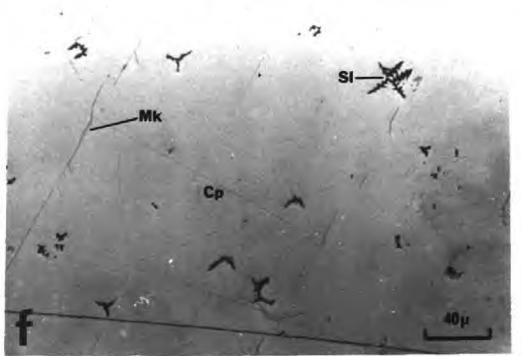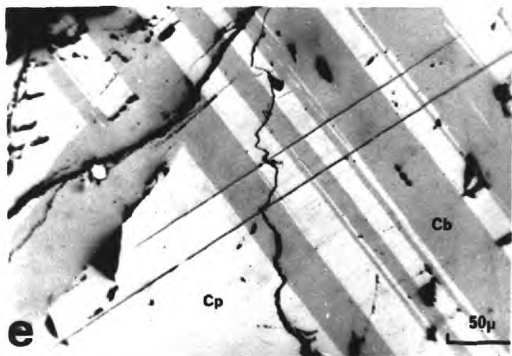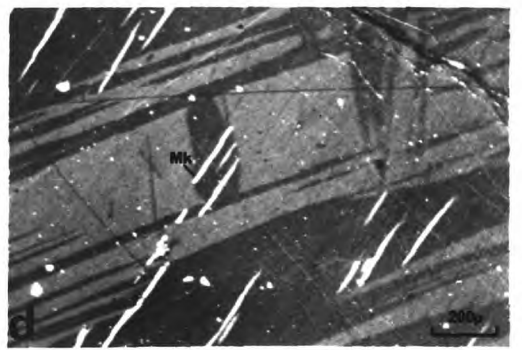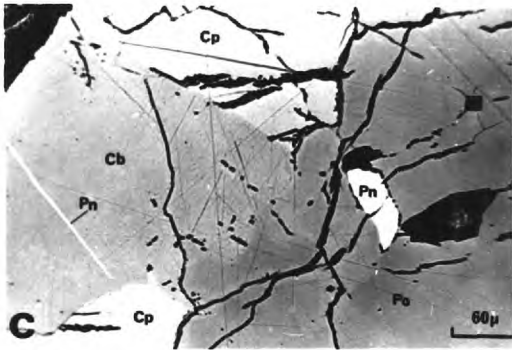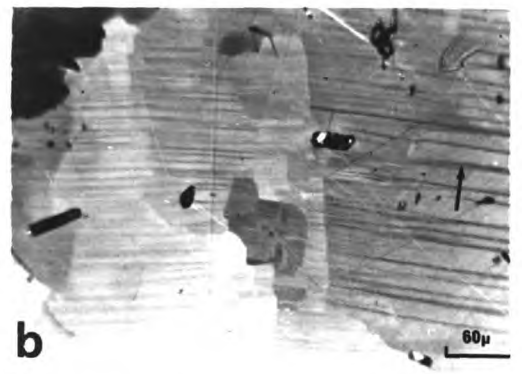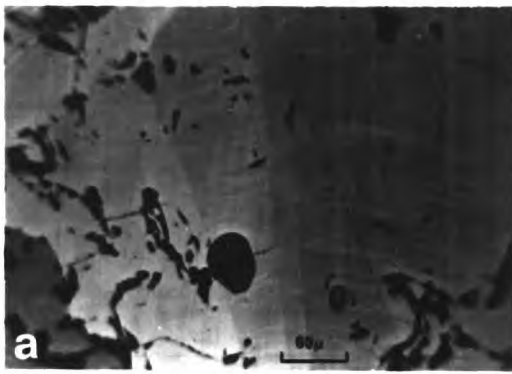
FIG.6-3

FIG. 6-4

(a,b) Characteristic high and low angle X-ray powder
diffraction peaks for high temperature hexagonal
pyrrhotite (CoKα radiation).

(c) A split (102) pyrrhotite peak indicates the presence
of both hexagonal and monoclinic polymorphs.

(d) The split peak is clearly shown by a fixed-counts,
step scan over the same 2θ interval as fig. c.

(e) Phase diagram for part of the Fe-S system (after
Desborough and Carpenter, 1965). The range of the
high-temperature pyrrhotite compositions in the
Kanmantoo ores is shown by the dark line placed
at an arbitrary temperature position.

(f) Relationship between the $d_{(102)}$ spacing and the
composition of hexagonal pyrrhotite (after Arnold
and Reichen, 1962).

(g) Hematite-magnetite and magnetite + quartz - fayalite
equilibrium curves as a function of oxygen fugacity and
temperature. Corrected for a total pressure of 5 kb
from data given by Eugster and Wones (1962).

(h) Stability fields for various phases at $600^{\circ}C$ and in
the presence of free silica as a function of sulphur
and oxygen fugacities (after Holland, 1965). For
explanation see text.

(i) Composition of pyrrhotite and the equilibrium curves
for pyrite-pyrrhotite and bismuth-bismuthinite as a
function of sulphur fugacity and temperature (after
Barton and Skinner, 1967). For explanation see text.
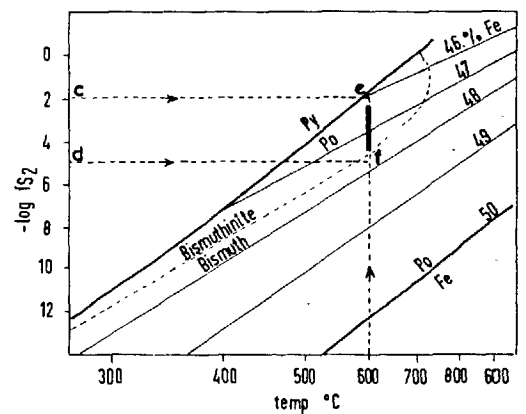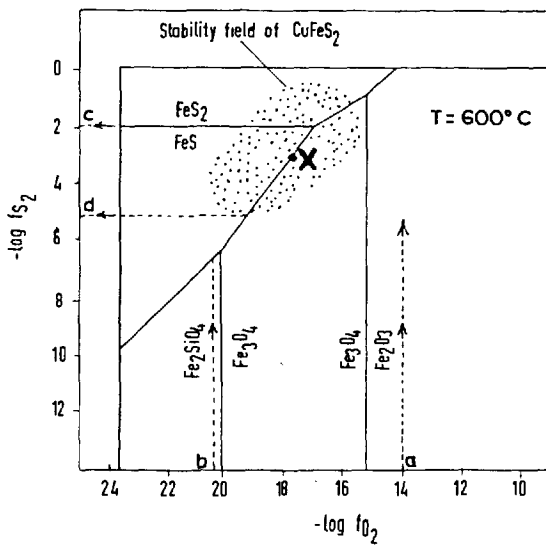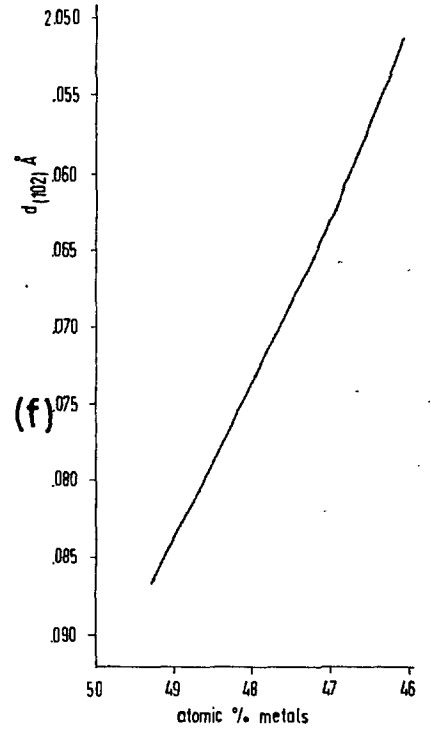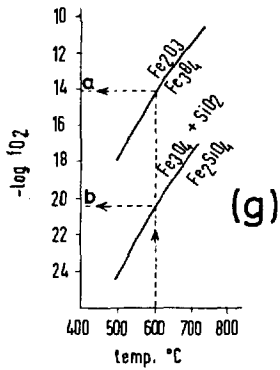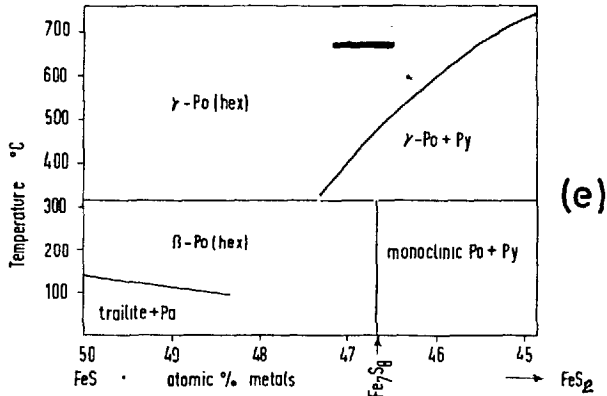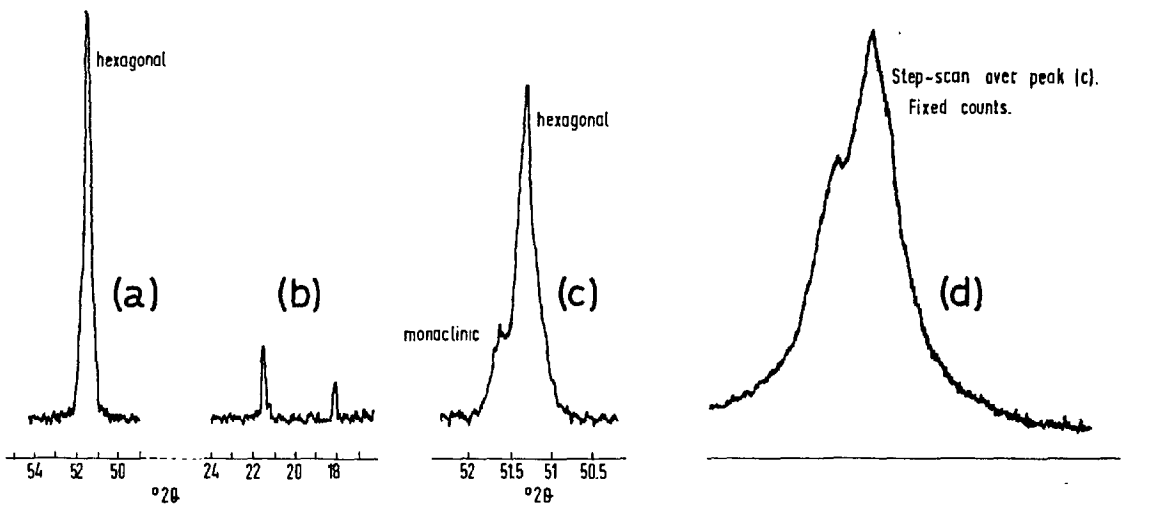
FIG. 6-4

TABLE 6-1. X-ray data and compositions of pyrrhotites based on the (102) lattice spacings. Fe filtered Co radiation.

sample	degrees 2θ	$d_{102}\text{\AA}^{\circ}$	atomic % Fe	remarks
21A-550[*]	51.35	2.064	47.10	step-scan, fixed counts
15-331	51.40	2.062	46.90	step-scan, fixed counts
12-793	51.43	2.061	46.85	step-scan, fixed time
31-1576	51.27	2.067	47.40	continuous scan
21A-540b	51.60	2.055	46.40	continuous scan
21A-540a	51.35	2.064	47.10	continuous scan
30-809	51.35	2.064	47.10	continuous scan

[*] The first number refers to the diamond drill hole and the second to the number of feet down the hole from where the core-sample was taken.

Ore Mineral Assemblages

21A-550	Po-Cp-Mt	
15-331	Po-Cp-Mt	Po: pyrrhotite
12-793	Po-Cp-Mt	Cp: chalcopyrite
31-1576	Po-Cp-Cb	Mt: magnetite
21A-540b	Po-Cp-Mt-Py	Cb: cubanite
21A-540a	Po-Cp-Mt	Py: pyrite
30-809	Po-Cp-Mt	

(b) <u>Possible Thermometric Implications of Pyrrhotite Compositions</u>

The pyrrhotite-pyrite geothermometer of Arnold (1962) is based on the changing composition of hexagonal pyrrhotite in equilibrium with pyrite with a change in temperature (see fig. 6-4e). However subsequent observations and experimental work have questioned the validity of this technique since (a) pyrrhotite tends to re-equilibrate with pyrite as the temperature falls(Schreyer et al. 1964), (b) pyrrhotite in equilibrium with chalcopyrite and pyrite at high temperatures contains up to 1% Cu and therefore has a different composition from that of pyrrhotite in equilibrium with pyrite alone at the same temperature (Yund and Kullerud, 1966), (c) similarly in nickel-bearing sulphide systems, pyrrhotite can hold large amounts of Ni in solid solution at elevated temperatures (Naldrett et al. 1967), and (d) the fugacity of sulphur (f_{S_2}) is reported by Barton and Skinner (1967) to be just as important as temperature in determining the composition of hexagonal pyrrhotite. Primary pyrite coexisting with pyrrhotite in the Kanmantoo orebody is very rare so even allowing for these limitations of the pyrite-pyrrhotite geothermometer, no temperature inferences can be made from the pyrrhotite compositions as such. However by a rather indirect method, it can be demonstrated whether or not the pyrrhotite <u>could</u> have formed at or around the inferred temperature and pressure conditions of metamorphism.

Since magnetite + quartz is apparently a stable assemblage through most of the pyrrhotite-bearing rocks and because both hematite and fayalite are absent, the oxygen fugacities are bracketed by the two buffer curves, corrected for a rock pressure of 5 kb, that are shown in fig. 6-4g. If 600°C is regarded as an approximate metamorphic temperature and if the corresponding possible range of values of f_{O_2} (a and b in fig. 6-4g) are transferred onto the f_{O_2} axis of the 600°C isothermal f_{S_2} - f_{O_2} diagram in fig. 6-4h (after Holland, 1965), clearly the Fe_3O_4 - FeS (pyrrhotite) univariant boundary is well within

these f_{O_2} limits. The stability field of chalcopyrite solid solution (stippled area in fig. 6-4h) and the absence of pyrite are f_{S_2} limiting factors. Therefore the possible range of sulphur fugacities at which magnetite, quartz, pyrrhotite and chalcopyrite solid solution can coexist at $600^{\circ}C$ is limited to between points c and d. If points c and d are now transferred onto the f_{S_2} axis of fig. 6-4i that shows the composition of high-temperature hexagonal pyrrhotite as a function of temperature and sulphur fugacity (after Toulmin and Barton, 1964), and orthogonal projections from c and d are made to intersect the $600^{\circ}C$ isotherm, the range of possible equilibrium pyrrhotite compositions at these conditions lies between points e and f. The actual range of pyrrhotite compositions is shown as a heavy line.

Although a number of simplifications have been made in this reasoning such as ignoring the effects of other dissolved metals on the composition and stability of pyrrhotite and the possibility of pyrrhotite growth at other combinations of temperature and f_{S_2} to give the same compositional range, the results at least show the compatability of the pyrrhotite compositions with the associated mineral assemblages and the estimated temperatures of metamorphism. One point that should be mentioned is that the pyrrhotite compositions determined from the d_{102} values are for the hexagonal phase only. Monoclinic pyrrhotite is thought to have a nearly constant composition around Fe_7S_8 (Clark, 1966a) so if the monoclinic phase, in the Kanmantoo ore formed by inversion from an original homogeneous hexagonal pyrrhotite, the range of pyrrhotite bulk compositions would be considerably reduced.

(c) **Pentlandite in Pyrrhotite**

Traces of pentlandite occur in both the fine-grained disseminated mineralization and the coarser grained ore and for the most part form as minute oriented blebs or star-like inclusions through the pyrrhotite host (fig. 5-6c). In only two sections have larger pentlandite grains been observed and in one of these a lamella of pentlandite is intergrown with

cubanite (fig. 6-3c). Pentlandite of all habits is optically
isotropic but the rare coarse-grained material has a slightly
but distinctly higher reflectivity than the smaller grains.
Electron probe analyses of pentlandite of three different
habits are given in table 6-2a. The small blebs of lower
reflectivity appear to be common Fe-Ni pentlandite whereas
the granular and lamellar grains are both rich in Co and
deficient in Fe and Ni. A comparison of the X-ray powder
diffraction spacings of one of the Co-rich phases with those
of Fe-Ni pentlandite and cobalt-pentlandite from the Outokumpu
Mine, Finland (Kuovo, Huhma and Vuorelainen, 1959) indicates
that this phase is the rather rare mineral cobalt-pentlandite
(table 6-2b). Departures from the composition M_9S_8 in table
6-2a are considered to be due largely to analytical error
rather than reflecting wide variations in the sulphur to metals
ratio.

The geometrical features of the minute Fe-Ni pentlandite
inclusions in the pyrrhotite plus the known complete solid
solution between pyrrhotite and pentlandite above $500^{\circ}C$
(Naldrett et al. 1967) indicate that they have probably exsolved
from a former Ni-bearing pyrrhotite phase. No nickel has been
detected in any of the pyrrhotite during electron probe micro-
analyses. There is little evidence either in the form of
textural relationships or from phase equilibria data to indicate
that the rare cobalt-pentlandite has also exsolved from pyrrhotite.
In fact the lamellar habit of this mineral in cubanite suggests
that much of the cobalt may have originally been in solid
solution in the copper-rich sulphide phase.

2. Chalcopyrite and Associated Phases

(a) General Features

Textural relationships discussed in chapter 5 indicate
that much of the chalcopyrite or its high-temperature parent
phase was subjected to the conditions of metamorphism although
a significant amount of chalcopyrite continued to form by
replacement of other minerals throughout the retrogressive

TABLE 6-2a. Electron probe analyses of pentlandites.

	(1) 39-1288	(2) 31-1576	(3) 18-537
Fe wt.%	34.12	11.54	6.78
Ni	39.15	7.11	5.11
Co	nd	51.90	49.25
S	39.16	33.68	35.27
	102.2	104.2	96.4
	$M_{7.46}S_8$	$M_{9.26}S_8$	$M_{7.6}S_8$

nd: not detected

Description of the Samples

(1) Minute blebs of low-reflectivity pentlandite in disseminated pyrrhotite in unaltered schist.

(2) Lamella of high-reflectivity pentlandite in cubanite of coarse-grained pyrrhotite-chalcopyrite-cubanite ore.

(3) Anhedral grain of high-reflectivity pentlandite in pyrrhotite of coarse-grained pyrrhotite-chalcopyrite ore.

TABLE 6-2b Comparison of X-ray posder data for sample (3) above with published data for cobalt-pentlandite (A) and pentlandite (B).

(3) I	(3) d	(A)* I	(A)* d	(B) I	(B) d	hkl
6	5.78	6	5.75	2	5.84	111
10	2.99	10	3.00	6	3.04	113
5	2.87	6	2.88	2	2.92	222
2	2.27	5	2.28	3	2.31	133
7	1.91	8	1.92	4	1.94	115/333
9	1.75	10	1.76	10	1.78	044
1	1.29	5	1.30	3	1.31	355/137
1	1.24	5	1.24	3	1.26	008
1	1.15	4	1.15	3	1.16	157/555
1½	1.02	6	1.02	5	1.03	448

* Composition of (A): 13.22% Fe, 9.78% Ni, 42.7% Co, 34.2% S.

and post-metamorphic history. Despite its manifold age, chalcopyrite of all habits is optically identical and both X-ray powder diffraction and electron probe analyses show its composition to be close to stoichiometric $CuFeS_2$ except for material within a few microns of exsolved sphalerite grains. Lamellar twinning is universally developed (fig. 6-3d) but it is difficult to decide in any instance whether the twinning is a result of growth, deformation or phase inversion from cubic to tetragonal symmetry.

(b) Minor Phases Intergrown with Chalcopyrite

(i) Cubanite

A very rare pale-yellow mineral with optical properties intermediate between chalcopyrite and pyrrhotite was identified from X-ray diffraction photographs as orthorhombic cubanite ($CuFe_2S_3$). Cubanite, detected in only a single polished section, occurs anhedrally intergrown with chalcopyrite and pyrrhotite and as rather coarse parallel lamellae within chalcopyrite (fig. 6-3c,e). The significance of the rarity of cubanite in the Kanmantoo mineralization is discussed in a later section.

(ii) Sphalerite

Minor sphalerite is intergrown with chalcopyrite in both the fine-grained disseminated mineralization and the coarser grained ore but the proportion of sphalerite to chalcopyrite is higher in the former than in the latter.

In the disseminated multiphase sulphide grains, sphalerite occurs usually as one or two sub-grains in contact with chalcopyrite (fig. 5-6c). The only indications that the chalcopyrite and sphalerite sub-grains were originally a single solid solution are (1) the sphalerite itself may contain very minute inclusions of chalcopyrite, and (2) the sub-grains are always in contact with each other.

In the coarser grained ore, sphalerite exists mainly as minute star-shaped and dendritic inclusions scattered through the chalcopyrite host (fig. 6-3f).

TABLE 6-3. Electron probe analyses of exsolved sphalerite
and adjacent chalcopyrite. Internal sphalerite
stars (1) and rims along external grain
boundaries (2).

	(1)		(2)	
	sphalerite	chalcopyrite	sphalerite	chalcopyrite
Cu	3.3 wt.%	33.2	0.3	33.7
Fe	7.7	29.8	5.7	30.1
Zn	52.7	2.3 .	60.8	nd
S	33.1	32.7	34.3	32.5
	96.8	98.0	101.4	96.3

nd: not detected

Such inclusions are rare or absent near the edges of the
chalcopyrite grains particularly where there is a semi-continuous
rim of sphalerite along the outside boundary fig. 6-3g).
Electron probe analyses of these two sphalerite types (table
6-3) show that the stars contain significantly more Fe and
Cu and less Zn than the rim phase. Chalcopyrite about 20
microns from the stars contains detectable amounts of Zn but
Znis not detectable in chalcopyrite at the same distance from
the rim phase. It seems likely that both sphalerite types
have formed by unmixing from a former zinc-bearing chalcopyrite
but that near the external grain boundaries, precipitation of
sphalerite along the interface has resulted in a more complete
separation of the two phases.

(iii) Mackinawite

Throughout the orebody and the weakly disseminated
mineralization there occurs in chalcopyrite small but persistent
amounts of a rather soft mineral that displays extreme bire-
flectance in colours from bright creamy pink to dull grey
(table 6-4a). Equally spectacular are the polarization colours
from deep blue through silvery brown to silvery white (in air).
In the disseminated multiphase sulphide grains this anisotropic
phase exists as rather irregular anhedral inclusions or sub-
grains (fig. 5-6c), but in the coarser grained chalcopyrite it
forms slim semi-regular lamellae running through the host in
two or more intersecting sets (fig. 6-3d,f). Individual lamellae
are usually no more than 100 microns long and about 10 microns
wide. They commonly show straight extinction but since two
sets of non-orthogonal intersecting lamellae often have
identical extinction positions, many lamellae display oblique
extinction as well. Sets of lamellae retain remarkably constant
orientations through even complexly twinned chalcopyrite grains
and single lamellae cut across twin boundaries with no visible
deviation (fig. 6-3d).

Both the optical characteristics given above and the
X-ray powder diffraction data in table 6-4b indicate that this
anisotroic phase is the tetragonal iron monosulphide,

mackinawite described by Evans et al. (1964). Electron probe analyses of four mackinawites from different parts of the Kanmantoo mineralization given in table 6-4c show that up to 14% Co and over 1% Ni are apparently substituting for Fe in the mackinawite lattice. Deviations from the ideal MS formula are probably partly real and partly due to analytical error.

There is some doubt over the discovery of mackinawite since it has often been mistaken for the similar looking highly anisotropic Cu-Fe sulphide, valleriite that contains essential Mg, Al, and OH components in the lattice (Evans and Allman, 1967). The first careful description of the optical properties of mackinawite is generally attributed to Milton and Milton (1958). Many papers dealing with mackinawite composition and occurrence appearing in recent years show that it is a rather common minor mineral found in a number of geological environments. Mackinawite has been found in recent sediments (Berner, 1964), hydrothermal-type basemetal ores (Clark, 1966b), basic volcanic rocks (Takeno, 1965), mafic intrusions (Van Rensburg et al. 1967 ; Clark, 1967), the Palabora carbonatite (Springer, 1967), the Witwatersrand conglomerate (Schidlowski et al. 1967), and in meteorites (Buseck, 1968). In most of these occurrences, mackinawite is always associated with pyrrhotite-chalcopyrite-pentlandite-sphalerite assemblages and it may be intergrown with any of these phases. Electron probe analyses given by these workers show that up to 14% combined Ni plus Co commonly substitutes for Fe, but the Co/Ni ratios are extremely variable even in a single deposit.

Considerable mystery surrounds the origin of mackinawite in ancient geological environments. Tetragonal FeS was first synthesised by Berner (1962) in aqueous solution at NTP by reacting dissolved H_2S with either finely ground goethite or metallic iron. So far, mackinawite has not been recognised in anhydrous phase equilibria studies and there is considerable evidence that an aqueous, sulphide-bearing environment is necessary for its formation (Rickard, 1968). Berner (1967) reported that tetragonal FeS is unstable with respect to

TABLE 6-4a.   Reflectivity data for a number of mackinawite
             laths in a single grain of chalcopyrite.

R_{max}	R_{min}	
42.8%	23.2%	Measurements
43.7	23.6	
43.0	23.9	a. in air
42.6	22.8	b. wavelength 589 nm
43.4	24.5	c. pyrite standard
42.9	22.3	(53.43%)
means 43.1	23.4	

TABLE 6-4b.   X-ray powder data for mackinawite from the Kanmantoo
             ore (1) compared with mackinawite data (2) given by
             Evans et al 1964.

(1)		(2)	
I	d	I	d
10	5.02	10	5.03
6	2.96	8	2.97
4	2.30	8	2.31
2	1.83	4	1.84
3	1.80	8	1.81

TABLE 6-4c.   Electron probe analyses of four mackinawite
             lamellae from chalcopyrite in the Kanmantoo ore.

	(1)[*] 16-660	(2) 39-1288	(3) 37-773	(4) 34-387
Fe wt.%	53.06	52.67	52.77	56.52
Co	13.68	6.64	8.85	4.87
Ni	0.56	0.90	1.15	1.10
Cu	0.43	0.60	nd	nd
S	37.14	36.00	36.26	35.23
	104.87	96.81	99.03	97.72
	$M_{1.033}S$	$M_{0.961}S$	$M_{0.983}S$	$M_{1.009}S$

                                         nd: not detected

[*]Samples (1), (3) and (4) from coarsed-grained ore.
Sample (2) from fine-grained disseminated mineralization.

pyrrhotite at 40 - 45°C but heating experiments by Takeno
(1965) on the natural material showed that pure Fe-mackinawite
begins to break down at around 130°C. Mackinawite containing
Ni and Co remains stable at temperatures up to about 250°C but
it has not yet been resolved whether the breakdown temperatures
are dependent on the cobalt and/or nickel content or on the
total metals to sulphur ratio (Takeno and Clark, 1967).

The mechanism whereby mackinawite lamellae form in
the interior of solid minerals is a problem. In conventional
textural interpretation the geometrical distribution of the
mackinawite lamellae would suggest an exsolution origin but
this would conflict with experimental results in both hydrous
and anhydrous systems. Rickard (op.cit) suggested that
mackinawite lamellae in pyrrhotite may have formed by the
reaction of metallic iron expelled from a cooling pyrrhotite-
iron solid solution with introduced aqueous sulphide.
Presumably the same mechanism could be applied to an Fe-Co-Ni
alloy expelled from the lattice of cooling chalcopyrite.
This proposed mechanism would seem to be supported by the
presence of minerals such as awaruite (Ni_3Fe), wairauite (CoFe),
native Fe and ·ative Ni together with mackinawite in serpentinised
ultrabasic rocks (Ramdohr, 1967).

3. Phase Relationships Among the Primary Ore Minerals

(a) General Statement

In the discussion of textural relationships given in
chapter 5, chronological implications of sulphide-sulphide
intergrowths were largely ignored for two reasons; firstly
because considerable textural changes can take place spontane-
ously down to temperatures as low as 200°C as shown by heating
experiments of Brett (1964) and annealing experiments of
Stanton and Gorman (1968) and secondly, because if the ore
minerals had been subjected to metamorphic conditions, the
present sulphide assemblages wouldmost likely be different
from those existing at metamorphic temperatures. The aim of
this section is to examine whether present day sulphide and

sulphide-oxide assemblages can be explained in the light of
phase equilibria studies in the Cu-Fe-S and other systems.

(b) The Cu-Fe-S System

If the small amounts of ubiquitous pentlandite, sphalerite
and mackinawite and the secondary FeS_2 minerals are not considered,
the dominant sulphide assemblage in the Kanmantoo ores is simply
pyrrhotite + chalcopyrite. Minor assemblages are pyrrhotite +
chalcopyrite + (primary) pyrite and pyrrhotite + chalcopyrite
+ cubanite.

Phase relationships in the Cu-Fe-S system from $700^{\circ}C$ down
to $200^{\circ}C$ have been determined by Yund and Kullerud (1966) by
heating various proportions of finely ground, pure elemental
starting materials in evacuated silica-glass tubes. At $700^{\circ}C$
the area of interest in the condensed phase diagram (fig. 6-5a)
contains the phases pyrite, chalcopyrite$_{ss}$ (solid solution),
a pyrrhotite$_{ss}$ containing about 1% Cu, and liquid sulphur. On
slow cooling, both the pyrrhotite and chalcopyrite solid solution
fields contract until at about $550^{\circ}C$ the latter splits into
separate chalcopyrite and cubanite solid solutions and a tie-
line is established between cubanite$_{ss}$ and pyrite. At tempera-
tures below $550^{\circ}C$(fig. 6-5b) chalcopyrite$_{ss}$ and pyrrhotite
cannot coexist in stable equilibrium. With further cooling,
the solid solution fields continue to contract but the phase
relationships in the area of interest remain unchanged until
about $330^{\circ}C$ when the assemblage pyrite + cubanite$_{ss}$ becomes
unstable and a tie-line is re-established between chalcopyrite
and pyrrhotite. These phase relationships hold down to at
least $200^{\circ}C$ (fig. 6-5c)

When considered in terms of the ideallised phase
relationships in the Cu-Fe-S system, the rare chalcopyrite +
pyrrhotite + cubanite and chalcopyrite + pyrrhotite + pyrite
assemblages in the Kanmantoo ore would be expected to be common
products of slow cooling whereas the dominant chalcopyrite +
pyrrhotite assemblage ought to be rare in comparison. The
restriction of the sulphide assemblages bulk compositions to
a tie-line or thin strip between $CuFeS_2$ and $Fe_{1-x}S$ is difficult

FIG. 6-5

(a,b,c)   Phase relationships in the Cu-Fe-S system at various
         temperatures (after Yund and Kullerud, 1966).

(d)   Sketch of pyrite, pyrrhotite and magnetite stability
      fields on a sulphur fugacity - oxygen fugacity
      diagram. For explanation see text.

(e)   Details of the stability relationships around the
      pyrrhotite field in the Cu-Fe-S system at a
      temperature of $700^{o}C$.

S

Field covered by (b) and (c).

Py

Po

Cp

Bn

Cu   700° C   Fe

(a)

S
80 wt % S
70
60
Py
50
40
Po
Cp   Cb
30
Cu   500° C   Fe

(b)

S

Py

Cp   Cb   Po

Cu   200° C   Fe

(c)

f_{S_2}

FeS₂   J
H   FeS   Fe₃O₄
I
G

f_{O_2} ⟶

(d)

43 wt % S
42
Py + Po   41
Py+Po+Cp   40
2.0515 Å
Composition range of
Kanmantoo pyrrhotites.
39
2.0692 Å
Po   38
Po+Cp   2.0892 Å   37
36

700° C

(e)

Py   Pyrite
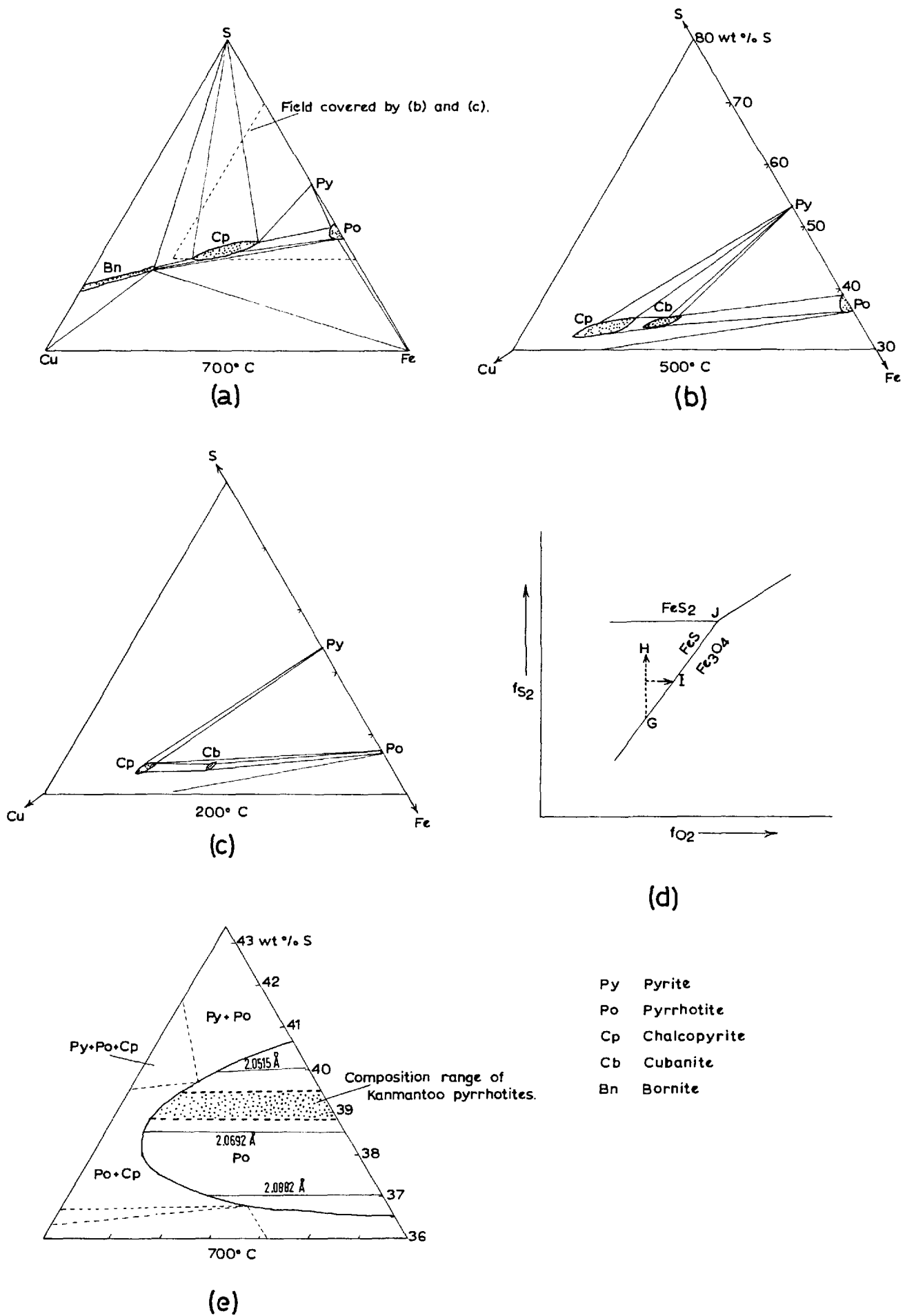Po   Pyrrhotite
Cp   Chalcopyrite
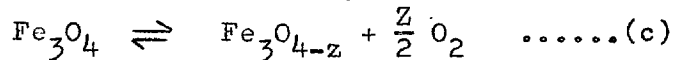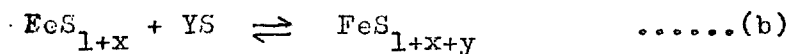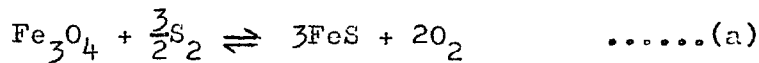Cb   Cubanite
Bn   Bornite

FIG. 6-5

to accept as being a result of chance; it would seem to
necessitate some external influence on the phase relation-
ships of the Cu-Fe-S system.

(c) Possible Effect of Magnetite on the Sulphide Assemblages

Magnetite is a constant associate of pyrrhotite and
chalcopyrite in the coarse-grained ore so it is possible that
its presence during cooling had some influence on the result-
ing sulphide assemblages.

Although variations in the total pressure of the
environment play only a very small role in anhydrous oxide
and sulphide systems, variations in the fugacities of oxygen
and sulphur have a great influence on the respective stabilities
of oxide and sulphide phases (Eugster and Wones, 1962; Barton
and Skinner, 1967). In a system containing coexisting iron
oxides and iron sulphides variations in either f_{O_2} or f_{S_2} can
effect all phases. As an illustrative example consider magnetite
and pyrrhotite coexisting at point G on the univariant phase
boundary in fig. 6-5d. If the temperature remains constant
and some change in the environment tends to raise the f_{S_2} towards
point H, the two phases will remain in stable equilibrium only
if a reactive change acts to increase f_{O_2}, decrease f_{S_2}, or
both in order to bring conditions back to the univariant
curve e.g. to point I. Such a reactive change could be
produced by slight movement to the right of the equilibrium
reaction (a) below, as well as by changes in the compositions of
the phases (b and c);

$$Fe_3O_4 + \tfrac{3}{2}S_2 \rightleftharpoons 3FeS + 2O_2 \qquad \ldots\ldots(a)$$

$$FeS_{1+x} + YS \rightleftharpoons FeS_{1+x+y} \qquad \ldots\ldots(b)$$

$$Fe_3O_4 \rightleftharpoons Fe_3O_{4-z} + \tfrac{z}{2}O_2 \qquad \ldots\ldots(c)$$

In the natural environment there would probably be complex
changes in the ferrous/ferric ratios of iron-bearing silicates
as well but it seems likely that the reaction of magnetite
with sulphur would be the principal factor in preventing large

changes in sulphur fugacity, and thus changes in pyrrhotite composition, from taking place.

In table 6-1, pyrrhotite in pyrrhotite + chalcopyrite + magnetite assemblages has a composition of around 47% Fe whereas the Fe content of pyrrhotite is slightly l̶o̶w̶e̶r̶ ^higher in the cubanite-bearing assemblage and slightly h̶i̶g̶h̶e̶r̶ ^lower in the pyrite-bearing assemblage. At around 600°C pyrrhotite with a composition of 47% Fe is some distance from the pyrite stability field (figs. 6-4i, 6-5e) therefore such a phase would coexist with magnetite at about point X on the univariant boundary in fig. 6-4H. If, during cooling the presence of magnetite enabled the pyrrhotite to maintain a composition around 47% Fe, the stability field of pyrite would be reached somewhere in the region between 300°C and 400°C (fig. 6-4i). It has been shown previously that below 550°C pyrrhotite can coexist only with cubanite$_{ss}$ but that around 330°C a tie-line is re-established between chalcopyrite and pyrrhotite. Thus if the pyrite stability field were approached at about the same temperature as this tie-line was re-established the bulk composition of the sulphide phases in the Cu-Fe-S system would be on or very close to the chalcopyrite-pyrrhotite boundary. Contraction of the solid solution fields with further cooling would cause practically all the cubanite to decompose to chalcopyrite plus pyrrhotite.

Whether such a cooling history occurred in the Kanmantoo ore is difficult to prove but support that the above explanation is correct in principle is given by (1) the lower Fe content of pyrrhotite in the pyrite bearing assemblage - the pyrite stability field would be intersected at a higher temperature and if entered, would almost certainly cause the complete breakdown of any cubanite, (2) the higher Fe content of pyrrhotite in the cubanite-bearing assemblage - the pyrite field would not be intersected thus the bulk composition of the sulphides would remain in the cubanite + pyrrhotite or cubanite + chalcopyrite + pyrrhotite field, and (3) the concentration of the monoclinic pyrrhotite phase around the grain-boundaries of pyrrhotite aggregates - this monoclinic phase may have formed directly from the decomposition of cubanite below 320°C.

More difficult to explain is the lack of both pyrite
and cubanite in the disseminated sulphide grains since there
is no associated magnetite to act as a possible stabilizer
of pyrrhotite compositions during cooling. It must be pointed
out however, that sphalerite forms a significant proportion
of the disseminated sulphide grains thus it is not possible to
discuss the cooling history in the context of the Cu-Fe-S system.

(d) Effects of Minor Elements on Sulphide Phase Equilibria

Craig, Naldrett and Kullerud (1967) have shown that
where 5% or more of Ni is present in the Cu-Fe-Ni-S system,
chalcopyrite + nickeliferous pyrrhotite remain stable at all
temperatures below $550^{\circ}C$. Unfortunately Ni is present in the
Kanmantoo ores in trace amounts only (see ch. 8) therefore
this attractive mechanism for explaining the dominant chalcopyrite
+ pyrrhotite assemblage cannot be applied. No data are available
on the analogous Cu-Fe-Co-S system but the small amounts of Co
present (ch. 8) are thought to be insufficient to affect signifi-
cantly the stability fields of the major phases.

A maximum of around 0.1% Zn can be held in the pyrrhotite
lattice at $850^{\circ}C$ (Barton and Toulmin, 1966) therefore at the
temperatures affecting the Kanmantoo rocks the solubility of
Zn in pyrrhotite would be negligible. In any case, textural
relationships indicate that practically all the sphalerite
in the coarse-grained ore was dissolved in the copper sulphide
phase at elevated temperatures. No data are available on
the effect of Zn on the stability fields of the copper-iron
sulphides.

4. Iron-Titanium Oxides

(a) General Features

Important mineralogical aspects of the magnetite-
hercynite-ilmenite intergrowths have been discussed in chapter
5. The slim hercynite lamellae in the undeformed magnetite
(fig. 5-11b) probably all exsolved from a former aluminous
magnetite phase (Turnock and Eugster, 1962). Solid solution
between ilmenite and magnetite is evidently very small

(Buddington and Lindsley, 1964) thus it appears that the associated ilmenite lamellae are of oxy-exsolution origin i.e. they formed through the sub-solvus oxidation of an original magnetite-ulvespinel solid solution. The large ilmenite porphyroblasts intergrown with magnetite in some sections (fig. 5-15g) appear to have developed originally as separate phases. Little in the way of temperature inferences can be made from the oxide intergrowths especially since most of them have been subject to post-formational plastic deformation and partial recrystallization.

(b) Heating Experiments on Magnetite Aggregates

Although considerable work has been done on the plastic deformation and recrystallization behaviour of many spinel-type phases in ceramic systems (Ryschkewitch, 1960), little information is available on the physical behaviour of magnetite at elevated temperatures. Therefore some preliminary heating experiments were carried out on naturally deformed and recrystallized magnetite-ilmenite-hercynite material from the Kanmantoo orebody to see whether any grain boundary mobility could be detected at or around the inferred temperatures of metamorphism.

Small pellets were drilled from lightly etched polished sections with a minature diamond studded core-drill having an internal diameter of 0.25 ins. Series of photographs taken across the polished area of each core under the reflected light microscope were used to build up a photo-mosaic of the entire surface. Each pellet was thoroughly cleaned with alcohol and air dried before being placed in a thick walled, pyrex-glass tube that was flushed with nitrogen, evacuated and sealed. The samples were heated in a muffle furnace having a manual, energy regulator-type temperature control and a nickel/chrome - nickel/aluminium thermocouple connected directly to the temperature indicator. An automatic, cold-junction compensator device was fitted. At the end of each run, the tubes were removed from the furnace and allowed to cool rapidly in air before being opened. The odour on opening

was noted and the samples were examined under a binocular
microscope and ore microscope before being mounted in a cold-
setting plastic medium to be lightly re-polished and re-etched.
Detection of textural changes was made by comparing the after-
heating intergrowths with the before-heating photo-mosaics.

Details of each run and the results are given in table
6-5. Above about $650^{\circ}C$ the pyrex-glass began to react with
the magnetite but there was usually enough unaltered oxide
left to observe whether or not textural changes had occurred.
Clearly, the results are largely negative except for some
slight straightening of the polyhedral magnetite boundaries
in one of the short runs at $940^{\circ}C$ (no. 4). It is interesting
to compare these results with those of Sergeyeva (1968) who
heated freshly cleaved magnetite in air for 6 hours at tempera-
tures from $300^{\circ}C$ to $900^{\circ}C$ using 100° intervals. Sergeyeva shows
convincing electron micrographs of incipient recrystallization
even at the lowest temperature but he reports that optical
examination of surfaces heated at all temperatures reveals
no discernable microstructural changes whatever.

It is felt that any future experiments ought to be done
for much longer times preferably under both dynamic and static
confining pressures and using less reactive containers. Also
it is important that the oxygen fugacity be controlled to
keep the magnetite chemically stable at the experimental
temperatures. Many of the "physical" changes reported by
Sergeyeva could conceivably be the result of magnetite reacting
with air to produce iron-deficient cubic phases of the maghemite
type. It is perhaps worth noting that the small amounts of
water vapour and other compounds released from the samples
during heating were capable of transporting relatively large
amounts of chalcopyrite even at the moderate temperature of
$470^{\circ}C$. The beautiful chalcopyrite euhedra found attached to
the polished magnetite surface after some runs provided ideal
material for testing the capabilities of a new technique in
scanning electron microscopy under the unfavourable viewing
conditions afforded by a magnetic sub-strate (Kelly, Lindqvist
and Muir, 1969).

Table 6-5.

TABLE 6-5. Details of heating experiments on magnetite aggregates from the Kanmantoo orebody.

| Run number	(1)	(2)	(3)	(4)	(5)	(6)	(7)
Sample	recrystallized magnetite	recrystallized magnetite	recrystallized magnetite	recrystallized magnetite	deformed magnetite	deformed magnetite	deformed magnetite
Approximate composition	70% magnetite 15% chlorite 15% chalcopyrite	70% magnetite 15% chlorite 15% chalcopyrite	90% magnetite 10% micas	70% magnetite 15% chlorite 15% chalcopyrite	90% magnetite 5% micas trace chalcopyrite	90% magnetite 5% micas trace chalcopyrite	90% magnetite 5% ilmenite 5% micas
Temperature	$470^{o}C$	$490^{o}C$	$740^{o}C$	$940^{o}C$	$470^{o}C$	$740^{o}C$	$940^{o}C$
Time	190 hrs	96 hrs	162 hrs	21 hrs	168 hrs	162 hrs	21 hrs
RESULTS	H_2O condensed on tube walls on cooling. Odour of H_2S on opening. No visible textural change in oxides. Needles of hematite on surface. Chalcopyrite severely corroded. Thin sulphide skin formed over polished surface of magnetite. Ilmenite surface unchanged. Large number of chalcopyrite euhedra attached to sulphide skin.	As for run number (1).	Devitrification of pyrex-glass tube. Tube shattered on cooling. Part of magnetite reacted with glass to hematite and Fe-silicates. No textural changes detected in the magnetite.	Flowage of pyrex-glass tube over bottom of furnace during heating. Magnetite and glass react. Some partial melting of the system. No increase in grain-size of the remaining oxides but a distinct straightening of the grain boundaries.	As for run number (1).	As for run number (3).	As for run number (4). But no textural changes detected.

5. Native Bismuth and Associated Minerals

Small anhedral grains of native bismuth are quite
common as inclusions in both pyrrhotite and chalcopyrite of
the coarse grained ore and in rare cases are accompanied by
one or two minute rounded grains of gold (fig. 6-3h).
No data are available on the extent to which Bi can dissolve
in pyrrhotite, chalcopyrite or cubanite at high temperatures
but it is likely to be very small. If native bismuth was in
contact with pyrrhotite during metamorphism it is difficult
to reconcile the position of the equilibrium bismuth/bismuthinite
boundary in fig. 6-4i (after Barton and Skinner op cit.) with
the pyrrhotite compositions. However it is interesting that
bismuth and pyrrhotite of the determined compositions are
compatible at a temperature a little over $700^{\circ}C$ which is not
far above the metamorphic temperature estimated from the
silicate assemblages.

Unchanged bismuth within the sulphide grains appears
to have been effectively isolated from subsequent changes in
the intergranular chemical environment since bismuth along
sulphide-silicate grain boundaries commonly displays reaction-
type intergrowths with chalcopyrite. One such intergrowth in
fig. 6-6 is shown by the accompanying X-ray scanning images
to contain Cu-Bi and Ni-Bi sulphides as reaction phases
between chalcopyrite and native bismuth. Electron probe micro-
analyses of the four phases designated A, B, C, D in the
optical image (fig. 6-6a) are given in table 6-6a. The results
are only semiquantitative since (a) a slight error in determin-
ing the small weight percent of sulphur produces a large error
in the calculated metals to sulphur atomic ratio, and (b)
no electron probe correction data were available for Bi;
extrapolations had to be made from Pb data. Phase B is
optically identical to _wittichenite_ (Cu_3BiS_3) but the
analysis indicates a little Fe substituting for Cu. Phase C
is optically similar to the rather rare mineral _parkerite_ ($Ni_3Bi_2S_2$)
and a comparison of X-ray powder diffraction data with parkerite
lattice spacings given by Peacock and Mc Andrew (1950)confirms
this indentification (table 8-6b). The origin of the Ni is unknown
but it was

FIG. 6-6

(a) Complex intergrowth between chalcopyrite (A)
     and various bismuth-bearing phases.

     Accompanying electron and X-ray scanning photo-
     graphs show the distribution of different elements
     in the various phases. The optical image is
     totated slightly with respect to the scanning
     images.

Optical Image

Bi

Bi + Ni + S

Bi + Cu + S

Fe + Cu + S

D

C

B

A

a

15μ

Electron

Fe

Cu

Bi

Ni

S
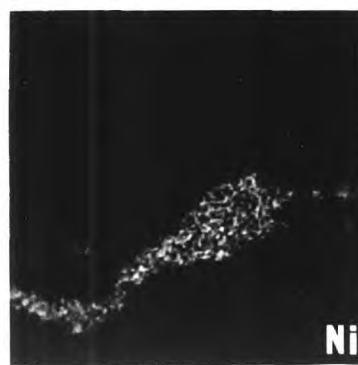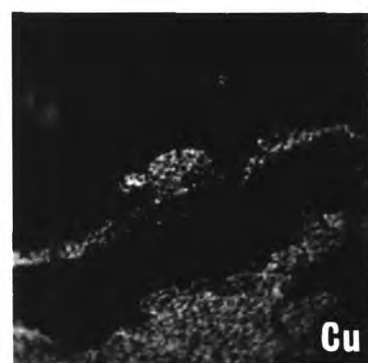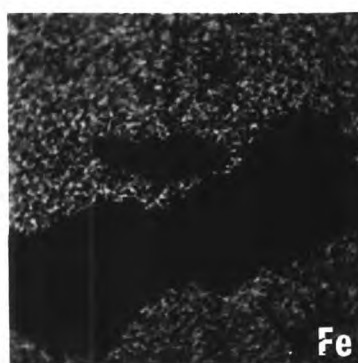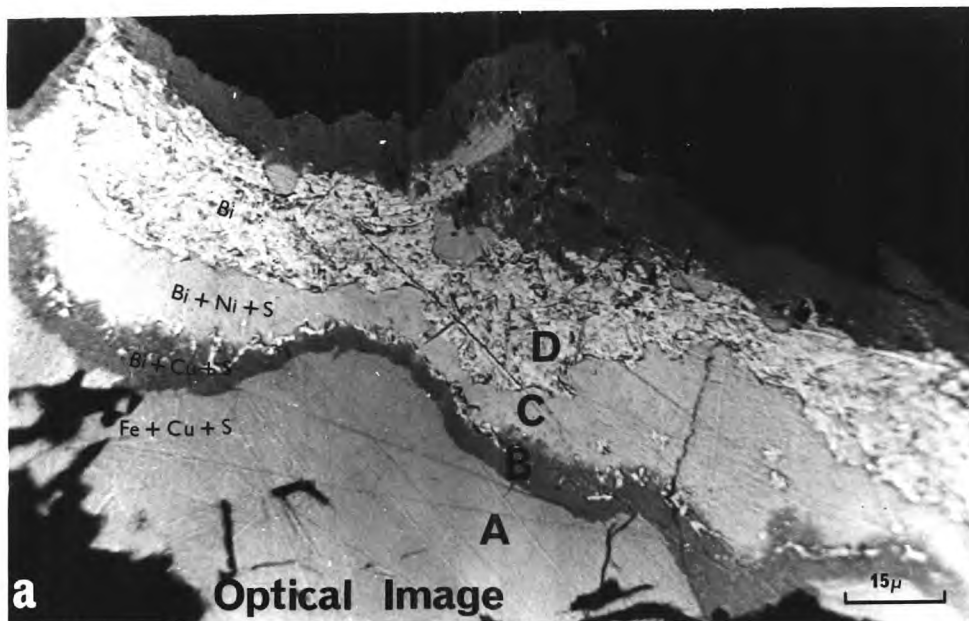
FIG. 6-6

TABLE 6-6a   Electron probe data for phases in fig. 6-6.

phase	A	B	C	D
Fe	maj	5.3wt%	0.3	0.6
Cu	maj	29.7	0.8	1.1
Ni	nd	nd	31.9	0.2
Co	nd	nd	nd	0.1
Bi	nd	51.0	55.7	96.3
S	maj	8.8	11.0	nd
		94.8	99.7	98.3
Approximate formula	$CuFeS_2$	$Cu_{10}Fe_2Bi_5S_6$	$Ni_5Bi_2S_3$	Bi
Probable mineral	chalcopyrite	wittichenite (Cu_3BiS_3)	parkerite ($Ni_3Bi_2S_2$)	bismuth

nd: not detected

TABLE 6-6b   Comparative X-ray powder data for
phase C and the mineral Parkerite.

phase C		Parkerite	
I	d	I	d
w	3.99	7	4.02
s	2.82	10	2.86
m	2.33	9	2.34
m	2.27	4	2.29
w	1.98	5	1.99

possibly introduced into the intergranular fluid phase during the breakdown of primary pyrrhotite.

6. Other Ore Minerals

Other ore minerals found in the Kanmantoo orebody include secondary pyrite and marcasite and small amounts of supergene sulphides and oxidized minerals (see chapter 5). Small molybdenite laths are not uncommon as inclusions in chalcopyrite and magnetite or along the cleavages of mica- ceous minerals. Where the sulphide or micas are deformed the included molybdenite exhibits striking folded and kinked microstructures. Rare euhedral grains of wolframite are intergrown with magnetite; both X-ray powder spacings and an electron probe analysis indicate that this phase is the iron-rich end member, ferberite.

Although sphalerite is a widespread minor phase in both the disseminated mineralization and coarse-grained ore, galena has a more restricted occurrence. A few small dissemin- ated grains have been found but most of the galena occurs with sphalerite in small veins in a few places in the orebody but mainly in quartz-mica schists outside the ore zones. The small veins up to an inch thick, all lie along the schistosity planes in relatively unaltered rock and consist of coarse-grained granular intergrowths of homogeneous galena and dark red sphalerite full of oriented laths of pyrrhotite and chalco- pyrite (fig. 6-3i).

SUMMARY

1. The experimentally determined stability fields of the aluminium silicate polymorphs and certain of the other silicates in the Kanmantoo rocks indicate that a temperature of around 675°C and a pressure of about $5\frac{1}{2}$ kb were reached during metamorphism.

2. Compositional zoning is prevalent in larger garnets in

nearly all mineral assemblages of the alteration zones but
no inferences of the physical conditions of growth can be
made from either the zoning or garnet compositions. No
specific garnet zoning or growth features seem to be peculiar
to sulphide-bearing or sulphide free assemblages.

3. The compositions of the high-temperature hexagonal
pyrrhotites are compatible with the inferred metamorphic
temperature.

4. Although there is strong textural evidence that many of
the primary sulphides were subject to the same metamorphic
conditions as the silicates, known phase relationships in the
relevant systems indicate that the present sulphide inter-
growths and assemblages developed from other assemblages
during cooling.

5. An explanation given to account for the rarity of both
primary pyrite and cubanite in the Kanmantoo ore is based
on the partial control of the oxygen and sulphur fugacities
of the environment and the stabilization of the pyrrhotite
compositions by an equilibrium pyrrhotite-magnetite assemblage.
As a result, the bulk compositions of the phases in the Cu-Fe-S
system were controlled to the extent that the breakdown of
cubanite below about $330^{o}C$ was able to proceed in most cases
to completion.

6. Part of the monoclinic pyrrhotite may have formed by
inversion from the high-temperature hexagonal pyrrhotite but
the concentration of the monoclinic material along the
pyrrhotite grain-boundaries is a possible indication that it
formed directly from the breakdown of cubanite below about
$320^{o}C$.

7. The small amounts of Ni, Co and Zn in the ores are not
thought to have had any appreciable affect on the sulphide
phase relationships. Probably all these minor metals were
in solid solution in the major phases at elevated temperatures
and formed into discrete minerals such as pentlandite and
sphalerite only during cooling.

8. Cobaltian mackinawite in exsolution-like intergrowths with chalcopyrite is a widespread but minor sulphide. Although available experimental data would seem to preclude mackinawite from being a simple exsolution product, there is no evidence to refute the suggestion that this mackinawite formed by a reaction between an Fe-Co-Ni alloy exsolved from chalcopyrite and introduced aqueous sulphide.

9. Preliminary heating experiments at temperatures from $470^\circ C$ $940^\circ C$ at periods from 190 hours down to 20 hours on what has been interpreted as naturally deformed and recrystallized magnetite, failed to produce any significant textural changes.

10. A number of accessory minerals probably present as discrete phases during metamorphism include native bismuth, gold, molybdenite and ferberite. Ore minerals considered to have formed during late and post-metomorphic times include pyrite and marcasite, bornite, covellite, chalcocite, hematite, goethite and the bismuth bearing sulphides, wittichinite and parkerite.

chapter 7

MINERAL VEINS

Introduction

Throughout the orebody and country rocks, there are
literally tens of thousands of silicate mineral veins ranging
in thickness from less than a millimetre to over six feet and
displaying a wealth of shapes, structural settings, mineralogies
and textures. Since an estimated 5% of the total rock volume
of the area consists of such veins, collectively they constitute
an important minor rock-type. Description of the veins involves
considerable difficulty; this is because their classification
under any heading such as size or mineralogy covers veins of
widely different shapes and ages and like-wise, veins of
similar ages may have different structural settings and
mineral assemblages.

Mineralogically, the veins are of two principal types;
the siliceous veins and the feldspar veins. In the siliceous
veins quartz is the major constituent, andalusite or muscovite
is locally dominant while minor phases include sillimanite,
biotite, staurolite, chlorite and sulphides; garnet is absent.
In the feldspar veins albite or adularia is the main phase
and minor minerals include siderite, chlorite, tourmaline,
rutile, chalcopyrite and pyrite.

Most of the siliceous veins are conformable or sub-
conformable to the schistosity and are more or less evenly
distributed through the different rockptypes as regards
numbers and size but not in relation to mineral assemblages.
Most of the andalusite-bearing veins occur in the andalusite-
staurolite schists, the muscovite-rich veins in areas containing
considerable late muscovite and the sulphide-bearing veins
are restricted to the mineralized regions. The feldspar veins
are all confined to cross-cutting joints and small fractures
and although tending to be more prevalent in areas adjacent
to chloritized alteration zones, as a group they are subordinate
to the siliceous veins.

In the following discussion emphasis is placed on the
origin of the veins i.e. whether by magmatic injection or by
metasomatic processes, the time relationships between vein
formation and the tectonic-metamorphic history, and any
genetic connections between vein and ore formation.

A. SILICEOUS VEINS

1. Form and Structural Relations

The conformable veins are the most common of siliceous
veins and vary in thickness from less than an inch to over
six feet, and in length from a few inches to about fifty feet.
In plan they all trend parallel to the schistosity surface
(map.1). In vertical cross-section the veins nearly all
display pinch and swell structures (fig. 7-1b) but since the
plunge of the "swells" appears to be gently to the north, the
plan shapes of the veins are sub-parallel to gently lenticular
(fig. 7-1a). The adjacent schistosity surfaces generally
follow faithfully the undulations of the vein walls (figs.
7-1b, 7-2a,b) although a few veins have walls showing slight
transgressions (fig. 7-2c).

There are a few fairly large siliceous veins that
bodily transgress the schistosity but these are mostly located
along the group-4 breccia zones (fig. 7-2d). Individual quartz
masses are extremely irregular in shape and the schistosity
at the quartz walls varies from being little disturbed to
severely contorted (fig. 7-2e,f).

In areas of interbanded quartz-feldspar and micaceous
schists, boudinage or pull-apart structures in the more competent
arenaceous bands contain quartz in the regularly spaced positions
between the boudins (fig. 7-1c). Such veins are termed tensional
veins. Individual boudins show slight necking but there is
clearly a component of simple shear across the veins (fig.
7-1c). Longer but thinner quartz veins illustrated in fig.
7-1d show similar features.

FIG. 7-1

Field Photographs of Various Quartz Veins

(a) Protrusion of a thick quartz vein above the erosion
     level of the surrounding quartz-mica schists; the
     vein has the same strike as the schistosity.

(b) Vertical section through a conformable quartz vein
     that possesses a pronounced pinch and swell
     structure. Note the biotite-rich, quartz-poor
     zones bordering the vein walls.

(c,d) Sub-planar tensional quartz veins in boudinaged
     quartz-feldspar schist bands. Note the offset of
     bedding across the veins.

(e) A ptygmatic quartz vein truncating the schistosity in
     quartz-mica schist. Cross fractures in the quartz are
     a common feature of this vein type.

FIG.7-1

FIG. 7-2

(a,b) Some cross-sectional sketches of conformable pinch
and swell quartz-rich veins.

(c) A pinch and swell quartz veins showing moderate
replacement of the surrounding schists.

(d) Irregular quartz mass developed along a large
cross-cutting breccia zone.

(e,f) Details of contacts between breccia zone quartz
masses and adjacent schist. There has clearly
been considerable replacement of the schist by
the quartz.

Schistosity
Trends

Quartz

4.0 ins

(a)

4.0 ins

(b)

3.0 ins

(c)

3.0 ins

(e)

18 ins

(d)

1.0 in

(f)
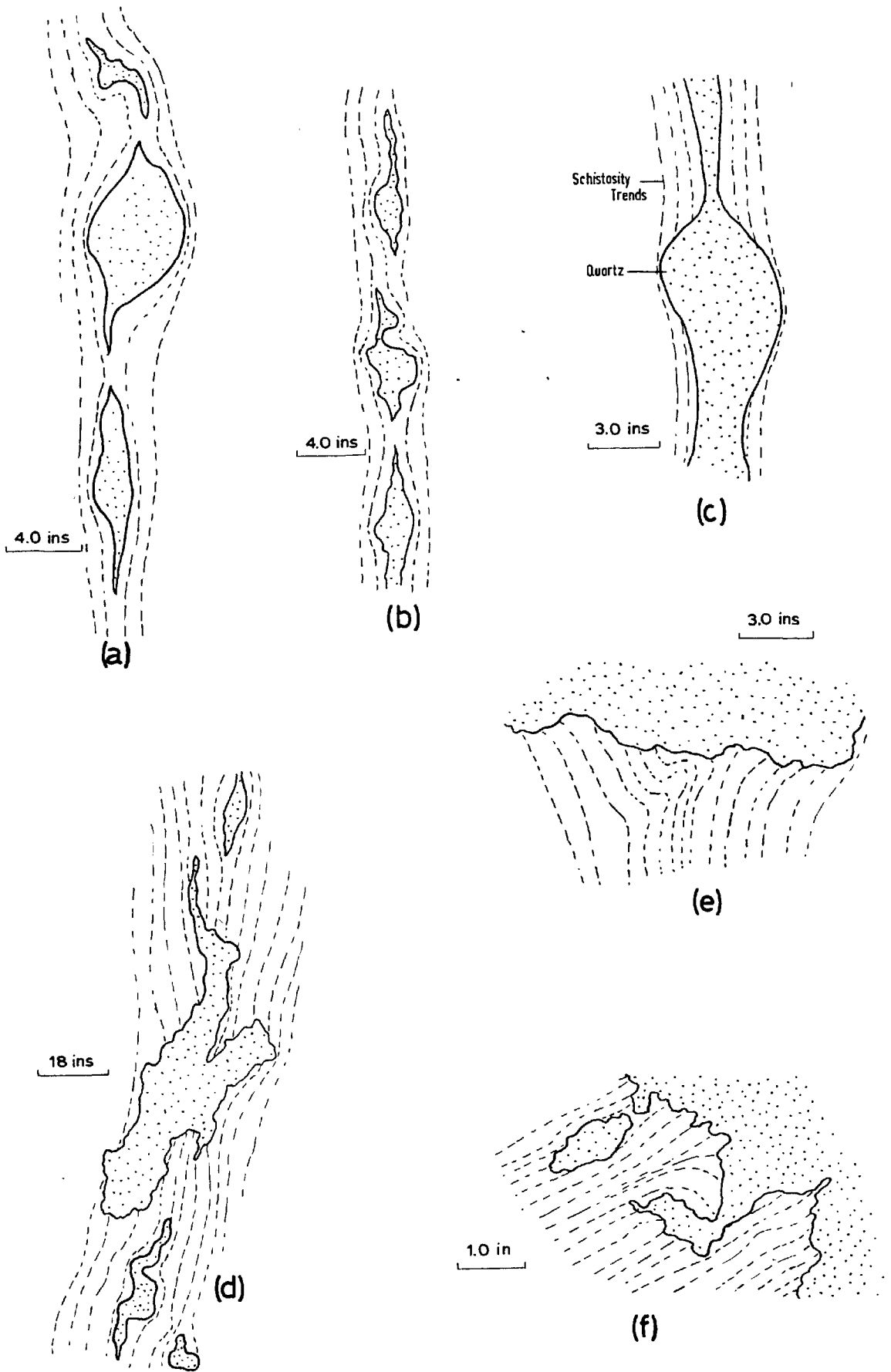
FIG. 7-2

Not found in the arenaceous rocks but quite common in the micaceous schists are thin highly contorted veins of the ptygmatic type. Gently lenticular in cross-section such veins rarely exceed three feet in unfolded length (fig. 7-1e). Ptygmatic veins always transgress the schistosity at moderate to high angles and generally display a series of cross fractures perpendicular to the walls. The schistosity at the vein contacts is usually little disturbed.

2. Internal Features and Mineralogy

Quartz, the main and often only mineral present, occurs as coarse to medium grained aggregates that vary in colour in hand specimen from clear grey to the more common milky white. The more milky the quartz the greater are the numbers of fractures, strain zones and fluid inclusions observed in thin section (fig. 7-4a). The clear quartz usually has a fairly well developed granular fabric with smooth grain boundaries whereas the milky strained quartz fabric is one of uneven grain-size, irregular grain shape and seriate grain boundaries. No vein quartz fabrics ever show a zonation in grain-size or any suggestion of columnar growth across a vein.

In contrast to the white to pale grey subidioblasts of andalusite in the schists, the vein andalusite occurs as large pink prismatic crystals that in thin section appear as moderately pleochroic grains largely free of small mineral inclusions (fig. 7-4b). Andalusite aggregates or crystals are scattered through all parts of a quartzitic vein and show no preference for either the walls or the vein centre.

Staurolite also occurs as large, inclusion-free idioblastic crystals in all parts of the veins (fig. 7-4c). There is no evidence for any age difference in the growth of vein andalusite and vein staurolite.

Biotite on the other hand is confined to the vicinity of the vein walls where it grows as large slim platy crystals through other minerals or along grain-boundaries (fig. 7-4d). A thin colourless zone on both sides of the biotite laths

<u>FIG. 7-3</u>

(all photographs approximately natural scale)

(a) Biotite-rich zone along the contact between a conformable quartz-vein and quartz-mica schist. Note the large muscovite flakes growing across the biotite of the border zone.

(b) Sub-conformable quartz vein in andalusite-staurolite schist. Anhedral pyrrhotite/chalcopyrite grains are scattered through the quartz as well as forming veinlets and blebs in the adjacent schist.

(c) A narrow quartz-rich tensional-type vein displaying a ptygmatic structure in the well foliated quartz-mica schist but assuming a sub-planar form in the massive quartz-feldspar schist.

(d) Albite infilling a joint in andalusite-staurolite schist. The dark material along the centre of the vein is siderite. Note the extremely irregular zone of feldspathization extending out from the vein proper into the adjacent schist. The black phase in both the albitization zone and vein proper (arrowed) is tourmaline.

(e) Another albite vein bordered by albitized schist although the boundary between infilled joint and altered schist is scarcely visible. Chalcopyrite (Cp) occupies the vein core and a few ragged grains are intergrown with albite in the alteration zone (arrowed).

(f) A thin adularia vein formed along a small cross-cutting fracture in andalusite-staurolite schist. The alteration of the schist adjacent to the vein is rather weak.
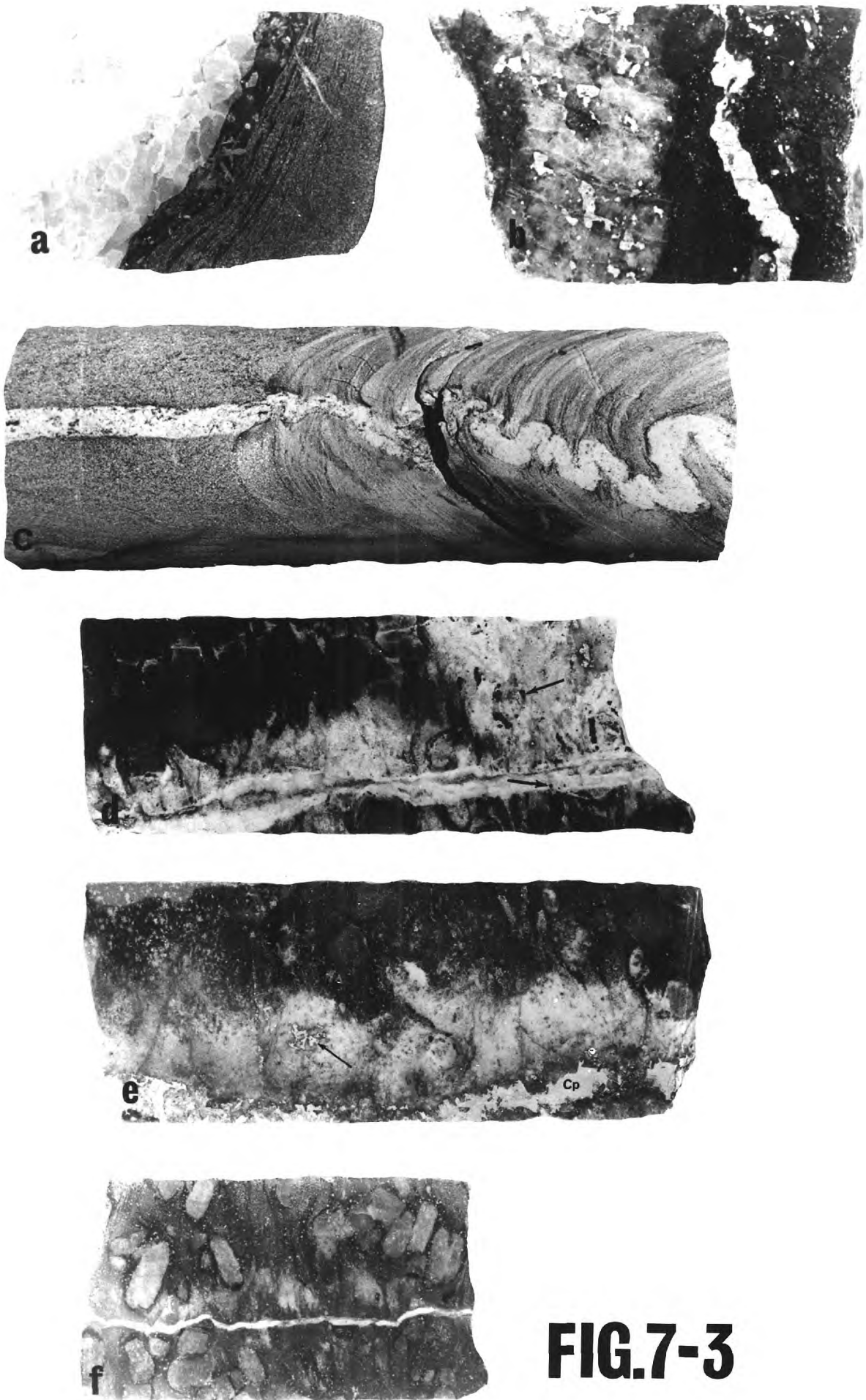
FIG.7-3

that have grown along grain-boundaries of pink vein andalusite, suggests that some iron for biotite growth has been extracted from the adjacent alumino silicate (fig. 7-5a). The amount of iron in the andalusite must nevertheless be very small as no Fe (nor Mn) could be detected with the electron probe. Vein muscovite first appears as thin wisps along andalusite-quartz interfaces (fig. 7-4b) but in the muscovite-rich veins or areas of veins quartz, andalusite and staurolite are severely corroded by the mica (figs. 7-4c, 7-5b). Thus there is considerable textural evidence that both biotite and muscovite grew later than some of the quartz and all of the vein andalusite and staurolite.

Sillimanite is a common though minor vein mineral and is found particularly in veins in schists themselves rich in late muscovite and sillimanite. A little sillimanite is found along the interfaces of various vein minerals especially where there is biotite along the same interface (fig. 7-4d) but most of the sillimanite is concentrated along the irregular interface between muscovite and andalusite (fig. 7-4e). Sillimanite is clearly a late mineral and in the latter example appears to be forming from the excess Al and Si produced during the alteration of andalusite to muscovite.

A few large euhedra of clear apatite are found near the walls of some siliceous veins. Fig. 7-4d shows some apatite crystals that appear to pre-date both the biotite laths and the sillimanite aggregates.

Chlorite is a rather rare vein mineral. Where present it occurs as coarse radiating aggregates corroding the other minerals,and displays a deep blue anomalous birefringence similar to that of the chlorite in the alteration zones.

Siliceous veins containing sulphides are restricted to schists that themselves contain sulphides. Pyrrhotite and chalcopyrite are the main vein sulphides and occur as small to large interstitial grains scattered evenly through the vein quartz (fig. 7-3b). The main textural features have

FIG. 7-4

Some Textural Relationships in Siliceous Veins

(all photographs in transmitted light)

(a) Sub-grain boundaries in strained vein quartz. The
small particles scattered through the quartz are
both mineral and fluid inclusions. Crossed nicols.

(b) Euhedral prism of andalusite surrounded by vein quartz.
Muscovite (Ms) occurs both as thin wisps along the
andalusite-quartz interface and as large anhedral grains
within the andalusite.

(c) Large subhedral staurolite grains (high relief)
intergrown with coarse-grained quartz and muscovite.

(d) Large apatite (Ap) subhedra intergrown with quartz.
Coarse biotite laths occur both within the apatite
and along the apatite-quartz interface; biotite in
the latter position is largely obscured by aggregates
of fine sillimanite needles (sill).

(e) Aggregates of sillimanite needles in muscovite near
the irregular interface between coarse-grained
muscovite and andalusite.

(f) A biotite-garnet-staurolite enrichment zone separating
a conformable quartz vein from unaltered quartz-
biotite-garnet schist.

(g) A large, late muscovite flake growing out into a
biotite-garnet enrichment zone from the walls of
a quartz vein.

(h) Outward growth of vein andalusite (Ad) into a garnet-
biotite enrichment zone. Note the numerous biotite
inclusions in the andalusite parallel to the enrichment
zone fabric.

(i) Quartz in the interior of a small irregular quartz
vein contains small muscovite laths oriented parallel
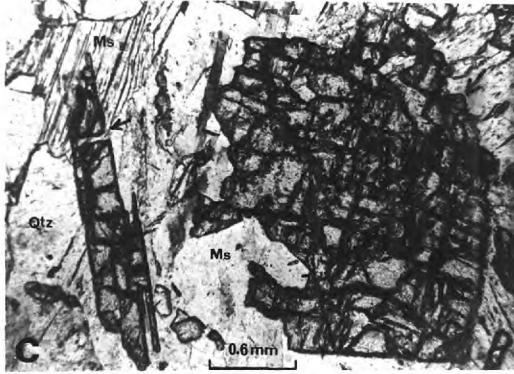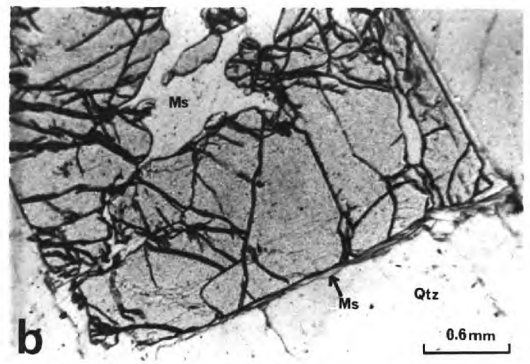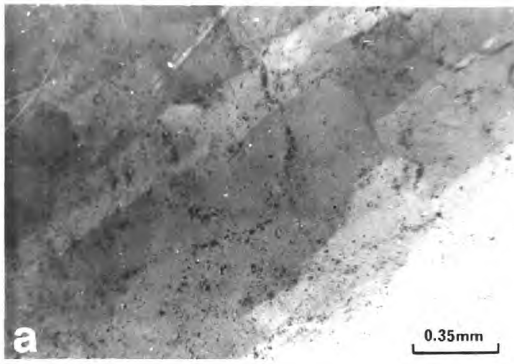to the schistosity of the adjacent schist.
Crossed nicols.
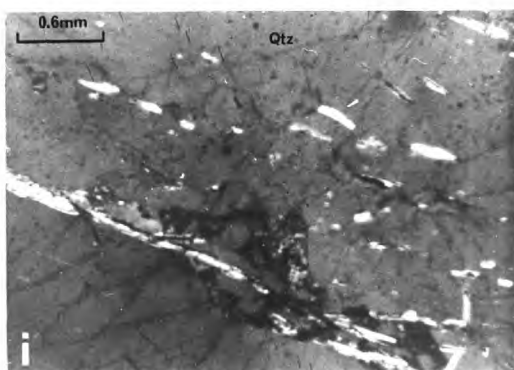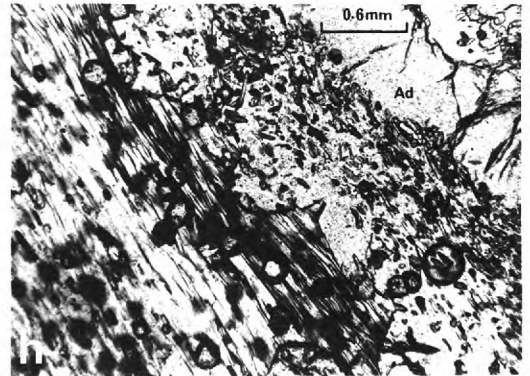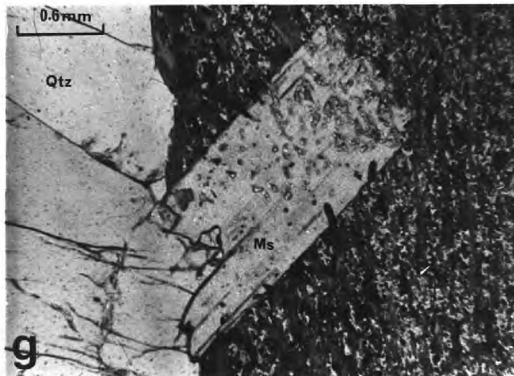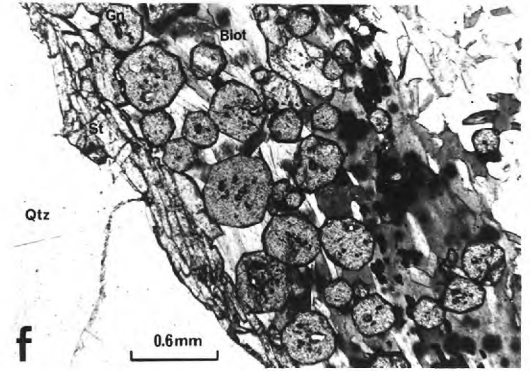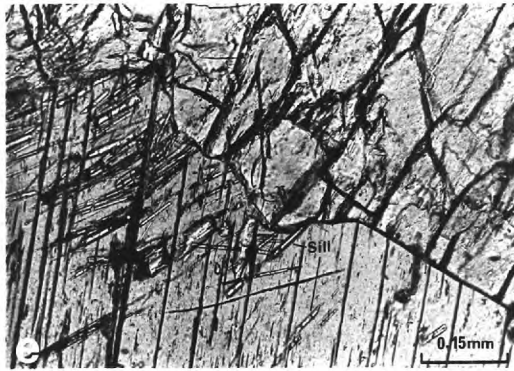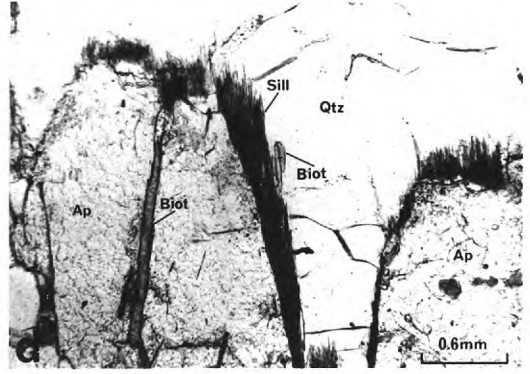
FIG. 7-4

been summarised in chapter 5 (see figs. 5-16g,h). Briefly, there is no definite evidence for any age difference between vein quartz and vein sulphide formation; the quartz is invariably strained and the sulphides tend to penetrate along the quartz interfaces and fractures. Such features could equally be produced by sulphides replacing vein quartz and by simultaneous deformation of quartz and sulphides.

3. Contact Relationships

Most of the conformable veins are bounded by a zone of schist depleted in quartz and enriched in the other schist minerals particularly biotite, garnet and staurolite; less commonly there is an enrichment of muscovite (figs. 7-1b, 7-3a). Although there is no consistent relationship between the thickness of an enrichment zone and the thickness of the adjacent vein particularly in the pinch and swell vein types, there is nevertheless a clear tendency for the thicker enrichment zones to be developed alongside the thicker veins. Photomicrographs of vein-enrichment zone contacts (figs. 7-4f,g) show a sharp break from "clean"inclusion-free vein quartz to the enrichment zone mineralogy and fabric. In a few veins there are indications of some replacement of enrichment zones by vein minerals other than quartz (fig. 7-4h) but such cases are uncommon.

Most of the tensional veins, ptygmatic veins and irregular cross-cutting quartz masses in breccia zones show a sudden break from vein quartz into apparently unaltered schists. There is no intervening zone of melanocratic minerals. But whereas the quartz in both the tensional and ptygmatic veins is usually clean and free from mineral inclusions, the qurtz of a few irregular veins is commonly loaded with small mica inclusions oriented parallel to the schistosity of the adjacent schists (fig. 7-4i).

4. Fluid Inclusions in Minerals Associated with Veins

Although fluid inclusions are rare in minerals of the

unaltered schists they are very common in certain minerals of the
siliceous veins and associated enrichment zones, and also in
minerals in the alteration zones.

(a)   Description of the Fluid Inclusions

        Fluid inclusions have not been found in the smaller
schist garnets but they are fairly common in garnets of the
alteration zones and in enrichment zones adjacent to conformable
siliceous veins. What are considered to be primary inclusions
i.e. trapped during mineral growth, are those that occur in
groups around zones parallel to the garnet crystal faces (fig.
7-5c). Individual inclusions reach a maximum size of only
10 microns and vary in cross-sectional shape from parallelo-
grams to triangles the sides of which are parallel to the garnet
dodecahedral faces. Only two phases are visible in the inclusions
- a bubble and a liquid. More abundant are the minute inclusions
of similar shape in radial zones across the garnet idioblasts
(fig. 7-5d); the origin of these inclusions is uncertain but
such radial arrangements are found in perfectly fresh garnets
showing no signs of plastic deformation or fracturing.

        Inclusions of unknown composition are found in deformed
staurolite crystals in the alteration zones of the lode schists,
in the enrichment zones and in the siliceous veins. These
inclusions have various shapes (fig.7-5e) but the rectangular
types are always aligned parallel to the prismatic faces of
the staurolite host. A clear and an opaque phase (iron oxide?)
are visible in the inclusions but bubbles have not been recognised.

        Fluid inclusions are absent in schist andalusite but a
few minute rectangular inclusions are found lying parallel to
the prismatic faces of undeformed vein andalusite crystals.
Such inclusions which appear to be primary, consist of three
phases - a liquid, a bubble and a small cubic crystal (fig. 7-5f).

        All the undeformed apatite crystals in the siliceous
veins contain scattered groups of elongated fluid inclusions
oriented along the c-axes of the grains. Some inclusions
are slightly curved but most appear to be perfect negative
prismatic crystals of apatite (fig. 7-5g). Usually three

FIG. 7-5

(a) A biotite lath growing along the interface of two large pale-pink vein andalusites. A thin zone of colourless andalusite occurs along both sides of the mica.

(b) Coarse plates of muscovite partially replacing andalusite (stippled) and quartz (clear) in a siliceous vein.

(c) Two-phase primary fluid inclusions in garnet. The inclusion faces are parallel to the garnet faces.

(d) Curved lines of two-phase fluid inclusions in unfractured garnets.

(e) Examples of some inclusions in staurolite. The dark phase is probably an oxide (ilmenite?) but the composition of the clear phase is unknown.

(f) Three phase fluid inclusions in andalusite; the clear phase is a saturated brine, the cubic crystal is an alkali chloride and the stippled phase is a bubble.

(g) Two and three phase fluid inclusions in vein apatite.

(h) Minute two and three phase fluid inclusions in a single enhedral quartz grain in unaltered quartz-mica schist.

(i) Two, three and four phase fluid inclusions in vein quartz. Individual inclusions vary in habit from perfect negative quartz crystals to anhedral attenuated worm-like forms.

(a) 0.3 mm

(b) 1.0 mm

(c) 25µ

(d) 150µ

(e) 10µ

(f) 10µ

(g) 10µ

(h) 50µ

(i) 10µ
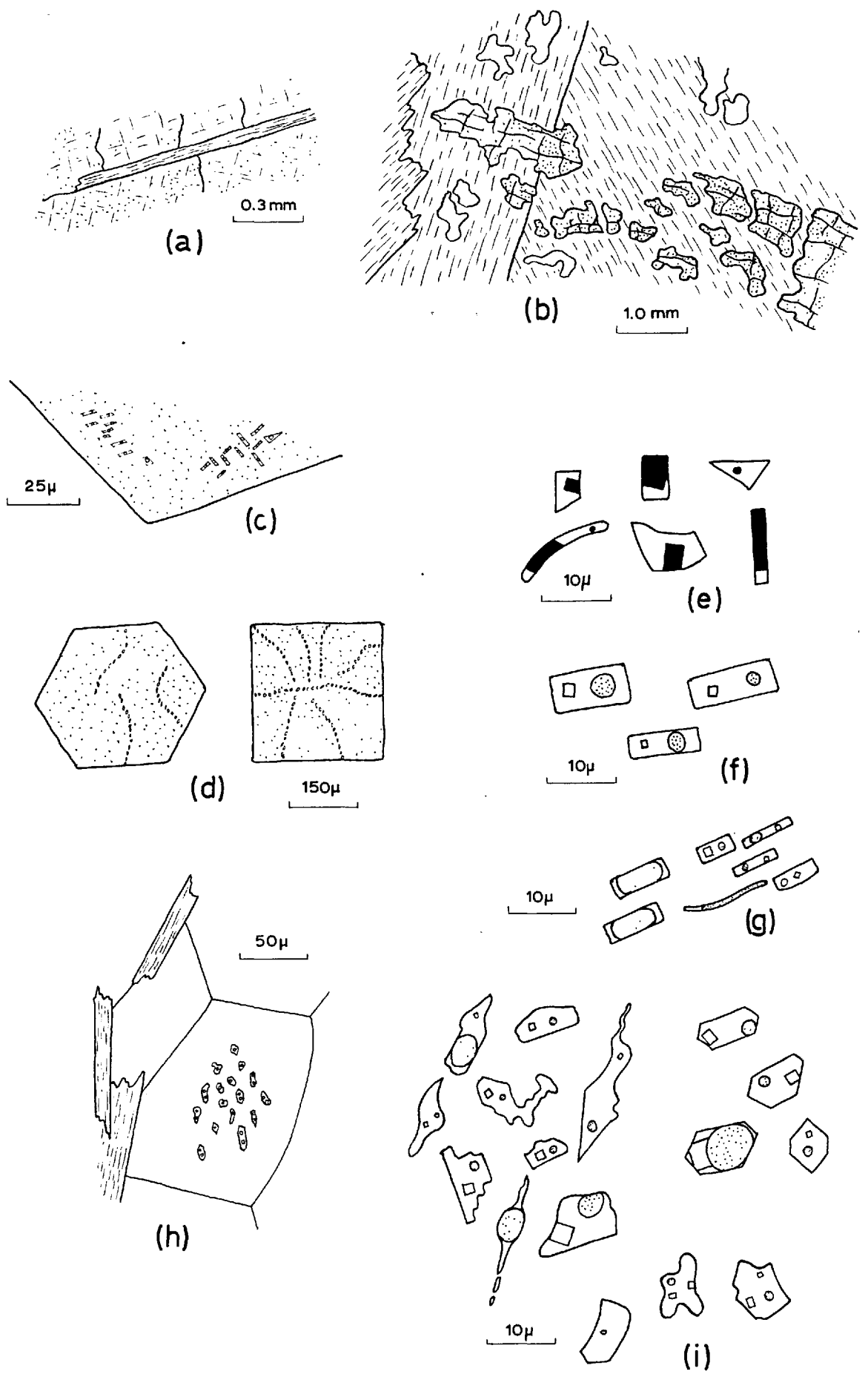
FIG. 7-5

phases are visible but some inclusions appear to contain only a little liquid and an enormous bubble that occupies about two thirds the volume of the inclusion.

Fluid inclusions are sometimes found in unstrained matrix quartz grains in the unaltered schists but for some reason they are concentrated in particular grains instead of being evenly distributed through the rock (fig. 7-5h). Fluid inclusions are not common in the clear, unstrained vein quartz but in the milky quartz enormous numbers of inclusions occur in planar zones that pass through many grains of different orientation without deviation. In quartz showing severe undolose extinction the inclusion zones appear to be independent also of the sub-grain boundaries. The shapes of the inclusions in the schist quartz vary from perfect negative crystals to slightly rounded grains but in the vein quartz, inclusions vary from negative crystals to highly irregular and attenuated worm-like forms even along a single line (fig. 7-5i). The majority of inclusions contain three phases but the relative proportions of bubble, liquid and cubic crystal are extremely variable. A small number of inclusions contain only a bubble and liquid whereas others contain an additional cubic crystal.

Although the inclusions in the unstrained schist quartz have the appearance of being primary the meaning of primary in quartz that may have recrystallized many times is not very clear. On the other hand, the inclusions in zones through the strained quartz all appear to be secondary and probably represent intergranular fluids that partially filled tectonic fractures that have since been re-cemented.

(b) Partial Analysis of the Fluid Inclusions in Vein Quartz

To confirm that the solid material in the fluid inclusions is an alkali halide in equilibrium with a concentrated brine the inclusions in a specimen of pure milky vein quartz were analysed by the following method. The quartz was crushed in a siliconcarbide impact mortar and the plus 30, minus 18 mesh fraction washed a number of times in deionised water, rinsed

in alcohol and dried in air at 75°C. 7.0 gm of the dried quartz was ground in deionised water for 15 minutes in a small vibratory rod-mill; this consisted of a small polythene jar of 130 ml capacity charged with 48 grinding elements of non-porous alumina (corundum). The resulting slurry was transferred to a beaker, diluted to about 150 ml with deionised water, agitated for 6 hours and then centrifuged to separate the fine quartz and alumina particles from the leach solution. After being analysed for Na^+ and K^+ on a flame photometer, the solution was gently boiled until all the water had evaporated. A portion of the small amount of residue was then X-rayed in a powder camera using iron filtered cobalt radiation. A blank i.e. deionized water was run through the rod-mill and subjected to the same procedure as the ground quartz up to the chemical analysis stage. The results are given below:

(a) Leach solution

wt of Na^+ in solution = 0.8 mgm (= 114 ppm of quartz)
wt of K^+ in solution = 0.3 mgm (= 43 ppm of quartz)

No detectable Na^+ or K^+ in blank.

(b) Residue

Strong reflections for halite, sylvite and quartz.
Weak reflections for an unidentified phase.
Alumina not detectable.

Of interest is the low Na/K ratio which is evidently a feature of inclusions in many quartz veins from metamorphic rocks (Roedder, 1967). No temperature inferences can be made from this data but the results do show that the intergranular phase at sometime during the metamorphic history was in part, a concentrated brine.

5. Origin of the Siliceous Veins

(a) Non-Replacement Siliceous Veins

Veins showing no or little sign that the emplacement of the vein material has involved significant replacement of the enclosing schist include the conformable veins, tensional

veins and ptygmatic veins.

Mono-mineralic quartz veins give little indication of
the conditions of formation except to virtually exclude
magmatic injection; the minimum melting point of quartz in
the presence of water is $1080^\circ C$ at 9.8 kb pressure (Kennedy
et al. 1962). Strong evidence that the multi-mineralic veins
formed during, or at least were subjected to, the physical
conditions of metamorphism is that the vein mineral assemblages
and textural time relationships are identical to those found
in the enclosing schists.

Pinch and swell pegmatite veins lying parallel to the
schistosity in some metamorphic rocks of West Greenland were
studied in great detail by Ramberg (1956). He attributes the
narrowing not to localised compressive stress normal to the
vein but rather to necking of an already formed or forming vein
during deformation of the enclosing rocks. Zones enriched in
certain rock minerals alongside the veins were termed extrac-
tion zones by Ramberg who believed they signify that some vein
material was derived metasomatically from the immediately
surrounding wall rock. Ramberg's theory, that such veins
probably developed in low pressure sites during dilational
deformation, has been supported and developed by many later
workers notably Carstens (1966), Gresens (1967) and Carpenter
(1967). The creation of such pressure lows causes chemical
potential gradients to be set up for both the dispersed (inter-
granular) phases and the solid phases. The more mobile compon-
ents will tend to diffuse along such gradients into the low
pressure sites as long as the pressure differential is maintained.
At no time is it necessary to postulate a cavity or opening
in the rock.

These genetic ideas correspond well with all the
observations made on pinch and swell veins in the Kanmantoo
area. The attitude of the veins parallel to the schistosity,
the orientation of the long axes of the swells at high angles
to the lineation, the largely non-replacement contact relation-
ships and the typical metamorphic assemblages all point to

vein formation during metamorphism and tectonism. The initial
period of vein formation was probably between the B_1a and B_1b
tectonic phases when the relaxation of the maximum compressive
stress normal to the schistosity was such as to allow tensional
forces to act in the same direction. In other words the
maximum compressive stress now acting along the schistosity
planes would tend to force them apart and, in so doing, create
considerable pressure gradients. The early veins would be
gently lenticular in shape but with renewal of compression
normal to the schistosity at the beginning of the B_1b phase the
tensional stress along the veins would cause them to deform
by necking. Thus a pinch and swell structure would be formed.
Primary fluid inclusions in many vein and enrichment zone
minerals suggest that an intergranular phase rich in dissolved
alkali chlorides acted at the same time as an important
transporting medium for the vein material and as a flux enabling
vein minerals to attain a considerable size. Thus the vein and
enrichment zones could be regarded in part as contemporary and
complementary products of metamorphic-tectonic differentiation.
Close similarities in mineralogy, texture and attitude of these
enrichment zones with the thicker alteration zones in the lode
schists suggest that the latter zones may have formed by a
similar mechanism although probably largely after the B_1b phase
when similar dilation stress fields were generated. It is
difficult to explain the lack of complementary quartz veins
close to the alteration zones except by postulating large
movements of iron and alumina into them or movement of silica
away. Sulphides in the quartz veins near the mineralized
areas appear to have been emplaced in the same manner as the
other vein minerals and give no clue to the origin of the ore
as a whole.

There seems little doubt that the tensional quartz veins were
formed by metasomatic infilling of the low-pressure zones
between boudins during or closely following one of the main
tectonic phases. Which tectonic phase is difficult to ascertain
but the non-chloritization and non-bleaching of the biotite in
the adjacent schists indicates quartz emplacement during
progressive metamorphism. Lack of any enrichment zones
suggest that the vein material was derived from a source

external to the immediate wall-rock. There is some evidence that
the ptygmatic veins formed originally in the same way as the
tensional veins. They are very similar in size and shape,
identical in composition (pure quartz) and both lack enrich-
ment zones. But the ptygmatic veins are confined to the
more micaceous host rocks. It is possible that after formation
as originally sub-planar tension veins, deformation and
flattening of the less competent host rocks perpendicular to
the schistosity caused the somewhat rigid veins to buckle.
Support for such a mechanism is shown in fig. 7-3c; a planar
tensional vein in an arenaceous bed becomes highly contorted on
passing into the less competent micaceous lithology. This
origin has been suggested for non-magmatic ptygmatic veins
by Wilson (1952), Ramberg (1959) and Watterson (1968) although
Ramberg points out that folding of the vein may in some cases
be contemporaneous with growth. Shelley (1968) on the other
hand found non-magmatic ptygmatic veins in rocks that showed
no signs of flattening. He believes that such veins developed
by metasomatic infilling and replacement along tortuous
fractures formed during deformation.

(b) Replacement Siliceous Veins

Since the breccia zones are either late or post -
metamorphic in age the irregular replacement quartz masses
in them must be late as well. The origin of the silica is
not known but it is probably partly derived from leaching of
the rocks in the breccia zones and partly from a deeper
seated source.

B. FELDSPAR VEINS

1. Albite Veins

Albite veins formed along joint planes are no more than
an inch or two thick and are rarely continuous along the joints
for more than a few tens of feet. The feldspar varies in
colour in hand specimen from pure white to pale green although
it is sometimes stained a pale brown. Typical examples of
such veins are illustrated in figs. 7-3d,e. Important

features are; (1) the vein proper i.e. the infilled joint, is fairly thin with gently undulating walls, (2) cavities in the veins are rare; the central portions are generally occupied by a thin core of brown siderite and/or discontinuous ragged chalcopyrite, (3) thick, extremely irregular altered zones extend into the immediate schist from the vein walls, and (4) crystals and aggregates of black tourmaline (arrowed in fig. 7-3d) are intergrown with feldspar in both the vein and altered zones.

In thin section there is visible a clear columnar arrangement of feldspar crystals into the vein centre from the walls but crystal faces are either destroyed by mutual growth interference or corroded by carbonate or sulphide minerals in the core. Lines of minute mineral inclusions reveal the zonal growth pattern in many of the albite grains (fig.7-6a). Tourmaline crystals in the veins and adjacent altered zones are generally euhedral to sub-hedral and are invariably delicately zoned in shades of olive green, pale blue and pale brown (fig. 7-6b). Alteration of the schist adjacent to the albite veins begins with the chloritization of biotite and garnet, sericitization of andalusite and replacement of quartz by albite (fig. 7-6c). Tourmaline forming in the altered zones is usually at first quite ragged in habit, commonly medium brown in colour and unzoned (fig. 7-6c). A few ragged aggregates of chalcopyrite in the altered zones apparently form largely by replacement of remnant quartz (fig. 7-6d). Eventually feldspar replaces even the chlorite and the final alteration zone is an anhedral granular aggregate of albite containing minor tourmaline, a little chalcopyrite and lines of small rutile prisms marking the former schisto-sity trends. In places albitization extends outwards for a few tens of feet into the country rocks to form thin albitite bands that faithfully preserve the lepidoblastic fabric of the original quartz-mica schist (fig. 7-6e).

2. Adularia Veins

Adularia veins are rather rare compared with the albite

FIG. 7-6

Some Textural Relationships in Feldspar Veins
(all photographs in transmitted light)

(a) Minute mineral inclusions outline the growth zones in anhedral vein albite.

(b) An irregular contact between vein albite (Ab) and chloritized schist (Chl). The zoned phase intergrown with the feldspar is tourmaline.

(c) Partially altered schist adjacent to an albite vein. Most of the biotite is altered to chlorite and the quartz partially replaced by albite. The garnet in the centre of the picture is largely altered to chlorite and is fringed by a ragged grain of brown tourmaline.

(d) Ragged interstitial chalcopyrite (Cp) intergrown with quartz in an albitized alteration zone. The albite (Ab) has a rather cloudy appearance.

(e) A quartz-mica schist near an albite vein that has been wholly replaced by a mosaic of fine-grained albite. Both the lepidoblastic albite fabric and lines of minute rutile prisms (not visible) preserve the formed schistosity trends. Crossed nicols.

(f) Granular adularia completely infilling a small fracture; the feldspar grain boundaries have been drawn on the photograph. Accicular chlorite aggregates extend for a short distance out into quartz-mica schist that is visible in the upper right part of the photograph.
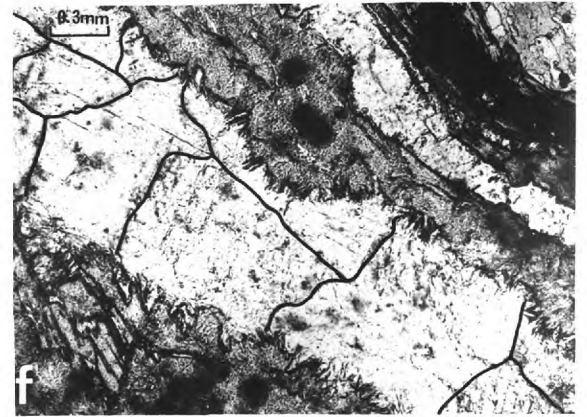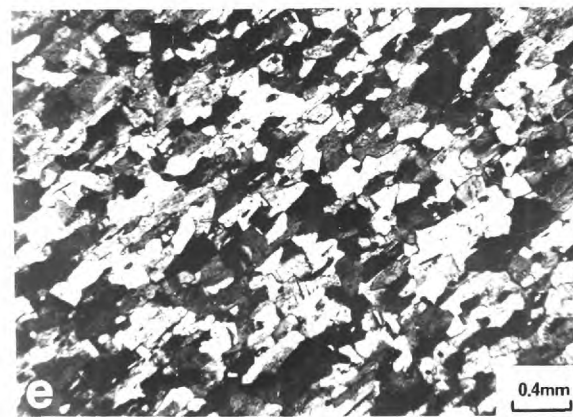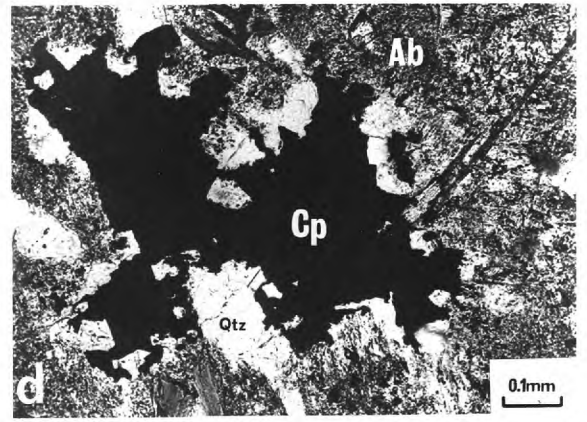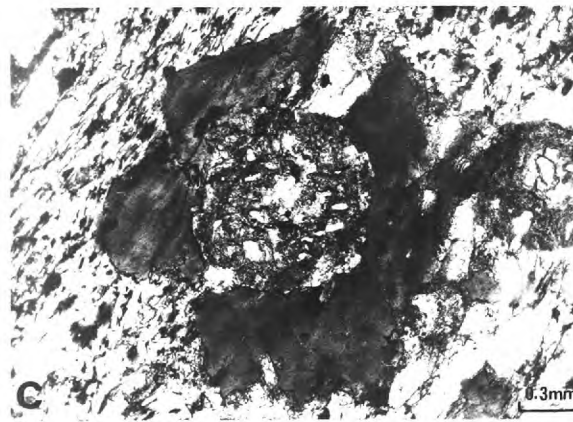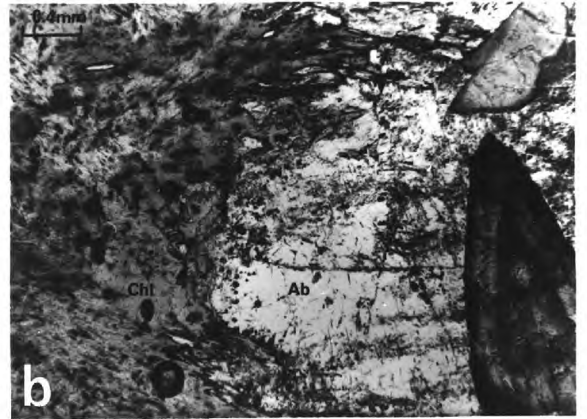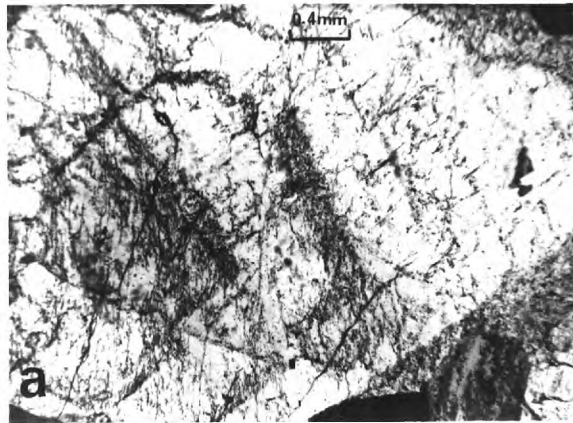
FIG. 7-6

veins and two examples are given in figs. 7-3f and 4-7e (ch.4).
The first example is a thin solid intergrowth of white adularia
along a narrow parallel sided fracture. In thin section (fig.
7-6f) the feldspar is seen as a coarse granular aggregate with
many grains growing from one side of the vein to the other. The
walls of the fracture are lined with fine-grained acicular
aggregates of pale green chlorite but there is only weak
alteration of the wall rocks. In the second example, the walls
of a rather larger irregular fracture are lined with columnar out-
growths of adularia on which the characteristic rhombic faces
are visible when viewed under a binocular microscope. In the
large central cavity a single pyrite crystal of cubic habit
is intergrown with the feldspar. Not clearly visible in the
photograph are bladed chlorite aggregates growing perpendi-
cular to the pyrite cube faces and a few specks of chalco-
pyrite intergrown with the feldspar. Alteration of the wall
rock is again weak.

3. Origin of the Feldspar Veins

The nearly mono-mineralic nature of most of the feldspar
veins virtually rules out any magmatic injection origin. Both
the textural features of the veins and their location along
late fractures point to deposition of feldspar from circulating
ground fluids late in the metamorphic history. The origin of the
feldspar constituents is difficult to prove but the proximity
of most of the veins to the chloritized alteration zones in
the lode schists suggests a genetic connection between chloriti-
zation and feldspar formation. Break down of biotite to
chlorite involves, among many possible chemical changes, a
liberation of alkalis and an addition of water. Chloritiza-
tion of the minerals along the walls of the joints probably
contributed some of the feldspar components but it seems
likely that the bulk of the alkalis and alumina were released
from the alteration zones in the lode schists and eventually
migrated into fractures and joints. This relationship between
chloritization of biotite and the formation of feldspar has
been observed in altered granites by Chayes (1955).

Accessory tourmaline is present in all the schists so quantitatively there is no problem of an indigenous boron supply. The large tourmaline grains in the altered zones alongside the veins probably formed partly by reconstitution of local tourmaline and partly from introduced components.

The formation of the small amounts of siderite and sulphides was probably later than most of the feldspar and possibly took place at the same time that pyrrhotite in the orebody was breaking down to pyrite plus marcasite. These veins minerals were most likely deposited from carbonated waters of meteoric origin that had leached pre-existing sulphides nearer the surface and percolated down through fractures and joints.

The segregation of feldspar veins into albitic and adularia types is an interesting problem. It seems likely that potash and soda were liberated simultaneously during shloritization so the cause for the separation must be in the depositional environment.

SUMMARY

1. Small quartz veins in tensional structures appear to have formed as metasomatic infillings between boudins prior to or in the early stages of progressive metamorphism. Such veins were all originally lens-shaped or planar in form but those in the less competent lithologies that were subject to later flattening, were buckled into ptygmatic shapes.

2. Pinch and swell veins lying parallel to the schistosity formed originally between the B_1a and B_1b tectonic phases as planar or gently lenticular veins. Subsequent deformation of the enclosing schists caused the veins to stretch and created the pinch and swell forms. There is little evidence that the veins formed by replacement but at the same time there are no signs of open cavity infilling. Thus it is concluded that the veins grew by diffusion of material into the low pressure zones during dilational strain of the surrounding

schists; vein growth probably kept pace with the strain.
Enrichment zones alongside many veins indicate that much of
the vein material came from the immediate wall rocks. Primary
fluid inclusions in many vein phases suggest that diffusion
of many of the mineral components was via a hydrous inter-
granular phase rich in alkali chlorides.

3. Sulphides in the quartz veins appear to have formed in
the same way as the other vein minerals i.e. by migrations of
material from the wall-rocks. These sulphide accumulations
are only a minor part of the mineralization.

4. The irregular quartz masses along the late breccia zones
were formed partly as cavity infillings and partly by replace-
ment of both the walls and the breccia fragments.

5. The few albite and adularia veins formed in joints and
fractures in the vicinity of the alteration zones in the lode
schists appear to be genetically related to the chloritization
of biotite in these zones. Small amounts of sulphides and
siderite associated with the feldspar veins were deposited from
meteoric ground waters, probably around the same time as
pyrrhotite in the orebody was breaking down to marcasite and
pyrite.

chapter 8

GEOCHEMICAL FEATURES OF THE SCHISTS AND

MINERALIZED ZONES

General Statement

 This chapter is divided into two parts; the first
section discusses the chemical variation among the principal
rock-types as a probable reflection of the original sediments,
and then compares the compositions of these unaltered rocks
with those of some alteration zone assemblages to see what
metasomatic changes have accompanied their formation. The
second section describes the concentrations of some major,
minor and trace elements through the ore zones, and discusses
the origin of these elements and the possible role metamorphism
and tectonism have played in their present distribution.

A. COMPOSITION OF THE SCHISTS

1. Sampling and Analytical Procedure

 Schist samples from in and around the Kanmantoo orebody
chosen for chemical analyses had to conform to the following
conditions; (a) they were typical representatives of the
rock-types, (b) there were no signs of supergene alteration
or weathering, and (c) thin sections were available for
studying the mineralogy and/or making modal analyses. Ten
samples were selected, five to show chemical variations among
the main rock-types and five to show variations among some
common alteration zone assemblages.

 Approximately 500 gm of each rock was crushed on a
tungsten carbide faced impact mortar and ground in a "Tema"
mill. The rock powder was thoroughly homogenised and then
coned and quartered until a convenient amount was obtained
or analysis. Silica was determined using a combined gravi-
metric and colorimetric method and alkalis were analysed by
flame photometry. Total iron, Al_2O_3, CaO, MgO and MnO were

all determined on an atomic absorption spectrophotometer (A.A.S.);
solutions were prepared by digesting small portions of the
powdered rock in a mixture of hydrofluoric, nitric and perch-
loric acids, evaporating to dryness, redissolving the residue
in HCl and diluting to the required degree with deionised
water. Rocks containing significant amounts of andalusite or
staurolite refused to break down completely by this method
so much material had to be fused with anhydrous sodium carbonate
and then dissolved directly in HCl; silica was allowed to
settle before the solution was analysed. For Mg and Ca
determinations small standard amounts of lanthanum solution
were added to the rock solutions to prevent these elements
complexing with Al. All A.A.S. analyses were made using an
acetylene-compressed air flame.

Repeat analyses were made for Al and alkalis and an
internal check was provided by running a previously analysed
standard rock sample concurrently with the Kanmantoo material.
Water, P_2O_5 and TiO_2 were not determined.

2. The Unaltered Rocks

Partial chemical analyses of the five principal rock-
types and modal analyses for two of them are given in table
8-1. As is to be expected from schists having such contrasting
mineral assemblages there are wide variations in the major
oxide chemistry. Important features of the quartz-feldspar
schists (1 to 4) that should be pointed out are; (a) the low
mica and high feldspar contents of the arenaceous schists are
reflected in the low iron and MgO and high alkali contents,
(b) silica, MnO MgO and CaO contents of the micaceous schists
are similar thus the contrasting mineralogies in these rocks
are a reflection of variations in the proportions of alumina,
iron and alkalis, (c) the high alkali content of the quartz-
mica schists has enabled practically all the iron, MgO CaO and
MnO to be used up in the micas, and (d) the lower alkali
contents of the andalusite-staurolite and lode schists means
that after formation of the micas, an excess of iron and

TABLE 8-1. Analyses of the principal rock-types.

(analyst: W. F. Lindqvist)

Chemical Composition

	(1)	(2)	(3)	(4)	(5)
SiO$_2$	74.66	60.72	61.81	64.92	62.74
Al$_2$O$_3$	11.11	12.90	16.97*	8.14	14.29
Fe as FeO	0.31	4.89	9.26	16.21	6.07
MnO	0.02	0.20	0.98	0.16	0.28
MgO	1.44	3.64	3.17	3.06	4.42
CaO	1.47	1.99	nd	0.44	10.61
Na$_2$O	3.38	2.57	0.25	0.19	1.29
K$_2$O	2.27	4.05	2.56	2.46	0.27
	94.66	90.96	95.0	95.49	99.97

* by subtraction from 95%
nd: not detected

Modal Composition

	(3)	(4)
quartz	36.98	42.45
biotite	30.71	28.37
andalusite	24.64	-
staurolite	1.41	-
garnet	5.97	27.65
chlorite	0.33	-
opaques	-	0.7
	100.01	99.97
points	3250	2365

(1)   Quartz-feldspar schist
(2)   Quartz-biotite-muscovite (quartz-mica) schist
(3)   Andalusite-staurolite schist
(4)   Quartz-biotite-garnet lode schist
(5)   Quartz-actinolite-anorthite (calc-silicate) schist

alumina was able to combine with silica to crystallize as andalusite and/or garnet.

Petrographic studies of the quartz-feldspar schists suggest that they were formerly slightly muddy arenaceous sediments and a comparison of analysis (1) in table 8-1 with (a) and (b) in table 8-2 indicates that the sediments were of the greywacke to arkosic sandstone type. The quartz-mica and andalusite-staurolite schists both appear to have been derived from varieties of siltstone or shale (c in table 8-2) while the unaltered quartz-biotite-garnet lode schists were probably ferruginous shales.

The pre-metamorphic nature of the calc-silicate schist bands is uncertain. Although the small-scale structural rela- tionships show that these bands are conformable with the folded bedding of the enclosing micaceous schists, the large scale stratigraphic relationships are unknown. Clearly the calc-silicate schist chemistry (5 in table 8-1) is markedly different from that of the other schists, the main points of departure being the high CaO and MgO contents of the former. Three possible origins for these lime-rich schists are:

(1) They represent thin beds of marl or dolomitic shale from which all the CO_2 was expelled during metamorphism. Little in the way of chemical evidence is available for such an origin since the resulting chemistry would depend on the original ratio of calcareous material to clay debris. Thicker, obviously bedded calc-silicate rocks and carbonate-bearing schists elsewhere in the Kanmantoo group are regarded by Mills (1964) as metamorphosed.

(2) They were thin doleritic dykes intruded before or during metamorphism. This would seem to be unlikely for the field relationships suggest that they are conformable with the bedding. Truly intrusive amphibolite rocks are known in the northern regions of the Kanmantoo Group (Mills, 1963) but a comparison of the composition of these rocks (d in table 8-2) with that of the calc-silicate schist

TABLE 8-2. Typical chemical compositions of some different rock-types.

	(a) greywacke	(b) arkosic sandstone	(c) shale	(d) meta-dolerite	(e) olivine andesite
SiO_2	73.04	75.57	60.64	48.67	57.74
Al_2O_3	10.17	11.38	17.32	15.05	17.70
Fe_2O_3	0.56	0.82	2.25	3.12	1.95
FeO	4.15	1.63	3.66	8.70	5.32
MnO	0.18	0.05	trace	6.17	0.09
MgO	1.43	0.72	2.60	6.63	5.00
CaO	1.49	1.69	1.54	11.49	9.14
Na_2O	3.56	2.45	1.19	2.42	1.59
K_2O	1.37	3.35	3.69	0.42	0.72
	95.95	97.66	92.89	96.67	99.25

a, b, c from Pettijohn (1957)

d from Mills (1963)

e from Turner and Verhoogen (1960)

is supporting evidence that the two rocks are not of the
same origin.

(3) They were originally thin tuffaceous bands. Contemporary
volcanism has been suspected during sedimentation in the
Kanmantoo Trough particularly in view of the sidespread
development of what are considered to be syngenetic
pyrite and pyrrhotite schist horizons (George, 1966).
However, as yet there is no direct evidence that this was
so. Rather interesting are the close chemical similarities
of the calc-silicate schist to a typical andesite (e in
table 8-2) a volcanic rock-type well known in Palaeozoic
to recent geosynclinal regions around the Pacific margins.

3. Alteration Zone Assemblages

Chemical and modal compositions of five typical altera-
tion zone assemblages are given in table 8-3. A comparison
of the compositions of the non- or only slightly chloritized
assemblages (1, 2 and 3) with those of the unaltered micaceous
schists (2,3 and 4 in table 8-1) shows that the development
of the alteration zones apparently involved the following
chemical changes:

(1) a large decrease in silica.
(2) a large increase in alumina.
(3) a tendency for an increase in Fe, MgO and MnO.
(4) a tendency for a decrease in alkalis.

It is difficult to prove in what direction the metasomatic
transfer of material has been i.e. whether the increase in
alumina and other components is real or whether it is a result
of extraction of a component such as silica, or both.
Development of small-scale, alteration zone-like concentrations
of biotite, garnet and staurolite along some quartz vein margins
has been attributed in the main to silica extraction (see ch. 7).
To examine the possibility that the alteration zones formed
in a similar manner analyses 1, 2 and 3 in table 8-3 have
been recalculated; if the weight percent of each component in
the analysis is regarded as grams then the amount of silica
added to each rock to bring the total silica content to about

TABLE 8-3. Analyses of alteration zone assemblages.
(Analyst: W. F. Lindqvist)

Chemical Composition

	(1)	(2)	(3)	(4)	(5)
SiO_2	32.29	36.16	44.49	30.16	24.51
Al_2O_3	24.74	35.27*	11.45	24.05	21.10
Fe as FeO	22.71	17.19	35.01	33.03	28.82
MnO	2.73	1.07	0.56	0.70	2.36
MgO	6.70	3.28	3.32	7.94	11.11
CaO	0.46	nd	0.59	1.05	0.47
Na_2O	0.93	0.22	0.25	0.92	0.56
K_2O	4.34	1.81	0.09	1.53	0.16
	94.90	95.0	95.76	99.38	89.65

* by subtraction from 95.0%
nd: not detected

Modal Composition

	(1)	(2)	(3)	(4)	(5)
quartz	trace	10.16	2.52	–	–
biotite	61.86	19.39	trace	2.53	1.0
muscovite	–	3.87	–	–	0.3
staurolite	trace	49.62	–	–	–
garnet	37.12	7.21	65.45	28.87	0.5
amphibole	–	–	29.30	–	–
chlorite	trace	8.96	1.04	63.44	97.4
opaques	trace	trace	1.57	5.15	0.7
apatite	–	0.66	–	–	–
	98.98	99.87	99.88	99.99	99.9
points	2352	4397	3566	4111	2524

(1) Garnet-biotite schist
(2) Staurolite-biotite schist
(3) Garnet-grunerite schist
(4) Garnet-chlorite schist
(5) Chlorite-rich rock

TABLE 8-4. Re-calculation of analyses 1, 2 and 3 of
table 8-3 (with silica added).

	(1)	(2)	(3)
silica added	80gm	70gm	50gm
SiO_2	61.7	61.3	61.8
Al_2O_3	13.6	20.3	7.5
Fe as FeO	12.5	9.9	22.9
MnO	1.5	0.6	0.3
MgO	3.7	1.9	2.2
CaO	0.2	–	0.4
Na_2O	0.5	0.1	0.16
K_2O	2.4	1.1	0.06
	96.1	95.2	95.32

61.5% (i.e. around that of the unaltered micaceous schists)
is shown in the second column in table 8-4. Comparison of
the recalculated analyses in table 8-4 with the unaltered
schists (2, 3 and 4 in table 8-1) shows a number of large
residual differences. Although there is a sampling problem
in a comparison of this type the indications are that simple
silica extraction does not explain the chemical evolution of
the alteration zones. Therefore it is tentatively concluded
that there has been significant introduction of components
like alumina and iron into these zones.

In the chloritized alteration zone assemblages (4 and
5 in table 8-3) there are further changes in chemistry although
some of these changes may only be apparent. For instance,
most of the chlorite is a breakdown product of biotite and
in the assemblages 1,2, 4 and 5 in table 8-3 the MgO contents
are fairly closely related to the respective combined chlorite
plus biotite contents. Thus it is not necessary to postulate
any significant introduction of magnesia during chloritization.
The same could probably be said of iron but the presence of
iron-bearing minerals in addition to biotite and chlorite
somewhat disguises the relationships. The most common biotite/
chlorite intergrowth in the rocks around the Kanmantoo orebody
indicates a volume by volume replacement of the former by
the latter. Chlorite contains about 11% H_2O and virtually
no potash whereas biotite contains about 3% H_2O and between
8-11% K_2O. Assuming the densities remain similar, the only
major chemical changes required to transform biotite to chlorite
are an addition of water and liberation of potash or, more
correctly, an addition of H^+ and release of K^+ (and Na^+).
It is possible that the alkalis so released eventually migrated
into joints and fractures to form vein feldspar.

B. SOME MAJOR, MINOR and TRACE ELEMENT VARIATIONS IN THE
    ENCLOSING SCHISTS

1. Sampling and Analytical Procedure

    A geochemical programme on core from selected diamond

drill holes was carried out on behalf of the writer by Mines
Exploration Pty Ltd. In order to gain the maximum useful
information from such work drill holes chosen were those that
as far as possible (a) passed through a number of schist
types, (b) showed no significant supergene alteration or
post-drilling weathering, and (c) passed through or close to
the orebody. No single drill hole complied with all such
conditions but the three holes selected, as a group, did;
these were nos. 5, 31, and 29 on cross-section 1250, 1200
and 1050 N respectively (map 4).

The drill core was split longitudinally and sampled
mainly in continuous 50 foot sections outside the mineralized
zones and in 10 foot sections within the mineralized zones.
iron and titanium were determined colorinetrically, sulphur
by roasting, copper, zinc, lead, cobalt, nickel, silver,
cadmium and chromium by A.A.S. and vanadium by emission
spectroscopy. The accuracies of all analyses are considered
to be within the limits of $\pm$ 5% (V $\pm$ 10%).

The geochemical results are shown in graphical form in
figs. 8-2,3,4. Two diagrams are given for each diamond drill
hole; one shows the variations in Fe, S and Cu and a sketch
of the cross-section geology while the other shows variations
in the important trace elements Co, Ni, Zn, Pb and Ag.
Different scales are used for the different elements depending
on their respective concentration ranges and, except for the
moving average curves and the silver distribution, the drill
hole positions are used as baselines for both the upright
and inverted histograms. Core was not available for analysis
where gaps are shown.

2. A possible Method for Interpreting Elemental Profiles

As an idealized model for interpretation consider the
two cases illustrated in fig. 8-1. The starting material in
each case is identical i.e. a volume of rock having a particu-
lar component evenly distributed through it. During meta-
morphism and deformation, a vein of material containing this
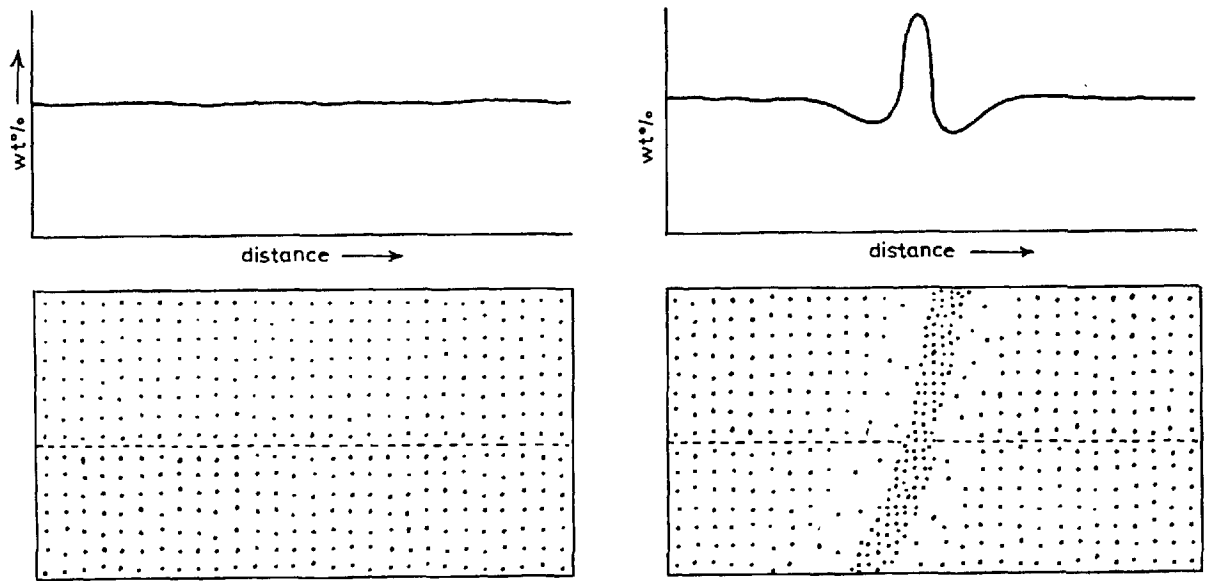
(a) Elemental profile across a vein formed by lateral secretion.
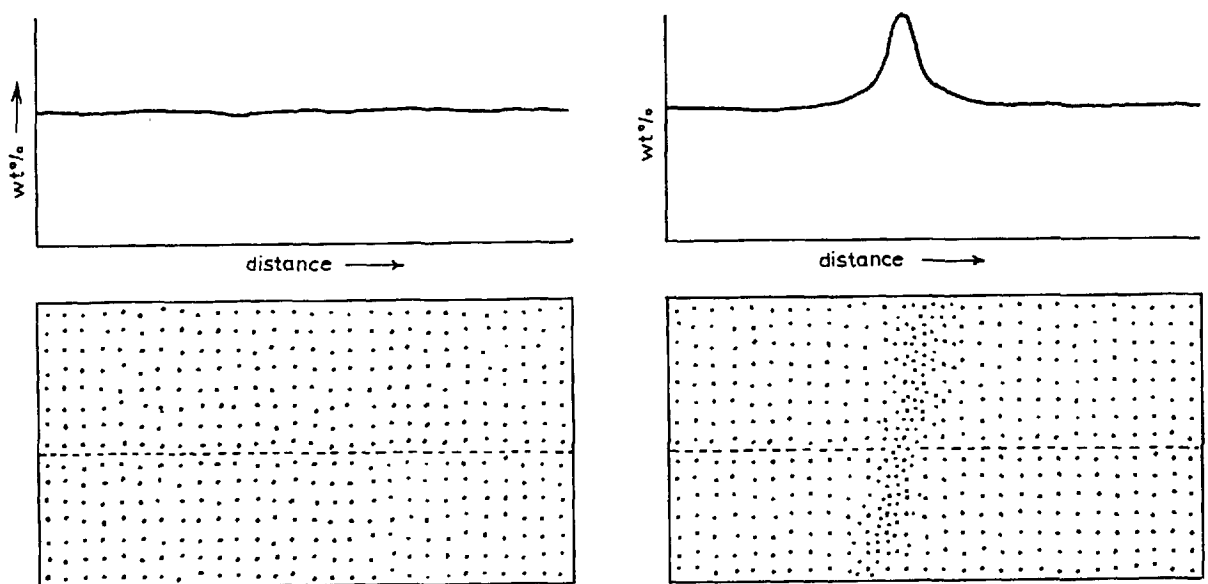
(b) Elemental profile across a vein formed from introduced material.

FIG. 8-1

component is formed along a structural surface. The problem
is to find evidence on where the vein components were derived.
In case (a) the component has migrated into the vein from the
immediate wall rock (lateral secretion) and the resulting
concentration profile of the component has two minima in the
positions shown. In case (b) the component has been introduced
and the resulting profile across the vein does not show any
minima. A hybrid vein formed partly through both processes
would contain more of the component in the vein than could be
accounted for in the depletion from the wall rocks. Serious
objections can be raised to such a model being applied to the
real situation particularly on a large scale. For instance
how can one distinguish between migrational changes and original
variations in the wall rocks and how does one recognise material
introduced from nearby from material introduced from a distant
source? A further complication is that migration of material
from large volumes of the wall rocks may be so complete as
to leave no sign of its former presence.

In the Kanmantoo orebody two important facts have
emerged from the structural and textural studies; these
are (1) much of the coarse-grained pyrrhotite and chalcopyrite
(or their high temperature parent phases) were present during
the growth of the surrounding metamorphic silicates, and (2)
the sulphide concentrations lie along tectonically developed
surfaces. Thus there seems little doubt that many of the ore
mineral components moved through the rocks during metamorphism.
The questions are what components and whence have they come?
There seem to be no easy answers to these questions nor solutions
to the problems outlined above, but simultaneous concentration
profiles for a number of elements may give some indication of
the history of at least some of them.

3.Relationships Among the Elements

(a) Iron, Sulphur, Copper

Although there may be fairly sharp variations in iron
content over small zones particularly in the mineralized

areas, iron shows a progressive increase from the quartz-mica schists through the andalusite-staurolite schists to the lode schists. This is to be expected from the analyses given in Table 8-1.

Disseminated sulphides are rather sparse through much of the quartz-mica schists thus sulphur is consistently low except in areas containing a few thin galena-sphalerite veinlets. Through the andalusite-staurolite schists and parts of the lode schists disseminated sulphides are fairly regularly dispersed as is evident from the small but consistent sulphur contents in these rocks. Along the 150 foot moving average S curve in drill hole no. 5 (fig. 8-2) there is an interesting minimum on the lower side of one of the mineralized zones that is similar to the concentration profile of case (a) in fig. 8-1. Thus there is the suggestion that some of the sulphur in the ore zones may have been derived from the surrounding rocks.

Chalcopyrite, which is virtually the only copper mineral in the Kanmantoo orebody, contains very nearly equal proportions by weight of Cu and S. An examination of the Cu and S variations along the three drill holes shows that outside the ore zones sulphur is present largely as an iron sulphide. In the ore zones the iron sulphide content of the rock tends to fall sharply as can be estimated by the difference in heights of the corresponding S and Cu histograms.

(b) Cobalt and Nickel

Both Co and Ni contents are low in the sulphur-poor quartz-mica schists but Co increases fairly regularly with S in the other rocks. Ni also increases with S but not to the same extent as Co thus the Co:Ni ratio tends to increase with increasing S. Clearly the moving average curve for Co in hole 5 is similar to that of S but very dissimilar to Cu.

(c) Zinc and Lead

Sphalerite is a persistent minor phase in the fine-grained disseminated mineralization thus Zn values run at
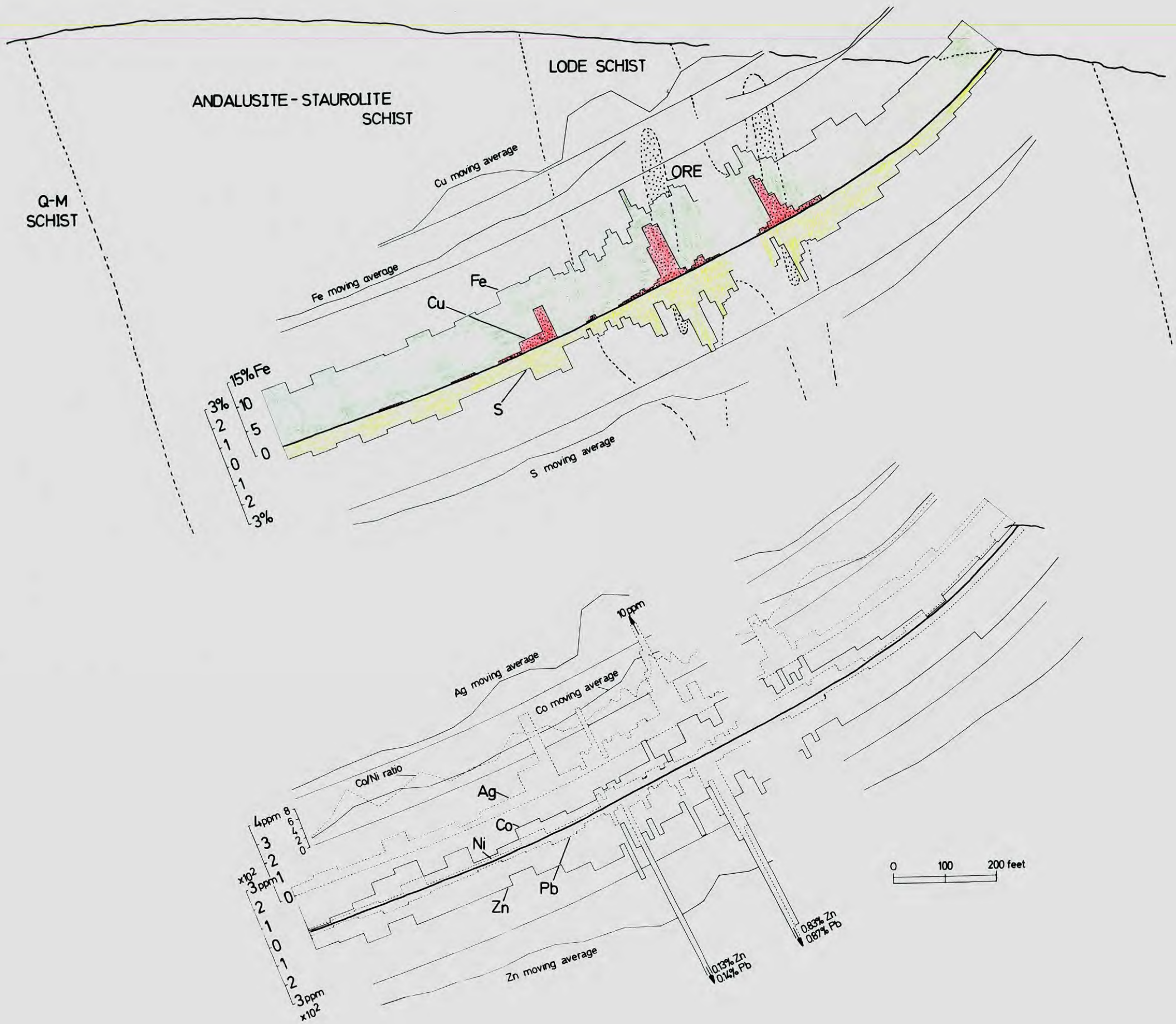
FIG. 8-2. GEOCHEMICAL PROFILE ALONG HOLE 5, SECTION 1250N

ANDALUSITE - STAUROLITE SCHIST

ORE ZONE

LODE SCHIST

QUARTZ - MICA SCHIST

Q-M SCHIST

Copper

Iron

Sulphur

Silver

Cobalt

Nickel

Zinc

Lead

0   100   200   300   400   500 feet

FIG. 8-3. GEOCHEMICAL PROFILE ALONG HOLE 31, SECTION 1200N

ANDALUSITE-STAUROLITE SCHIST

LODE SCHIST

QUARTZ-MICA SCHIST

Fe

Cu

ORE

15% Fe
10
2% 5
1 0
0
1
2
3%

12ppm Ag

Ag

Co

Ni

2ppm
1
0
200
100ppm
0
100
200
300
400 ppm

Pb

Zn

S

0.22% Zn

0.12% Zn

0.72% Zn
0.85% Pb

0   100   200 feet
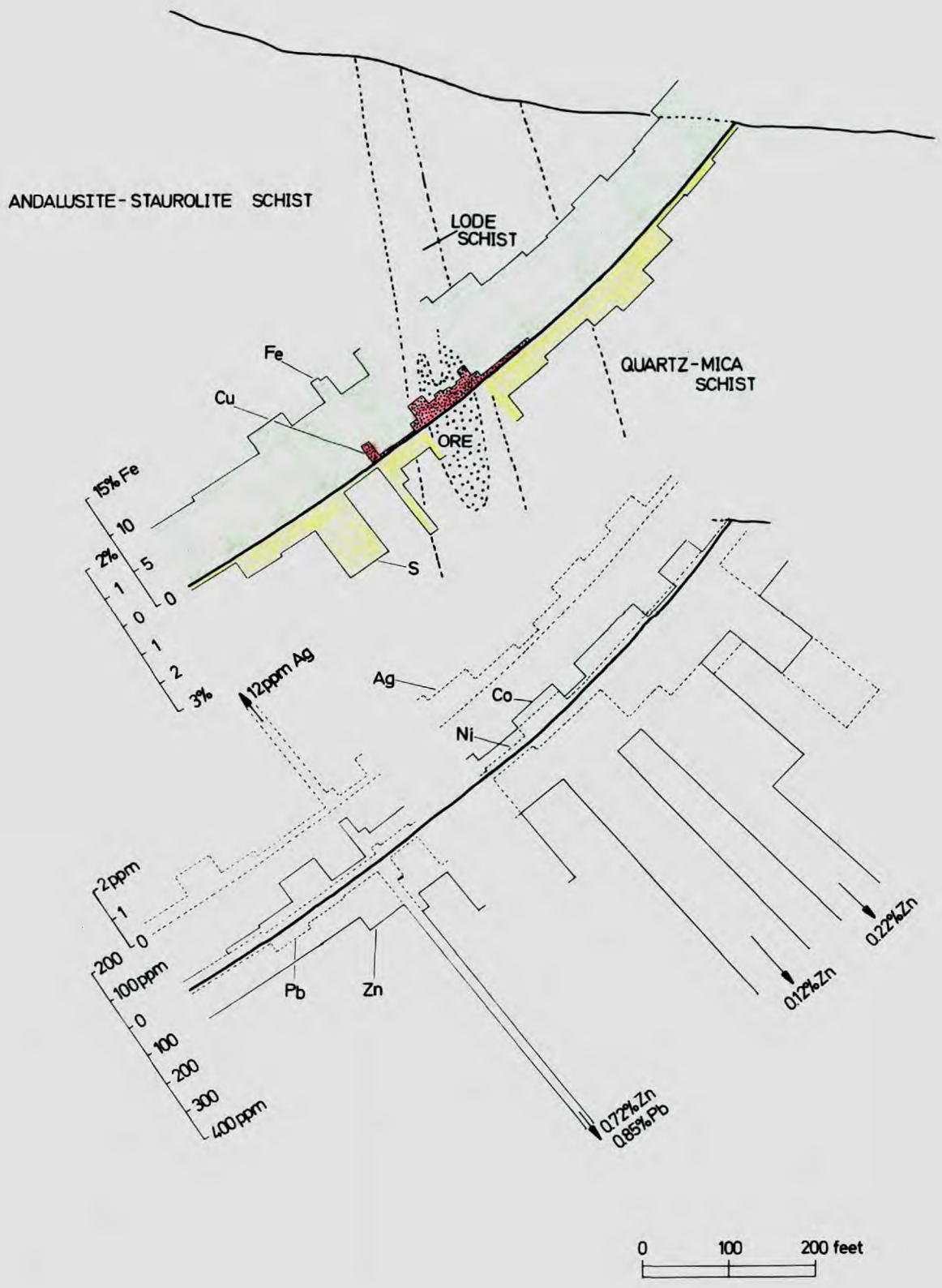
FIG. 8-4.   GEOCHEMICAL PROFILE ALONG HOLE 29, SECTION 1050N

high trace levels through the andalusite-staurolite schists and
lode schists. Galena is relatively uncommon thus Pb is low. In
the mineralized zones and in parts of the quartz-mica schists
there are a few thin veinlets of coarse-grained galena-
sphalerite along the schistosity surfaces; these produce the
locally high Zn and Pb values. The broad zones of high Zn
and Pb in the upper parts of drill holes 31 and 29 are some-
what misleading since at these positions the drill holes cut
across the schistosity and the enclosing veins at rather acute
angles.

Zn and Pb tend to vary sympathetically with each other
and Zn is generally greatly dominant over Pb except in areas
containing the sphalerite-galena veinlets. Both metals
appear to vary rather independently of all the other metals
except for silver.

(d) Silver

Although silver tends to increase with both increasing
Pb(+Zn) and increasing sulphur, it is partly sympathetic with
Cu variations as well. No silver minerals have been recognised
in the mineralization therefore it is thought that the small
amounts of Ag are in solid solution partly in galena and
partly in chalcopyrite.

(c) Other Metals

Other metals analysed for but not shown graphically
are titanium, cadmium, chromium, and vanadium. Ti shows
little departure in the different rock-types from an average
around 0.38% (see table 8-5a). Cd is everywhere less than
3 ppm except in zones of high Pb and Zn values where it reaches
30 ppm, Cr is present to the extent of only 20 to 30 ppm
and V is mostly in the range 50 to 70 ppm.

4. Origin of the Disseminated Mineralization

It has been shown in previous chapters that the fabric
of the fine-grained sulphide grains is identical to that of
the metamorphic matrix silicates with which they are intergrown

i.e. the grains are flattened in the schistosity plane and
elongated along the lineation direction. The conclusion
that the sulphides have been present from the earliest
recognisable stages of metamorphism is further supported by
the time implications of the intergrowths between the sulphide
minerals and the silicate porphyroblasts.

In the field, disseminated sulphide bearing schists
are seen to form both thick and thin units conformable with
what has been deduced as bedding, and it has been demonstrated
that this conformability persist down to a very small scale.
It seems likely therefore that the sulphur, the minor amounts of
Cu and Zn and the traces of Co, Ni and Pb that make up the
disseminated mineralization were present in the original
sediments. That the average metal contents of the quartz-
mica and andalusite-staurolite schists (table 8-5a) are
more or less typical of pelitic rocks is shown by a comparison
with the average metal contents of some unmetamorphosed
sediments (a and b in table 8-5b). Cu is not shown in table
8-5a because in most samples amounts less than 200 ppm were
reported as such. A number of earlier analyses made on schists
outside the ore zones gave copper values of around 50 ppm which
is similar to the average Cu content of black shales (Vine,
1966). Whether any of the original sediments were of the
sapropelic type (c and d in table 8-5b) is not known since
neither organic matter nor graphite has been detected. Indirect
evidence that the organic matter content was originally low is
the low vanadium content; there is a marked enrichment of
this metal in shales containing only a moderate amount of
organic matter (Marmo, 1960). Both Zn and Pb values appear
to be rather high in the quartz-mica schists and suggest
perhaps that some of the sphalerite and galena in the veinlets
has been introduced from beyond the vein environments.

A possible indication that not all the disseminated
mineralization is of sedimentary origin is seen in the different
Co:Ni ratios of the quartz-mica and andalusite-staurolite
schists. The Co:Ni ratios of minerals and rocks have been used

TABLE 8-5a. Average concentrations and standard deviations of some elements in the three major schist units surrounding the Kanmantoo orebody.

	quartz-mica schists		andalusite-staurolite schists		lode schists and ore zones	
	avg.	S.D.	avg.	S.D.	avg.	S.D.
Fe wt%	5.1	1.3	9.2	1.8	13.4	2.2
S	0.24	0.2	0.71	0.58	1.58	0.87
Ti	0.39	0.04	0.38	0.06	0.37	0.05
Co ppm	21	9	77	54	131	46
Ni	24	8	34	17	57	18
Zn	363	422	141	49	214	73
Pb	113	139	20	15	60	72
Ag	0.4	0.3	0.5	0.5	1.2	0.8
Cd	<3	-	<3	-	<3	-
Cr	31	14	21	2.5	20	2
V	65	17	62	14	61	12
Co/Ni	0.87		2.3		2.3	
Co/S x 10^6	0.9		1.1		0.9	
Ni/S x 10^6	1.0		0.58		0.37	
Zn/S x 10^6	15.0		2.0		1.4	

TABLE 8-5b. Average abundances of metals in some sediments and schists derived from sapropelic muds.

	(a)	(b)	(c)	(d)
	Shale	deep-sea clay	black schists	sulphide schists
Ti wt%	0.46	0.46	0.36	0.05-0.4
Co ppm	19	74	150	0-150
Ni	68	225	400	200-900
Zn	95	165	300	500-1800
Pb	20	80	50	0-500
Ag	0.07	0.11	2	1-7
Cd	-	-	-	trace
Cr	90	90	4600	100-200
V	130	120	500	0-1500
Co/Ni	0.28	0.33	0.37	-

a, b from Turekian and Wedepohl (1961)
c from Peltola (1960)
d from Marmo (1960)

as a possible indicator of metallogenesis by Davidson (1962)
and Loftus-Hills and Solomon (1967). The premise is that
Co:Ni ratios in practically all sediments of all ages are less
than unity and usually considerably so; in the primary i.e.
magmatic environment, Co is found in excess of Ni commonly
only in late stage acid plutonic rocks. Thus sulphides or
sulphides in rocks having low Co:Ni ratios are postulated to
be of sedimentary origin whereas those having high ratios have
probably been formed epigenetically from introduced hydrothermal
solutions given off by acidic magmas. By well reasoned
arguments on this basis Davidson (op cit) attempted to show
that the copper in the deposits of the Zambian copper belt
is of hydrothermal-epigenetic origin. But the overwhelming
stratigraphic evidence that these ores are of sedimentary
origin e.g. Garlick (1967) suggests that the application of
Co:Ni ratios genesis problems must be treated with considerable
caution. Thus it is difficult to draw any conclusions on the
genetic significance of the Co:Ni ratios of the Kanmantoo
mineralization.

5. Formation of the Ore Zones

The ore zones are characterised by coarse-grained
pyrrhotite-chalcopyrite-magnetite mineralization and the
presence of small amounts of bismuth, molybdenum and gold
that are not found in the disseminated mineralization. There
is no evidence that any of the coarse-grained ore was present
in the alteration zones prior to the cessation of the B_1b
tectonic phase but textural relationships show that some of the
oxides and sulphides had formed, been deformed and had partially
recrystallized prior to the crystallization of many of the
silicates in these zones. In general however, the very complex
sulphide-silicate-oxide intergrowths indicate a prolonged
period of growth of all phases. Whether there was a continuous
introduction of sulphide components during this time or
simply a re-arrangement of pre-existing material is difficult
to ascertain from textural studies.

In the disseminated mineralization which is concluded
to be of sedimentary origin, pyrrhotite is the dominant
sulphide phase while both chalcopyrite and sphalerite are
minor and present in about equal amounts. Trace amounts of
Ni occur mainly as pentlandite laths in pyrrhotite whereas most
of the Co is apparently concentrated in mackinawite laths that
are spatially related more to chalcopyrite than pyrrhotite.
Thus it seems likely that at the elevated temperatures of
metamorphism most of the disseminated sulphide grains were
made up of two phases; a major pyrrhotite phase containing
most of the Ni and a minor Cu-Fe-Zn sulphide phase containing
most of the Co. It has been suggested that the sulphur in the
ore zones may have been derived from the wall rocks and a
glance at the S profile of drill hole no. 5 in fig. 8-2
shows that this is highly feasible. If then the sulphide
concentrations along the dilational alteration zones were
formed by the bulk migration and segration of disseminated
material from the wall-rocks during metamorphism, the Co:S,
Zn:S and Cu:S ratios in both types of mineralization would be
expected to be similar. Only the andalusite-staurolite and
lode schists will be considered in such a comparison since
the quartz-mica schists contain very little disseminated
mineralization and lie well outside the ore zones. The Co:S
ratios are nearly identical (table 8-5a) but the Ni:S ratios
are not so close. The differences nevertheless are not so
great as to dismiss such a migrational hypothesis as unlikely.
Zn:S ratios are not very close but the chemical relationships
are probably complicated by some of the sphalerite-galena
veinlets forming independently of and possibly subsequent to
the copper sulphide ore zones. Although no figures can be
given, the Cu:S ratios (and consequently the Cu:Co ratios)
of the two types of mineralization are enormously different
(fig. 8-2); this suggests that the depositional histories of
the S and most of the Cu in the ore zones have not been parallel.

The alteration zones in which the ore has formed must
have been subjected to considerable hydrous activity as
witness the large grain size of the minerals (water promotes

the diffusion of atoms on surfaces and along interfaces thereby
accelerating rates of crystal growth), primary fluid inclusions
in many silicates, and the large proportion of hydrous phases
like biotite, staurolite and grunerite. It seems likely that
such fluids were hydrous products of metamorphic dehydration
reactions and that they were locked in grain boundaries until
induced to migrate along pressure gradients into low-pressure
zones. If it were assumed that small amounts of copper and
perhaps zinc were also released from silicate lattices during
metamorphic reactions and were able to be transported in this
migrating intergranular fluid as chlorides, then the arrival of
such fluids in pyrrhotite-bearing alteration zones may have
caused reactions of the type:

$$2FeS + Cu^{++} \longrightarrow CuFeS_2 + Fe^{++}$$

$$3FeS + Cu^{++} \longrightarrow CuFe_2S_3 + Fe^{++}$$

$$FeS + Zn^{++} \longrightarrow ZnS + Fe^{++}$$
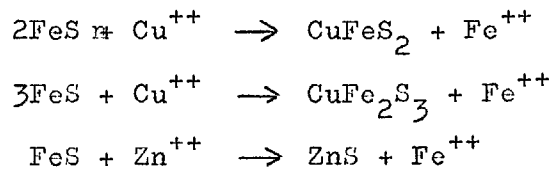
It is possible that the present ore zones were originally
quartz-rich siliceous veins containing a significant amount
of pyrrhotite-rich sulphide mineralization derived from the
country rocks in the same manner as the silicate components.
Much of the iron released from the pyrrhotite may then have
combined with components like silica, alumina, potash and
water in the vein environment to form garnet, biotite,
magnetite, staurolite and other ferriferous silicates. In
areas free of disseminated sulphides, no pyrrhotite would
form in the siliceous veins therefore there would be no way
of precipitating the copper ions introduced in the hydrous
fluids.

This hypothesis envisages two separate though probably
contemporaneous processes both of which were necessary for
the formation of concentrations of copper sulphides. Initially
there was the diffusion of disseminated sulphides from the
country rocks into low-pressure dilational zones between or
after the two major fold-forming tectonic phases. The

resulting pyrrhotite concentrations then acted as chemical traps for copper ions introduced via an intergranular hydrous phase that migrated into the same zones. Important facts that support such a mechanism are (1) the reduction in the proportion of iron-sulphide to sulphur but the increase in iron oxides and ferriferous silicates from the unaltered weakly mineralized country schists to the ore zones, (2) the fairly close abundance relationships among Ni, Co and S in both the country schists and the ore zones, (3) the intimate spatial and time relationships among the coarse-grained sulphides, oxides and ferriferous silicates in the ore zones, and (4) the paucity of free silica in the ore-bearing altera-tion zones. Similar mechanisms for the concentration of base-metals have been proposed for deposits in the Bathhurst District (N.S.W.) by Stanton (1955), in the Yanahara District of Japan by Higashimoto (1960) and for the copper in the Zambian Copper Belt by Davidson (1962). All these writers envisage metal-laden fluids migrating through the rocks during metamorphism and reacting with in situ, bedded syngenetic pyrite.

chapter 9

CONCLUSIONS

Opening Statement

Examination of all the field and laboratory evidence
leads to the following conclusions on the geological history
and localization of the ore, and on guides to further ore
concentrations in the Kanmantoo Group and similar geological
environments.

A. DEPOSITIONAL ENVIRONMENT OF THE SCHISTS

1. Sprigg and Campana (1953) considered the sedimentary facies
in the Kanmantoo Group to be comparable with the Alpine Flysch.
According to Pettijohn (1957) flysch-type environments are
marked by great thicknesses of greywackes and regularly inter-
bedded silts and shales, the last sometimes carbonaceous.
Carbonate rocks are scarce. Cross-bedding and ripple marks
are uncommon but slump structures and graded bedding are
widespread. The coarser sediments accumulated rapidly in
comparatively deep water and the shales represent periods of
quiet deposition.

2. The schists enclosing the Kanmantoo orebody are all
argillaceous in character and are part of a thick sequence of
greywacke-shale type lithologies that display typical flysch
characteristics. Well developed lithological banding in all
the schists is concluded in the main to represent bedding.
Iron sulphides disseminated through most of the aluminous and
ferruginous micaceous schists, and a lack of graphite, suggest
that the shales were deposited in a reducing environment.

3. Of the three common types of reducing environments -
a euxinic or restricted basin type, a stagnant depression in
the open sea, and a lagoonal or estuarine type - the last is
the least likely. The narrow elongated form of the Kanmantoo
Trough, the certainty of land to the west and the probability

of land to the east suggest that a restricted basin type
environment prevailed.

4. The contribution of contemporary volcanism to the sediments
and metals in the Kanmantoo Trough is unknown. No volcanic
rocks have been found or proved anywhere in the sequence.

B. METAMORPHISM AND DEFORMATION OF THE ENCLOSING ROCKS

1. The main structural features in the area are dominated by
folding that was produced by two major tectonic phases during
an Ordovician orogeny. These two phases, termed B_1a and B_1b,
produced folds having similar profiles and axial surface
attitudes. In this respect they are essentially sub-phases
of a single major phase (B_1). Evidence from deformed concretion-
like bodies in the aluminous schists indicates that the
schistosity surface, formed during deformation and accompanying
metamorphism, represents a plane of flattening, and that the
mineral lineations on the schistosity surface are parallel to
the direction of extension or flow of the rocks.

2. By the end of the B_1a phase most of the shales had been
transformed into phyllites or slates and soon afterwards great
volumes of alumina, silica and iron began crystallizing as
andalusite and almanditic garnet.

3. In the interval between the B_1a and B_1b tectonic phases
when the compressive forces responsible for deformation and
folding were relaxed, small dilational stresses acted normal
to the schistosity surfaces. The pressure gradients induced
in the rocks by such stresses promoted diffusion of the more
mobile rock components towards the low pressure sites. As a
result there were formed parallel to the schistosity surfaces
a great many lenticular, segregation quartz veins containing
small amounts of other metamorphic silicates. Renewed
compression normal to the schistosity during the B_1b tectonic
phase set up tensile stresses along these veins which stretched
by a process of necking.

4. By the end of the B_1b tectonic phase most of the argilla-
ceous rocks had recrystallized into medium-grained micaceous
schists containing varying amounts and proportions of garnet,
andalusite and staurolite porphyroblasts. Argillaceous rocks
near the arenaceous units are much finer grained and have
responded much less to metamorphism. In the arenaceous rocks
themselves only the clay fraction has crystallized into meta-
morphic minerals. The detrital quartz and feldspar are evi
evidently relatively unchanged.

5. The relaxation of compressive forces following the B_1b
tectonic phase allowed small dilational stresses again to
act normal to the schistosity surfaces. This prolonged period
of small dilational movements is termed the B_2 tectonic phase.
Siliceous veins probably continued to form through most of the
rocks but in the ferruginous and aluminous schists, hydrous
activity along the dilational zones caused the crystallization
and growth of garnet, biotite, muscovite and staurolite to
sizes considerably greater than those in the adjacent schists.
These zones have been termed the alteration zones. The
appearance of sillimanite in such zones indicates that early
in the B_2 tectonic phase the peak metamorphic temperature of
about $675^{\circ}C$ was reached.

6. As the temperature decreased, continual dilational move-
ments and accompanying hydrous activity along these alteration
zones caused much of the biotite and small amounts of garnet
and muscovite to break down to chlorite. Large volumes of
former garnet-biotite rocks were transformed into garnet
chlorite rocks. It is thought that late in the chloritization
stage some of the alkalis released from the biotite migrated
into joint planes and fractures and crystallized as albite
and adularia.

7. Small tectonic movements, perhaps late in the B_2 phase,
caused local kinking, crenulation and shearing of the schisto-
sity planes. Much later in the Tertiary, regional block
faulting movements caused minor faulting, brecciation, and
fracturing of the schists around the Kanmantoo orebody.

C. INVOLVEMENT OF ORE MINERALS IN THE METAMORPHIC-TECTONIC HISTORY

1. The fabric and shapes of the disseminated sulphide grains are identical to those of the matrix silicates in both the fine-grained and coarse-grained schists. In addition, a number of silicate porphyroblasts have trapped sulphide as well as oxide and silicate inclusions during growth. Thus the disseminated mineralization has been present in the schists from the earliest recognisable stage of metamorphism.

2. All the coarse-grained chalcopyrite-pyrrhotite-magnetite mineralization is located along or in schists adjacent to the post-B_1b alteration zones. Textural studies show that much of the sulphide-oxide mineralization was present before the growth of many of the coarse-grained silicate grains but generally, the very complex sulphide-oxide-silicate intergrowths indicate a long period of growth of all phases that lasted through the temperature peak of metamorphism. There is no textural evidence that any of this ore was in its present location prior to the cessation of the B_1b tectonic phase.

3. Although the chemical environment in the alteration zones during the crystallization of the ore minerals was probably extremely complex and varied both in time and space, attempts to resolve the ore mineral assemblages with the inferred metamorphic temperatures, the deduced values of oxygen and sulphur fugacities and the expected mineralogical changes on cooling have nevertheless been partially successful. The present ore mineral assemblage is dominantly hexagonal pyrrhotite + monoclinic pyrrhotite + chalcopyrite + magnetite. Between about $330°C$ and $550°C$ the assemblage was probably hexagonal pyrrhotite + cubanite solid solution + magnetite while above $550°C$ it was pyrrhotite + chalcopyrite solid solution + magnetite. A number of minor metals in the ore were in solid solution with the major minerals at these elevated temperatures and formed discrete mineral phases only during cooling. Most of the nickel was in the pyrrhotite (pentlandite), cobalt partly in the pyrrhotite and partly in

the copper sulphide phase (cobalt-pentlandite and cobaltian mackinawite), zinc in the copper sulphide phase (sphalerite) and aluminium and titanium in magnetite (hercynite and ilmenite).

4. During later deformations and the accompanying chloriti-zation of silicates along the alteration zones, a little magnetite was altered to chlorite but the sulphide phases appeared to have suffered mainly local solution and redeposi-tion. Probably the sulphides underwent some localized plastic deformation and recrystallization as well but if we are to believe the results of some recent heating experiments on sulphide aggregates, internal strain effects from these deformational events should not be visible today. The undulose extinction commonly observed in pyrrhotite must therefore be attributed to a very late, low-temperature deformation.

5. Probably early in Tertiary times ground waters of meteoric origin circulating through small fractures and joints caused a significant proportion of the pyrrhotite to break down to concentric, possibly originally colloidal, aggregates of pyrite and marcasite. A lateritic peneplain formed over a large part of the eastern regions of the Mt Lofty Ranges in later Tertiary times, had the effect of restricting the downward percolation of surface waters through the Kanmantoo orebody. Thus the oxidation of the ore is restricted to about the upper 100 feet and secondary copper enrichment is generally weak.

D. ORIGIN OF THE ORE CONSTITUENTS

1. The fine-grained disseminated sulphide mineralization through the aluminous and ferruginous schists appears to be conformable to the bedding on all scales. The iron, sulphur and small amounts of base metals that constitute this minerali-zation are therefore considered to have been present in the original sediments. This conclusion is in agreement with most of the other workers who have studied disseminated sulphide horizons in the Kanmantoo Group.

2. All the coarse-grained ore is located along or near the tectonically controlled alteration zones and both structural and textural evidence suggests that the ore minerals were introduced into these positions after the B_1b tectonic phase.

3. The similarities in the Co:S and Ni:S ratios of the disseminated mineralization and the coarse-grained ore, combined with the implications of some of the elemental profiles through the ore zones, have led to the conclusion that the initial sulphide concentrations along the alteration zones were possibly rich in pyrrhotite and poor in chalcopyrite, and were formed by bulk migration of disseminated sulphides from the surrounding schists. Although the cause of this migration was probably tectonically induced pressure gradients operative both before and after the B_1b phase, the exact mechanism of sulphide migration is unknown. Three possibilities can be envisaged: (a) the sulphides moved in the solid state along grain boundaries by simultaneous deformation and recrystallization, (b) they moved by molecular, atomic or ionic diffusion through silicate lattices or along silicate grain boundaries, and (c) they moved as dissolved ions or ionic complexes in an intergranular hydrous fluid along the silicate grain boundaries.

4. The enormous contrast in the Cu:S ratios of the two types of mineralization has led to the further, albeit tentative, conclusion that most of the copper was introduced later, not as a sulphide, but possibly as a chloride dissolved in the metamorphic fluids that travelled probably considerable distances through rock before entering the alteration zones. A reaction between these copper ions and the pre-existing pyrrhotite produced chalcopyrite or cubanite, and the iron released from the pyrrhotite combined with other components and crystallized as magnetite, garnet and various iron-rich hydrous silicate minerals.

5. The origin of this copper is unknown but it could conceivably have been leached from large volumes of the geosynclinal rocks by migrating metamorphic fluids or else released into the intergranular phase from silicate minerals undergoing recrystallization or replacement reactions.

E. GUIDES TO FURTHER ORE

Based on the theory that the copper sulphide minerals
in the Kanmantoo orebody have accumulated through a reaction
between dissolved copper ions in migrating metamorphogenic
hydrous fluids and pre-existing pyrrhotite-rich
sulphide concentrations in dilational zones parallel to the
tectonic foliation, the following geological features are
important in searching for similar orebodies. These apply
both to the Kanmantoo Group as a whole and to similar litholo-
gical and metamorphosed regions.

1. Areas with schists containing disseminated iron sulphides
are the most favourable.

2. Within such areas, zones parallel to the tectonic foliation
containing coarse-grained iron-rich silicates like garnet,
staurolite, biotite and amphibole. Chloritization appears to
be only incidental to ore development but zones of intense
chloritization point to both metasomatic activity and the
former presence of concentrations of iron-rich or iron/
magnesium-rich silicates.

3. Extensive development of quartz or other metamorphic,
silicate veins parallel to the tectonic foliation. These
point to a dilational deformation phase in the geological
history favourable for concentrating disseminated sulphides
and for localizing migrating metamorphic fluids.

4. Pyrrhotite and/or magnetite concentrations along tectonic
zones. These are obviously important and may be detected by
magnetic means.

References

Althaus, E.,1967. The triple point andalusite-sillimanite-kyanite. Contr . Mineral. and Petrol., 16, pp. 29-44.

Althaus, E., 1968. Der Einfluss des Wassers auf metamorphe Mineralreaktionen. N. Jb. Mineral., pp. 289-306.

Amstutz, G.C., 1960. Some basic concepts and thoughts on the Space-time analysis of rocks and mineral deposits in orogenic belts. Geol. Rdsch., 50, pp. 165-185.

Arnold, R.G., 1962. Equilibrium relations between pyrrhotite and pyrite from 325° - $743^{\circ}C$. Econ. Geol. 57, pp. 72-90.

Arnold, R.G., and Reichen, L.E., 1962. Measurement of the metal content of naturally occurring, metal-deficient, hexagonal pyrrhotite by an X-ray spacing method. Am. Miner., 47, pp. 105-111.

Atherton, M.P., 1965. The chemical significance of isograds. (In) Controls of metamorphism (W.S. Pitcher and G.W. Flinn, eds). Oliver and Boyd, Edinburgh.

Atherton, M.P., and Edmunds, W.M., 1966. An electron microprobe study of some zoned garnets from metamorphic rocks. Earth and Plan. Sci. Ltrs., 1, pp. 185-193.

Barton, P.B., and Skinner, B.J., 1967. Sulphide mineral stabilities. (In) Geochemistry of hydrothermal ore deposits (H.L. Barnes, ed.). Holt, Rinehart and Winston, New York.

Barton, P.B., and Toulmin, P., 1966. Phase relations involving sphalerite in the Fe-Zn-S system. Econ. Geol., 61, pp. 815-849.

Bastin, E.S., 1931. Criteria of age relations of minerals with especial reference to polished sections. Econ. Geol., 26, pp. 561-610.

Bateman, A.M., 1950. Economic mineral deposits (2nd ed.) John Wiley and Sons, New York.

Berner, R.A., 1962. Tetragonal iron sulfide. Science, 137, p. 669.

Berner, R.A., 1964. Iron sulphides formed from aqueous solutions at low temperatures and pressures. J. Geol., 72, pp. 293-306.

Berner, R.A., 1967. Thermodynamic stability of sedimentary iron sulphides. Am. J. Sci., 265, pp. 773-785.

Berry, L.G., and Mason, B., 1959. Mineralogy. W.H. Freeman, San Francisco.

Billings, M.P., 1962. Structural geology. Prentice-Hall, New Jersey.

Boyd, F.R., 1959. Hydrothermal investigations of amphiboles. (In) Researches in Geochemistry (P.H. Abelson, ed.), John Wiley and Sons, New York, pp.377-396.

Brett, R., 1964. Experimental data from the system Cu-Fe-S and their bearing on exsolution textures in ores. Econ. Geol., 59, pp. 1241-1269.

Buddington, A.F., and Lindsley, D.H., 1964. Iron-titanium oxide minerals and synthetic equivalents. J. Petrology, 5, pp.310-357.

Buerger, M.J., 1928. The plastic deformation of ore minerals. Am. Miner., 13, pp. 1-17 and 35-51.

Burnham, C.W., 1962. Private Report. Carnegie Inst. Wash.

Buseck, P.R., 1968. Mackinawite, pentlandite and native copper from the Newport pallasite. Mineralog. Mag., 36, pp. 717-725.

Campana, B., 1954. The structure of the eastern South Australian ranges: The Mt. Lofty - Olary arc. J. Geol. Soc. Aust., 12, pp. 47-62.

Carey, S.W., 1962. Folding. Bull. Am. Assoc. Petrol. Geol., 10, pp. 95-144.

Carpenter, J.R., 1967. Apparent retrograde metamorphism: Another example of the influence of structural deformation on metamorphic differentiation. Contr. Mineral. and Petrol., 17, pp. 173-186.

Carstens, H., 1966. Exaggerated grain growth in the metamorphism of monomineralic rocks. Norsk. Geol. Tidsskr., 46, pp. 353-358.

Chayes, F., 1955. Potash feldspar as a by-product of the biotite-chlorite transformation. J. Geol., 53, p. 75.

Chinner, G.A., 1961. The origin of sillimanite in Glen Clova, Angus. J. Petrology, 2, pp. 312-323.

Chowdhury, M.K.R., and Das Gupta, S.P., 1965. Ore localization in the Khetri copper belt, Rajasthan, India. Econ. Geol., 60, pp. 69-89.

Clark, A.H., 1966a. Stability field of monoclinic pyrrhotite. Inst. Min. Metall., 75, pp. 232-235.

Clark, A.H., 1966b. Some comments on the composition and
          stability relations of mackinawite. N. Jb. Miner.
          Mh., 10, pp.300-304.

Clark, A.H., 1967. Mackinawite from the Lizard, Cornwall.
          Mineralog. Mag., 36, pp. 614-615.

Clark, S.P., Robertson, E.C., and Birch, F., 1957.
          Experimental determination of kyanite-sillimanite
          equilibrium relations at high temperatures and
          pressures. Am. J. Sci., 255, pp. 628-640.

Cloos, E., 1946. Lineations. Geol. Soc. Am., Mem. 18.

Clough, C.T., and Hill, J.B., 1887. The geology of Cowal.
          Mem. Geol. Surv. Scotland.

Craig, J.R., Naldrett, A.J., and Kullerud, G., 1967.
          Succession of mineral assemblages in pyrrhotite-
          rich Ni-Cu ores. Carnegie Inst. Wash. Yb., 66,
          pp. 431-434.

Crook, T., 1933. History of the theory of ore deposits.
          Thomas Murby, London.

Dahl, O., 1968. Hydrothermal studies of garnet-mica equilibria
          in the system $3(FeO, MnO)-2Al_2O_3-12SiO_2-K_2O-H_2O$.
          Geol. Foren. Stockh. Forf., 90, pp. 331-348.

Daily, B., 1963. The fossiliferous Cambrian succession on
          Fleurieu Peninsular, South Australia. Records of
          the S. Aust. Museum, 14, pp.579-601.

Davidson, C.F., 1962. On the cobalt:nickel ratio in ore
          deposits. Min. Mag., Lond., 106, pp. 78-85.

Davies, D.K., 1966. Sedimentary structures and sub-facies
          of a Mississippi river point delta. J. Geol., 74,
          pp. 234-239.

Davis, G.R., 1954. The origin of the Roan Antelope copper
          deposit of Northern Rhodesia. Econ. Geol., 49,
          pp. 575-615.

Desborough, G.A., and Carpenter, R.H., 1965. Phase relations
          of pyrrhotite. Econ. Geol., 60, pp. 1431-1450.

Desch, C.H., 1919. The solidification of metals from the
          solid state. J. Inst. Metals, 22, pp. 241-263.

Dickinson, S.B., 1942. The copper deposits of the Callington-
          Kanmantoo district. (In) The structural control of
          ore deposition in some South Australian copper
          fields. Geol. surv. S. Aust., Bull. 20, pp. 79-99.

Edwards, A.B., 1954. Textures of the ore minerals and their significance. Aust. Inst. Min. Met., Melbourne.

Emmons, W.H., 1909. Some regionally metamorphosed ore deposits and so-called segregated veins. Econ. Geol., 4, pp. 755-781.

Ernst, W.G., 1966. Synthesis and stability relations of ferrotremolite. Am. J. Sci., 264, pp. 37-65.

Evans, B.W., 1965. Application of a reaction-rate method to the breakdown equilibrium of muscovite and muscovite plus quartz. Am. J. Sci., 263, pp. 647-667.

Evans, H.T., and Allman, R., 1967. Crystal chemistry of valleriite, a hybrid iron-copper sulphide, magnesium-aluminium hydroxide species. Program Ann. Meetings, Geol. Soc. Am., p. 61 (abstract).

Evans, H.T., Milton, C., Chao, E.C.T., Adler, I., Mead, C., Ingram, B., and Berner, R.A., 1964. Valleriite and the new iron sulphide, mackinawite. U.S. Geol. Surv. Prof. Paper, 475D, pp. 64-69.

Evernden, J.R., and Richards, J.R., 1962. Potassium-argon ages in Eastern Australia. J. Geol. Soc. Aust., 9, pp. 1-49.

Eugster, H.P., and Wones, D.R., 1962. Stability relations of the ferruginous biotite, annite. J. Petrology 3, pp. 83-125.

Ewer, W.E., 1967. Physico-chemical aspects of recrystallization. Mineral. Deposita, 2, pp. 221-227.

Flinn, D., 1965. Deformation in metamorphism. (In) Controls of metamorphism (W.S. Pitcher and G.W. Flinn, eds), Oliver and Boyd, Edinburgh.

Ganguly, J., and Newton, R.C., 1968. Thermal stability of chloritoid at high pressure and relatively high oxygen fugacity. J. Petrology, 9, pp. 444-466.

Garlick, W.G., 1967. Special features and sedimentary facies of stratiform sulphide deposits in arenites. (In) Sedimentary ores, ancient and modern (C.H. James, ed.), Proc. 15th Inter-Univ. congr., Univer. of Leicester.

George, R., 1966. Observations on the sedimentation and metamorphism of the Nairne pyrite deposit. Geol. Soc. Aust. specialists meeting; Mineragraphy and ore genesis, Adelaide.

Gilbert, M.C., Bell, P.M., and Richardson, S.W., 1968. The andalusite-sillimanite transition and the aluminium silicate triple point. Carnegie Inst. Wash. Yb., 67, pp. 135-137.

Grasso, R., and McManus, J.B., 1954. The geology of the
        Callington area. Unpublished B.Sc (Hons.). thesis,
        Univer. of Adelaide.

Gresens, R.l., 1967. Tectonic-hydrothermal pegmatites;
        1. The model. Contr. Mineral. and Petrol., 15,
        pp. 345-355.

Grühn, A., 1918. Kunstliche Zwillingsbildung des Magnetit.
        N. Jb. Mineral., pp. 99-112.

Han, Tsu-Ming., 1968. Ore mineral relations in the Cuyuna
        sulphide deposit, Minnesota. Mineral, Deposita,
        3, pp. 109-134.

Harris, A.L., and Rast., 1960. The evolution of quartz
        fabrics in the metamorphic rocks of Central Perthshire.
        Trans. Geol. Soc. Edinb., 18, pp.51-78.

Harte, B., and Henley, K.J., 1966. Occurrence of compositionally
        zoned almanditic garnets in regionally metamorphosed
        rocks. Nature, Lond., 210, pp. 689-692.

Higashimoto, S., 1960. Pyritic ore deposits of the Yanahara
        district, Japan. Jour. Sci. Hiroshima Univ., 3,
        pp. 25-68.

Hobbs, B.E., 1965. Structural analysis of the rocks between
        the Wyangala batholith and the Copperhannia thrust,
        New South Wales. J. Geol. Soc. Aust., 12, pp. 1-24.

Hobbs, B.E., and Talbot, J.L., 1966. The analysis of strain
        in deformed rocks. J. Geol., 74, pp. 500-513.

Holland, H.D., 1965. Some applications of thermochemical
        data to problems of ore deposits 11. Mineral
        assemblages and the composition of ore-forming
        fluids. Econ. Geol., 60, pp. 1101-1166.

Hollister, L.S., 1966. Garnet zoning: and interpretation
        based on the Rayleigh fractionation model. Science,
        154, pp. 1647-1650.

Hornstra, J., 1960. Dislocations, stacking faults and twins in
        the spinel structure. Jl. Phys. and Chem. Solids,
        15, pp. 311-323.

Horwitz, R.C., Thomson, B.P., and Webb, B.P., 1959. The
        Cambrian-Precambrian boundary in the eastern Mt.
        Lofty Ranges region, South Australia. Trans. Roy.
        Soc. S. Aust., 82, pp. 205-218.

Howard, P.F., 1959. Structure and rock alteration at the
        Elizabeth mine, Vermont. Pt.1, Econ. Geol., 54,
        pp.1214-1249. Pt.2, Econ. Geol., 54, pp. 1414-1443.

Hsu, L.G., 1968. Selected phase relationships in the system
Al-Mn-Fe-Si-O-H: A model for garnet equilibria.
J. Petrology, 9, pp. 40-83.

Johnson, M.R., 1963. Some time relations of movement and
metamorphism in the Scottish Highlands. Geologie
Mijnb., 42, pp. 121-142.

Johnson, W., 1965. Copper and lead deposits of South Australia.
(In) Geology of Australian ore deposits, 8th Comm.
Min. Met. Congr., vol. 1, pp. 285-296.

Kalliokoski, J., 1965. Metamorphic features in North American
massive sulphide deposits. Econ. Geol., 60, pp.
485-505.

Kanehira, K., 1959. Geology and ore deposits of the Chihara
mine, Ehime Prefecture, Japan. Tokyo Univ. Fac.
Sci Jour., sec. 2, 11, pp. 308-338.

Kato, T., 1925. The problem of the cupriferous pyrite deposits.
Econ. Geol., 20, pp. 97-100.

Kelly, T.K., 1969. Quantitative electron probe microanalysis
in mineralogy. Unpublished Ph.D. thesis, University
of London (in preparation).

Kelly, T.K., Lindqvist, W.F., and Muir, M.D., 1969. Y-modulation:
an improved method of revealing surface detail using
the scanning electron microscope. Science, 165,
pp. 283-285.

Kennedy, G.C., Wasserburg, G.J., Heard H.C.,and Newton, R.C.,
1962. The upper phase region in the system SiO_2 -
H_2O. Am. J. Sci., 260, pp. 501-521.

Kinkel, A.R., 1962. The Ore Knob massive sulphide copper
deposit, North Carolina: An example of recrystallized
ore. Econ. Geol., 57, pp. 1116-1121.

Kinkel, A.R., 1967. The Ore Knob copper deposit North Carolina,
and other massive sulphide deposits of the Appalachians.
U.S.geol. Survey, Prof. Paper 558.

Kleeman, A.W., 1954. A reconnaisance of the structural petrology
of the Mt. Lofty Ranges. Unpublished Ph.D. thesis,
University of Adelaide.

Kleeman, A.W., and Skinner, B.J., 1959. The Kanmantoo Group
in the Strathalbyn - Harrogate region, South Australia.
Trans. Roy. Soc. S. Aust., 82, pp. 61-71.

Kopp, O.C., and Harris, L.A., 1967. Synthesis of grunerite
and other phases in the system SiO_2-NaOH-Fe-H_2O
Am. Miner., 52, pp. 1681-1688.

Kuovo, O., Huhma, M., and Vuorelainen, Y., 1959. A natural
cobalt analog of pentlandite. Am. Miner., 44,
pp. 897-900.

La Ganza, R.F., 1959. Talisker Mine - Bore Hole No.1. Mining
Review, S. Aust. Dept. Mines, 110, pp. 49-56.

Leake, B.E., 1968. Zoned garnets from the Galway granite and
its aplites. Earth and Plan. Sci. Ltrs., 3, pp. 311-316.

Lindgren, W., 1933. Mineral deposits (4th ed.). McGraw-Hill,
New York.

Lindgren, W., and Irving, J.D., 1911. The origin of the
Rammelsberg ore deposit. Econ. Geol., 6, pp 303-313.

Loftus-Hills, G., and Solomon, M., 1967. Cobalt, nickel and
selenium in sulphides as indicators of ore genesis.
Mineral. deposita, 2, pp. 228-242.

Lord Kelvin., 1887. On the division of space with the minimum
partitional area. Phil. Mag., 24, pp. 503-514.

Markham, N.L., 1968. Some genetic aspects of the Mt. Lyell
mineralization. Mineral. Deposita, 3, pp. 199-221.

Marmo, V., 1960. On the sulphide and sulphide-graphite schists
of Finland. Bull. Comm. Geol. de Finlande, 190.

McDonald, J.A., 1967. Metamorphism and its effects on sulphide
assemblages. Mineral. Deposita, 2, pp.200-220.

McLean, D., 1965. The science of metamorphism in metals.
(In) Controls of metamorphism (W.S. Pitcher and
G.W. Flinn, eds). Oliver and Boyd, Edinburgh.

McNamara, M.J., 1966. Chlorite-biotite equilibrium reactions
in a carbonate free system. J. Petrology, 7,
pp. 404-413.

Mills, K.J., 1963. The geology of the Mt. Crawford granite
gneiss and adjacent metasediments. Trans. R. Soc.
S. Aust., 87, pp. 167-183.

Mills, K.J., 1964. The structural petrology of an area east
of Springton, South Australia. Unpublished Ph.D.
thesis, University of Adelaide.

Milton, C., and Milton, D.I., 1958. Nickel gold ore of the
Mackinaw mine, Snohomish County, Washington. Econ.
Geol., 53, pp.420-477.

Mining Review, 1939. no. 70, South Australia Dept. Mines,
p.66.

Mirams, R.C., 1962. The geology of the Mt. Barker - Callington
area. Mining Review, S. Aust. Dept. Mines, 117,
pp. 9-16.

Miyashiro, A., 1953. Calcium poor garnet in relation to metamorphism. Geochim. Cosmochim. Acta, 4, pp. 179-208.

Miyashiro, A., 1961. Evolution of metamorphic belts. J. Petrology, 2, pp. 277-311.

Moh, G.H., Kullerud, G., Kingman, O., and Diffenbach, R., 1964. Studies of Ducktown, Tennessee ores and country rocks. Carnegie Inst. Wash. Yb., 63, pp. 211-213.

Naldrett, A.J., Craig, J.R., and Kullerud, G., 1967. The central portion of the Fe-Ni-S system and its bearing on pentlandite exsolution in iron-nickel sulphide ores. Econ. Geol., 62, pp. 826-847.

Newhouse, W.H., and Flaherty, G.F., 1930. The texture and origin of some banded or schistose sulphide ores. Econ. Geol., 25, pp. 600-620

Newton, R.C., 1966. Kyanite-andalusite equilibrium from 700° to $800^{\circ}C$. Science, 153, pp. 170-172.

Offler, R., and Fleming, P.D., 1968. A synthesis of folding and metamorphism in the Mt Lofty Ranges, South Australia. J. Geol. Soc. Aust., 15, pp. 245-266.

Paterson, M.S., and Weiss, L.E., 1966. Experimental deformation and folding in phyllite. Bull. geol. Soc. Am., 77, pp. 343-374.

Peacock, M.A., and McAndrew, J., 1950. On parkerite and shandite and the crystal structure Ni_3PbS_2. Am. Miner., 35, pp. 425-439.

Peltola, E., 1960. On the black schists in the Outokumpu region in eastern Finland. Bull. Comm. Geol. de Finlande, 107.

Pettijohn, F.J., 1957. Sedimentary rocks. Harper and Bros., New York.

Pitcher, W.S., 1965. The aluminium silicate polymorphs. (In) Controls of metamorphism (W.S. Pitcher and G.W. Flinn, eds). Oliver and Boyd, Edinburgh.

Ramberg, H., 1956. Pegmatites in West Greenland. Bull. geol. Soc. Am., 67, pp. 185-214.

Ramberg, H., 1959. Evolution of ptygmatic folding. Norsk. Geol. Tidsskr., 39, pp. 99-152.

Ramdohr, P., 1951. Die Lagerstätte von Broken Hill in New South Wales im Lichte der neuen geologischen Erkenntnisse und erzmikroskopischer Untersuchungen. Heidelberg Beiträge Miner. u. Petrol., 2, pp. 291-333.

Ramdohr, P., 1967. A widespread mineral association connected with serpentinization. N. Jb. Miner. Abh., 107, pp.241-265.

Ramsay, J.G., 1962. Interference patterns produced by the superposition of folds of similar type. J. Geol., 70, pp. 466-481.

Ramsay, J.G., 1964. The uses and limitations of β-diagrams and Pi - diagrams in the geological analysis of folds. Q. Jl. geol. Soc. Lond., 120, pp. 435-454.

Ramsay, J.G., 1967. Folding and fracturing of rocks. McGraw-Hill, New York.

Read, H.H., 1949. A contemplation of time in plutonism. Q. Jl. geol. Soc. Lond., 105, pp. 101-156.

Read, H.H., 1952. Metamorphism and migmatization in the Ythan Valley, Aberdeenshire. Trans. Edinb. geol. Soc. 15, pp. 265-279.

Read, R.A., 1967a. Deformation and metamorphism of the San Dionisio pyritic orebody, Riotinto, Spain. Unpublished Ph.D. thesis, Univ. of London.

Read, R.A., 1967b. Geometrical and time relationships for three fold systems and a subsidiary movement phase in metamorphic rocks south of Bagneres-de-Bigorre, French Pyrenees. Geologie Mijnb., 46, pp. 425-445.

Richardson, S.W., 1968. Staurolite stability in a part of the system Fe-Al-Si-O-H. J. Petrology, 9, pp. 467-488.

Rickard, D.T., 1968. The geological and microbiological formation of iron sulphides. Unpublished Ph.D. thesis, University of London.

Roberts, W.M.B., 1965. Recrystallization and mobilization of sulphides at 2000 atmospheres and in a temperature range 50-145°C. Econ. Geol., 60, pp. 168-171.

Roedder, E., 1967. Fluid inclusions as samples of ore fluids. (In) Geochemistry of hydrothermal ore deposits (H.L. Barnes, ed.). Holt, Rinehart and Winston, New York.

Ryschkewitch, E., 1960. Oxide Ceramics. Academic Press, New York.

Schidlowski, M., and Ottemann, J., 1967. Mackinawite from the Witwatersrand conglomerates. Am. Miner., 51, pp. 1535-1541.

Schreyer, W., Kullerud, G., and Ramdohr, P., 1964. Metamorphic conditions of ore and country rock of the Bodenmais, Bavaria, sulfide deposit. N. Jb. Miner. Abh., 101, pp. 1-26.

Schröcke, H., 1953. Gefügeanalyse und metamorphie Lagerstätten. N. Jb. Mineral. Mh., 5, pp.100-105.

Schwartz, G.M., 1951. Classification and definitions of textures and mineral structures in ores. Econ. Geol., 46, pp. 578-591.

Sen Gupta, P.R., 1965. Practical implications of certain aspects of mineralization in the singbhum copper belt, Bihar. Min. Geol. Met. Inst. India, Wadia Commen. Vol., pp. 772-778.

Sergeyeva, N.E., 1968. An electron-microscope study of changes occurring in ferrispinellides on heating. Int. Geol. Rev., 10, pp. 970-975.

Shelley, D., 1968. Ptygma-like veins in graywacke, mudstone, and low-grade schist from New Zealand. J. Geol., 76, pp. 692-701.

Singh, D.S., 1965. Measurement of spectral reflectivity with the Reichert microphotometer. Inst. Min. Metall., 74, pp. 901-916.

Skinner, B.J., 1956. Physical properties of end members of the garnet group. Am. Miner., 41, pp. 428-436.

Skinner, B.J., 1958. The geology and metamorphism of the Nairne pyrite formation, a sedimentary sulphide deposit in South Australia. Econ. Geol., 53, pp. 546-562.

Smith, C.S., 1948. Grains, phases and interfaces: an interpretation of microstructure. Trans. A.I.M.E., 175, pp. 15-51.

Sprigg, R.C., 1952. Sedimentation in the Adelaide Geosyncline and the formation of the continental terrace. Sir Douglas Mawson Anniv. vol., University of Adelaide, pp. 153-159.

Sprigg, R.C., and Campana, B., 1953. The age and facies of the Kanmantoo group, eastern Mt. Lofty Ranges, and Kangaroo Island, South Australia. Aust. J. Sci., 16. pp.12-14.

Springer, G., 1967. Electron probe analysis of valleriite and
    mackinawite from Palabora and other localities.
    (In) Abstracts: Int. Assoc. on Genesis of Ore
    Deposits., Sympos. St. Andrews, Scotland.

Spry, A., 1963. The chronological analysis of crystallization
    and deformation of some Tasmanian Precambrian rocks.
    J. Geol. Soc. Aust., 10,pp. 193-208.

Stanton, R.L., 1955. Lower Palaeozoic mineralization near
    Bathurst, N.S.W. Econ. Geol., 50, pp. 681-714.

Stanton, R.L., 1959. Mineralogical features and possible mode
    of emplacement of the Brunswick Mining and Smelting
    orebodies, Gloucester County, New Brunswick.
    Canad. Min. Met. Bull., 52, pp. 631-643.

Stanton, R.L., 1964. Mineral interfaces in stratiform ores.
    Inst. Min. Metall., 74, pp. 45-79.

Stanton, R.L., and Gorman, H., 1968. A phenomenological study
    of grain boundary migration in some common sulphides.
    Econ. Geol., 63, pp. 907-923.

Stevenson, J.S., 1937. Mineralization and metamorphism at
    the Eustis mine, Quebec. Econ. Geol., 32, pp. 335-363.

Takeno, S., 1965. Thermal studies on mackinawite. Jour.
    Sci. Hiroshima Univ. Ser.C, 4, pp. 455-478.

Takeno, S., and Clark, A.H., 1967. Observations on tetragonal
    $(Fe,Ni,Co)_{1-x}S$, mackinawite. Jour. Sci. Hiroshima
    Univ. Ser. C, 5, pp. 287-293.

Talbot, J.L., and Hobbs, B.E., 1968. The relationship of
    metamorphic differentiation to other structural
    features at three localities. J. Geol., 76,
    pp. 581-587.

Thomson, B.P., 1965. Geology and mineralization of South
    Australia. (In)Geology of Australian ore deposits,
    8th Comm. Min. Met. Congr., vol. 1, pp. 270-284.

Toulmin, P., and Barton, P.B., 1964. A thermodynamic study
    of pyrite and pyrrhotite. Geochim. Cosmochim.
    Acta, 28, pp. 641-671.

Turekian, K.K., and Wedepohl, K.H., 1961. Distribution of the
    elements in some major units of the earth's crust.
    Bull. geol. Soc. Am., 72, pp. 175-192.

Turner, F.J., 1948. Review of current hypotheses of origin and
    tectonic significance of schistosity (foliation) in
    metamorphic rocks. Trans. Am. Geophys. Union, 29,
    pp. 558-564.
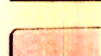
Turner, F.J., and Verhoogen, J., 1960. Igneous and metamorphic petrology. McGraw-Hill, New York.

Turner, F.J., and Weiss, L.E., 1963. Structural analysis of metamorphic tectonites. McGraw-Hill, New York.

Turnock, A.C., and Eugster, H.P., 1962. Fe-Al oxides: phase relationships below $1000^{\circ}C$. J. Petrology, 3, pp. 533-565.

Van Hise, C.R., 1900. Some principles controlling the deposition of ores. Trans. A.I.M.E., 30, pp.1-151.

Van Rensburg, W.C.J., and Liebenberg, L., 1967. Mackinawite from South Africa. Am. Miner., 52, pp. 1027-1035.

Verhoogen, J., 1948. Geological significance of surface tension. J. Geol., 56, pp.210-217.

Vine, J.D., 1966. Element distribution in some shelf and eugeosynclinal black shales. U.S. geol. Survey, Bull., 1214-E.

Vokes, F.M., 1957. The copper deposits of the Birtavarre District, Troms, northern Norway. Norges geol. unders., 199.

Voll, G., 1960. New work on petrofabrics. Lpool. Manchr. geol. J., 2, pp.503-537.

Watterson, J., 1968. Homogeneous deformation of the gneisses of Vesterland, South-west Greenland. Meddr. Gronland, 175, pp. 1-72.

Weiss, L.E., 1959. Structural analysis of the basement system at Turoka, Kenya. Overseas Geol. and Miner. Resources, 7, pp. 3-35 and 123-153.

White, A.J.R., 1956. The granites and associated metamorphic rocks of Palmer, South Australia. Unpublished Ph.D. thesis, University of London.

White, A.J.R., 1966. Petrology and structure of the Rathjen granite gneiss of the Palmer region, South Australia. J. Geol. Soc. Aust., 13, pp.471-490.

White, A.J.R., Compston, W., and Kleeman, A.W., 1967. The Palmer granite - A study of a granite within a regional metamorphic environment. J. Petrology, 8, pp.29-50.

Williams, D., and Nakhla, F.M., 1951. Chromographic contact print method of examining metallic minerals and its applications. Inst. Min. Metall., 60, pp.257-296.

Wilson, G., 1952. Ptygmatic structures and their formation. Geol. Mag., 89, pp. 1-21.

Wilson, G., 1961. The tectonic significance of small scale structures, and their importance to the geologist in the field. Annales Soc. Geol. de Belgique, 84, pp. 423-548.

Winkler, H.G.F., 1965. Petrogenesis of metamorphic rocks. Springer-Verlag, Berlin.

Yund, R.A., and Kullerud, G., 1966. Thermal stability of assemblages in the Cu-Fe-S system. J. Petrology, 7, pp. 454-488.

Zwart, H.J., 1958. Regional metamorphism and related granitization in the Valle de Aran (Central Pyrenees). Geologie Mijnb., 20, pp. 18-30.

Zwart, H.J., 1962. On the determination of polymetamorphic mineral associations and its application to the Bosost area (Central Pyrenees). Geol. Rdsch., 52, pp. 38-65.

Zwart, H.J., 1963. Some examples of the relations between deformation and metamorphism from the Central pyrenees. Geologie. Mijnb., 42, pp. 143-154.
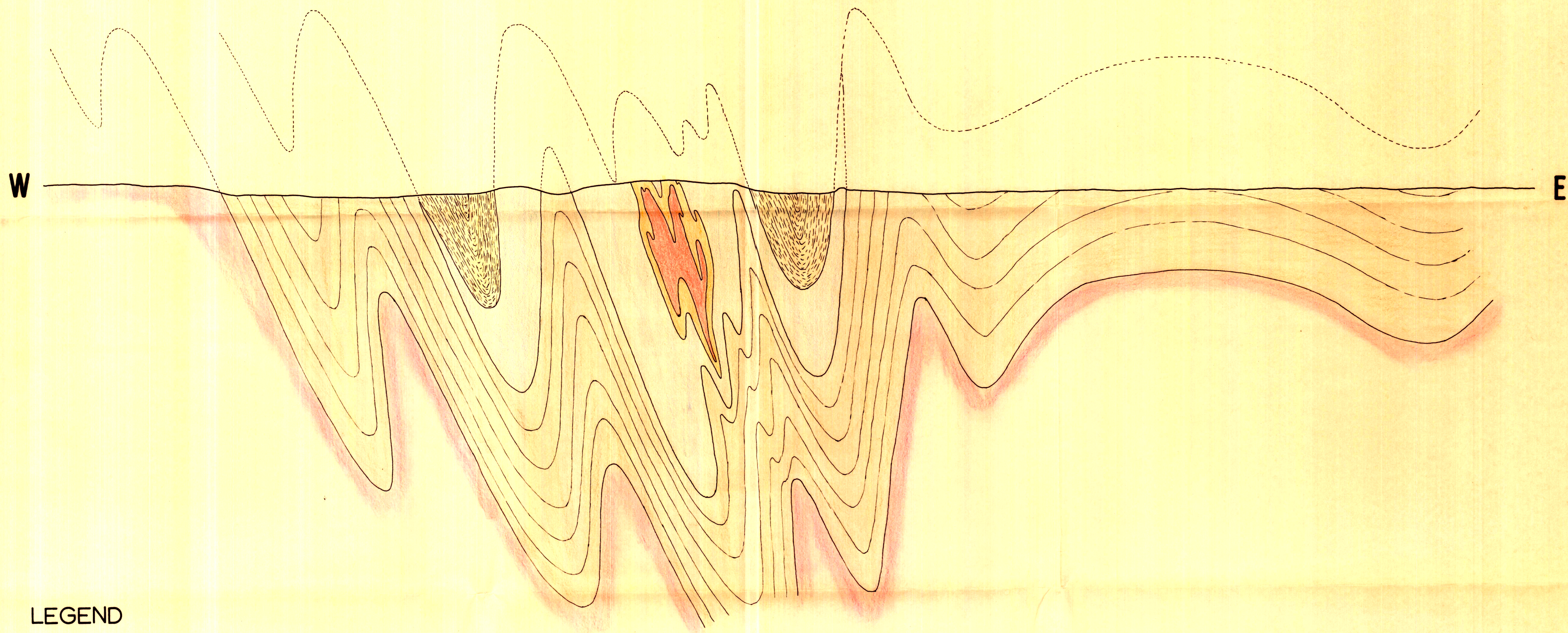
LEGEND
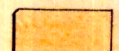
- UPPER QUARTZ - MICA SCHIST
- ANDALUSITE - STAUROLITE SCHIST
- LODE SCHIST
- KANMANTOO OREBODY
- LOWER QUARTZ - MICA SCHIST
- LOWER QUARTZ - FELDSPAR SCHIST

GENERAL SECTION THROUGH 1200 NORTH

W

E

0   1/8   1/4   1/2 MILE

0   1/8   1/4   1/2 KILOMETER

WFL. 1968.

Map 3.
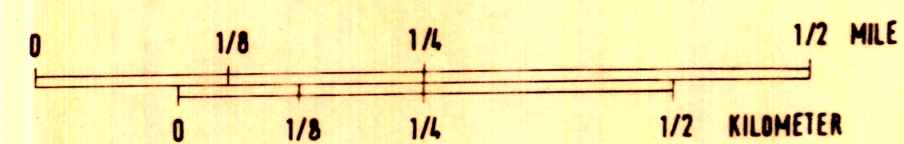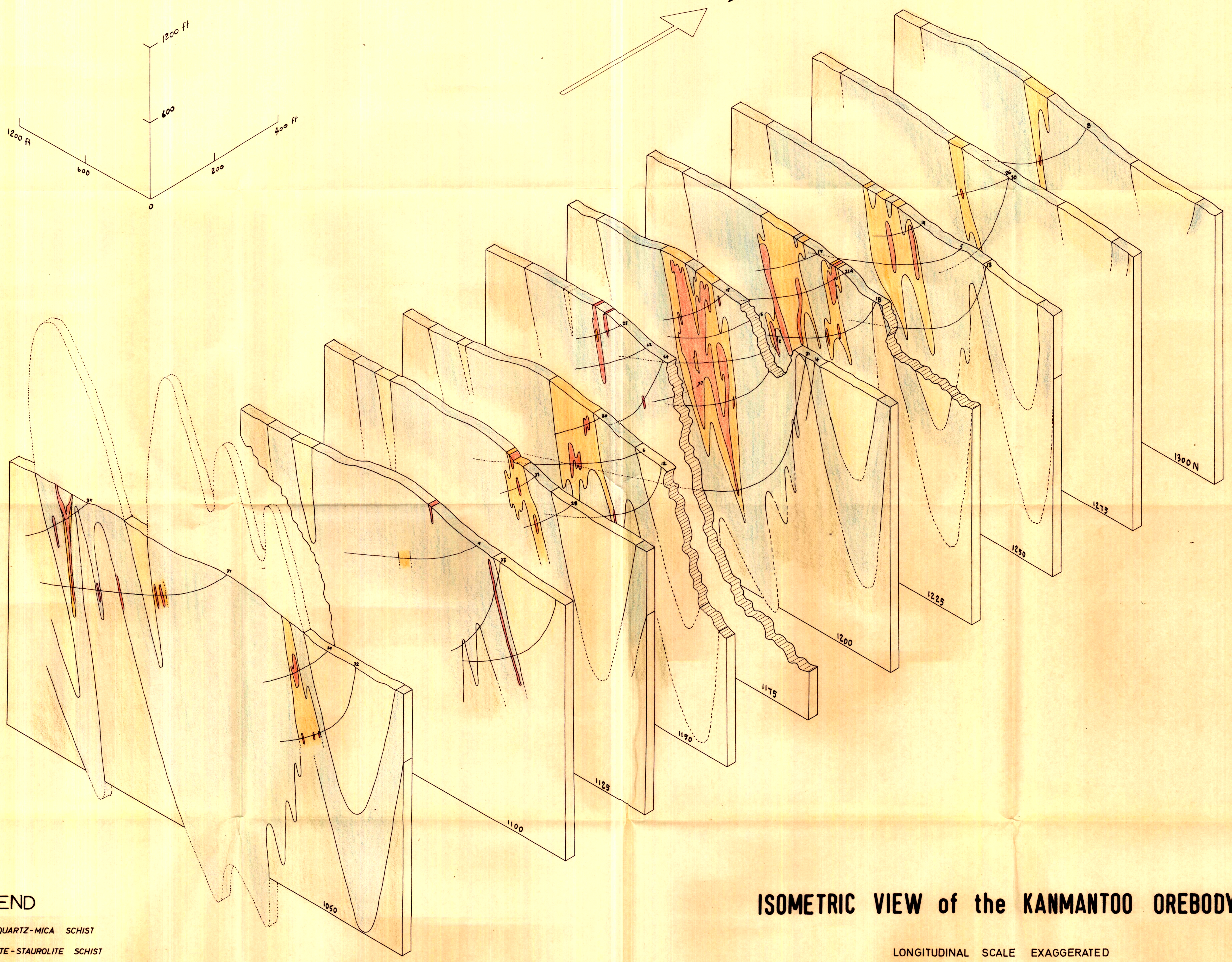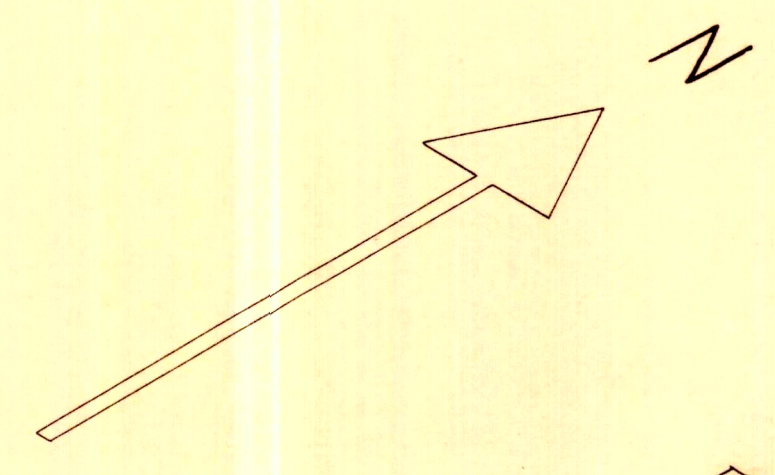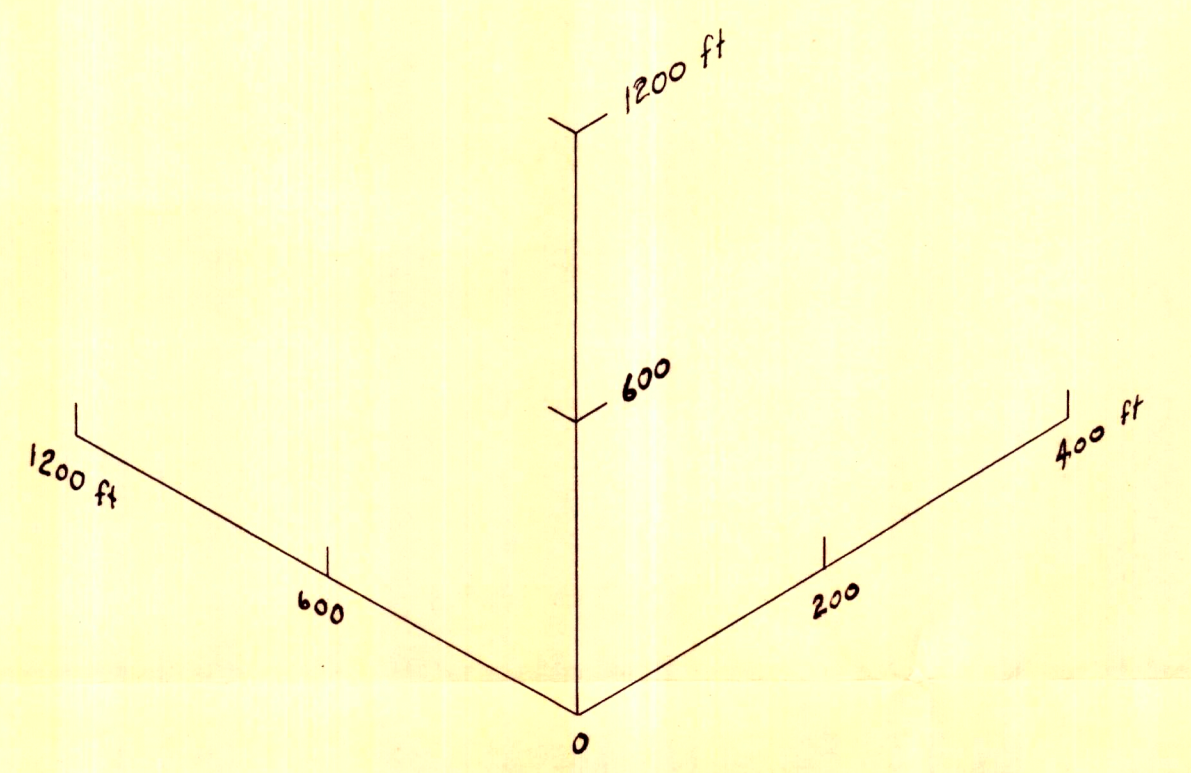
LEGEND

▢ UPPER QUARTZ-MICA SCHIST
▢ ANDALUSITE-STAUROLITE SCHIST
▢ LODE SCHIST
▢ ORE ZONES
▢ LOWER QUARTZ-MICA SCHIST

〜 DIAMOND DRILL HOLES

ISOMETRIC VIEW of the KANMANTOO OREBODY

LONGITUDINAL SCALE EXAGGERATED

WFL. 1968.

Map 4.
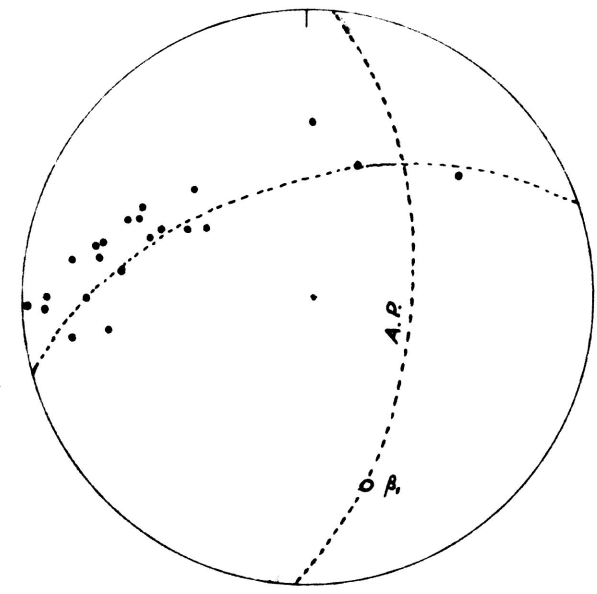
(a) POLES to S_0
sub-area 1.
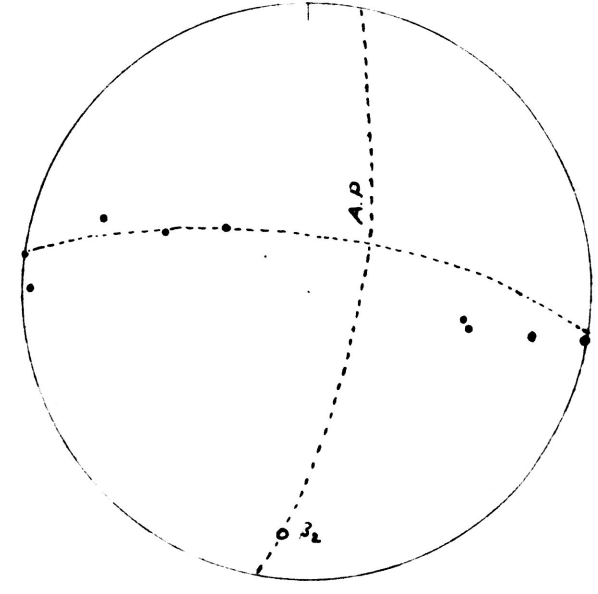
(b) POLES to S_0
sub-area 2.
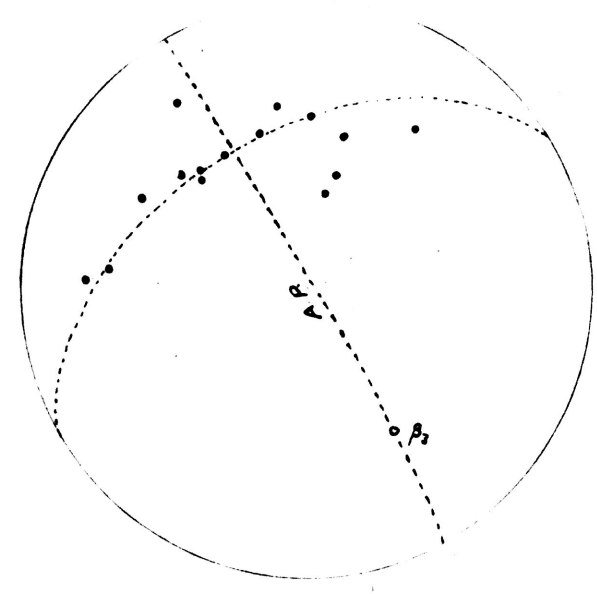
(c) POLES to S_0
sub-area 3.
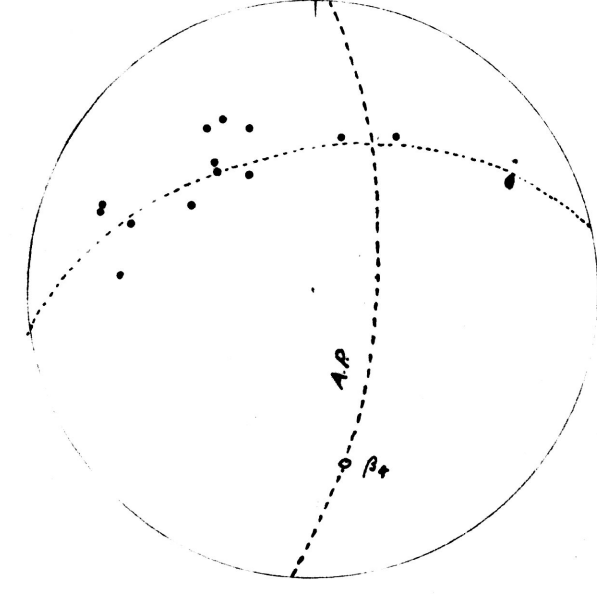
(d) POLES to S_0
sub-area 4.
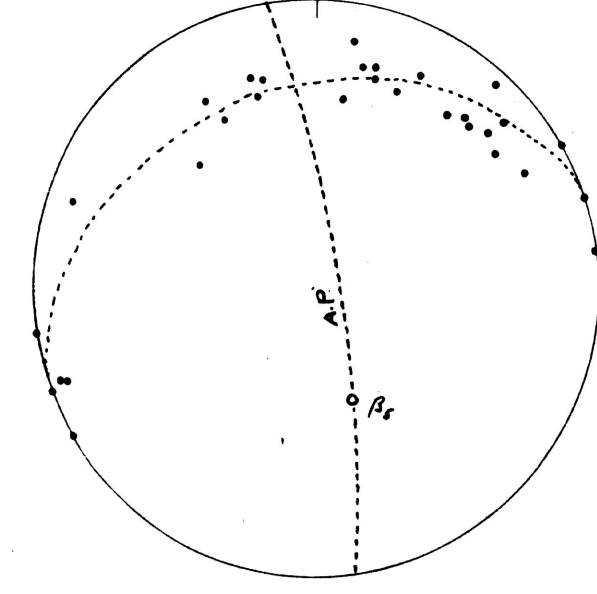
(e) POLES to S_0
sub-area 5.
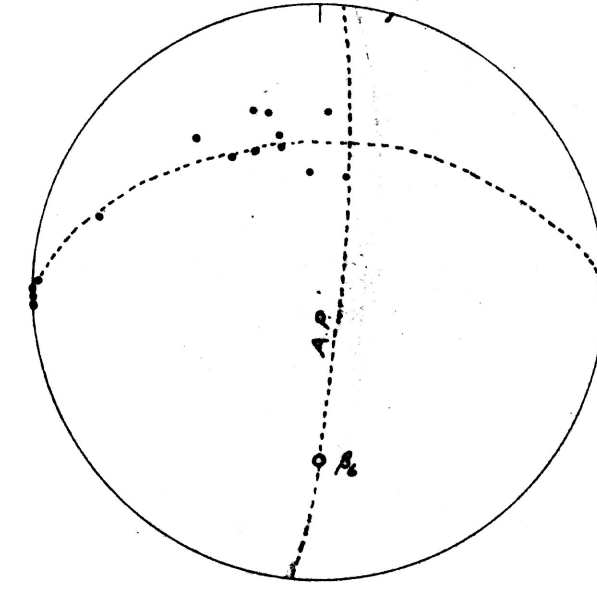
(f) POLES to S_0
sub-area 6.
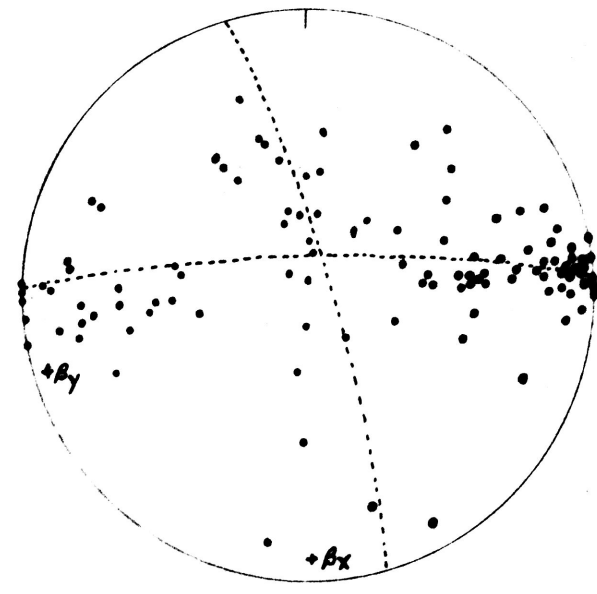
(g) 103 POLES to S_0
mine area
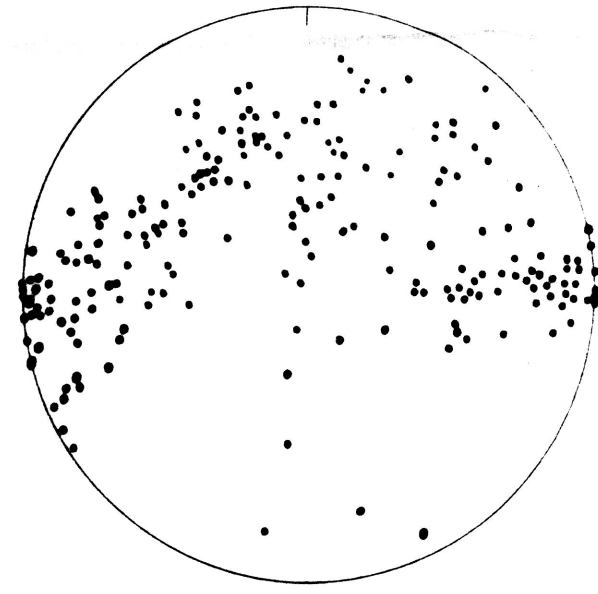
(h) 208 POLES to S_0
whole area
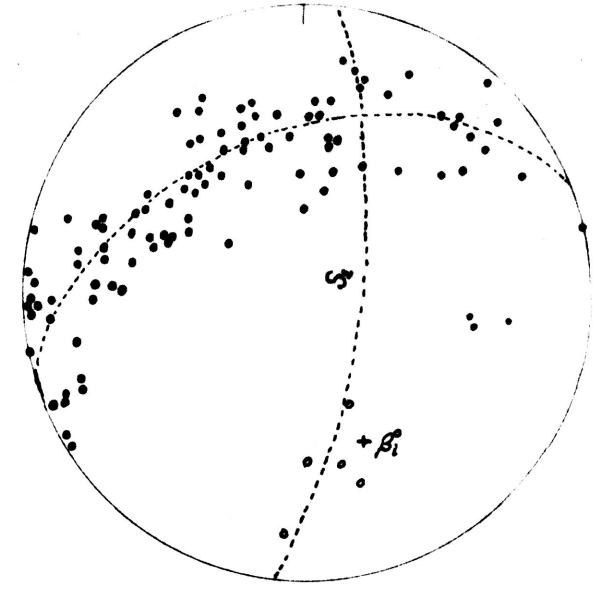
(i) 105 POLES to S_0
outer area
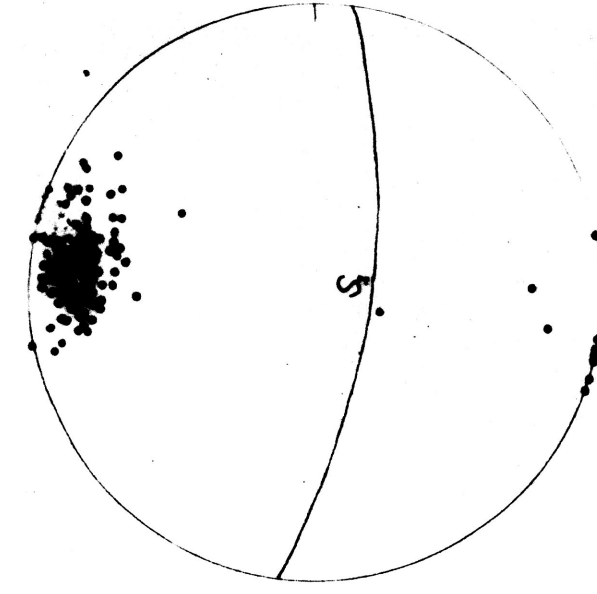
(j) 157 POLES to S_1
whole area
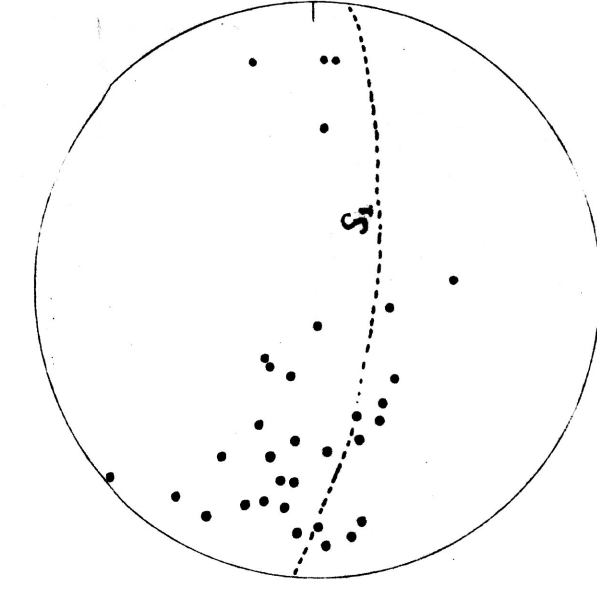
(k) 34 SMALL FOLDS in S_0
whole area
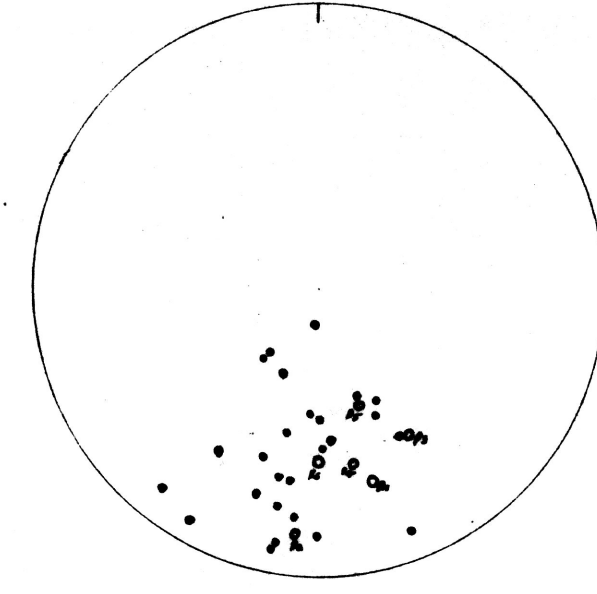
(l) SMALL FOLDS in S_0
outer area
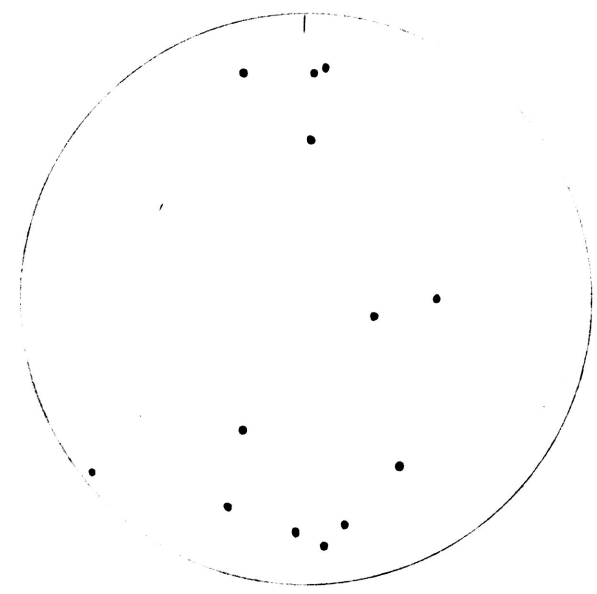
(m) SMALL FOLDS in S_0
mine area
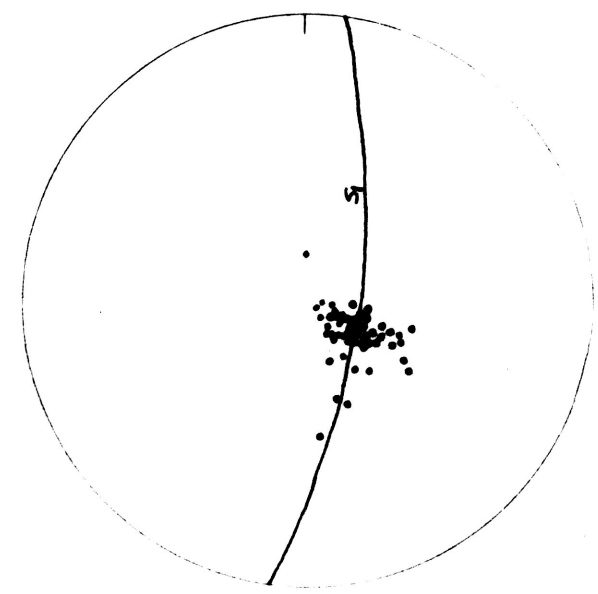
(n) 60 LINEATIONS in S_1
whole area
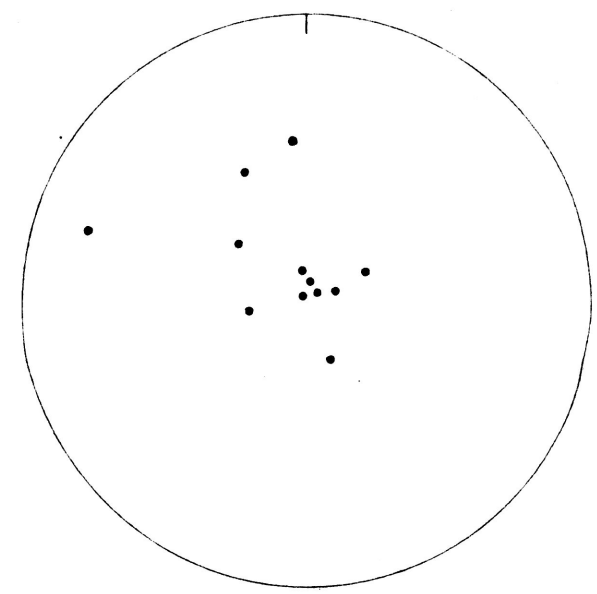
(o) 12 KINK-BANDS in S_1
whole area
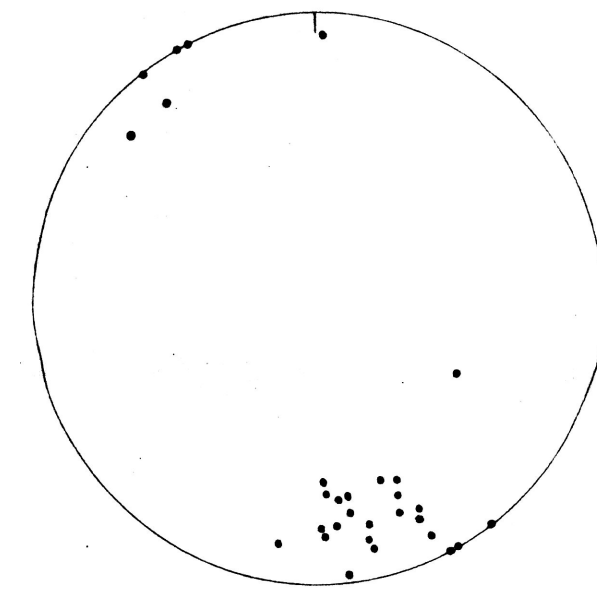
(p) 27 JOINTS
whole area
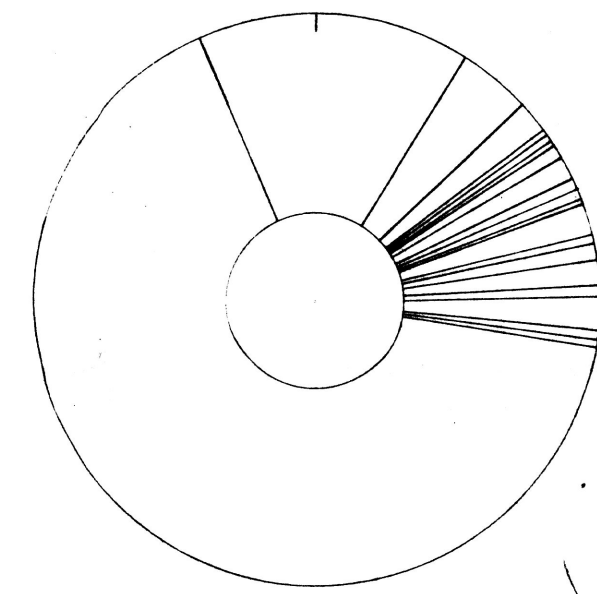
(q) STRIKES of BRECCIA ZONES
(strike diagram)
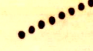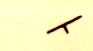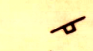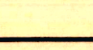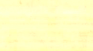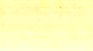
S_0 LITHOLGICAL BANDING (bedding?)

S_1 AXIAL PLANE SCHISTOSITY

$\circ_{\beta_s}$ STATISTICAL FOLD AXES of SUB-AREAS

$+$ OVERALL STATISTICAL FOLD AXIS

PLOTS of STRUCTURAL ELEMENTS on EQUAL AREA NETS

(lower hemisphere)

WFL. 1968.

NORTH

Magnetic
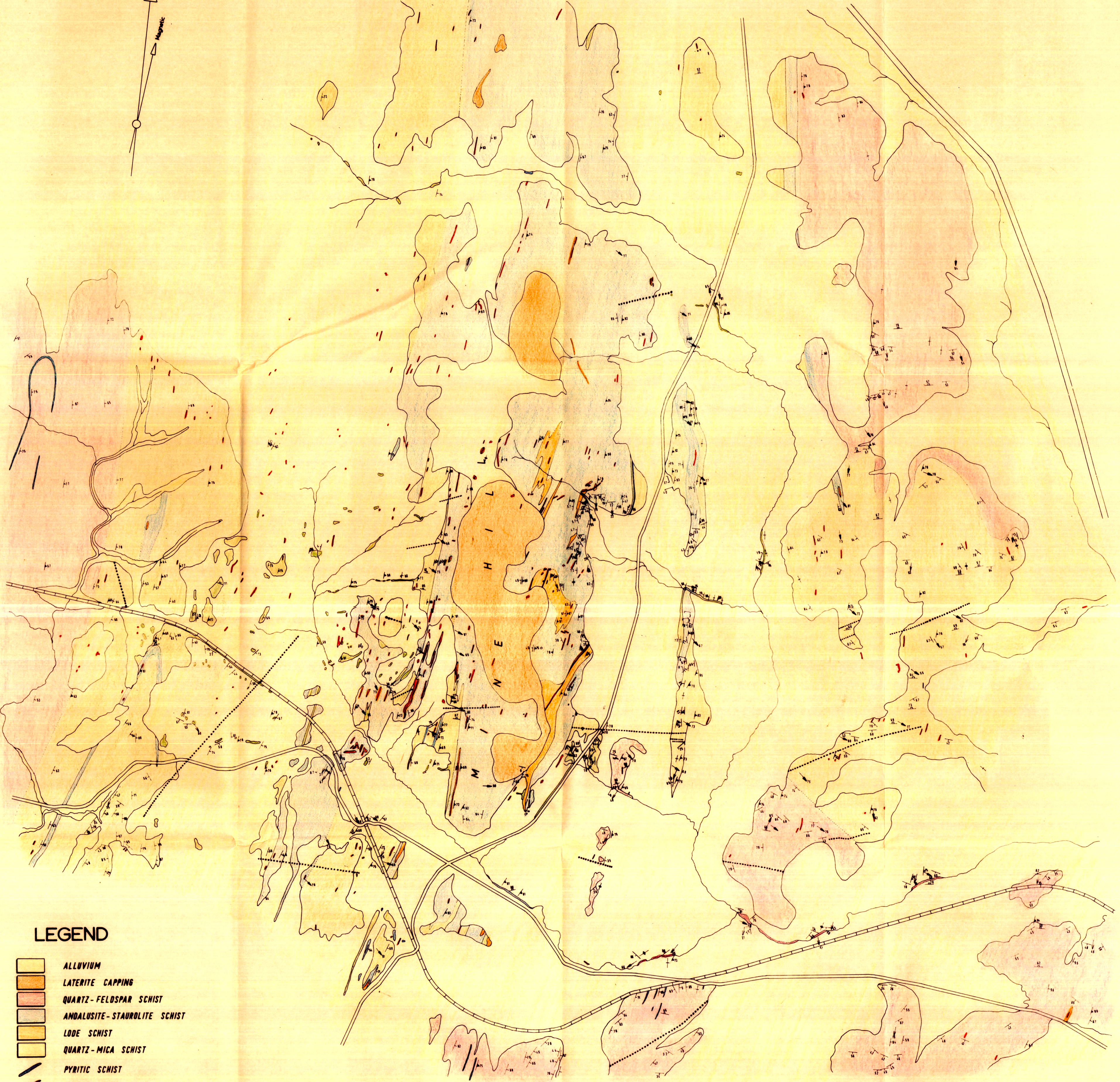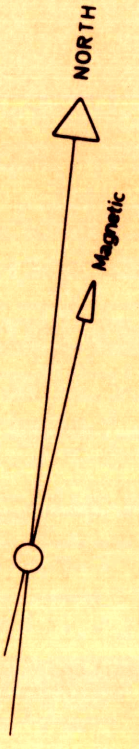
LEGEND

ALLUVIUM
LATERITE CAPPING
QUARTZ-FELDSPAR SCHIST
ANDALUSITE-STAUROLITE SCHIST
LODE SCHIST
QUARTZ-MICA SCHIST

PYRITIC SCHIST
QUARTZ VEINS
BRECCIA ZONES

LITHOLOGICAL BANDING (S_0)
AXIAL PLANE SCHISTOSITY (S_1)
KINK BANDS IN S_1
JOINTS
SMALL FOLDS IN S_0
LINEATIONS IN S_1
GEOLOGICAL CONTACTS
APPROXIMATE GEOLOGICAL CONTACTS
STREAM BEDS
ROADS
RAILWAY

GEOLOGY around the KANMANTOO OREBODY

0   1/8   1/4   1/2 MILE

0   1/8   1/4   1/2 KILOMETER

WFL. 1968.

Map 1.

STRUCTURAL INTERPRETATION
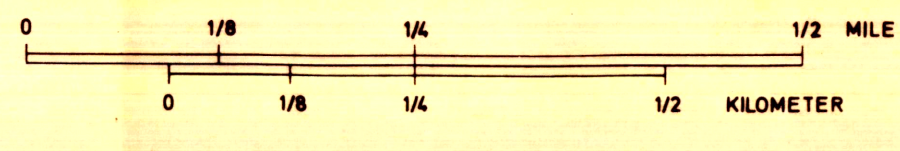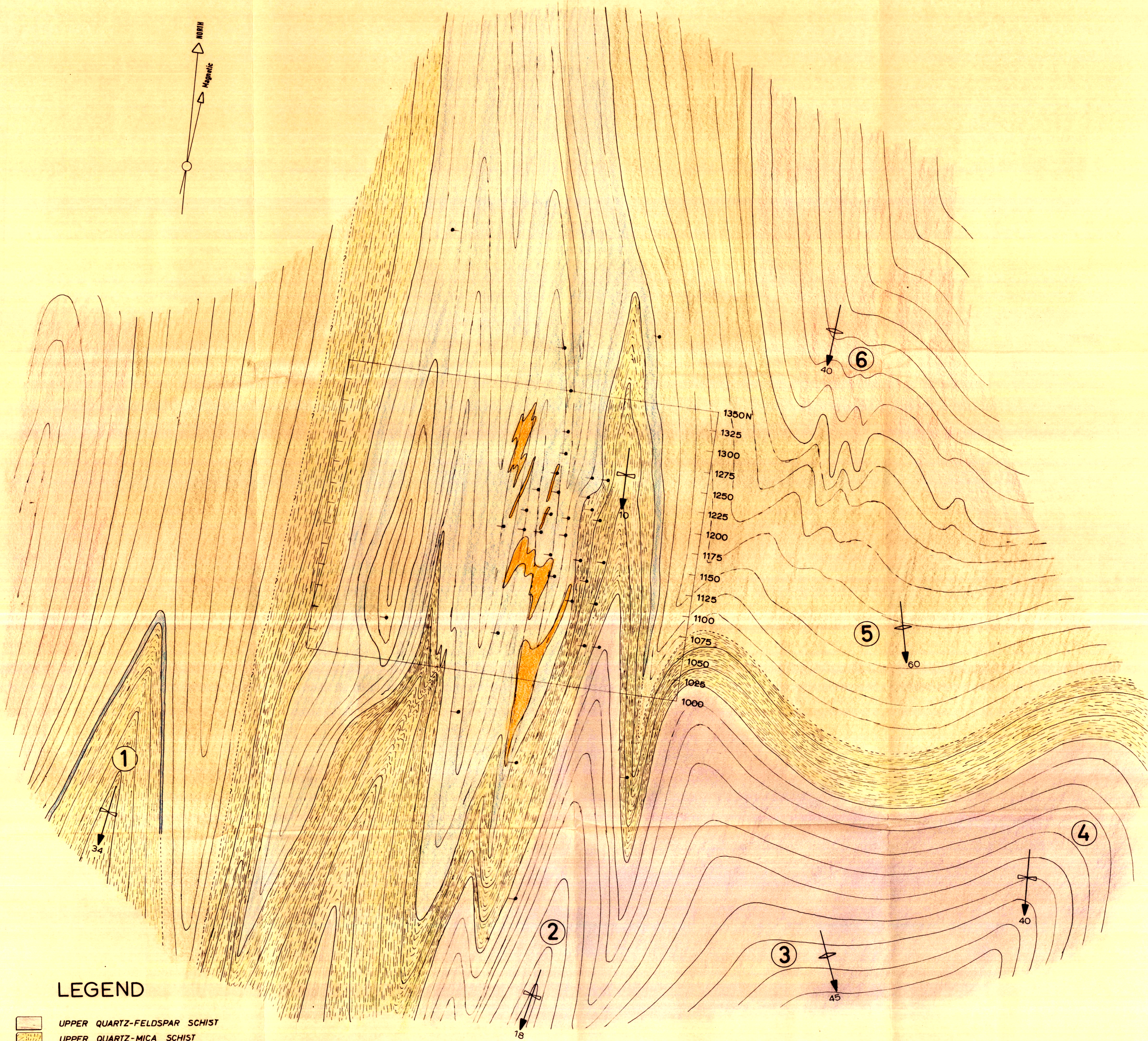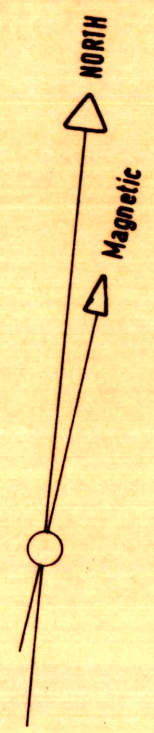
LEGEND

UPPER QUARTZ-FELDSPAR SCHIST
UPPER QUARTZ-MICA SCHIST
ANDALUSITE-STAUROLITE SCHIST
LODE SCHIST
LOWER QUARTZ-MICA SCHIST
LOWER QUARTZ-FELDSPAR SCHIST

〰 STRUCTURAL TREND LINES
➤ TREND & PLUNGE OF MAJOR FOLDS
⋮ DRILLING GRID - MINE AREA
• POSITION & DIRECTION OF INCLINATION
  OF DIAMOND DRILL-HOLES
① STRUCTURAL SUB-AREAS

NORTH
Magnetic

1350N
1325
1300
1275
1250
1225
1200
1175
1150
1125
1100
1075
1050
1025
1000

① 34
② 18
③ 45
④ 40
⑤ 60
⑥ 40

0   1/8   1/4   1/2 MILE
0   1/8 1/4   1/2 KILOMETER

WFL 1968.

Map 2.